Final Report

FORMATION OF URANIUM ORES BY DIAGENESIS OF VOLCANIC SEDIMENTS

Christopher D. Henry and Anthony W. Walton, Principal Investigators

Project funded May 15, 1977 - June 30, 1978
by Bendix Field Engineering Corporation,
a prime contractor with the U.S. Department of Energy
Subcontract No. 77-067-E

Bureau of Economic Geology
The University of Texas at Austin
Austin, Texas 78712

1978

FORMATION OF URANIUM ORES BY DIAGENESIS OF VOLCANIC SEDIMENTS

Christopher D. Henry and Anthony W. Walton, Principal Investigators

CONTENTS

I. INTRODUCTION

by Christopher D. Henry[1] and Anthony W. Walton[2]

SCOPE OF INVESTIGATION

Silicic igneous rocks are relatively rich in uranium; both granites (plutonic) and rhyolites (volcanic and volcaniclastic) have been considered sources of uranium for some sandstone deposits. Uranium in sandstone deposits of the Texas Gulf Coast is probably derived from volcanic ash incorporated in the sediments (Galloway, 1977). In turn, the volcanic ash is probably derived from a belt of rhyolitic volcanoes active during the Middle Tertiary in western Mexico and Trans-Pecos Texas. It therefore seems appropriate to examine the volcanic source rocks to determine whether uranium deposits could form in them or from uranium derived from them.

The importance of rhyolitic volcanic rocks and volcanic centers is particularly underscored by the discovery of major uranium deposits in the Sierra Peña Blanca, Chihuahua, Mexico. The uranium deposits are in rhyolitic ash-flow tuffs and volcaniclastic sediments. Chapter IX by Goodell and others reports on the first detailed study of Peña Blanca.

Most of this study focused on the Chinati Mountains volcanic center and associated volcanic and volcaniclastic rocks in Trans-Pecos Texas

---

[1]Bureau of Economic Geology, The University of Texas at Austin.
[2]Department of Geology, University of Kansas, Lawrence.

(fig. 1). The initial purpose of this project was to investigate the Tascotal Formation, a thick sequence of tuffaceous sediment and minor air-fall tuff, as a possible source or host for uranium mineralization. The project examined the kinds of sedimentary deposits within the Tascotal, the sedimentary processes that acted to form the deposits, and the effect of diagenesis on volcanic glass and uranium contained within the glass in the sediments. A general model of sedimentation and uranium mineralization applicable to other volcaniclastic sedimentary deposits is reported in several chapters by Walton or in the chapter by Jordan. Also, Robinson (chapter V) describes limestones deposited in shallow lacustrine environments within the Pruett Formation, a volcaniclastic sequence older than the Tascotal Formation. A lacustrine environment is not found in the Tascotal, and uranium mineralization is associated with the limestones.

Although much of the investigation focused on the Tascotal Formation, we recognized that the volcanic source area from which the Tascotal was derived, the igneous rocks of the source area, and the processes acting on them could be equally important in the formation of uranium deposits. The source of the Tascotal had not previously been a subject of thorough investigation, but several lines of evidence, including regional distribution, clast composition, and sedimentary structures, indicate that the Tascotal Formation is derived from the Chinati Mountains.

Derivation of the Tascotal Formation from the Chinatis is consistent with general geologic relationships also. The Chinati Mountains

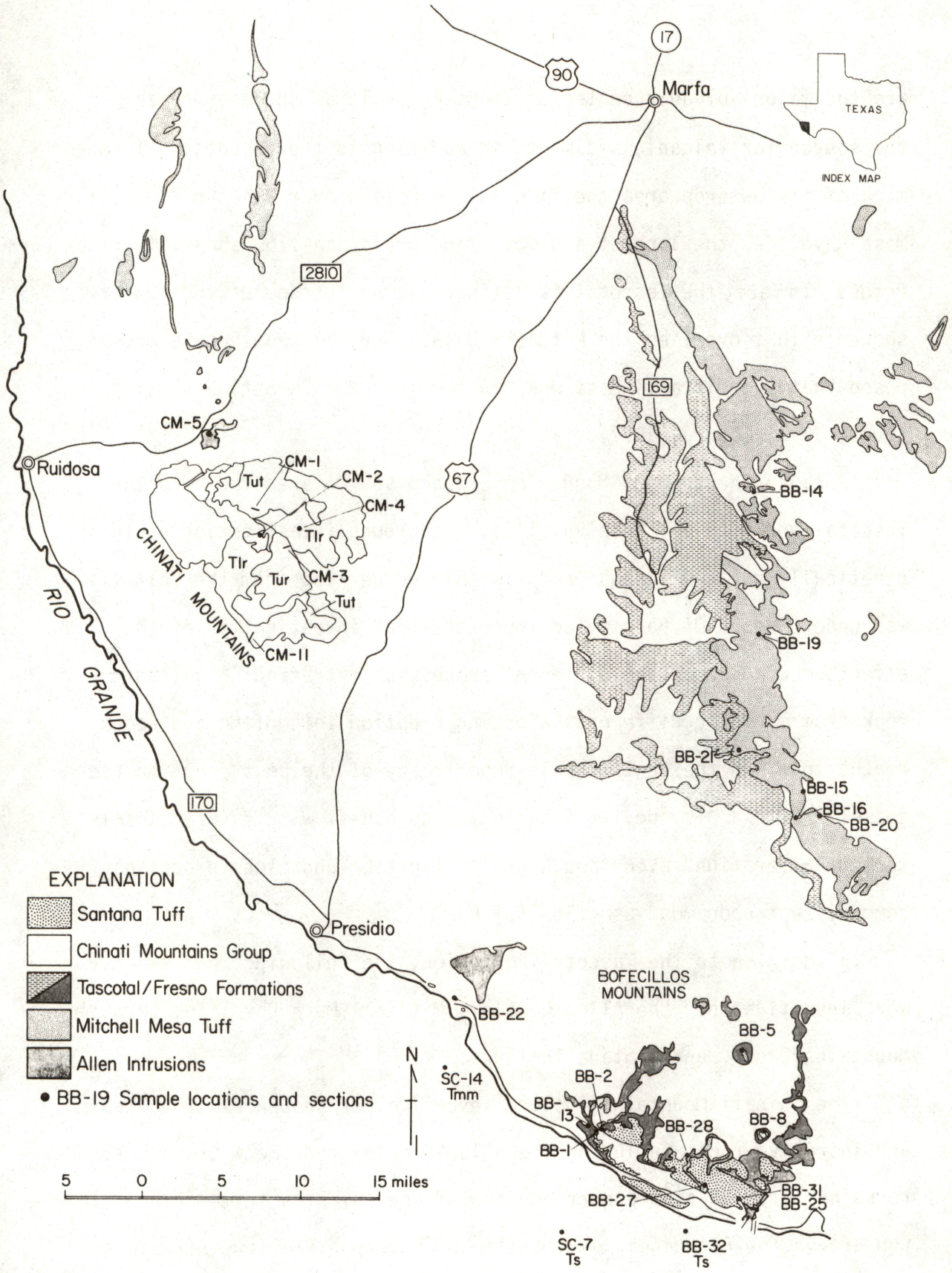

Figure 1. Generalized geologic map of part of Trans-Pecos Texas showing distribution of formations discussed in text and sample locations.

are the major volcanic center of Trans-Pecos Texas and are probably the source for volcanic sediments in addition to the Tascotal. Through much of its outcrop area the Tascotal Formation overlies the Mitchell Mesa Rhyolite, the largest and most widespread ash-flow sheet of Trans-Pecos. In fact, the Tascotal is defined as the tuffaceous sedimentary sequence that overlies the Mitchell Mesa. Several people have proposed that the Mitchell Mesa was erupted from the Chinati Mountains (Burt, 1970; Cepeda, 1977).

Because the Chinati Mountains are the source area for both the Tascotal and Mitchell Mesa Rhyolite, a thorough investigation of the genetically related igneous rocks within or derived from the Chinatis was undertaken. Of particular importance was investigation of the effect on uranium of the different processes that affect a volcanic rock from magmatic differentiation and eruption to cooling and recent weathering. In the text of this report many of the post-eruption processes, for example, devitrification of an ash-flow tuff, are loosely termed "alteration" even though devitrification and other processes commonly act upon most ash-flow tuffs.

In addition to the Tascotal Formation, the following rock types were investigated: the Allen Complex, Mitchell Mesa Rhyolite, Chinati Mountains Group, and Santana Tuff.

The Chinati Mountains include several older sequences of volcanic and intrusive rocks including the Allen Complex and Shely Group. These rocks are exposed at the northern end of the Chinatis in the Pinto Canyon area. The Allen Complex consists of numerous shallow intrusions

and lava flows of rhyolite. Investigation of the Allen Complex is particularly important because it contains numerous small concentrations of uranium that have recently been investigated for possible economic-grade deposits (Reeves and others, 1978).

The Mitchell Mesa Rhyolite is the major ash-flow tuff of Trans-Pecos Texas and is derived from the Chinati Mountains. Evidence for this assertion includes regional distribution, thickness, and elevation of the Mitchell Mesa (Burt, 1970) and similarities in petrochemistry and age between the Mitchell Mesa and rocks of the Chinati Mountains (Cepeda, 1977). Additional evidence is discussed in more detail by Burt and Cepeda. The Mitchell Mesa Rhyolite directly underlies the Tascotal throughout the outcrop area, and the Tascotal is in part derived from the Mitchell Mesa. Upper nonwelded parts of the Mitchell Mesa were eroded and redeposited as tuffaceous sediment in the basal part of the Tascotal. The Mitchell Mesa was investigated to see if a variety of processes that commonly act upon an ash-flow tuff could release or redistribute uranium. Thus the Mitchell Mesa could be a source for uranium concentration either within the Mitchell Mesa or within the Tascotal or other tuffaceous sediments.

Eruption of the Mitchell Mesa produced the Chinati Caldera which was subsequently filled by volcanic rocks of the Chinati Mountains Group (Cepeda, 1977). The Chinati Mountains Group consists of trachyte and rhyolite lava flows and rhyolite ash-flow tuff. Many of the processes that could influence uranium concentration and distribution in the Mitchell Mesa Rhyolite could also act upon rocks of the Chinati

Mountains Group. However, because the Chinati Mountains Group was deposited as caldera fill at the locus of continued igneous activity, additional processes that do not affect the extra-caldera Mitchell Mesa Rhyolite could affect the Chinati Mountains Group. For example, high-temperature processes should be far more significant within a caldera (or as a result of resurgent intrusion) than outside a caldera and could give rise to hydrothermal alteration.

A final volcanic unit, the Santana Tuff, was investigated even though it is not genetically related to the Tascotal Formation, Mitchell Mesa Rhyolite, or Chinati Mountains Group. The Santana Tuff is an ash-flow tuff overlying the Fresno Formation, the Tascotal equivalent in the southern part of Trans-Pecos. The Santana Tuff is in many respects similar to the Mitchell Mesa Rhyolite, and investigation of the Mitchell Mesa Rhyolite allows broader generalization of results. A major difference, at least in the particular parts examined, is that the Mitchell Mesa is mostly thin distal ash-flow tuff where it is in contact with the Tascotal, and the Santana Tuff where it overlies the Fresno Formation is thick, near-source ash-flow tuff. Thus, although both have undergone a variety of alteration processes common to ash-flow tuffs, the style and intensity of alteration acting on each is different. Also, because the Santana Tuff overlies the tuffaceous sediment being studied (in this case the Fresno Formation), it is a more likely source for uranium than is the Mitchell Mesa Rhyolite.

To broaden the results of this study, several areas outside Trans-Pecos Texas were examined to evaluate the conclusions derived from the

Trans-Pecos study. Areas selected were Virgin Valley, Nevada, Thomas Range, Utah, and the previously mentioned Peña Blanca, Chihuahua. Each area was selected because it was reported to have abundant silicic volcanic rocks and volcaniclastic sediments and significant uranium concentrations associated with the rocks.

BRIEF SUMMARY OF RESULTS

To understand the formation of uranium deposits and to predict where they could occur, one must understand the processes that act in formation and alteration of potential source and host rocks. Thus, this study has focused on the types of volcanic and volcaniclastic rocks that can form around a major volcanic center.

Rocks accumulate in volcanic regions in several settings, including volcanic center areas, volcanic and sedimentary aprons, valley areas, lakes, and eolian regions. In each of these, a variety of igneous and sedimentary processes act to accumulate material and form rocks. Each set of processes leaves distinctive rock types or structures, so that the rocks that form in each area are recognizable. From the existence of rocks of one such setting, the current or former presence of the others can be inferred.

Each part of a volcanic region can be considered separately for its favorability for accumulation of uranium deposits. In general, the principles of evaluating volcanic and sedimentary parts of the system should be different because the kinds of uranium deposits that can be formed in each are different. In sedimentary sequences, sandstone-type,

calcrete, and lacustrine deposits are likely, and uranium can leak across unconformities into underlying units. In volcanic rocks, both high- and low-temperature processes can act to release, transport, and concentrate uranium. Uranium released from the volcanic rocks can accumulate either within the volcanic rocks or within adjacent rocks including the volcanic sedimentary sequence.

Analysis of the formational systems of the Tascotal Formation, an Oligocene unit that crops out in the Trans-Pecos volcanic field of Texas and includes the Fresno Formation, leads to the conclusion that the Tascotal formed in a number of different environments. Most of the sediment that makes up the Tascotal was derived from the active phase of the Chinati Mountains volcanic center. The sediment was deposited by braided streams to form the active apron member that crops out in eastern Presidio County. Simultaneously, deposition of sediment took place in three other environments: (1) braided streams that were part of the regional drainage net deposited the lower conglomerate member to form a valley facies south of the active apron region; (2) alluvial fans formed around the Solitario Uplift; and (3) active apron sediments were deposited in southeastern Presidio County in the Bofecillos Mountains. Later, three other formational systems operated to create other members. The Fresno member in the Bofecillos Mountains consists of flows from a local volcanic center. A sequence of eolian sand overlies the active apron member north of the Bofecillos Mountains. The conglomeratic Perdiz member contains debris eroded from the Chinati Mountains after volcanic activity ended there.

Uranium deposits are likely to occur in the valley facies of the Tascotal where conditions were suitable for uranium release from volcanic glass, migration through permeable sandstones and conglomerates, and entrapment within potential reducing environments or calcretes. The other members lack one or more of the factors necessary to form secondary uranium deposits. Most lack reducing environments. In some of the members, uranium was released from glass shards, then almost immediately reprecipitated in disseminated fashion. In the eolian member, the glass shards have not been altered. Tables 1 and 2 summarize criteria for mobilization, migration, and entrapment of uranium.

Uranium can be released from volcanic rocks both by high-temperature processes unique to volcanic rocks and by low-temperature processes similar to those acting on the volcanic sediments. Release and transport of uranium are intimately connected, and specific transport mechanisms can occur only with certain release mechanisms. Any process that breaks down or dissolves glass releases uranium, including high-temperature devitrification with or without vapor-phase cryztallization, granophyric crystallization, and solution of glass by cool or heated ground water. However, each release process dictates the transport mechanism available, and not all are effective in transporting uranium. Volcanic rocks formally composed of glass but now altered by ground water have been efficiently depleted of uranium. Thus ground water must be an effective transporting agent in addition to releasing uranium from glass. Ligands to complex uranium in ground water are required but many exist (Langmuir, 1978). Uranium mineralization in the Allen Complex, Trans-Pecos Texas, in Virgin

Table 1. Favorability criteria for accumulation of uranium in volcanic sediments: uranium mobilization and migration (preliminary).

Sequence of events	Criteria
Release of uranium from glass	1. Ghosts or pseudomorphs of shards 2. Shard-free layers in sequences containing abundant glass--if evidence exists that shard-free layers originally contained glass
Migration of uranium from site of release	1. Evidence of alteration of glass at slightly basic to slightly acid pH--for example, no zeolites formed as glass was altering 2. Evidence that potential complexing agents (for example, $CO_3^=$, $PO_4^=$, F^-) were <u>not</u> depleted at the time of migration 3. Alteration of glass in soil systems
Integrated flow path for ground water	1. Porous, permeable, sheet-like or channel-like sands and conglomerates that extend down dip, especially those with few mud interbeds
Trap for accumulation of uranium A. Internal	1. Similar to sandstone-type deposits a. Disseminated pyrite or organic matter in part of sequence, oxidized rock in remainder, oxidation-reduction interface between b. Situation favoring passage of sour gas or other reductants through the system 2. Areas of discharge of ground water a. Discharge calcretes b. Lacustrine sediments c. Closed-system zeolite assemblages (indicating lakes or playas)
B. External	1. Unconformable relations between glass-rich sediments and permeable channels into underlying rocks

Table 2. Volcanic sedimentary systems: their character and uranium potential.

Depositional system	Active processes	Grain size	Sedimentary structures	Source	Uranium potential migration	Trap
Apron						
Proximal	Surge, stream flood, debris flow	Coarsest in the system, but may be only sand; always gravel in inactive phase	Depends on grainsize; small to very large-scale crossbeds in gravels, massive gravels, diamictite conglomerates and other mudflow deposits	Poor potential unless fine-grained and glass-rich	Excellent except in debris-flow beds	Poor--no reductants
Mid fan	Stream flood, braided stream	Finer than proximal; conglomerates present, but probably not dominant; sand in active phase, sand and gravel in inactive phase	Braided-stream sequences: (Miall, 1977) deposition from linguoid bars	Glass-rich sediments have some source potential if altered at low pH	Excellent	Poor--no reductants
Distal fan	Braided stream, sheet flood	Sand and mud	Sand-rich braided-stream sequences (Miall, 1977)	Same as mid fan	Poor to excellent--depends on mud content	Poor--no reductants

Table 2. Continued.

Depositional system	Active processes	Grain size	Sedimentary structures	Source	Uranium potential migration	Trap
Valley Fluvial	Braided or meandering stream	Variable--mud to gravel	Braided-stream sequences (Miall, 1977), point bars and overbank deposits, swamps and small lakes	Excellent if paleosoils present	Poor to excellent; ground waters may initially be reducing	Poor to excellent; if redunctants accumulate soil or ground water, may have oxidation reduction; may be area of ground-water discharge and calcrete formation
Lacustrine	Orthochemical sedimentation, allochemical sedimentation (diatomites, oolites, etc.); algal growth; turbidity currents, eolian fallout, wave reworking, beach and fluvial deltaic systems at margins	Muds to sands	Laminated to massive muds and allochemical or orthochemical sediments	Glass-rich beds good to excellent, if glass can react	Abundant fine beds reduce chances of long migration	Organic matter may be abundant; may be area of ground-water discharge; should be good
Eolian	Grain fall, traction, avalanching	Sand	Large-scale crossbeds and parallel lamination	Good if altered under favorable circumstances	Excellent, unless permeability reduced by alteration	Poor--no reductants

Valley, Nevada, in the Thomas Range, Utah, and in the Sierra Peña Blanca, Chihuahua, probably formed from uranium released by ground-water alteration of glass.

Rocks having undergone devitrification with or without vapor-phase crystallization are not depleted in uranium. Thus, normal vapor-phase transport of uranium is apparently not effective because either (1) the vapor is of the wrong composition (lacks a complexing agent such as fluorine), or (2) the vapor does not migrate far enough to concentrate uranium. Granophyrically crystallized rocks of the Upper Rhyolite of the Chinati Mountains Group are moderately depleted in uranium. The depletion is apparently related to much more extensive volatile flushing than occurs in normal vapor-phase crystallization.

Concentration of uranium transported by ground water can occur in the same environments that concentrate uranium released from sediments (table 1) as well as in the volcanic rocks themselves. Solubility controls include oxidation reduction, concentration by evaporation, or mixing of waters of different chemistry. The latter could occur at or near the contact of volcanic and nonvolcanic rocks, such as carbonates. Uraniferous opal, chalcedony, or uranophane occur at all four areas studied. Uranium and silica are associated because they are both released in relatively large quantities by solution of glass, and because opal apparently efficiently adsorbs uranium.

Localization of mineralization is also controlled by permeability. In fracture systems of volcanic rocks, brecciated zones along faults (especially at intersections of faults), lithophysal zones, or nonwelded

parts of ash-flow tuffs are possible sites. Permeability of sedimentary environments are given in tables 1 and 2.

A general conclusion of this study is that low-temperature solution of glass by ground water (diagenesis) is highly favorable for release and transport of uranium. In some settings transport of uranium released by diagenesis is inhibited by lack of complexing agents in the ground water; identification of transport controls is of critical importance. A variety of environments exists for concentration of uranium, but their existence at a specific site depends entirely on the geologic setting of the site.

REFERENCES

Burt, E. R., 1970, Petrology of the Mitchell Mesa Rhyolite, Trans-Pecos Texas: The University of Texas at Austin Ph. D. dissertation, 94 p.

Cepeda, J., 1977, Geology and geochemistry of the igneous rocks of the Chinati Mountains, Presidio County, Texas: The University of Texas at Austin, unpublished Ph. D. dissertation, 153 p.

Galloway, W. E., 1977, Catahoula Formation of the Texas Coastal Plain: Depositional systems, composition, structural development, groundwater flow history, and uranium distribution: The University of Texas at Austin, Bureau of Economic Geology Report of Investigations 87, 59 p.

Langmuir, D., 1978, Uranium solution-mineral equilibria at low temperatures with applications to sedimentary ore deposits: Geochimica et. Cosmochimica Acta, v. 42, p. 547-569.

Miall, A. D., 1977, Paleocurrent and paleohydrologic analysis of some vertical profiles through a Cretaceous braided stream deposit, Banks Island, Arctic Canada: Sedimentology, v. 23, p. 459-483.

Reeves, C. C., Kenney, P., Wright, E., 1978, Known radioactive anomalies and uranium potential of Cenozoic sediments, Trans-Pecos Texas, in Walton, A. W., ed., Cenozoic geology of the Trans-Pecos volcanic field of Texas, p. 86-99.

II. ROCK-FORMING SYSTEMS OF VOLCANIC REGIONS

by Anthony W. Walton[1]

INTRODUCTION

Efficient, systematic exploration for uranium deposits requires understanding of the geologic regimes in which the deposits form and of the processes by which they form. Currently, exploration is very active for uranium deposits in volcanic rocks and volcanic sediments, spurred perhaps by large discoveries in the Sierra Peña Blanca of Chihuahua, Mexico, or by the widely known fact that products of silicic or alkalic volcanos commonly contain abundant uranium. Unfortunately, little is known about sedimentary rocks of volcanic regions and about the geochemistry of uranium in those areas. Volcanic sequences and volcanic sedimentary sequences may offer a range of possible types of uranium deposits different from both those found in the sandstone-type deposits so prolific in the western part of the United States and the great diversity of types that are important sources of the metal elsewhere. Alternatively, close analogues may exist between volcano-related types and other rock types so that the differences of types of uranium deposit may be more differences of degree. In any case the guides to ore formation may be different in volcanic terrains.

---

[1]Department of Geology, University of Kansas, Lawrence.

Exploration in nonvolcanic areas, especially in normal sedimentary sequences, is aided by well-developed conceptual models of the formational processes of the rocks and uranium deposits in them. After studying parts of an area, it is possible to make confident guesses about sediments or rocks that occur in other parts of it, and especially, about their uranium potential. A lack of the necessary information in volcano-related sequences together with the lack of models of ore formation in such environments has reduced the exploration process there to following models more applicable to other environments, to relying on techniques best applied to the exploration for shallow deposits, or to applying methods in use since the earliest days of the uranium industry.

This report describes studies on volcano-related sequences that were conducted by several workers. The objectives of the studies were to increase understanding of sedimentology and uranium geology of volcanic areas. The objectives of this report are (1) to aid in development of facies models of volcanic and volcanic sedimentary terrains; (2) to describe one process of alteration of volcanic glass, a key step in formation of uranium deposits in such regions; and (3) to report a possible method of determining whether alteration of volcanic glass has released uranium to solution to migrate and be concentrated into deposits, or whether the uranium was almost immediately precipitated as dispersed uranium minerals or impurities in clay, opal, or zeolite.

The report is based largely on the Trans-Pecos volcanic field of Texas, and thus represents only one example of volcanic processes and alteration. Although only a minor amount of comparison with other volcanic districts has been possible, some information on Thomas Range,

Utah, and Virgin Valley, Nevada, is included in the report. Particularly interesting is the section describing the Peña Blanca uranium deposit in Chihuahua, Mexico, where proven reserves of 4,000 tons of U_3O_8 and a potential reserve of several times that amount occur in volcanic rocks and sediments (R. Chavez, oral communication, 1977). Because of the limited sample, the conclusions of this report should not be taken as indicative of conditions in all volcanic regions. Instead they provide examples for comparison and a beginning on which to build.

A Systematic Approach

The approach in describing the rocks of the volcanic area is patterned on the depositional systems concept applied previously to terrigenous sediments to elucidate the environments of their formation (Fisher and McGowen, 1967). This scheme provides a framework for depositional analysis of sedimentary units by encouraging close comparison with modern analogues and reference to laboratory model studies, and by focusing the attention of the investigator on crucial evidence. The term "system" refers to the group of processes characteristic of a large, but distinct, geomorphic environment in which sediment accumulates. This environment could be a river system, for example, in which channel and overbank processes transport and deposit material. The river region is geomorphically distinct from an alluvial fan at its head and a delta near its mouth. In the context of volcanic fields, a system might be a vent system in which uniquely volcanic processes can combine with sedimentary processes to produce a vent facies. Such

systems can be studied by the methods of systems analysis, for their boundary conditions, input, internal machinations, and output are related, and variation of one such parameter affects the others. Provided that reliable and sufficient information about one or more of these qualities is available, conclusions can be drawn about the others. In his lucid exposition, Galloway (1977, p. 5-8) uses the term "depositional system" in a different sense: to him it is a body of rock that formed in a geomorphic environment, not the system of processes that led to formation of the rock. In this report, bodies of rock that Galloway (1977) might term "depositional systems" are identified as "informal members."

Each system is characterized by a number of processes that act to produce a diversity of facies or types of rocks. Fluvial systems include the processes of unidirectional flow of fresh water, variation of amount of that flow, and lateral migration of the flow axis, among others. Under certain conditions, these processes operate to form the characteristic channel-lag, point-bar, and floodplain deposits of meandering streams. Under different boundary conditions--regional slope, grain size of the sediment available, or amount of discharge--the character of the stream can be altered and the nature of the deposit changed. By studying the processes and deposits of a large number of modern depositional environments, and by referring to appropriate laboratory studies, sedimentologists have set up a series of models that summarize the characteristics of sediment produced in that environment. In studies of ancient rocks, the investigator compares critical features of

the rocks with those of modern sediments. From this comparison, he can deduce the nature of the process or processes responsible for each facies of the ancient rock, and the geomorphic environment in which the sediment formed.

Particular systems produce not only sediments of a diversity of different facies, but also sediments of nearly or completely identical character. This apparent complexity results from the fact that similar processes can be found in a large number of different systems: for example, unidirectional flow in channels occurs in deltas and alluvial fans as well as in rivers. But analysis of depositional systems allows us to escape this dilemma by pointing out that each depositional system has a unique set of processes. Though several or all of the processes may be shared with other depositional systems, and hence, similar facies may occur in deposits of several systems, the particular set of processes--and facies--is found associated in only one depositional system.

The advantages of studying sediments as depositional systems are (1) The attention of the investigator is focused on the aspects of the rock that contain information useful for interpreting the depositional environment of the rock. Because conceptual models of the processes and sediment character of most depositional environments exist, the investigator need only collect relevant information on sedimentary facies of the rocks he is studying and compare it with well-established models. (2) Once these interpretations are made, it is possible to predict distribution of other facies and to estimate probability of finding facies--controlled accumulations of valuable materials in various areas. Pro-

specting for economically valuable deposits in sedimentary rocks, such as uranium deposits, is speeded if knowledge of any facies controls on distribution of the deposits is available, and if the techniques and concepts necessary to interpret the facies are available.

Volcanic Sediment and Volcanic Cycles

Historically, sedimentologists have studied rocks with an objective other than determination of the immediate, geomorphic environment of their formation. Many workers have placed emphasis on determining the relation of sedimentary rocks to tectonic cycles or tectonic regimes. In applying this alternative objective of studies of sedimentary rocks to areas of volcanic sediment, the appropriate cycle to observe is that of activity and extinction of volcanic source areas. Active volcanic centers are constructive, building themselves rather rapidly, and shedding sediment that has properties that depend on the nature of the volcanic activity, climate, and other such conditions. After extinction, the volcano is eroded away; it still produces sediment, but the nature of that sediment results more from the transporting processes and the climate, which controls rates of weathering and erosion, than it does from the volcanic rocks.

This report recognizes the basic depositional framework of volcanic sediments first in terms of the depositional environments expected to occur near volcanos, and then in terms of the cycle of activity and extinction of volcanic centers. In the next chapter, the Tascotal Formation and associated strata of the Trans-Pecos volcanic field of Texas

will be examined in light of both the environmental and volcanic cycle models.

DEPOSITIONAL SYSTEMS IN VOLCANIC REGIONS

Earlier work in volcanic fields has distinguished between a vent region in which volcanic processes predominate and a region in which sedimentary processes rework volcanic material into sedimentary rocks (Dickinson, 1968; Smedes and Prostka, 1972; and Walton, 1977a). Although the sedimentary region has been inadequately studied, it can be subdivided into several areas, each characterized by the activity of one depositional system. The analysis presented here is in part directed at that, first describing the systems in an idealized way, then in a later section interpreting the Tascotal Formation in terms of those systems. Before embarking on this discussion, however, it is necessary to state some definitions to clarify particular usage of terms in this paper.

Volcanic and Sedimentary Rocks

The distinction between volcanic debris and sediment is one of origin; inherently it is interpretative and genetic (Rodgers, 1950). Volcanic debris is formed by volcanic processes--eruption of magma at the earth's surface and associated activities, such as explosions resulting from pressure release or interaction with ground water, and autobrecciation caused by cooling stresses and flow. Volcanic processes include direct, though perhaps delayed, fall or settlement of

particles either from explosion-produced clouds or from other situations in which volcanic processes cause the particles to rise above the earth's surface. Once such volcanic processes have ceased to operate on material or as their intensity declines, sedimentary processes can begin. These may include reworking of loose material or erosion of fragments liberated from solid rock, and transportation and deposition, generally by air or water, but possibly by glaciers. All of these sedimentary processes operate at temperatures characteristic of the earth's surface. Hence, in this report, volcanic rocks are formed by volcanic processes; sediments and sedimentary rocks are formed by sedimentary processes. Volcanic sediments and volcanic sedimentary rocks are formed by sedimentary processes from particles derived directly or indirectly from volcanic sources. Gradations and intermediate types exist, and the distinction among volcanic, volcanic sedimentary, and sedimentary rocks, however easy in principle, is commonly difficult in practice. In any case, it is important for many purposes.

This usage is at variance with that of most geologists, who follow R. V. Fisher (1961) and consider volcanic rocks those that contain mostly material of volcanic origin, regardless of the actual formation process of the accumulation or rock they make up. Fisher considers size and the process of forming the particles in constructing his classification. In this report, the depositional or formational process of the accumulation of particles not the source of the particles themselves, is considered the first-order distinction. The rocks considered volcanic sediments in this report include the epiclastic volcanic rocks

and certain of Fisher's (1961) pyroclastic volcanic rocks--those that have been reworked. Autobreccias, flow breccias, vent breccias, and so forth, as well as air-fall and ash-flow tuffs, that is, primary pyroclastic rocks, are considered the result of volcanic processes.

The experience of the author during the course of the research that led to this report and research elsewhere in Trans-Pecos Texas must be at variance with the experience of Fisher (1961) who suggests that pyroclastic volcaniclastic rocks, including reworked pyroclastic rocks, and epiclastic volcaniclastic rocks should be kept as separate categories as much as possible. Glass shards are normally of pyroclastic origin; volcanic rock fragments are mostly of epiclastic origin, but may be either "autoclastic" or "pyroclastic" in Fisher's (1961) terminology. Hence, most volcaniclastic rocks composed of volcanic rock fragments would be assigned to a category different from that of volcaniclastic rocks composed of shards. But Walton (1977) has shown that the composition of volcanic sedimentary rocks ("volcaniclastic" in the terminology of Fisher, 1961) in the Vieja Group of Trans-Pecos Texas is a function of grain size and the composition of their source and depositional environment: generally, coarse rocks are rich in volcanic rock fragments, and therefore "epiclastic" in Fisher's terms, whereas fine rocks are composed of shards and therefore are "pyroclastic." The rocks are all of sedimentary origin (fluvial or alluvial fan). Coarse and fine rocks are interbedded on all scales from centimeters to hundreds of meters. Remarkably similar rocks are described in the chapter of this report on the

Tascotal Formation. A distinction between reworked pyroclastic volcaniclastic rocks and epiclastic volcanic rocks in this circumstance is pointless.

This report adopts the alternative system primarily because both the methods of study of volcanic rocks on one hand and of sedimentary rocks including volcanic sedimentary rocks on the other and the kinds of information that can be extracted from each kind of rock differ so greatly. Volcanic rocks can be interpreted in terms of formation process, analyzed chemically to learn of magma origin and for purposes of comparison with other volcanic rocks, and dated by radiometric means. Sedimentary rocks can be interpreted in terms of a different set of formational processes, mapped for facies interpretation, and dated by fossils. Isotopic ages of the formation of sediments can be determined only under special circumstances requiring extensive knowledge of their history. Chemical analyses of volcanic sedimentary rocks tell little or nothing of magma chemistry because of the effects of mixing, weathering, differential sedimentation, and diagenesis on the composition of the rock. Volcanic rocks and sedimentary rocks should be recognized as distinct rock types not only because different researchers work on each rock type, but also because work on them proceeds from different assumptions to different conclusions. Fisher's (1961) classification glosses over this fundamental distinction.

Physiography of Volcanic Regions

Physiography and the geomorphic processes of modern volcanic regions are the key to understanding ancient volcanic sediments. Un-

fortunately, the attention of most geologists studying volcanic fields has focused on the volcanos themselves and volcanic processes. Detailed observations of surrounding areas where sedimentary processes are influenced by the presence of the volcano have been made by only a few workers. The following statement on physiography is based largely on observations of the distribution of rocks and facies in the Trans-Pecos volcanic field of Texas with some contribution from other workers' descriptions of other volcanic fields.

Volcanic fields consist of individual centers more or less separated by areas of less intense volcanic activity. The centers consist of nests of adjacent or overlapping calderas, up to 10-inch areas sevearal times the size of individual calderas. In the Trans-Pecos field, these volcanic centers are a few kilometers to several tens of kilometers in diameter. Major volcanic centers include the Davis Mountains and the Chinati Mountains, highlands that still dominate the field. The Eagle Mountains, Quitman Mountains, and Chisos Mountains also contain large centers. Concentrations of lava flows or collapse structures mark centers in the Bofecillos Mountains, Oak Hills, and the Paisano Pass region. Many smaller centers are known or suspected, and sediments or flows may hide still others. Each of these centers has a history of activity, ranging up to perhaps a few million years for larger centers, followed by a quiescent period of erosion that continues to the present. Activity of the several centers was not simultaneous; flows and sediments from each interfinger in a way that reveals the order of their activity.

In volcanic-center areas, volcanic rocks and intrusions predominate, including the caldera-filling sequences, ring plutons, precaldera volcanic

rocks, and outflow-facies volcanic rocks from adjacent centers. These range from dense, solidified lavas and intrusions to loose pyroclastic deposits. Loose pyroclastic deposits were important sources of sediment for adjacent sedimentary aprons. Such deposits of nonlithified pyroclastic material are rarely common in preserved volcanic centers, but the fact that some sedimentary aprons are largely constructed from products of their erosion indicates that they are formed abundantly and were rapidly removed by erosion. Sedimentary rocks interbedded in volcanic-center regions are either very coarse grained deposits of sediment gravity flows and high-gradient streams or fine lake deposits formed in collapse depressions or other low areas. The abundance of volcanic rocks in large center regions indicates that they were major sites of volcanic activity. Calderas in volcanic-center regions indicate that the regions were the source of the major ignimbrite units also.

Between volcanos in areas that were and still are the lower parts of the field, deposits total up to about 1 kilometer thick. The largest accumulations are the Buck Hill Volcanic Series of the east side of the field (Goldich and Elms, 1949) and the Vieja Group of the Sierra Vieja on the west side (DeFord, 1958; Walton, 1977). These deposits consist of large amounts of sediment, mainly volcanic sediment, and small amounts of volcanic rocks.

It is possible to subdivide the sedimentary areas of the field into an apron region and a basin or valley region. Together with the volcanic-center region, these regions form a group of related environments also dependent on the occurrence of the volcanic activity (Walton, 1977).

If material accumulates in any of these regions more rapidly than erosion removes it, a corresponding rock facies will develop. Ideally the rock of each facies will be distinct from the others, recognizable by its properties and interpretable in terms of processes that acted upon it.

In addition to those formed in the three volcano-related regions, certain rocks of the Trans-Pecos volcanic field appear to be the result of eolian deposition. These rocks represent a distinct depositional system and form a separate facies not directly related to the presence of volcanic activity beyond the fact that their constituents are of volcanic origin.

Stages of Volcanic Activity

Volcanic centers that produce silica-rich or intermediate rocks have an active period of up to perhaps a few million years, during which they may undergo several events of caldera formation. Generally, adjacent volcanic sediment deposits could be expected to reflect the several events of caldera formation and the overall history of activity and quiescence of the volcanic center.

The caldera-formation sequence is shorter in duration than the overall history of the volcanic center. Smith and Bailey (1968) describe the normal sequence of events that occurs at resurgent calderas over a period of 1 to 2 million years: regional tumescence and volcanism, ash-flow extrusion, caldera collapse, pyroclastic and lava eruptions, structural resurgence of the caldera floor, ring-fracture eruptions, and terminal fumarolic activity. During this sequence, only a

few years or tens of years are required for ignimbrite emplacement and caldera collapse.

The caldera cycle consists of four main stages: (1) The precaldera volcanic stage during which a series of volcanic and volcano-tectonic events, such as regional tumescence, faulting, and extrusion of lava and pyroclastic material from the fractures, occurs with gradually increasing tempo. This period may last for about 100,000 years (Smith and Bailey, 1968). (2) The stage of major ash-flow tuff emplacement and caldera collapse might last only a few years (3) The stage of ring fracture and caldera-filling volcanism that, like the initial phase of activity, might last about 100,000, years. This stage may or may not include resurgence. (4) Finally, volcanic activity slows, and the area of the caldera gradually slips into a stage of senescence. This process might take hundreds of thousands of years. This sequence is more general than that of Smith and Bailey, but should be applicable to all calderas that produce ash-flow and includes the phases that are recognizable in sediment outside the caldera.

Outside the caldera are two phases of sediment deposition--the active phase and the inactive phase. The active phase includes three stages of the generalized caldera cycle. During the crescendo that precedes caldera formation, tumescence of the volcanic center causes increasing gradients even as more volcanic debris becomes available for transport. This period is ended by caldera collapse, and the sedimentary record is punctuated by a major ignimbrite unit that separates the pre-ash-flow tuff part of the active-phase sediment record from the

post-ash-flow tuff part. Subsequently, caldera-filling activity contributes great amounts of pyroclastic debris, but flows tend to concentrate inside the caldera rather than outside it. Consequently, abundant sand-sized material derived from that pyroclastic debris dominates the sedimentary system for the rest of the active phase. With the decrease of volcanic activity and eventual extinction of the center, the supply of fine sediment is exhausted, and erosion cuts into the flow rocks of the volcano core. With this, the sediment size grows coarser, and streams must adjust their gradients to transport it. The postcaldera part of the active phase eventually grades into the inactive phase, but the stratigraphic contact between the two phases may be sharp or disconformable. Table 1 summarizes these relations between volcanic and sedimentary events.

Sedimentary Aprons

Fans or aprons of sediment commonly form at the foot of escarpments and at other places where gradient or stream capacity decreases. Where volcanic highlands are built on a relatively flat, preexisting surface by solidification of high-viscosity lava flows, a gradient decrease will exist at the outer margin of the accumulation. Stream flow, mudflow, sheetwash, and other processes that reach equilibrium at gradients lower than those of the lava flows will erode the volcanic accumulation. Material transported by these processes will be deposited where the carrying medium loses energy--at the gradient change. Erosion of a volcanic center in certain places will first form gulleys, then canyons

Table 1: Caldera development and sedimentation (modified from Smith and Bailey)

	Time Span (Valles Caldera) Years	Intracaldera Sediments	Generalized Caldera Cycle	Apron Sedimentary Phases	Apron Sediments (Trans-Pecos Texas)
VII Terminal solfatara and hot spring activity	$>10^5$	Erosion	Senescence	Inactive phase	Coarse gravels rich in volcanic rock fragments
VI Major ring-fracture volcanism	1×10^5	Late-stage caldera filling			
V Resurgent doming	$<10^5$	Caldera breaching	Postcaldera extrusions and intrusions, possibly including resurgence	Post-ash-flow tuff	Abundant
IV Preresurgence, volcanism, and sedimentation		Caldera filling: slides, avalanches, sedimentation on fans and in lakes		Active phase	Fine Sediment
III Caldera collapse	<10	Slides and avalanches	Caldera collapse and ash-flow emplacement		Ash-flow tuff
II Caldera-forming volcanism	<10	None			
I Regional tumescence and generation of ring fractures	$<4 \times 10^5$	Erosion	Precaldera tumescence, faulting and extrusions	Pre-ash-flow tuff	Abundant, fine at base, coarsening upward

that become major routes of flow. Where streams confined by the canyon wall debouch onto the heads of growing aprons, flow spreads over the fan surface, thereby reducing the capacity of the stream to carry sediment. The sedimentary fan or apron grows because of either reduced gradient or change from confined to unconfined flow. In most respects volcanic-sediment aprons are almost identical to bajadas that are formed by the coalescence of alluvial fans.

Process of Development of Volcanic Aprons

Miall (1977) suggests that the distinction between braided-stream facies and alluvial-fan facies may be arbitrary, implying that the processes may be the same, even though it is possible to draw a geomorphic distinction between streams and fans. Certainly, much of the sediment on alluvial fans is deposited by unconfined flows that divide around or flow over low bars. A gradiation probably exists between such flows and those described by Bull (1972) as sheet floods. But Miall's statement is a simplification because alluvial fans are marked by a somewhat greater diversity of processes than are braided streams, including debris flows and stream floods (Bluch, 1967; Miall, 1970a, 1970b; Bull, 1972; and Steel, 1974). Studies of sedimentation on alluvial fans have emphasized fans where fluvial processes predominate.

The review of braided-stream deposits by Miall (1977) probably serves as the best guide to the type of sediment to be expected as a result of the sheet flood--braided-stream continuum. Miall lists four basic types of vertical sequence: (1) the Scott type, dominantly gravel deposited as longitudinal bars with interbedded debris flood deposits

and minor sand lenses; (2) the Donjek type, consisting of fining-upward sequences of sand, gravel, and mud deposited by individual channels of the system; (3) the Platte type, mostly sand deposited by linguoid bars; and (4) the Bijou Creek type in which each flood even in the ephemeral stream leaves a fining-upward sand deposit. Any of these types might be expected on alluvial fans, depending upon local conditions of grain size of available sediment, gradient, and rainfall character. Furthermore, other configurations may be possible; Miall's (1977) models are limited by published studies of recent streams.

Volcanic-apron systems, however, have certain characteristics that may somewhat limit the possibilities. They have rather small drainage basins and, unless glaciated, should have ephemeral streams with flashy discharge. Grain size of sediment will be a function of the type of volcanism and the climate. The explosive volcanic activity of the Trans-Pecos field produced sand-sized glass shards. Deposits formed on aprons near such volcanos would be similar to Miall's (1977) sand-rich types. Other volcanos with a more placid mode of eruption would make more flow rock, which could break down to coarse epiclastic debris and less sand-sized material, permitting development of some of Miall's (1977) coarser facies types.

Many authors agree that stream floods are important processes on alluvial fans (Bull, 1972; Schumm, 1977). These differ from the braided-stream, sheet-flood activity in that the flows are confined to a relatively narrow channel--in a canyon or fan-head trench (Denny, 1967; Hooke, 1967). Probably, confined streams would be ephemeral or subject

to large fluctuations of discharge. If a volcano produced abundant coarse debris, the deposits of surrounding stream flood channels would be almost entirely conglomerate flood-surge or debris-flow deposits and longitudinal bar deposits, and only thin sand beds (McGowen and Groat, 1971; Bluck, 1967; Steel, 1974; and Boothroyd and Ashley, 1975). Deposits of ephemeral streams that carry sand are of Miall's (1977) Bijou type: mostly horizontally laminated sand beds that overlie scour surface and are overlain by small-scale ripple cross-stratified sand that may grade into a mud drape. Each cycle represents the result of a single flood; most of the deposition takes place as the flood begins to wane, but while velocity/grain size/depth relations are still in the upper flow regime. The ripples are lower flow regime deposits, formed near the end of each event. Desiccation, bioturbation, soft-sediment deformation, eolian activity, and erosion may affect these deposits, especially their upper parts, and may modify or obliterate their peculiar character (McKee and others, 1967; Picard and High, 1973).

Unless especially favorable circumstances prevail, it may be difficult to distinguish between the deposits of confined flows and those of unconfined flows. It is possible that the proportion of debris flood deposits would be greater in confined than in unconfined flow or that individual confined flood events might leave thicker deposits. But there is little reason to suspect that the sedimentary structures of the deposits would differ greatly. In fact, the confined and unconfined flow are probably parts of a continuum. In the active-apron member of the Tascotal Formation, discussed in a subsequent chapter of this

report, a distinction is drawn between thin fining-upward sequences and thick fining-upward sequences--one being attributed to unconfined flow; the other, to confined flow. This interpretation is inferred from other depositional systems that operate in a similar fashion and from the sequence of the deposits of several flood events, rather than individual events.

Deposition by debris flow is a common feature of volcanic regions in either the volcanic apron or the vent area. Basic principles of debris-flow mechanics are outlined in Middleton and Hampton (1973), Johnson (1970, chapters 12-14), and Rodine and Johnson (1977). Deposits of debris flows are also described in Walker (1976), Crandell (1971), and Bull (1972). Debris flows are sediment gravity flows in which particles are at least partly supported by a pastey matrix of mud and water that has finite strength and density greater than water. Rodine and Johnson (1977) point out that debris flows can occur on slopes of a few degrees and transport immense blocks of rock.

Debris flows can arise by any of several processes in volcanic regions. Lydon (1968) describes lahars of the Tuscan Formation in northern California, interpreting them as essentially volcanic rocks, that incorporated debris from autobrecciated lava and were mobilized by mixing of magmatic water. Anderson (1971) describes mudflow breccias interbedded with normal stream sediment in the Bear Valley Formation of Utah. These probably result from mixing of debris and water just as happens in arid regions (Bull, 1972). Crandell (1971) describes mudflows, which may be related to glacial melting episodes on the slopes

of Mt. Rainier. Similarly, Indonesian volcanos have been known to produce lahars as a result of catastrophic draining of caldera lakes.

Debris-flow deposits range from mudrocks to conglomerates and sandstones with fine mud matrix. Conglomerate clasts need not be touching, and the deposit may have a partially or completely matrix-supported texture. Internally, debris-flow deposits have no stratification or very indistinct stratification. Clast sizes may be graded normally or inversely through the deposit or may not be graded at all. Having been rafted along, supported by the strength of the mud matrix, the largest clasts may be found in the upper part of the flow or even protruding from its top. Because of their high viscosity, debris flows deposit sediment on slopes steeper than those characteristic of pure water flows. For this reason, interbedding of stream and coarse debris-flow deposits should be the exception rather than the rule.

In areas where weathering or unstable composition of volcanic detritus promote formation of mud, debris flows may be important constituents of volcanic-apron sequences. They are common products of volcanos that produce lavas of intermediate composition. The Absaroka field contains great thicknesses of them (Hay, 1956; Parsons, 1969); those of the Tuscan Formation in California are composed of andesite and basaltic andesite clasts (Lydon, 1968). South Park, Colorado, and the Southern High Plateau area of Utah contain immense deposits of debris flows (DeVoto, 1971; Rowley, oral communication). These flows may be volcanic like those of the Tuscan Formation, or they may be sedimentary. The Colmena Formation of the Vieja Group of Trans-Pecos Texas is made mostly

of debris-flow deposits that contain clasts of intermediate rock types (Walton, 1977). Otherwise, the Trans-Pecos volcanic field may be anomalous in its relative paucity of this type of deposit.

Alluvial fans, and presumably volcanic-sediment aprons, are built segment by segment (Denny, 1967). Only part of the fan is active at any one time; the activity either migrates slowly across the fan surface or jumps from place to place as each locus of activity becomes unstable with respect to another. By this building of successive segments, the entire fan or apron maintains a regular, smooth profile and shape within the limits imposed by boundary conditions. The segment-by-segment construction patterns are reflected by changes of grain size and sedimentary structures that mark the history of each segment's activity, similar to that described for deep-sea fans (Walker and Mutti, 1973; Ricci Lucchi, 1975; Walton, in press). Each segment on a volcanic apron should be progradational, consisting of a coarsening- or thickening-upward sequence of individual flood or flow deposits; the deposit of one segment's activity should be a few meters to several tens of meters thick. Each segment can be fed by a channel that crosses the proximal part of the fan.

Factors that affect the nature of fan or apron deposit include the grain-size distribution of the source sediment and the climate. The slope of the fan will depend partly on the grain size of the material and the nature of the depositing medium. Where stream processes dominate, such as on fans with little mud available for transport or on fans developed in humid climates, gradients will be lower where sand

is the dominant sediment and higher if gravel is most abundant. Sediments will be well sorted sands and gravels with abundant primary sedimentary structures. Mudflows require more mud among the available sediments and greater slopes of the fan--hence they cannot occur in distal regions of stream-deposited aprons. Mudflows are believed to be favored in arctic regions and in areas with little rainfall, especially if that rainfall comes in occasional downpours (Leggett and others, 1966).

Because of the interplay between grain size and apron slope, the nature of volcanic aprons is controlled by the nature of volcanism and modified by climatic factors. In Trans-Pecos Texas, where explosive volcanism produced abundant fine debris, characteristically in the sand-size range, low apron slopes were constructed by streams. Mudflow activity was not important because of the low slopes and lack of available mud except on some intermediate volcanos that produced little sand-sized debris. However, where rainfall is greater, where mafic to intermediate lavas that might break down into clay are common, or where, as in the Cascades, glaciation promotes conditions favorable for mudflow development, mass flows rather than stream flows would dominate apron sedimentation.

Uranium Potential of Apron Deposits

Volcanic aprons can be potential sources of large amounts of uranium, because they may include very great numbers of uranium-rich glass shards. Apron sediments commonly contain little mud--unless debris-flow deposits dominate--and they are initially highly permeable, permitting free movement of fluids through them. Water enters the apron along

stream courses or channels and elsewhere along the surface and flows downward through the body of sediment, reacting with the sediment grains as it goes. In glass-rich sediment, precipitation of diagenetically formed minerals in pores reduces permeability, but to an unknown extent. Coarse sediment should retain much of its initial permeability. Generally, little organic matter is present, and other reducing constituents are rare so that the waters may be suitable for transport of uranium; but few suitable oxidation-reduction traps should be present. This factor prevents accumulation of deposits similar to the familiar roll-front deposits of many sandstones. Furthermore, chemical peculiarities that may occur in volcanic aprons may prevent transportation of uranium, as explained in another chapter of this report. The possibilities of uranium deposits in apron sediments are thus limited by the lack of reducing environments and possibly by the lack of effective release of uranium, even from rather uranium-rich glass.

Valley Systems

Regional drainage in volcanic regions is accomplished through valleys that generally run tangentially to the aprons and collect water runoff from several of them. The major depositional processes in valleys are fluvial. Sediments accumulate by normal channel and overbank processes of rivers. The gradients of valleys should be lower than those of adjacent aprons, and the valleys should be marked by braided or meandering rivers. Furthermore, because of their larger watersheds and potential for ground-water contributions, the discharge of the

valley-following streams should be less flashy than that of apron streams. Deposits should be compositionally more heterogeneous because they are derived from a number of sources. Descriptions of fluvial sedimentology and geomorphology are numerous. Interested readers should refer to Allen (1965), Reinich and Singh (1975), Fisher and Brown (1972), Brown (1973), Leopold and others (1964), and Schumm (1972, 1977), or to other works for discussions of river systems and sediments. Recent work in understanding braided-stream systems includes Eynon and Walker (1974), Miall (1976,1977), and Rush (1971). The discussion of the four braided-stream models of Miall (1977) is applicable to valley as well as apron systems.

Lacustrine Systems

Lakes are likely to form in either of two situations in volcanic terrains. Smith and Bailey (1968) suggest that lakes are the rule rather than the exception within calderas. Certainly such lakes occur at Crater Lake, Oregon, and in the Toba Cauldron, Sumatra. Lake sediment was important in filling the Valles Caldera, New Mexico. Lakes can also occur where volcanic, sedimentary, or tectonic activity closes off a low part of a volcanic field. Such low-area lacustrine systems would be an alternative to a valley system in the volcanic-sediment facies tract.

Caldera lakes are deep but have small watersheds. Were it not for the local volcanic activity, they might be expected to have a long history before the slow input of epiclastic debris filled them. In the Valles Caldera, 2,000 ft (about 600 m) of caldera fill, including some proportion of lake sediments, accumulated in about 100,000 years. Nelson

(1967) described Crater Lake, providing one of the best recent studies of caldera-filling lakes. In contrast with the lakes Smith and Bailey (1968) expect in resurgent calderas, Crater Lake is receiving sediment only at a slow rate, apparently because its watershed is very small and because volcanic activity since the Mount Mazama eruption has not been very intense. Nelson (1967) reports about 60 cm of sediment in the deepest part of the lake. At the present rate of accumulation, about 10 m of sediment would accumulate in 100,000 years, a much lower rate than that implied by Smith and Bailey.

In terms of facies and process, the sediments of Crater Lake are probably similar to those of other caldera lakes. The outer margin of the lake is rimmed and floored by landslide debris from the crater walls or deltas and sublacustrine accumulations at the mouth of canyons. The lake floor is underlain by organic sediments--ooze debris from algae where the lake bottom is in the photic zone and diatom tests in deeper water. Occasional thin intercalations of sand and silt have been introduced by turbidity currents. Eolian contribution of sediments to lake floor regions is also potentially large. Were Crater Lake to again become the site of active volcanism, much pyroclastic debris could accumulate there. Basically, then, caldera lakes can be expected to have two facies, a coarse marginal facies and a fine central facies. Only where volcanism is active, however, can significant amounts of lacustrine sediment accumulate in caldera lakes.

Constructive volcanic activity, tectonics, or accumulation of sediments may create basin-center lakes that would bear the same relation

to volcanic aprons that the playas of the Basin and Range Province bear to adjacent alluvial fans. Such lakes would be shallow and would have shorelines that would migrate rapidly in response to changes of their budget of inflow from rivers, direct rainfall, and ground-water discharge, outflow over the barrier, and evaporation loss. Unlike caldera lakes, basin-center lakes have large watersheds and would receive large quantities of sediment. Shallow basin-center lakes can thus be rapidly filled with sediment and may spill over whatever sill or topographic barrier contains them. Ground-water discharge into lakes would provide large quantities of dissolved solids and promote formation of orthochemical sediment in the lake. Basin-center lake sediments should include interbeds of lake-center turbidites, silts, calcareous rocks, diatomites, eolian material, and air-fall tuffs. Shoreline and fluvial rocks that accumulated during low stands or progradational episodes. Away from the basin center, lake-center facies would become less common and fluvial or apron facies more common.

In arid regions or regions of predominant ground-water discharge, basin-center lake sediments could include orthochemical materials. Carbonate sediments and evaporites are important in lakes unrelated to volcanism, but in lakes around volcanos the abundance of silica in readily soluble minerals and glass would make silica-rich organic and chemical sediments more important. Diatomites or high-silica clay and zeolite beds should be abundant, and most carbonate beds should contain chert or opal. Diagenesis of playa lake beds is described by Surdam (1977).

Uranium in Valley Systems or Lakes

Many sandstone uranium deposits are in fluvial rocks, and several aspects of valley systems in volcanic sediment terrains make them the most favorable targets for exploration for uranium deposits. Stream channelways are better defined in them than in apron regions, and resulting sediments should form excellent channelways for the passage of ground water. Areas of poor drainage such as lakes and swamps might exist on floodplains, and organic matter might accumulate in them. If the rate of accumulation is low, soil-forming processes may be important in valley regions, leading to effective release of uranium from volcanic glass, as will be explained in another section of this report. Consequently, valley systems of volcanic regions combine all three elements necessary to produce sandstone uranium deposits: sources of uranium, permeability channels, and reducing conditions. Conversely, if there are areas of ground-water discharge, concentration of uranium into caliche or other evaporative phases may occur.

Lake sediments that contain abundant volcanic material are also potential hosts for uranium deposits. Deposits in the Date Creek Basin (Otten, 1977) and shows of uranium in the Virgin Valley region (Henry, this report, Chapter VIII) occur in lake deposits. Lakes trap much local surface runoff and may receive ground-water discharge. Organic matter, which may be common in lake waters and sediments, may trap the uranium, or it may accumulate in uraniferous opal.

Eolian Systems

Eolian deposits are common wherever loose sediment is available for wind transport, in deserts, in glacial or periglacial regions, and along coasts. Volcanos that produce abundant fine glass shards, as those in Trans-Pecos Texas did, might also favor formation of abundant eolian deposits unless growth of vegetation was rapid enough to stabilize the accumulation of volcanic debris. Two kinds of deposits form as a result of eolian activity: sand dunes and other deposits that represent accumulations of bed load, and loess--sediments built of airborne suspended load. Generally the two kinds of deposits are found in different regions because the atmosphere separates bed load and suspended load more completely than do rivers. Only dune sediments have been reported from volcanic regions, so this discussion will not include loess even though silt-sized ash particles are abundant and loess derived from volcanic sources may be common.

Eolian systems are commonly thought to be the result of wind activity where environmental conditions leave broad areas unprotected by plants from wind erosion, such as on floodplains, beaches, or glacial outwash fans. Sand dunes are most common in coastal or desert regions. Loess is most often ascribed to conditions related to glaciers, though students of the subject point out that desert loess is also common. Flint (1971) emphasizes that the common condition of coastal, desert, and periglacial regions is the abundance of loose, unvegetated sediment. He then points out that if such loose sediment could form in humid areas, loess and sand dunes might result. Flint points out that lowering of

the water table, as might occur on alluvial fans as a result of entrenchment of streams or migration of channel ways, may kill vegetation and leave marshy areas dry, increasing availability of loose sediment for wind erosion.

Dune sediments consist of fine to medium sand, with some interbeds of bimodal sand and granular sand (Folk, 1968). The deposits are cross-bedded in large-scale sets or parallel laminated. Processes of eolian sand deposition and the resulting stratification types have been studied by Hunter (1977). Though his work was done on small (1 to 10 m) coastal dunes, the observations are probably applicable to larger inland forms; certainly his are the most useful observations to date. Hunter recognizes three basic processes active in dunes: deposition from a traction carpet where saltating and creeping grains are trapped in sheltered positions between grains; fall of grains into flow-separation zones where the air flow does not reach the ground surface; and avalanching on slip faces of dunes. The first and second of these, which Hunter calls "traction deposition" and "grain-fall deposition," respectively, form the ends of a continuum of processes. Avalanching, which may occur by slumping or by grain flow, is really a secondary process, but one which forms a distinctive kind of sedimentary structure.

Traction deposition occurs on either ripple or planar bedforms. Plane-bed deposition forms faint, horizontal laminae a few millimeters thick, but is rare. Rippled beds are the common depositional bed form for traction deposits, and climbing ripple stratification is the common type of internal structure. Hunter describes translatent strata, ripple-form laminae, and ripple foreset cross-laminae as three types of

stratification formed by these processes. Translatent strata are deposited by climbing ripples in which the foreset lamination is not visible. Because eolian ripples have coarser material in their upper parts and finer in their troughs, translatent strata deposited by eolian processes coarsen upwards. Ripple-form laminae and ripple foreset cross-lamination are rare in eolian deposits.

Grainfall lamination forms in areas of flow separation where grains fall from the saltation cloud directly to the depositional surface. Grainfall forms poorly defined laminae a few millimeters thick that closely parallel the surface on which they are deposited. They resemble the rare horizontal laminae formed by traction deposition during high winds, but have high initial dips and are among the most common of eolian sedimentary structures.

Because of the steep angles of dune slip faces, grain flows, slumps, and slumps that convert to grain flows are common. The most common are grain flows in which the grains are temporarily supported by dispersive pressure and transported by gravity. Dispersive pressure sorts the larger grains upward in the moving mass and they tend to outrun finer grains. Hence the deposits coarsen from the lower to the upper boundary of the layers they form, and the toe generally contains more coarse grains than does the head of the deposit. The layers themselves are generally arcuate to complex in cross section and are found on preserved slip faces, commonly interbedded with grain-fall deposits (Hunter, 1977).

McKee (1966) describes large-scale cross-stratification developed in eolian dunes by the grain fall and avalanching processes of Hunter

(1977). Though stratification differs slightly in different dune types, five features appear to be common in cross-stratification in dunes developed by unidirectional winds: medium to large-scale cross strata are characteristic and commonly attain dips of 30° to 34° downwind. Bounding surfaces of these sets are horizontal or dip downwind at low angles. In the downwind parts of large dunes, bounding surfaces of sets of medium to large-scale cross-strata dip downwind at 20° to 28°. The thickest sets of cross-strata occur at the bottom of the dune, and the sets thin progressively up through the dune. Finally, the sets of cross-strata grow thicker downwind within each dune (McKee, 1966).

Several authors have made studies of broader aspects of dune fields and added to knowledge of eolian stratification (Ellwood and others, 1975; McKee, 1966; McKee and others, 1971; Walker and Harms, 1972; Bigarella, 1972; Wilson, 1972). Wilson describes hierarchies of eolian bedforms, from ripples through conventional sand dunes, to large forms comprising several sand dunes. McKee (1966) describes several types of conventional sand dunes--features with heights of a few meters and wave lengths of tens to hundreds of meters--transverse dunes, barchans, parabolic dunes, and dome dunes. McKee points out that in White Sands, New Mexico, the form of dunes changes from dome dunes to transverse dunes to barchans or parabolic dunes in a downwind direction.

The presence of eolian deposits in volcanic sediments in Trans-Pecos Texas results primarily from the abundance of loose debris available for wind transport and only indirectly from volcanic activity. In this respect, these deposits differ from the vent-apron-valley facies sequences

that are the deposits of the three geomorphic environments characterizing the area. The occurrence of eolian facies is consequently less predictable--it may form at any time that the loose debris is present and may have any spatial relation to the remainder of the volcanic sediment deposits: eolian deposits will lie in a direction downwind of their sediment source. Their presence is favored by the lack of effective plant cover: abundant paleosoil horizons, which indicate extensive plant cover, may indicate that eolian facies did not develop.

Uranium Potential of Eolian Facies Rocks

The eolian facies of the Tascotal has not undergone extensive diagenesis; parts of the eolian facies in the Vieja Group have (Walton, 1975, 1977a). The potential for uranium deposits in eolian sediments is similar to that of fine-grained apron sediments. The sand-rich nature of the sediment promotes considerable primary permeability that may be reduced if the glass undergoes diagenesis. Eolian sediment is almost devoid of reducing material, so uranium, if released and complexed, can be transported, but no suitable traps exist to form ore-grade deposits. Like fine apron sediments, eolian deposits are better sources of uranium than they are sites of mineralization, but may not ever have effectively released uranium to solution.

REFERENCES

Allen, J. R. L., 1965, A review of the origin and characteristics of recent alluvial sediments: Sedimentology, v. 5, p. 89-191.

Anderson, J. J., 1971, Geology of the southwestern high plateaus of Utah: Bear Valley Formation, and Oligocene-Miocene volcanic arenite: Geological Society of America Bulletin, v. 82, p. 1179-1206.

Bigarella, J. J., 1972, Eolian Environments: their characteristics, recognition, and importance: Society of Economic Paleontologists and Mineralogists, Special Publication 16, p. 12-62.

Bluck, 1967, Deposition of some upper Old Red Sandstone conglomerates in the Clyde area: Scottish Journal of Geology, v. 3, p. 139-167.

Boothroyd, J. C., and Ashley, G., 1975, Process, bar morphology, and sedimentary structures on braided outwash fans, northeastern Gulf of Alaska: Society of Economic Paleontologists and Mineralogists, Special Pulbication 23, p. 193-222.

Crandell, D. R., 1971, Postglacial lahars from Mount Rainier Volcano, Washington. U.S. Geological Survey, Professional Paper 677.

DeFord, R. K., 1958, Tertiary formations of Rim Rock Country, Presidio County, Texas: Texas Journal of Science, v. 10, p. 1-37.

De Voto, R. H., 1971, Geologic History of South Park and geology of the Antero Reservoir quadrangle, Colorado: Colorado School of Mines Quarterly, v. 66, no. 3, 90 p.

Dickinson, W. R., 1968, Sedimentation of volcanic clastic strata of the Pliocene Korominunua Formation in northwest Viti Levu, Fiji, American Journal of Science, v. 266, p. 440-453.

Ellwood, J. M., Evans, P. D., and Wilson, I. G., 1975, Small scale aeolian bedforms: Journal of Sedimentary Petrology, v. 45, p. 554-561.

Eynon, G. and Walker, R. G., 1974, Facies relationships in Pleistocene outwash gravels, southern Ontario: a model for bar growth in braided rivers; Sedimentology, v. 21, p. 43-70.

Fisher, R. V., 1961, Proposed classification of volcaniclastic sediments and rocks: Geological Society of America Bulletin, v. 72, p. 1409-1414.

Fisher, W. L., and Brown, L. F., 1972, Clastic depositional systems--a genetic approach to facies analysis: The University of Texas at Austin, Bureau of Economic Geology.

Fisher, W. L., and McGowen, J. H., 1967, Depositional systems in the Wilcox Group of Texas and their relationship to occurrence of oil and gas: Gulf Coast Association of Geological Societies Transactions, v. 17, p. 105-125.

Flint, R. F., 1971, Glacial and Quaternary geology: New York, Wiley.

Folk, R. L., 1968, Petrology of sedimentary rocks: Austin, Texas, Hemphills.

Galloway, W. E., 1977, Catahoula Formation of the Texas Coastal Plain: Depositional systems, composition, structural development, groundwater flow history, and uranium distribution: The University of Texas at Austin, Bureau of Economic Geology Report of Investigations 87.

Goldich, S. S., and Elms, M. A., 1949, Stratigraphy and petrology of the Buck Hill Quadrangle, Texas: Geological Society of America Bulletin, v. 60, p. 1133-1182.

Hay, R. L., 1956, Pitchfork Formation-detrital facies of early basic breccia, Absoroka Range, Wyoming: American Association of Petroleum Geologists Bulletin, v. 40, p. 1863-1898.

Hooke, R. LeB., 1967, Processes on arid-region alluvial fans: Journal of Geology, v. 75, p. 438-460.

Hunter, R. E., 1977, Basic types of stratification in small eolian dunes: Sedimentology, v. 24, p. 361-387.

Leggett, R. F., Brown, R. J. E., and Jonston, G. H., 1966, Alluvial-fan formation near Aklavik, Northwest Territories, Canada: Geological Society of America Bulletin, v. 77, p. 15-30.

Lydon, P. A., 1968, Geology and lahars of the Tuscan Formation, Northern California: Geological Society of America, Memoir 116, p. 441-475.

McGowen, J. H., and Groat, C. G., 1971, Van Horn Sandstone, West Texas: An alluvial fan model for mineral exploration: The University of Texas at Austin, Bureau of Economic Geology Report of Investigations No. 72, 57 p.

McKee, E. D., 1966, Structures of dunes at White Sands National Monument, New Mexico: Sedimentology, v. 7, p. 1-69.

McKee, E. D., Crosby, E. S., and Berryhill, H. L., 1967, Flood deposits, Bijou Creek, Colorado: Journal of Sedimentary Petrology, v. 37, p. 829-851.

McKee, E. D., Doeglass, J. R., and Rittenhouse, S., 1971, Deformation of leeside laminae in eolian dunes: Geological Society of America Bulletin, v. 82, p. 359-378.

Miall, A. D., 1970a, Continental marine transition in the Devonian of Prince of Wales Island, Northwest Territories: Canadian Journal of Earth Sciences, v. 7, no. 1, p. 125-144.

Miall, A. D., 1970b, Devonian alluvial fans, Prince of Wales Island, Arctic Canada: Journal of Sedimentary Petrology, v. 40, no. 2, p. 556-571.

Miall, A. D., 1976, Paleocurrent and paleohydrologic analysis of some vertical profiles through a Cretaceous braided stream deposit, Banks Island, Arctic Canada: Sedimentology, v. 23, p. 459-483.

Miall, A. D., 1977, A review of the braided-river depositional environment: Earth Science Review, v. 13, p. 1-62.

Middleton, G. V., and Hampton, M. A., 1973, Sediment gravity flows; mechanics of flow and deposition: in Turbidites and Deep-Water Sedimentation, p. 1-38: Society of Economic Paleontologists and Mineralogists, Pacific Section, Los Angeles.

Otten, J. K., 1977, Criteria for uranium deposition in the Date Creek Basin and adjacent areas, west-central Arizona (abs.): 1977 NURE Uranium Geology Symposium, Bendix Field Engineering Corps., Grand Junction, Colorado, Sedimentary Host Rock Session, p. 41-49.

Parsons, W. H., 1969, Criteria for the recognition of volcanic breccias-review, Geological Society of America Memoir 115, p. 263-304.

Picard, M. D., and High, L. R., Jr., 1973, Sedimentary structures of ephemeral streams: Developments in Sedimentology, v. 17, New York, Elsevier.

Reineck, H. -E., and Singh, I. B., 1975, Depositional sedimentary environments, New York, Springer-Verlag.

Ricci Lucchi, R., 1975, Depositional cycles in two turbidite formations of northern Apennines (Italy): Journal of Sedimentary Petrology, v. 45, p. 3-43.

Rodgers, J., 1950, The nomenclature and classification of sedimentary rocks: American Journal of Science, v. 248, p. 297-311.

Rodine, J. D., and Johnson, A. M., 1977, The ability of debris, heavily freighted with coarse clastic materials, to flow on gentle slopes: Sedimentology, v. 23, p. 213-234.

Rust, B. R., 1972, Structure and process in a braided river: Sedimentology, v. 18, p. 221-245.

Schumm, S. A., 1972, Fluvial paleochannels, in Recognition of ancient sedimentary environments: Society of Economic Paleontologists and Mineralogists, Speical Publication, no. 16, p. 98-107.

Schumm, S. A., 1977, The Fluvial System: New York, John Wiley.

Smedes, H. W., and Prostka, H. J., 1972, Stratigraphic framework of the Absoroka Volcanic supergroup in the Yellowstone National Park region: United States Geological Survey, Professional Paper 729-C.

Smith, R. L., and Bailey, R. A., 1968, Resurgent caldrons: Society of America Memoir, 116, p. 613-662.

Steel, R. J., 1974, New Red Sandstone floodplain and piedmont sedimentation in the Hebridean Province, Scotland: Journal of Sedimentary Petrology, v. 44, p. 336-357.

Surdam, R. C., 1977, Zeolites in closed hydrologic systems; in Mumpton, F. A., ed., Mineralogy and geology of natural zeolites: Mineral Society America Short Course Notes, no. 4.

Walker, R. G., 1976, Generalized facies models for resedimented conglomerates of turbidite association: Geological Society of America Bulletin, v. 86, p. 737-748.

Walker, R. G., and Mutti, E., 1973, Turbidite facies and facies association: in Middleton, G. V., and Bouma, A. H., Turbidites and deep water sedimentation: Society of Economic Paleotologists and Mineralogists Pacific Section Short Course Notes.

Walker, T. R., and Harms, J. C., 1972, Eolian origin of flagstone beds, Lyons sandstone (Permian) type area, Boulder County, Colorado: Mountain Geologist, v. 9, p. 279-288.

Walton, A. W., 1972, Sedimentary petrology and zeolitic diagenesis of the Vieja Group (Eocene-Oligocene), Presidio County, Texas: The University of Texas at Austin, Ph.D. dissertation.

Walton, A. W., 1975, Zeolitic diagenesis in Oligocene volcanic sediments, Trans-Pecos Texas: Geological Society of America Bulletin, v. 86, p. 615-624.

_____ 1977a, Petrology of volcanic sedimentary rocks, Vieja Group, Southern Rim Rock Country, Trans-Pecos Texas: Journal of Sedimentary Petrology, v. 47, p. 137-157.

_____ 1977b, Oligocene volcanic sedimentary apron in Trans-Pecos volcanic field of Texas (abs) AAPG-SEPM Program and Abstracts, Washington, D. C. meeting, June 12-16, 1977, p. 108.

_____ in press, Volcanic sediment apron in the Tascotal Formation (Oligocene?), Trans-Pecos Texas: Journal of Sedimentary Petrology.

Wilson, I. G., 1972, Aeolian bedforms-their development and origins: Sedimentology, v. 19, p. 173-210.

III. SYSTEMATIC ANALYSIS OF A VOLCANIC SEDIMENT SEQUENCE: THE TASCOTAL FORMATION

by Anthony W. Walton[1]

ABSTRACT

The Tascotal Formation is a volcanic sedimentary part of the Buck Hill Volcanic Series. Five informal volcanic sedimentary members of the Tascotal are (1) the active-apron member, (2) the lower conglomerate member, (3) the southern apron member, (4) the eolian member, and (5) the Perdiz member. The Solitario fan member and the Fresno volcanic member make up the rest of the outcropping Tascotal. These members are lithologically distinct because they result from different depositional systems, that is, they formed in different geomorphic environments of deposition.

The active-apron member is a sequence that generally coarsens upward from distal-fan to mid-fan deposits that accumulated in Platte-type braided systems. These deposits are overlain by channel-fill deposits that accumulated in fanhead trenches. The active-apron member contained abundant volcanic glass shards when it was formed, and it must have accumulated during the time of activity of a large volcano that had an explosive mode of eruption. Paleocurrent data and other considerations indicate that the active volcanism was in the Chinati Mountains.

The Perdiz member, which is continuous with the Perdiz Conglomerate, is the coarse-grained fan of material that accumulated around the Chinati

---

[1]Department of Geology, University of Kansas, Lawrence.

Mountains after volcanic activity ceased there. The contrast between the Perdiz member and the active-apron member illustrates the differences between sedimentation around an active volcano and sedimentation around an inactive volcano.

The Fresno volcanic member, consisting mostly of lava flows, accumulated around the Bofecillos volcano, which had a quiet rather than explosive mode of eruption. No active apron formed around it. Instead, the lava flows overlie or interfinger with sediments of three other members: (1) the Solitario fan member that formed as alluvial fans around the Solitario Uplift; (2) the southern apron member that formed around an unidentifiable active volcano; and (3) the Perdiz member.

The lower conglomerate member formed in a Donjek-type braided stream that flowed between the Chinati-derived aprons to the north and the Solitario-Bofecillos area to the south. The eolian member lies between the active-apron member and the Perdiz member. It accumulated while the apron streams adjusted their gradients from the low values characteristic of active-apron sedimentation to the higher values that mark inactive aprons.

TASCOTAL FORMATION

The Tascotal Formation is an eastward-thickening wedge of sediment up to 250 m thick that crops out along the valley of Alamito Creek in the bluffs of Tascotal Mesa and in the Bofecillos Mountains of Presidio County, Texas (fig. 1). The formation has been truncated on the east by erosion and pinches out against flows of the lower slopes of the Chinati volcano

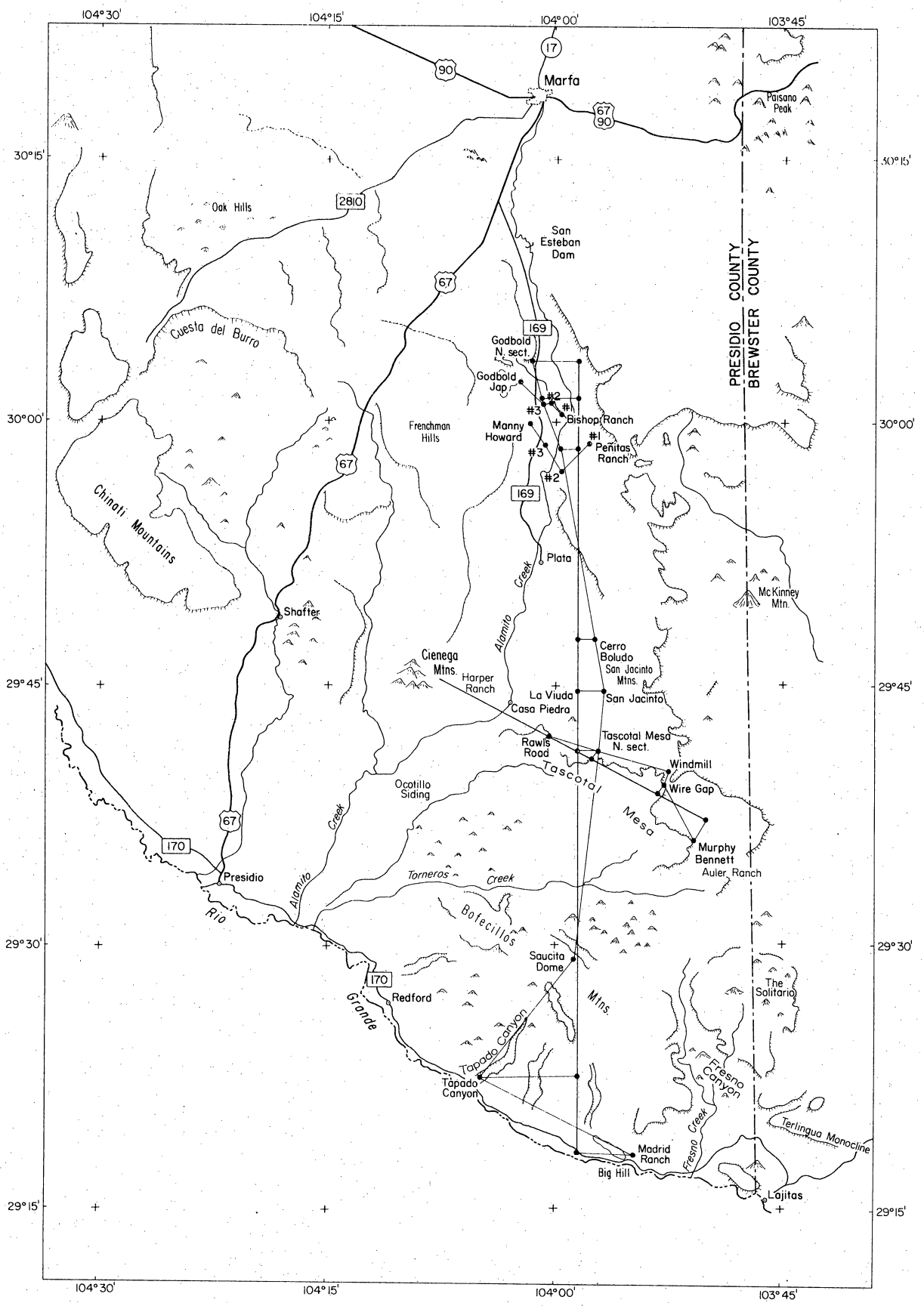

Figure 1. Location map of the eastern part of the Trans-Pecos Volcanic Field. Lines show locations of cross sections in fig. 2.

along a north-south line not far west of its outcrop belt. The Tascotal consists of sandstone with smaller amounts of conglomerate and shale and a trace of limestone. Most of the constituents are of volcanic origin and are material Fisher (1961) would describe as "pyroclastic" or "epiclastic." With the exception of a few air-fall tuff layers, this part of the Tascotal is the result of sedimentary processes, and the rocks are best described as "volcanic sediments." In the Bofecillos Mountains, the Tascotal includes much volcanic rock.

The objective of this chapter is to describe the deposition of the Tascotal Formation in order to understand it in terms of its depositional environments and its relation to activity at the Chinati volcano. See chapter VI for a description of the effects of diagenesis on its uranium content.

Stratigraphy

Boundaries

The name "Tascotal" was suggested by Goldich and Seward (1948) for a sequence of white rock that lay between the Mitchell Mesa Rhyolite and the Rawls Basalt of the Buck Hill Volcanic Series. This interval was studied by Erickson (1953), who described a type section at Wire Gap where he found a lower tuff member and an upper sandstone and conglomerate member. The type section actually consists of four units. The lowest unit, 145 m thick, consists of white to pink, thin-bedded or crossbedded volcanic sediment in which most glass has been dissolved and turned into zeolite. The next interval, 57 m thick, consists of light-colored vol-

canic sediment that displays large-scale crossbeds that are interpreted to be of eolian origin. Above this interval is 30 m of interbedded sandstone and conglomerate containing grains ranging up to cobble size, including both volcanic rock fragments and carbonate rock fragments. The uppermost interval of the type section is 15 m thick and consists of pumice-rich sandstone and conglomerates. This interval is mentioned again below in conjunction with a discussion of the upper boundary of the Tascotal. These and other members of the Tascotal are summarized in table 1; their distribution and the boundaries of the Tascotal are indicated in figures 2 and 3.

The Tascotal Formation overlies Mitchell Mesa Ignimbrite, a welded ash-flow tuff erupted from the Chinati Mountains Volcanic Center and spread over much of the Trans-Pecos volcanic field (Goldich and Seward, 1948; Burt, 1970). The Mitchell Mesa consists of two members. The lower member is a crystal-rich ash-flow tuff with characteristic chatoyant sanidine crystals. This member is widely distributed throughout the Trans-Pecos volcanic field; it is the part originally described by Goldich and Elms (1949) and is the Brite Ignimbrite of DeFord (1958). The upper member is a lithic ash-flow tuff described by Burt (1970) from localities north of the Chinati Mountains. It has also been found in localities at the foot of San Jacinto Mountain and on the Peñitas Ranch in the valley of Alamito Creek. The Mitchell Mesa is absent over some domes in the Bofecillos Mountains, and in these places, the Tascotal (or Fresno) directly overlies Tule Mountain Trachyandesite or Cretaceous strata (McKnight, 1970).

Table 1. Informal members of the Tascotal Formation.

Member	Area of Occurrence	Characteristics	Mode of Formation
Active apron	Face of Tascotal Mesa from Wire Gap north along valley of Alamito Creek to San Esteban Dam, lower part of formation	Generally volcanic sandstone with some conglomerate and mud rock. Arranged in thin and thick fining-upward sequences	Alluvial fan deposition during volcanic activity in Chinati Mountains
Eolian	Tascotal Mesa from Auler Ranch north to Harper Ranch; overlies active-apron member. Also present in some domes in Bofecillos Mountains	Fine to medium volcanic sandstones, crossbedded in sets a few meters to 25 m thick	Eolian deposition in dunes, etc.
Perdiz	Tascotal Mesa northwest to Alamito Creek, merges with Perdiz Conglomerate that extends northwest across Frenchman Hills, Cuesta del Burro, and Oak Hills. Also in western Bofecillos Mountains. Forms upper part of Tascotal where exposed	Crossbedded conglomerates and sandstones, containing abundant felsic VRF's and limestone clasts	Braided-stream activity, mostly after cessation of volcanic activity in the Chinatis
Lower conglomerate	Lower part of Tascotal, Murphy Bennett Section; near mouth of Torneros Creek, along the Rio Grande	Conglomerate and sandstone, mostly, but some mudrock and traces of limestone. Clasts are VRF's and CRF's	Fluvial or alluvial fan deposition, may have been site of regional drainage between fans spread from Solitario and Chinatis
Solitario fan	Lower part of Tascotal, Auler Ranch, Fresno Creek Valley, eastern Bofecillos Mountains	Conglomerates and sandstones containing black, green and white chert fragments in addition to VRF's and CRF's	Alluvial fan spread off Solitario uplift

Table 1. Informal members of the Tascotal Formation (continued)

Member	Area of Occurrence	Characteristics	Mode of Formation
Southern apron	Most of sedimentary Tascotal in Bofecillos Mountains, exposures in canyons near Rio Grande and in domes	Volcanic sandstone with some conglomerate in thin fining-upward sequences and medium scale crossbeds	Active apron developed around unidentified volcano
Fresno volcanic	Upper part of the Tascotal in central Bofecillos Mountains, extending to Rio Grande. Includes McKnight's (1970) mafic trachyandesite, latite and latiteporphyry and his valley-fill sequence	Lava flows of several compositions and some massive unsorted, matrix-rich conglomerate	Lava flows from vents in the Bofecillos Mountains and associated mudflow activity

Figure 2. Nomenclature and boundaries of the Tascotal and related strata

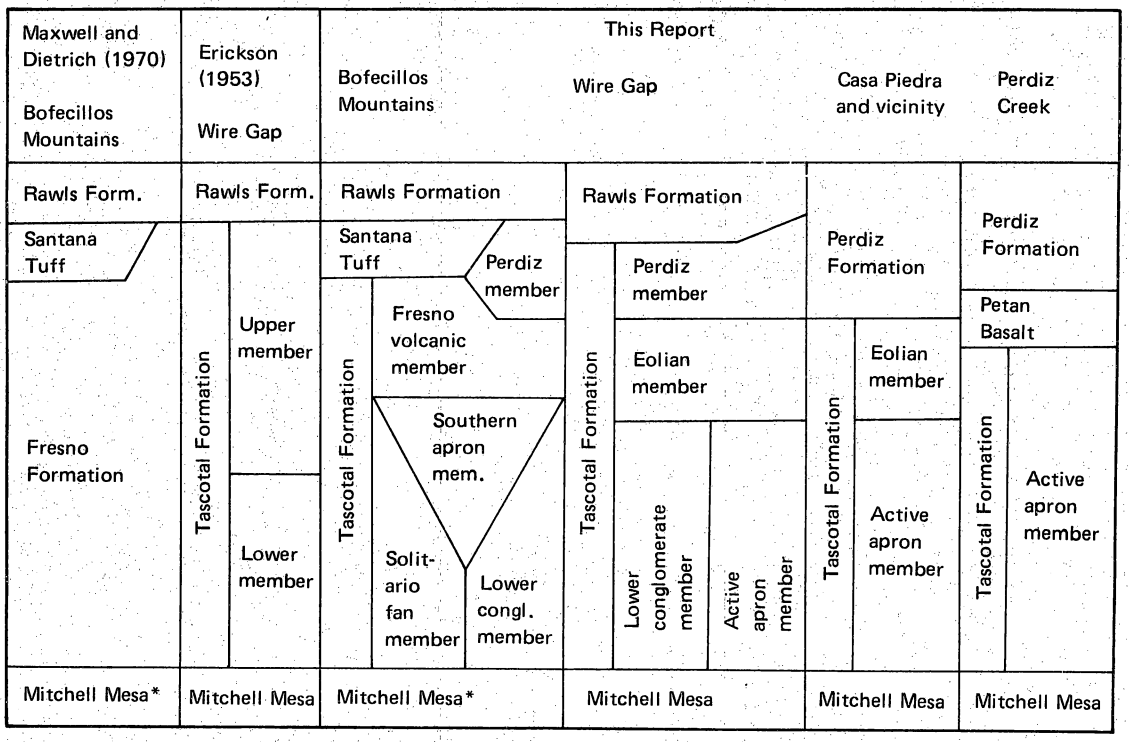

Figure 2. Nomenclature and boundaries of the Tascotal Formation and related strata.

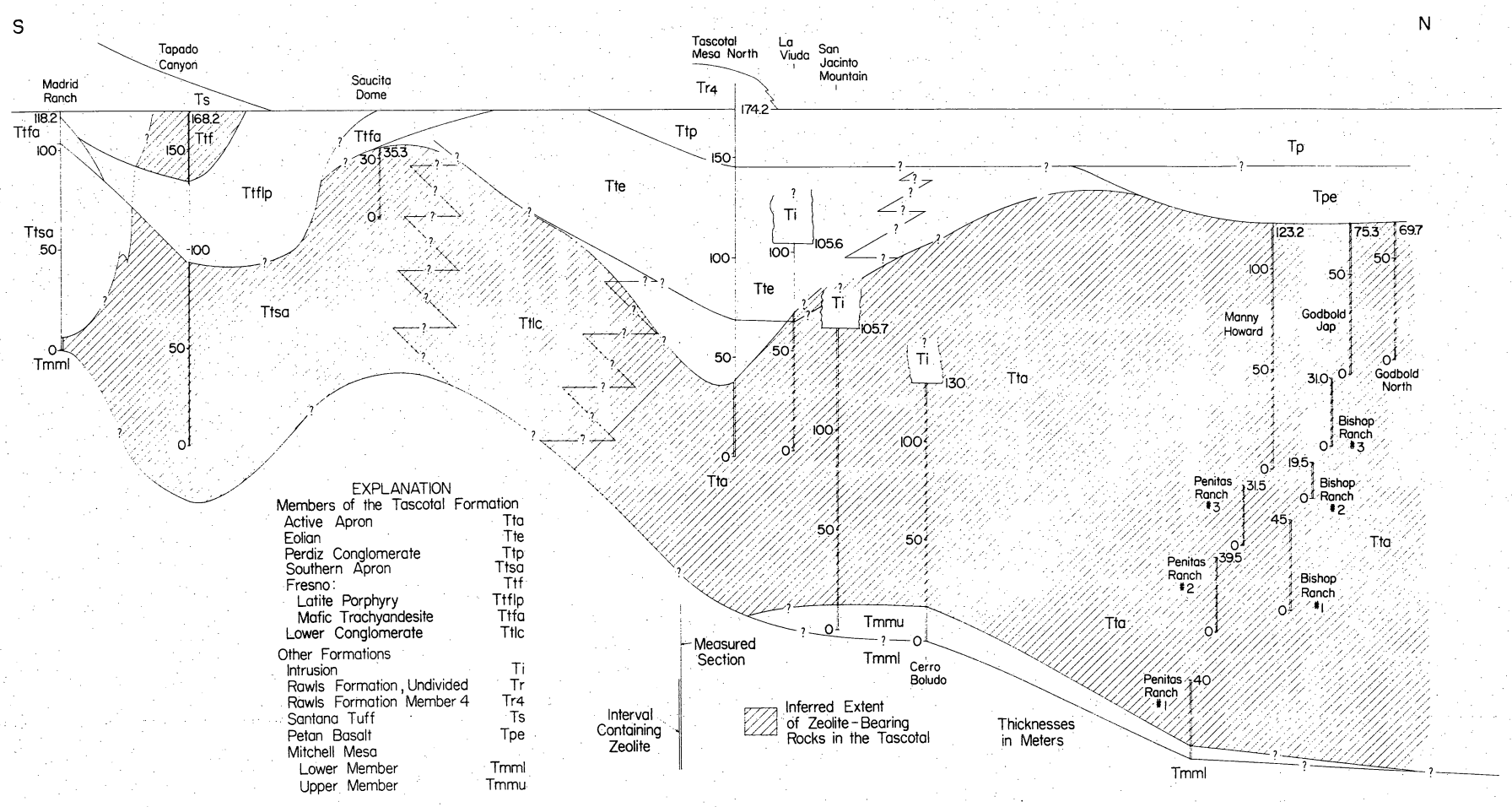

Figure 3A

Figure 3. Schematic cross sections of the Tascotal Formation showing stratigraphic subdivisions and distribution of diagenetic assemblage. Measured sections indicated in brown, intervals containing zeolite indicated in maroon. See also McKnight (1970) for cross sections through the Bofecillos regions. A. North-south cross section from the Godbold Ranch to Big Hill on the Rio Grande. B. East-west section from Murphy Bennett Section to the Cienega Mountains.

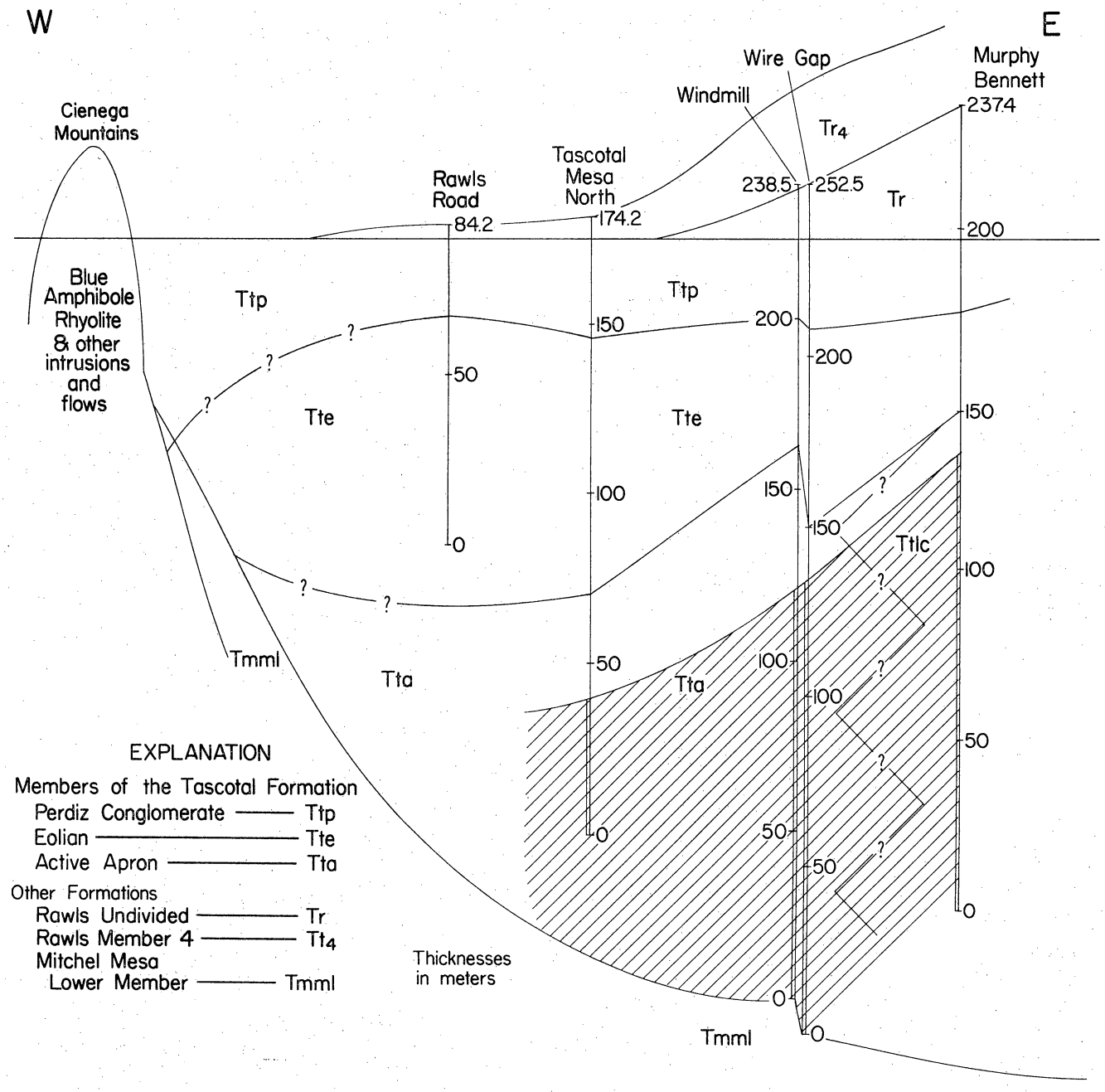
W
E
Cienega Mountains
Blue Amphibole Rhyolite & other intrusions and flows
Rawls Road
84.2
Tascotal Mesa North
174.2
Windmill
Wire Gap
238.5
252.5
Tr4
Tr
Murphy Bennett
237.4
200
Ttp
Tte
Tta
Tmml
Ttlc
150
100
50
0
EXPLANATION
Members of the Tascotal Formation
Perdiz Conglomerate — Ttp
Eolian — Tte
Active Apron — Tta
Other Formations
Rawls Undivided — Tr
Rawls Member 4 — Tt4
Mitchel Mesa Lower Member — Tmml
Thicknesses in meters

Figure 3B

The upper boundary of the Tascotal Formation is not so neatly defined. Erickson (1953) used the base of the flow rocks of the Rawls Formation as the top of the Tascotal. However, at the type section, the uppermost interval of Erickson's Tascotal Formation is a conglomerate composed of pumice and clasts of dark flow rocks. It is 15 m thick at Wire Gap and thickens to about 40 m at the Murphy Bennett section to the south. As will be clear from the discussion below, this unit must represent a cycle of volcanic activity different from that which formed other strata originally included in the Tascotal. Because of this and because the pumice-rich conglomerate is so unlike the rest of the Tascotal, it should not be included in the Tascotal. Dietrich (oral communication) reminded me that an ash-flow tuff layer a few meters thick occurs at the top of this pumice-rich layer in the southern part of the escarpment of Tascotal Mesa. He correlated this unit with the Santana Tuff (Maxwell and Dietrich, 1970). If his correlation is correct, the pumice unit might be included in Tascotal, but probably represents events closely related to emplacement of the several ash flows of the Santana. If so, the pumaceous conglomerate should be considered a facies of the Santana. This interval might also be assigned to the Rawls Formation because it closely resembles the nonwelded ash-flow tuffs that McKnight (1970) mapped as part of member 2 of the Rawls, clearly overlying the Santana. This member consists of pumice clasts up to several centimeters in diameter mixed with dark volcanic rock fragments (VRF's) that appear to have a mafic to intermediate composition, similar to that of flows in the Bofecillos Mountains. Although Rawls member 2 is volcanic and

the pumice-rich conglomerates are sedimentary, the two sequences are similar in appearance.

Dietrich (1966) demonstrated that the conglomerate layer near the top of the Tascotal Formation (the third member from the base of the type section) is continuous with the Perdiz Conglomerate, a major sheet of gravel spread from the Chinati Mountains to the northeast and southeast. This gravel layer is part of the Tascotal Formation as far west as the course of Alamito Creek. West of that creek, the Perdiz will be listed as a separate formation. The Perdiz is described by Jordan in chapter IV.

North of the latitude of Plata, the Tascotal Formation is overlain by a sequence of black trachyandesite porphyry, generally called the Petan Basalt. The Petan Basalt was originally defined by DeFord (1958) as part of the Vieja Group, a sequence of volcanic sediments and volcanic rocks that occurs in the Sierra Vieja on the western side of the Trans-Pecos volcanic field. In the Sierra Vieja, the Petan directly overlies the Mitchell Mesa. Ramsey (1961) correlated the Petan Basalt, as DeFord defined it, and the black lava rocks that crop out along the west side of the valley of Alamito Creek. Where the Petan is present, it forms a separate formation overlying the Tascotal and separating it from the Perdiz Conglomerate.

The Fresno Formation

On the basis of outcrops of the interval between the Mitchell Mesa Rhyolite and the Santana Tuff in the Bofecillos Mountains, Maxwell and Dietrich (1970) defined the Fresno Formation. Where the Santana is absent,

This definition is exactly equivalent to that of the Tascotal by Erickson (1953) because the Rawls Formation overlies the Santana. More of the Fresno area as mapped by McKnight (1970) and Dietrich (1966) is overlain by Rawls than is overlain by Santana. Maxwell and Dietrich (1970) justified this new name by stating that, in the Bofecillos area, the interval in question is mostly occupied by volcanic rocks.

In the center of the mountains, this is true; but along the Rio Grande near Redford in the vicinity of Big Hill, and in the lower part of the valley of Fresno Creek, the Tascotal interval is predominantly made up of sediments. The "Fresno" is a lens of volcanic material from a few local vents surrounded by sediment from several sources, the Solitario Uplift, the Chinati Mountains, an unknown source of volcanic material in Mexico, and highlands where sedimentary rocks were exposed to the west of the area of outcrop. Each of these, the volcanic lens and the several masses of sediment, is the result of a rock-forming system in the sense developed in the previous section of this report. As a mapping unit, the Fresno of Maxwell and Dietrich (1970) is useful, but in terms of understanding the development of this region as a volcanic field during Oligocene times, it is better to divide the interval between the Mitchell Mesa and the Rawls, or Santana, into a number of members that are lithologically and genetically distinct. The name "Fresno" will be retained for some of these--the lens of volcanic rocks in the Bofecillos Mountains.

The lower boundary throughout the area, the Mitchell Mesa, is an excellent time horizon. Different volcanic units overlie the Tascotal Formation at different places, and the interval assigned conveniently to the

Tascotal differs from place to place. At the type section, the Tascotal is overlain by sediments and flow rocks of the Rawls Formation. To the south, it is overlain by the Santana Tuff in outcrops along the Rio Grande and along Fresno Creek. To the north of the type section and west of Alamito Creek, the boundaries are stratigraphically lower. The Tascotal is overlain by the Perdiz Conglomerate over a small area east of the Cienega Mountains. Along the valley of Alamito Creek, north of the latitude of Plata, the Tascotal is overlain by the Petan Basalt. The Rawls is not a time horizon, but it serves as an easily correlatable boundary. Because of its well-marked boundaries, the Tascotal is an ideal package of sediment to analyze in terms of its formational systems.

Age

No radiometric age determinations are available for the Tascotal itself, nor have enough vertebrate fossils been collected from it to permit accurate placement within the system of North American land-mammal ages. But the volcanic units above and below the Tascotal Formation have been dated by the K-Ar method, and the period of time in which the Tascotal was formed is known. Eighteen samples from the Mitchell Mesa, which underlies the Tascotal, have yielded an average age of 31.5 million years (McDowell, 1978). The Santana Tuff, above the Tascotal along the Rio Grande, has been dated by McDowell (1978) at 26.3 million years. McDowell (1978) has also determined ages of 22 to 26.2 million years for several samples from the Rawls Formation overlying the Tascotal in the Bofecillos Mountains. Clark and Gilliland (1978) report ages of 26.7 million years

for the Rawls and 33.0 million years for the Petan Basalt. The single age for the Petan is probably unreliable because it overlies the well-dated, 31.5-million-year-old Mitchell Mesa.

The Chinati Mountains Group is reported by McDowell (1978) to range in age from 32.1 to 31.2 million years. Cepeda (1977, 1978) concludes that these flows fill a caldera that formed as the Mitchell Mesa Rhyolite was emplaced. If this conclusion is correct, at least part of the Tascotal formed while the Chinati Volcanic Center was active.

Stratigraphic Subdivision

Erickson (1953) recognized two parts of the Tascotal, a lower interval of thin-bedded, flaggy, white or light-gray tuff (for example, sedimentary rock composed of material of volcanic derivation) and an upper part that is gray or buff and consists of sandstone and conglomerate. McKnight (1970) described a similar two-fold subdivision of the Fresno in the Bofecillos Mountains. However, the subtle color differences between the upper and lower parts of the Tascotal are the results of diagenesis. Furthermore, the differences in grain size noticed by Erickson (1953) and attributed by McKnight (1970) to change of depositional mode from air-fall to fluvial sedimentation are the effects of changes of sediment character related to processes occurring in the Chinati Mountains as active volcanism climaxed and waned there and other events in the history of the Trans-Pecos Volcanic Field. For this reason, I propose an alternative informal subdivision, based on the process of formation of the rocks. Lithologic character and interpretation of these

members will be discussed after their geographic distribution is described and some information about the source of the Tascotal is presented (table 1, figs. 2 and 3). These members are more akin to the depositional systems of Fisher and McGowen (1967) or Galloway (1977) than they are to formal members.

Active Apron Member

The active-apron member makes up the lower 145 m of the 250 m type section of the Tascotal at Wire Gap and forms the great bulk of the formation. It extends from the northermost outcrops of the Tascotal, west of San Esteban Dam, about 10 km south of Marfa, to south of Wire Gap. The white outcrops all along Alamito Creek and east of Plata and Casa Piedra are assigned to this member.

The active-apron member consists of white, pale-buff, light-gray, or pink sandstone with rare interbeds of conglomerate and claystone. Grains in sandstone are predominantly of volcanic origin--glass shards and pumice, plagioclase, sanidine, volcanic quartz (Folk, 1968), volcanic rock fragments, and heavy minerals such as pyroxene, biotite, hornblende, and lamprobolite. The rocks are bedded, sorted, and crossbedded, and they display scour-and-fill structures in a manner that implies deposition by flowing water. A few beds of air-fall tuff occur in most sections, but they constitute less than 1 percent of the volume of the formation.

Eolian Member

Dietrich (1966) and McKnight (1970) noticed eolian crossbeds in the Tascotal Formation in several locations, especially along the rim of

Tascotal Mesa and at several places in the Bofecillos Mountains. In addition eolian sandstones occur west of Alamito Creek to a point north of the latitude of Casa Piedra. From there, southeast to the south end of Tascotal Mesa on the Auler Ranch, the eolian member makes a continuous layer that is about 40 m thick near Wire Gap and 25 m thick at the Tascotal Mesa North Section on the San Jacinto Ranch due south of San Jacinto Mountain. The eolian member consists of crossbedded fine to medium sandstones in which crossbed sets range up to 25 m thick. Its constituent grains are similar to those of the active-apron member but are better sorted by size and are better rounded. Glass shards are more abundant in the eolian member than in parts of the active-apron member.

Perdiz Member

The upper part of the Tascotal at Wire Gap and elsewhere along the face of Tascotal Mesa consists of coarse sandstones and conglomerates. At Wire Gap, at the Windmill Section, and at the Tascotal Mesa Section this interval totals 30 m thick. At the Murphy Bennett Section to the south, it is thinner, 21 m. Dietrich (1966) was able to trace this layer south of the Cienega Mountains to outcrops assigned to the Perdiz Formation. It also continues--with only small interruptions east of the Cienegas--to link up with outcrops of Perdiz Formation that overlie Petan Basalt and cap the Frenchman Hills, the Cuesta del Burro, and the Oak Hills (Ramsey, 1961; Jordan, this report, chapter IV). East of Alamito Creek and in the western part of the Bofecillos Mountains, gravels at the top of the Tascotal are thinner and difficult to map separately. I will consider them to be a member of the Tascotal Formation. Thus the

Perdiz member of the Tascotal crops out along the face of the Tascotal Mesa from Alamito Creek to the Auler Ranch. It also crops out in the Botella Horst and in the Torneros Dome regions in the western part of the Bofecillos Mountains; it is 20 m thick near the mouth of Tapado Canyon. Conglomerates are not present at the top of the Tascotal in the southeastern part of the Bofecillos Mountains or along the Rio Grande, southeast of Tapado Canyon.

Lower Conglomerate Member

The section exposed on the face of Tascotal Mesa, near the headquarters of the Murphy Bennett Ranch, is quite different from the type section only 6 km to the north northwest at Wire Gap. The bottom 146 m of exposed section consists of interbeds of conglomerate and sandstone, with some clay beds and a single bed of limestone. The conglomerates are composed of a mixture of volcanic rock fragments and limestone fragments. Some beds contain white and green chert clasts probably derived from the Solitario Uplift. This type of rock is not exposed elsewhere along the Tascotal Mesa escarpment but outcrops of this level are not good at other locations nearby. However, similar rocks occur low in the Tascotal near the International Boundary and Water Commission Gauging Station on the Rio Grande below Presidio (Dietrich, 1966).

Solitario Fan Member

The Solitario Uplift lies just east of the Bofecillos Mountains. In its core are exposures of igneous rock and Cretaceous sediments as well as the only outcrops of early Paleozoic rock, including white and green

chert, in the vicinity. Adjacent to the Solitario, conglomerates contain clasts of these distinctive cherts. Outcrops of such conglomerates occur in Fresno Canyon, elsewhere in the eastern Bofecillos Mountains, and on the Auler Ranch, near the south end of Tascotal Mesa. Some conglomerates in the lower part of the Murphy Bennett section of the Tascotal contain clasts of these cherts as well. Outcrops of this interval are rare; mostly this member underlies gravel-covered slopes. Little conclusive evidence of its mode of formation is available.

Southern Apron Member

In most outcrops in the Bofecillos Mountains, the lowest part of the Tascotal consists of volcanic sandstones with some interbeds of conglomerate or mudrock, very much like the active-apron member of the Wire Gap region but probably not continuous with it. This member displays cross-bedded or structureless, water-deposited sediments. The sediments are commonly a pale-green color that distinguishes them from most sediments of the active-apron member. The southern apron member is commonly about 100 m thick in outcrops along the Rio Grande; the thickest measured sections are in Tapado Canyon, but the base is not exposed. The unit is generally thinner and has a smaller extent of diagenesis in the southeastern part of the Bofecillos than it does elsewhere. McKnight (1970) interprets it as pinching out under the Bofecillos volcano. It also crops out in a dome north of the Bofecillos volcano, so that it may have predated activity of the volcano and may continue as a layer of more or less constant thickness beneath the volcanic edifice, thinning over domes that stood above the general elevation. This unit underlies flows of the Fresno

volcanic member of the Tascotal. McKnight (1970) discerned an upper layer of sediment and tuff in the Fresno Formation above the flow rocks. His measured-section descriptions indicate that this unit is commonly conglomeratic, where exposed, but outcrops were poor at many sections. Probably the sediments that formed after the Fresno volcanic member can be assigned to the Perdiz member of the Tascotal Formation.

Fresno Volcanic Member

Dietrich (1966), and Maxwell and Dietrich (1970) argue that rocks that crop out in the interval between the Mitchell Mesa Rhyolite and the Rawls Formation or Santana Tuff in the Bofecillos Mountains are different from those in that interval in the Tascotal Mesa Quadrangle mapped by Erickson (1953). They therefore propose to assign these rocks to the Fresno Formation, which, they point out, is almost exactly equivalent to the Tascotal. The major purpose of this report is to interpret the stratigraphic interval that includes the Tascotal of Erickson (1953) and the Fresno of Dietrich (1966) and Maxwell and Dietrich (1970) in terms of the mosaic of depositional facies that led to accumulation of rock at that place and time. To separate the Fresno Formation from the Tascotal Formation calls attention to differences between them, but the Fresno, as mapped by Dietrich (1966) and McKnight (1970), includes amounts of sediment that are comparable to the amounts of igneous rock in the Tascotal. Furthermore, some members can be traced from Fresno to Tascotal, and both formations include volcanic apron members. Recognizing a Fresno volcanic member of the Tascotal Formation emphasizes the true differences between the type Tascotal and rocks of the same age in the central

Bofecillos, but it also points out the similarity of rocks exposed along the Rio Grande to typical Tascotal.

The Fresno volcanic member includes the large flow rock units of the Bofecillos Mountains, McKnight's (1970) mafic trachyandesite, latite, and latite porphyry. These flows crop out in the area of the Bofecillos vents and in several small domes near them, south from there at the mouth of Tapado Canyon. They extend eastward under outcrops of Santana into the cliffs of the southeast margin of the Bofecillos and the west wall of Fresno Canyon to the north. The member also includes a valley-fill sequence exposed in the upper part of Fresno Canyon. It overlies the southern apron member and is overlain by the Perdiz member, the Santana Tuff, or the Rawls Formation.

Volcanic and Structural Background

At the time the Tascotal began to form, the Chinatis had just undergone a major ash-flow and caldera-forming event that led to the emplacement of the Mitchell Mesa welded ash-flow tuff. This caldera-forming event was succeeded by a sequence of eruptions of magma into the Chinati Caldera which led to the formation of the several flow units described recently by Cepeda (1977). These rocks postdate major caldera--forming activity in the Chinatis. Consequently, the Tascotal records the period of time during which the Chinati Mountains were undergoing a gradual decline of volcanic activity leading to their eventual demise as a volcanic center. The Bofecillos Mountains, which lie to the south of the type area of the Tascotal outcrop, were the site of volcanic activity forming

the Fresno member and much of the Rawls Formation. Activity at this center began late during the period in which the Tascotal was formed. Further to the south, beyond the Rio Grande in Mexico, activity began late in the period during which the Tascotal formed in an area centering on Sierra Rica. The Santana Tuff and a quartz-feldspar welded ash-flow tuff, mapped by McKnight (1970) as the Big Hill Intrusion, may have come from that center.

The Paisano volcano described by Parker (1970) serves as the northeastern boundary of the Tascotal depositional basin. This volcano had a history of eruption that preceded formation of the Mitchell Mesa Tuff. Consequently, that center was in its declining stages or was actually inactive at the time the Tascotal was formed; it was probably a high area that was undergoing erosion. Most of the activity in the Davis Mountains also preceded formation of the Tascotal.

Just before the beginning of the period during which the Tascotal was deposited, the Mitchell Mesa ash-flow had filled topographic lows and subdued local relief, leaving a gently sloping plain. This gently sloping plain was interrupted by a few highlands; for example, no Mitchell Mesa was deposited west of Alamito Creek in the vicinity of the Cienega Mountains in an area which may form the wall of an early caldera of the Chinati volcanic center complex. The slopes at this time were generally east of the Chinatis and the highlands south of that range. Slopes on the northern side of the Chinatis are not known: probably they were to the north or northeast, away from the center of volcanic activity.

Pre-existing topography locally influenced slope directions elsewhere. The Solitario Uplift east of the Bofecillos Mountains began to rise before the Mitchell Mesa formed (Wilson and others, 1978) and shed its characteristic debris composed of Cretaceous limestone clasts and distinctive cherts from Paleozoic sediments exposed within the uplift. Evidence in the southeastern part of the Bofecillos Mountains in the vicinity of Lajitas and Big Hill suggests that slopes there were locally to the west off the Terlingua monocline and other structural features that had developed earlier in the history of the region (McKnight, 1970). Thus the known limits of deposition of the Tascotal Formation in the United States were the Solitario and Terlingua monocline areas on the southeast and the Chinati Mountain area on the west. Unfortunately the limits due east of the Chinatis, where erosion has removed the Tascotal north of the Solitario, are not known. The limits of the basin on the north, in the vicinity of Marfa and the northwest are not known because they are buried under later rocks.

The actual limit of the Tascotal Formation on the west can be located with some degree of precision. It does not crop out in the valley of Alamito Creek in the vicinity of the Ocotillo siding in the Ocotillo (15-minute) Quandrangle (Dietrich, 1966). In this area the Perdiz laps directly onto Cretaceous and Permian rocks. Similarly, along the ridge extending north from the Cienega Mountains, the Tascotal does not occur, and rocks of the Morita Ranch Formation crop out on the divide between Alamito Creek and Cienega Creek. Near the crest of the Frenchman Hills, just east of Highway 67, outcrops of Morita Ranch Formation units are

overlain by the Petan Basalt and by the Perdiz Conglomerate. In the banks of Perdiz Creek, even farther north, the Mitchell Mesa and the Petan are separated by a thin interval of volcanic sediment (Maxwell and Dietrich, 1970). The Tascotal is exposed only east of a line connecting these points.

SEDIMENTOLOGY OF THE TASCOTAL

Current Directions and Source Indicators

The major kinds of information available on sources of the Tascotal are its rock and mineral-fragment composition and the orientation of imbricated clasts in conglomerate deposits. Although the sediments are crossbedded in places, few good crossbedding directions could be measured because the crossbeds are low-angle varieties or are not well exposed. Only in some eolian deposits can crossbeds be measured accurately. Both clast type and clast imbrication indicate derivation from source areas that lay to the west for most, though not all, of the Tascotal. The Chinati Mountains lay to the west, and were active at least during deposition of the lower Tascotal and were probably, as they remain today, a major highland throughout the time of deposition of the Tascotal; they and their associated highlands are a likely source of most of the sediment in the Tascotal.

Clast Types

In order to determine the types of clasts present in conglomerates, counts of clast types were conducted on populations in two ranges of long dimension: 5/8 to 2-1/2 inches and 2-1/2 to 10 inches. These sizes cor-

respond closely to -4 to -6 phi, the coarse half of the pebble range, and -6 to -8 phi, the cobble size range. Coarser material is rare and finer pebbles or granules were difficult to identify with precision in the field; identification of cobbles and coarse pebbles was much more precise than that of the finest pebbles used for the study. In each size class, 100 clasts were selected, beginning at a randomly chosen point on the outcrop and spreading outward from it, taking all clasts of the right size. Clasts were identified as limestone, chert, and volcanic rock fragments. Chert was subdivided by color; volcanic rock fragments were subdivided into felsic and mafic varieties. Distinctive types, such as fragments of the Mitchell Mesa, were counted separately. Results of the counts are indicated in the appendix to this chapter, sample localities are plotted in figure 1, and areas characterized by particular rock types are shown in figure 4.

The results clearly show that several areas of distinctive clast composition exist. Four are indicated in figure 4: Fans 1, 2, and 3, and the Solitario Fan. Fan 1 contains conglomerates that have abundant limestone and other sedimentary rock fragments (SRF) mixed with the felsic fragments and other VRF's that make up most of the clast population. This fan crops out in the face of the Tascotal Mesa. A second fan lies north of Fan 1 and contains no limestone clasts and few other SRF's, but contains blue amphibole rhyolite (riebeckite rhyolite) derived from the Cienega Mountains. This fan can be divided into northern and southern parts; the northern part contains no clasts of Mitchell Mesa, but does contain fragments from some trachytes that crop out north of the Cienegas. The northernmost fan, Fan 3, contains a few Mitchell Mesa clasts and

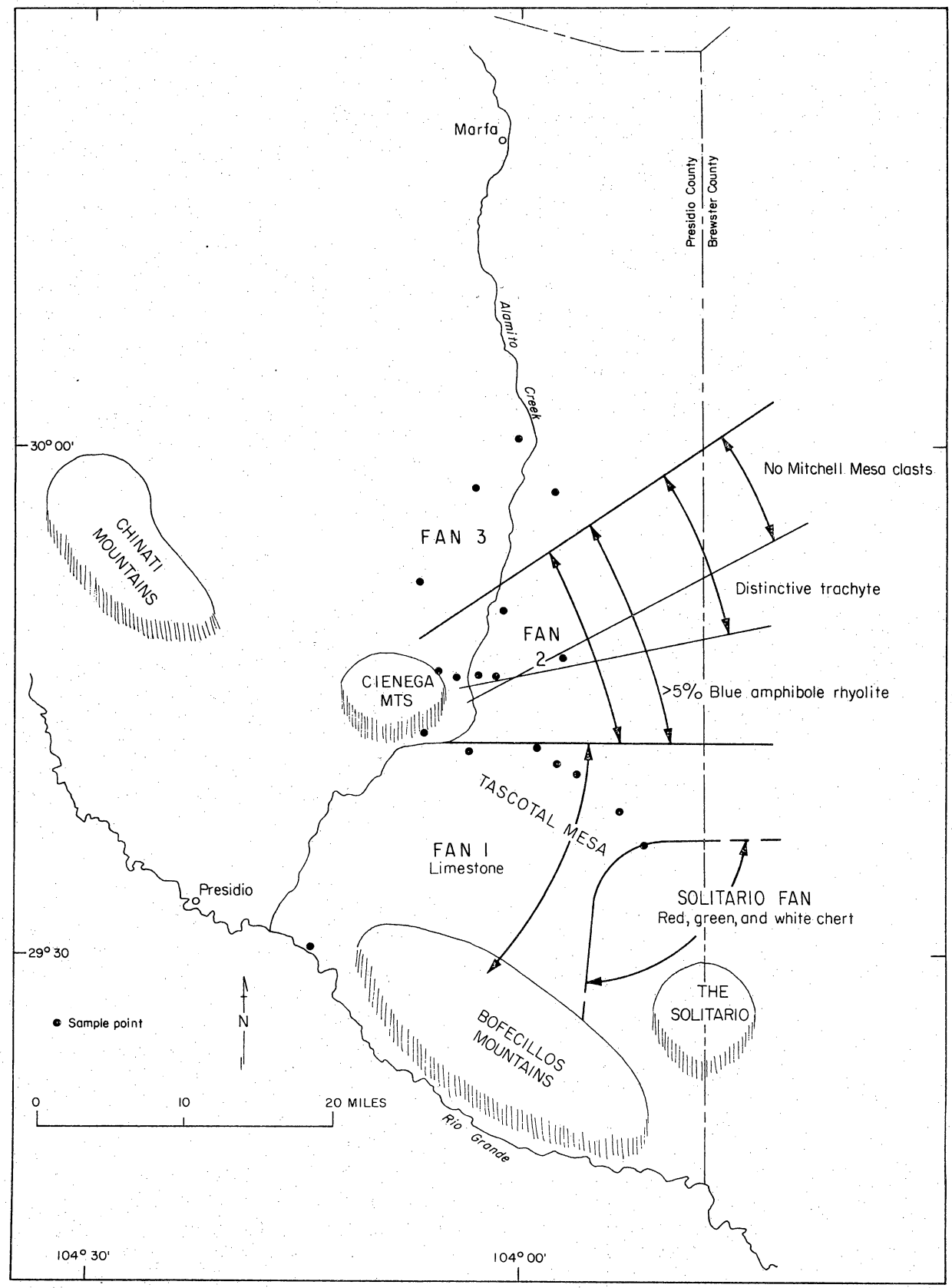

Figure 4. Fans defined by distinctive clasts in Tascotal Conglomerates.

includes a few fragments of intrusive igneous rocks, some of which contain biotite, in addition to abundant felsic VRF's, but none of the clasts characteristic of Fan 2. The Solitario fan corresponds to the Solitario fan member and contains clasts of limestone and green or red chert, but few VRF clasts.

Further pebble counts in the Bofecillos Mountains would confirm a qualitative assertation that two conglomerate sources are important within the Bofecillos. The Solitario Uplift was an important source of gravels in the lower Tascotal for the region from just south of the southern end of Tascotal Mesa on the Auler Ranch; along the west side of the Solitario, in the upper part of Fresno Canyon and in nearby domes. These conglomerates are distinct because of their abundance of green or white chert, derived from Caballos Novaculite outcrops in the center of the uplift. The second type of gravel occurs on the Botella Horst and on the Torneros Dome. These deposits are mapped as Fresno Formation by Dietrich (1966) but, they may be assignable to either the lower conglomerate member or the Perdiz member of the Tascotal. They consist of a mixture of limestone clasts, Mitchell Mesa, and other felsic volcanic rocks and clearly were not derived from the Solitario. These compositions are similar to those in the lower part of the Tascotal at the southern end of Tascotal Mesa.

The best explanation of these patterns of conglomerate clast distribution is that the majority of material was derived from the west, from the Chinati Mountains, and from areas of limestone outcrop such as those southwest of Casa Piedra along Alamito Creek (Dietrich, 1966).

Outcrops of limestone also occur today in Mexico south and west of Presidio, and it is easy to postulate a continuous belt of outcrop of limestone and other sedimentary rocks of Permian or Cretaceous age south and southeast from the Chinati Mountains across the area of what is now the Presidio Bolson. Henry (oral communication) indicates that oil tests near Presidio encountered bolson fill material directly overlying Cretaceous rocks, with no volcanic material between. The only conglomerate clasts not derived from the west are those in the Solitario fan member.

Paleocurrents

Pebble imbrication proved to be a satisfactory source of paleocurrent information for the Tascotal Formation. Dip direction of the maximum projection plane (that is, the upstream direction) of 30 clasts was measured at a number of outcrops, commonly at more than one conglomerate bed in each section, for a total of 34 stations; results are displayed in figure 5. Although directions of flow indicated by the several samples range from north northwest through east to south southeast, the generally easterly flow directions substantiate the conclusion drawn from the clast composition data of a westerly source.

Primary Mineralogy of the Tascotal

In mineralogically immature sedimentary rocks like the Tascotal, studies of the minerals that were deposited to form the sediment simply and directly reveal the nature of the source. The primary composition of the Tascotal indicates unequivocally the importance of volcanic activity

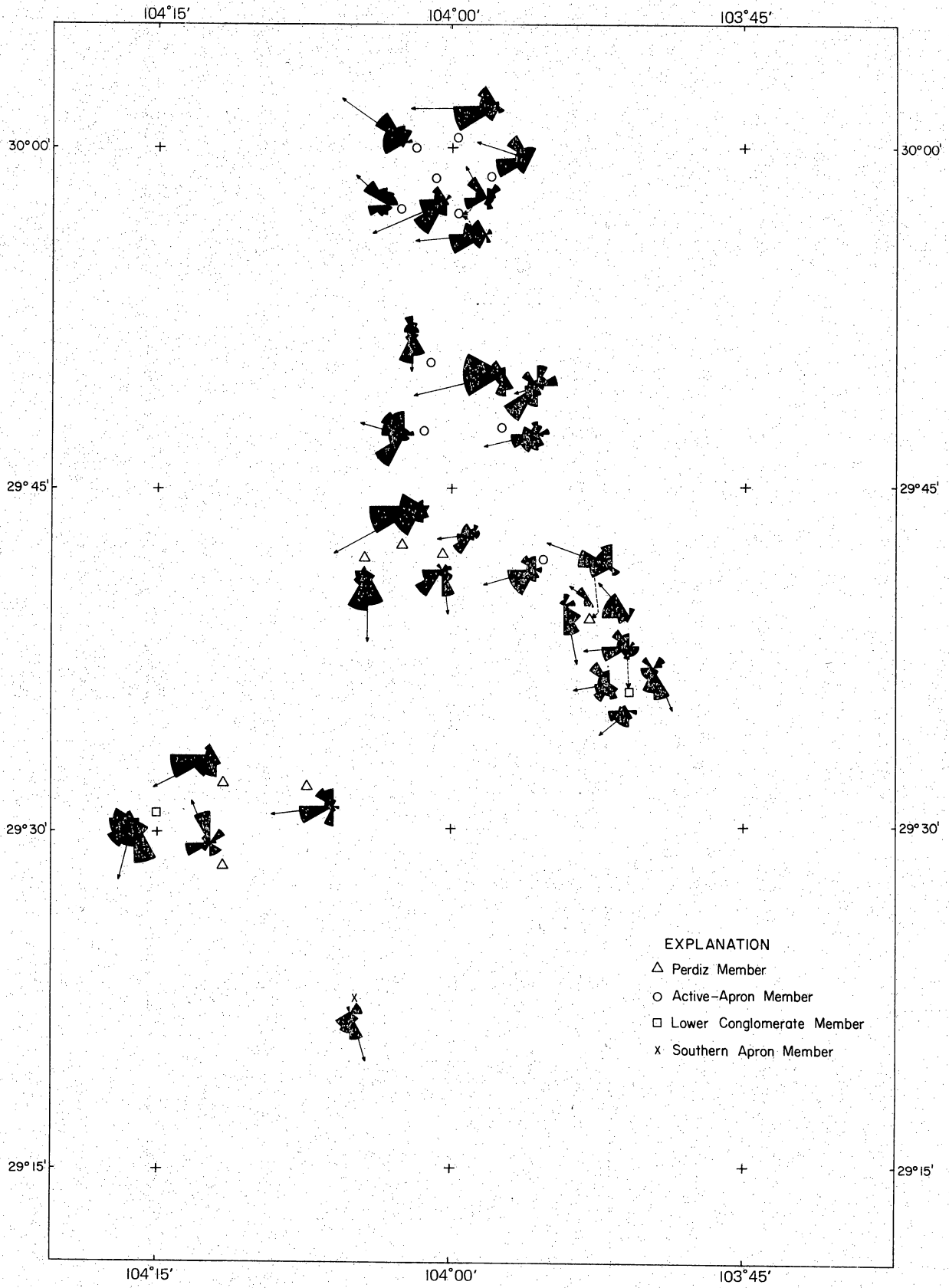

Figure 5. Paleocurrents measured on imbricated clasts in conglomerates. Arrows point upstream, their length is proportional to vector magnitude. Symbols indicate member: circle for active apron, square for lower conglomerate, X for southern apron, and triangle for Perdiz. Orientation of thirty clasts measured, unless otherwise noted.

in its source area. In this section, mineralogy will be reviewed only as it is important in interpreting the Tascotal (table 2).

Volcanic Glass

Volcanic glass, as simple shards and as frothy or long tube pumice, is a common constituent in most of the Tascotal. Simple shards are the finest grained fraction of the grain-size distribution. They range from silt to coarse sand size. Pumice differs in that it includes whole bubbles or tubes and generally has a coarser grain size. Pumice fragments up to several centimeters long are found. Volcanic glass is most common in fine sandstones; it forms the fine fraction of rocks of the active apron and is common in fine to medium sands of the eolian member. Both kinds of glass are less common in coarser rocks of the active apron and in rocks of the Perdiz or other conglomerates. A few layers are especially rich in pumice grains. One such layer, about a meter thick, was present in both the Wire Gap and Murphy Bennett sections. Of course, the pumice conglomerate that I have exiled to the Rawls or Santana is anomalously glass-rich.

The importance of glass is two-fold. (1) Its abundance in these rocks implies a source that yielded abundant glass fragments, a volcano characterized by an explosive mode of eruption. Because these glass shards must have some from non-lithified deposits, the volcano must have constantly replenished those deposits to provide material for a stratigraphic section that totals 150 to 200 m thick. The thick intervals of shard-rich rocks must have formed during the time the glass-producing volcano was active. (2) Glass is extremely unstable at or near the earth's surface.

Table 2. Implications of observations of primary mineralogy

Observation	Implication
Glass shards are a major constituent.	a. Much of Tascotal formed from debris produced by a volcano that was active while the formation accumulated. b. Intense diagenesis occurred as glass reacted with ground water.
Plagioclase is the most abundant constituent of crystal fraction except in lower part of active-apron member.	Most of the Tascotal does not consist simply of reworked debris from the upper, nonwelded part of the Mitchell Mesa; only the lowest part of the active apron is. There sanidine, like that in the Mitchell Mesa, is common.
Fine VRF's are common in sandstones of active apron.	Flows were exposed in parts of the source area, but coarse debris from them could not be transported by streams because of low gradients.
Coarse VRF's are abundant and glass shards rare in Perdiz member.	This interval accumulated <u>after</u> cessation of volcanic activity in the Chinatis and erosion of the accumulation of loose pyroclastic debris.
Tuffs in active-apron member are of different mineral composition than apron sediments: less hornblende or pyroxene, more biotite, few VRF's, and finer glass shards occur in tuffs.	Active-apron sediments are not simply the result of reworking of local, ash fall deposits, but include coarser pyroclastic material (nearer source) and epiclastic material.

In the Tascotal, much of the glass has dissolved into circulating water and all constituents of the glass including uranium have been released to form new minerals or to migrate through the system. During diagenesis, mineral precipitation has preserved the original texture of the rock, so that areas where shards or pumice once existed can be differentiated by their shape from areas that were primary pore space. Diagenesis of shards and its relation to uranium migration are discussed in the next chapter.

Crystals

Quartz, sanidine, plagioclase, and various heavy minerals that occur as monocrystalline grains form the crystal fraction of the Tascotal. Quartz and the feldspars are generally common in fine to coarse sandstones and occur in virtually all rocks, throughout the entire range of average grain size. They may be euhedra, broken euhedra, or angular to subrounded fragments.

In most rocks, plagioclase is the most abundant, followed by sanidine and quartz. The one exception to this pattern is found at the base of the active apron member, just above the Mitchell Mesa, where sanidine and quartz are more abundant than plagioclase. The Mitchell Mesa contains sanidine but virtually no plagioclase. The observed composition implies that the lowest part of the active apron member may be the result of reworking of the upper, nonwelded part of the Mitchell Mesa, but the bulk of the Tascotal came from other sources.

Opaque, iron-rich oxide grains, probably magnetite and biotite, are widely distributed in the Tascotal and are only slightly altered along their margin. Pyroxene, hornblende, and lamprobolite are common in rocks

that have not undergone extensive diagenesis and are present as etched crystals in rocks that are more altered. Presumably they were a source of several elements for the diagenetic system, especially iron.

Volcanic Rock Fragments (VRF's)

The coarsest volcanic clasts of most rocks are VRF's, but they occur in grains of silt to boulder size and in all rocks. Fine VRF's, of silt to granule size, are common in rocks of the active apron and eolian members of the Tascotal. These imply that areas of flow rock were exposed to erosion during accumulation of these members, in addition to the areas of fine volcanic glass shards. Transport of coarse clasts from these deposits was prevented by stream gradients maintained at low declivity by the abundant sand-sized pyroclastic debris.

Conglomeratic members of the Tascotal that contain abundant VRF's must have been derived from source areas where the cover of fine pyroclastic debris was absent. Such areas could be where volcanic activity had ceased, or where it was too distant to provide much air-fall tuff, where the volcanic activity produced little fine pyroclastic material, or where that produced was rapidly stripped by erosion.

Sedimentary Rock Fragments

The presence of carbonate rock fragments (CRF's), chert fragments, and some clasts of terrigenous rocks, such as siltstone and sandstone, in the Tascotal indicates that the source area was not exclusively volcanic. Such material is restricted to the southern part of the outcrop of the formation, from the vicinity of Casa Piedra to the south. These

sources included the Solitario, which provided white and green chert, the area around Ocotillo and perhaps that around Shafter where rocks of Permian and Cretaceous age crop out now, the folded mountain ranges of the Chihuahua tectonic belt where large anticlinal mountains now expose Cretaceous sediments, and exposures of sedimentary rocks that now underlie the Presidio Bolson. In view of the generally easterly flow directions indicated by pebble imbrication, it is appropriate to suggest a generally high area, lying west of the present extent of the Tascotal but south of the Chinati Mountains, that served as a major source of sedimentary rock fragments. Noticeable in the conglomerate derived from that source are silicified fossils similar to those found in Cretaceous limestones near Ocotillo.

Tuff Beds

Beds of air-fall tuff, a few centimeters to a meter or so thick, are interbedded with sedimentary rocks of the Tascotal Formation. They are easily distinguished from the normal apron sediments because they are finer grained, contain a simpler heavy mineral assemblage, normally just biotite, and lack the fine volcanic rock fragments that are so common in apron sediments. The apron sediments are not the result of simple reworking of these air-fall beds, but are derived from coarser pyroclastic material and from sources of epiclastic detritus of volcanic provenance. Consequently, they formed as an apron of sediments around an active volcanic source.

Sedimentological Analysis

The mineralogy, paleocurrent indicators, and age of the Tascotal lead to the conclusion that the bulk of the formation was derived from the Chinati Mountains at the time they were the site of active volcanism and in the period after their history of activity. Other sources include a sedimentary terrain south of the Chinatis and the Solitario Uplift. The discussion of the sedimentology of the Tascotal Formation will concentrate on the following aspects: description of rocks formed during the active phase of volcanic history; description of contemporaneous rocks that may be the valley facies; and description of the changes of sedimentation that occur when a volcanic center passes from its active to its inactive phase (table 3).

Sedimentology of the Active-Apron Member

The active-apron member of the Tascotal includes two especially distinctive rock types, thin fining-upward sequences and thick fining-upward sequences. These are arranged in sequence with crossbedded sandstones in such a way to suggest progradation of this unit from its volcanic source eastward. The interpretation here follows that of Walter (1977b, in press) comparing these deposits with those of alluvial fans and deep sea fans. The character of this active apron is intimately connected with the fact that it formed around a volcano that was erupting abundant fine pyroclastic debris.

The lower part of the active apron member consists of sequences, on the order of a meter thick, that include the following units in succession

Table 3. Rock-forming systems of the Tascotal.

SYSTEM	CHARACTERISTICS	EXAMPLES
Vent system	Abundant lavas and ash flow tuffs, various intrusions. Some sediments of very coarse grain size.	Fresno volcanic member
Sedimentary aprons system		
a. Active apron	Sand-dominated, composed of progradational sheetwash deposits and aggradational channel deposits. Overall system is progradational and has bajada morphology.	Active apron, southern apron members
b. Inactive apron	Gravel-dominated bar and channel deposits with braided-stream sedimentary structures, but overall bajada morphology.	Perdiz member and Perdiz
Valley system	Fluvial sediments of diverse provenance, evidence of lake or swamp deposition. Develops between two or more sedimentary aprons or fans.	Lower conglomerate member
Associated facies, not intimately related to the volcanic activity		
Alluvial fan systems	Gravels deposited by alluvial fan process, mostly resembling braided streams deposits.	Solitario fan member
Eolian system	Fine to medium sand in large-scale crossbeds interbedded with near horizontal stratification. Little or no gravel or clay.	Eolian member

above a scour surface (fig. 6): (1) structureless or medium-scale cross-bedded sandstone that may be of medium to granular or pebbly coarse sand-size. This lower part of the sequence commonly shows evidence of smaller internal scours as though several events were necessary for its deposition. (2) Thinly-bedded, laminated sand, or interbeds of thin sand beds and laminae or drapes of pink mud. Mud drapes or surfaces between sandstone laminae are commonly mudcracked, tracked or burrowed, or show other evidence of the passage of time between depositional events.

These sequences are like those described by Boothroyd and Ashley (1975) in the distal region of a glacial outwash fan where they form in linguoid bars. The glacial fan sequences consist of medium scale bar slipface crossbedding, overlying a scour surface and grading up into ripple and ripple drift cross-lamination that was deposited on bar surfaces. The Tascotal thin fining-upward sequences differ in three respects. First is the evidence of episodic deposition in the Tascotal, while Boothroyd and Ashley believe that the sequence they studied was the result of one continuous depositional event. The second difference is that sedimentary structures are not as obviously abundant in the Tascotal as they are in the glacial outwash. Finally, the linguoid bar deposits of Boothroyd and Ashley (1975) are interbedded with longitudinal bar deposits consisting of large scale planar crossbeds overlain by flat beds, in turn overlain by ripple-drift bedding. Such deposits are not present in the Tascotal.

Despite these differences the thin fining-upward sequences are probably the deposits of migrating linguoid bars. The lack of sedimentary

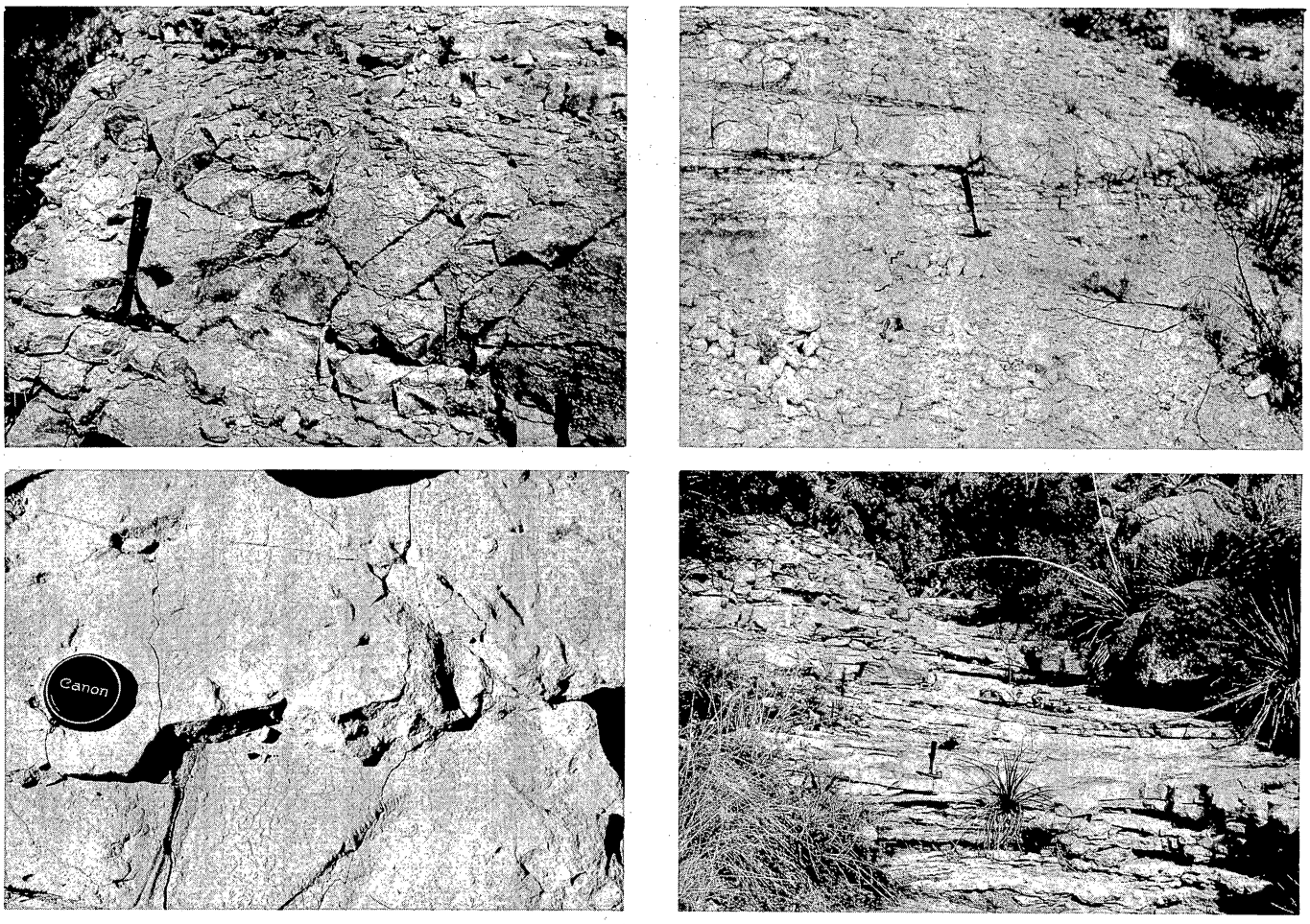

Figure 6. Field photographs of rocks of thin fining-upward sequences. A. The hammer sits on a scour surface which truncates thin beds to the right of it. Massive lower part of the sequence is overlain by thin, reddened beds of the upper part. B. A well-displayed sequence begins just about the butt of the hammer. C. Mudracked mud drape in the upper part of a thin fining-upward sequence. D. A number of thin fining-upward sequences. E. Exposure of a sequence of beds of the sort characteristic of the active-apron member. Hammer is 28 cm long.

structures may be a result of diagenesis or of the lack of material suitable to mark individual laminae or cross-laminae. The lack of interbedded longitudinal bar deposits may have been caused by less intense flow of water during flood events, perhaps because the Tascotal deposits were relatively more distal than those of the glacial outwash fan. The episodic nature of deposition might be caused by a more distal position or by the fact that the flood events on the Tascotal apron, which were a result of precipitation, were of shorter duration than were those on the outwash fan, which are caused by seasonal melting of the glacier. All in all, the thin fining-upward sequences are best interpreted as the distal deposits of an alluvial fan.

Overlying the well marked, mud-draped, thin fining-upward sequences of the lower part of the Tascotal are slightly coarser grained, cross-bedded sediments in which mud is less common and granules, some pebbles, and a very few cobbles occur (fig. 7). These deposits commonly are interrupted by scour surfaces with relief of about one meter, but ranging up to two meters. These deposits are similar to those Platte type of braided river of Miall (1977). Because they are coarser grained than the thin fining-upward sequences, and contain larger scale sedimentary structures arranged in thicker sequences, they must represent more proximal deposits of the volcanic apron. They probably were deposited in a manner similar to that in which the thin fining-upward sequences formed, but by more energetic flows. The position of these deposits relative to the underlying thin fining-upward sequences and the overlying thick fining-upward sequences as well as their internal structures suggest they are mid-fan deposits.

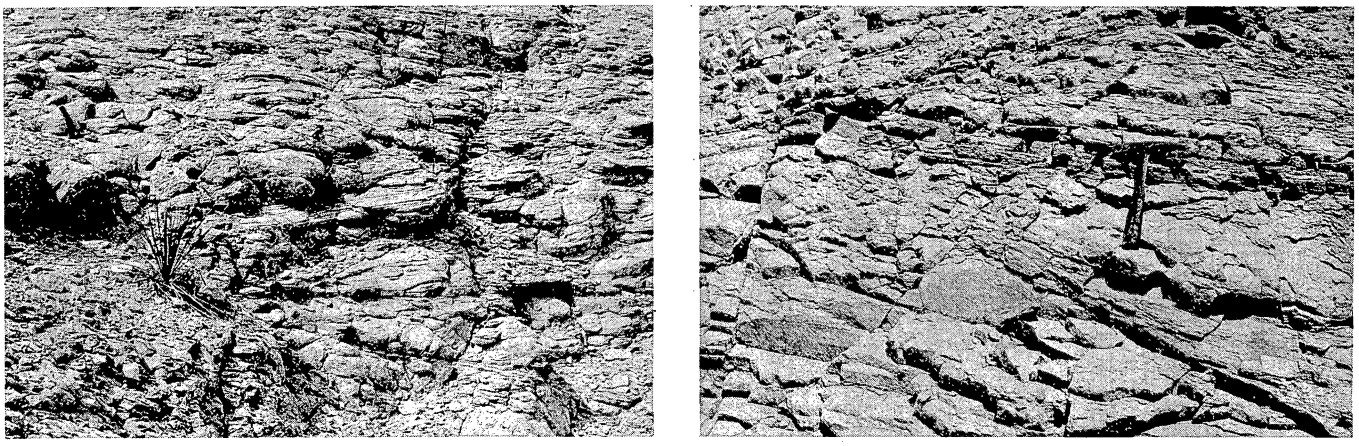

Figure 7. Photographs of beds in the mid fan region of the active apron, overlying the thin fining-upward sequences. A. Crossbeds in the Windmill section. The sotol bush is about 0.5 m tall. B. Crossbedded sediments of the southern apron member in Tapado Canyon, Bofecillos Mountains.

Thick fining-upward sequences overlie a scour surface and consist of a cobble pavement and a number of overlying subsequences, all of which fine upwards (fig. 8). Subsequences ideally are composed mostly of sand-sized volcanic sediment with some pebble conglomerate at the base and mudrocks at the top. Sandstones are crossbedded or laminated, generally in a sequence that goes from large scale crossbedding at the base, with sets up to a meter thick, passing upward into a laminated interval that passes into another crossbedded interval where medium scale crossbeds (one to a few decimeters) prevail. An ideal subsequence, containing

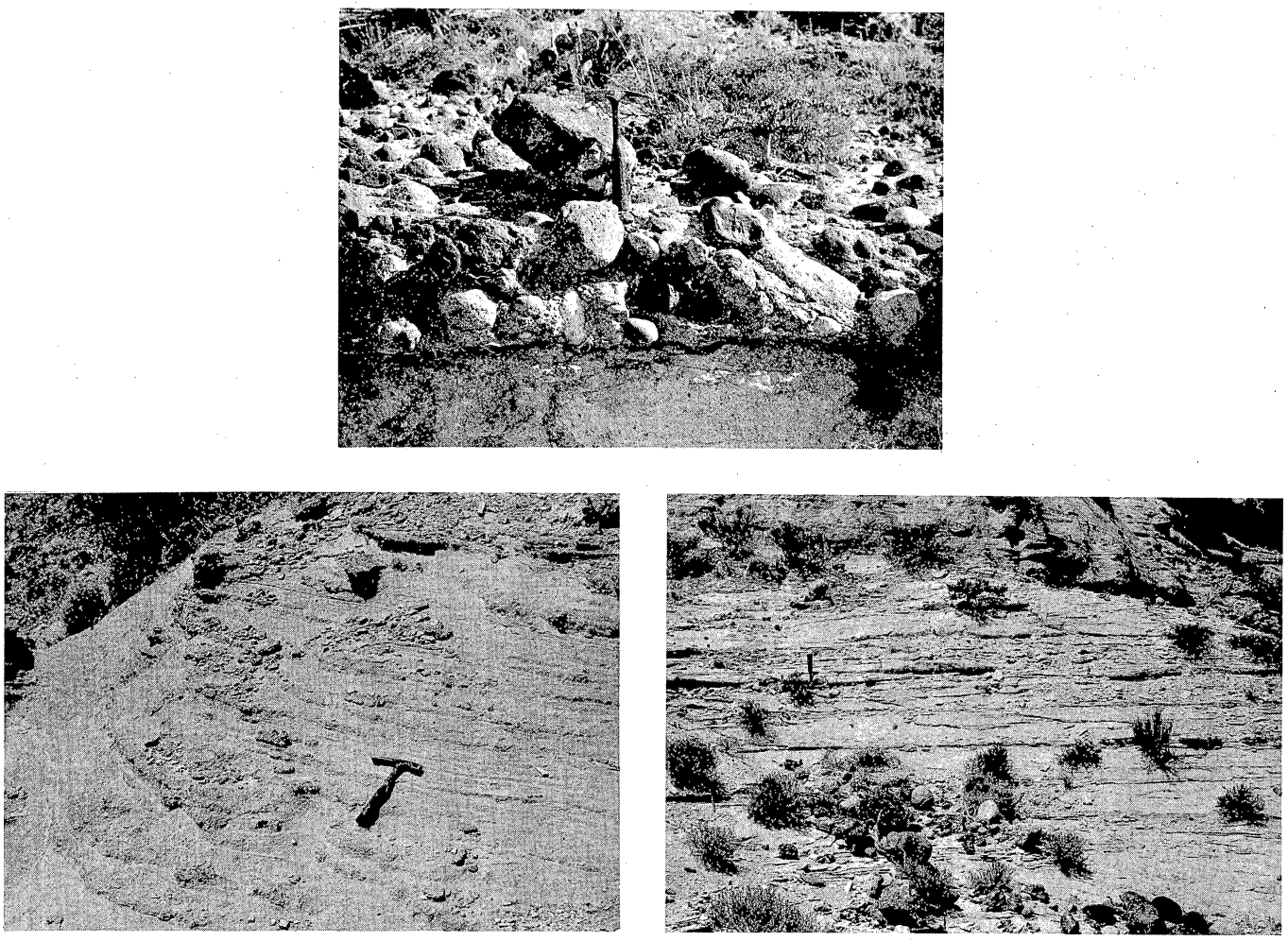

Figure 8. Thick fining-upward sequences of the active apron member. A. Conglomerate armor overlying scour surface at the bottom of the sequence. B. Horizontally bedded sediment from a thick fining-upward sequence. C. Trough crossbedded sediments and horizontally bedded interval of a thick fining-upward sequence.

everything from pebbles through mudrocks, would total 10 m thick. Real subsequences are thinner, totaling a few meters because either the base or top part is missing. In the lower part of the thick fining-upward sequence, the subsequences preserve most of the lower part of the ideal subsequence. In the upper part of the thick fining-upward sequence, the lower part of the ideal subsequence is absent and only the upper part is preserved (Walton, in press).

Individual subsequences are remarkably similar to the channel-fill sequences described by Picard and High (1973, p. 198-201). They describe a sedimentation unit overlying a scoured base that consists of a lag deposit, inclined or horizontally discontinuous stratification, festoon cross-stratification, ripple scale cross-stratification, and horizontal parallel stratification as the result of a single flood which eroded a channel and then back filled it. Picard and High (1973) report that individual cycles are dominated by either the basal parts of the sequence or the upper parts.

The overall thick fining-upward sequence represents flows of successively less intensity, probably deposited in a channel scoured into the apron surface. A likely course of events represented by these deposits began when a major feeder channel was scoured into the pre-existing sediments of the active phase apron. While this scouring took place, a thin lag of cobbles was deposited covering the channel floor. Because cobbles are so rare elsewhere in apron sediments, the lags that over channel floors must represent the selection of coarse fragments from many flows. Hence, the cobble lag represents a long period of mature

activity in the channel. Because of gradient instability or some other cause, feeder channels were gradually abandoned. Each flood during this abandonment process encountered a smaller channel because the deposits of the last one partially filled the water course. Consequently, each flow event was smaller and deposited less of the early parts of the idealized fining-upward subsequence and more of the upper parts that give evidence of less vigorous flow. Virtually the entire channel was eventually abandoned, and only muddy waters deposited sediment in it (Walton, 1977b, in press).

Schumm (1977, p. 246-247, 256-259) described the development of fanhead trenches on dry fans, those characterized by episodic stream flow or mudflow events, and wet fans, which have a constant flow of water. Such fanhead trenching may be closely analogous to the formation of the channels that are filled by the thick fining-upward sequences of the Tascotal. Dry fan channels may result from climatic changes or tectonic activity in the source area or from erosive reduction of the source area, reducing the available sediment (Bull, 1968; Eckis, 1928). Schumm (1977) also described experimental evidence of fanhead trench formation and filling under conditions of constant water discharge as the sediment discharge was reduced by sheet flood deposition near the fanhead and then increased by entrenchment of those deposits and source area channels. They may also be related to decrease of fine sediment production as the rate of volcanism declines, as explained below. This is in some respects similar to the mechanism proposed by Eckis (1928).

Thin fining-upward sequences of the Tascotal are found mostly at the base of the active apron member where they represent distal fan deposits,

but are also present in the rest of that member, interbedded with other rock types. Crossbedded sandstones overlie the interval where thin fining-upward sequences predominate. Their coarser grain size and larger scale sedimentary structures suggest a depositional position more proximal than that of the thin fining-upward sequences, perhaps the mid-fan region. The thick fining-upward sequences are found only in the upper part of the active apron. Overall, this is a progradational sequence with coarser grained sediments that display larger scale crossbeds overlying the finer sediments with smaller scale structures (fig. 9).

In work on deep sea fan deposits, Ricci Lucchi (1975) recognized progradational and aggradational sequences. The active apron member is closely comparable to such systems both in that it accumulates in a sediment dispersal system in which new material is constantly added at the source and in that it shows both kinds of sequences: the overall progradational sequences observed by Ricci Lucchi (1975) are equivalent to the progradational sequences of the Tascotal. The thick fining-upward sequences are equivalent to the aggradational sequences.

Inactive-Phase Apron

The character of the active-phase apron is determined by the fact that the source volcano produced abundant, fine pyroclastic debris which required that streams maintain rather low gradients. This prevented the inclusion of gravel among the sediments. As the eruption of fine pyroclastic debris slowed and then stopped, the supply of such material to streams became less, because erosion quickly stripped the patches of loose material. Streams then cut into flow rocks of the volcanic center and

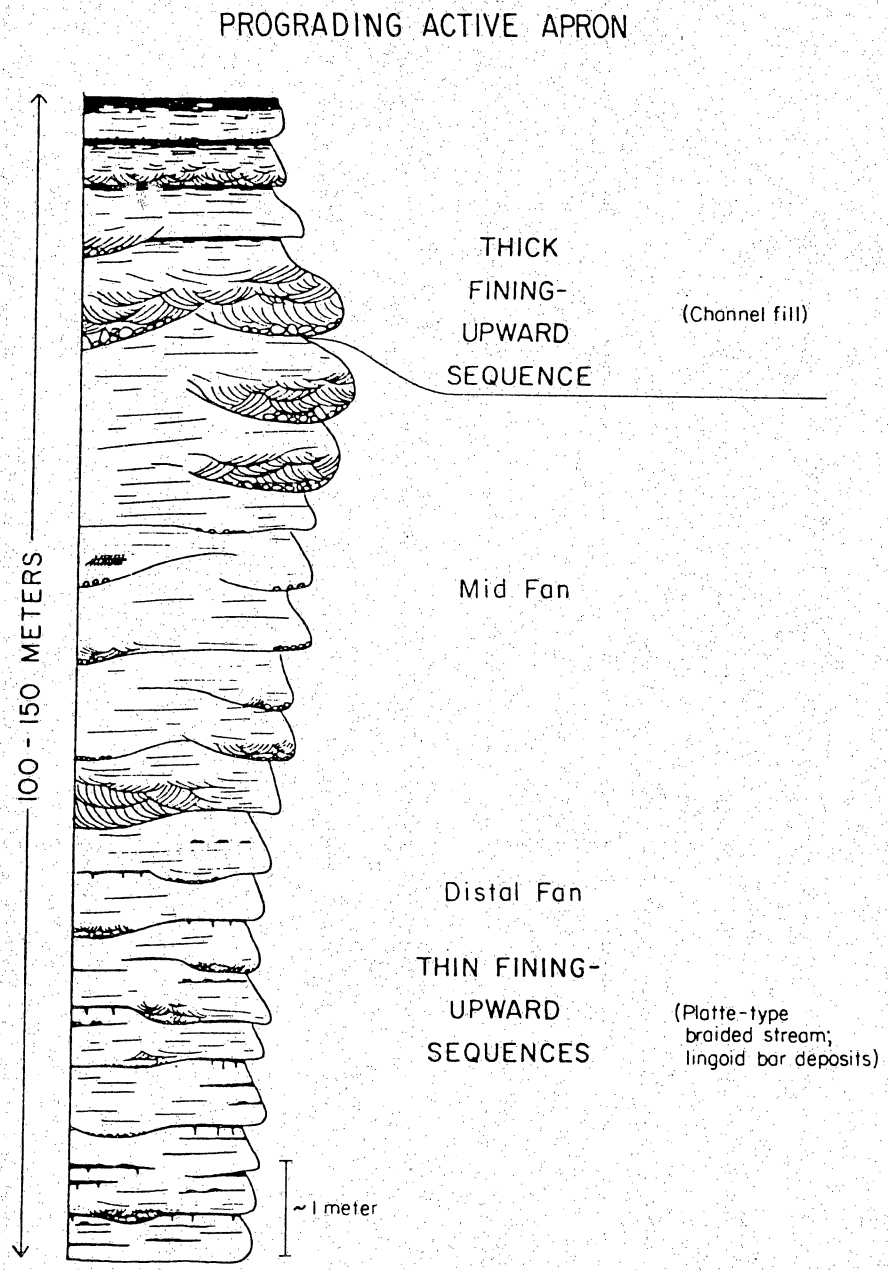

Figure 9A

Figure 9. Comparison of active apron sequence (A) and valley sequence from the lower conglomerate member (B).

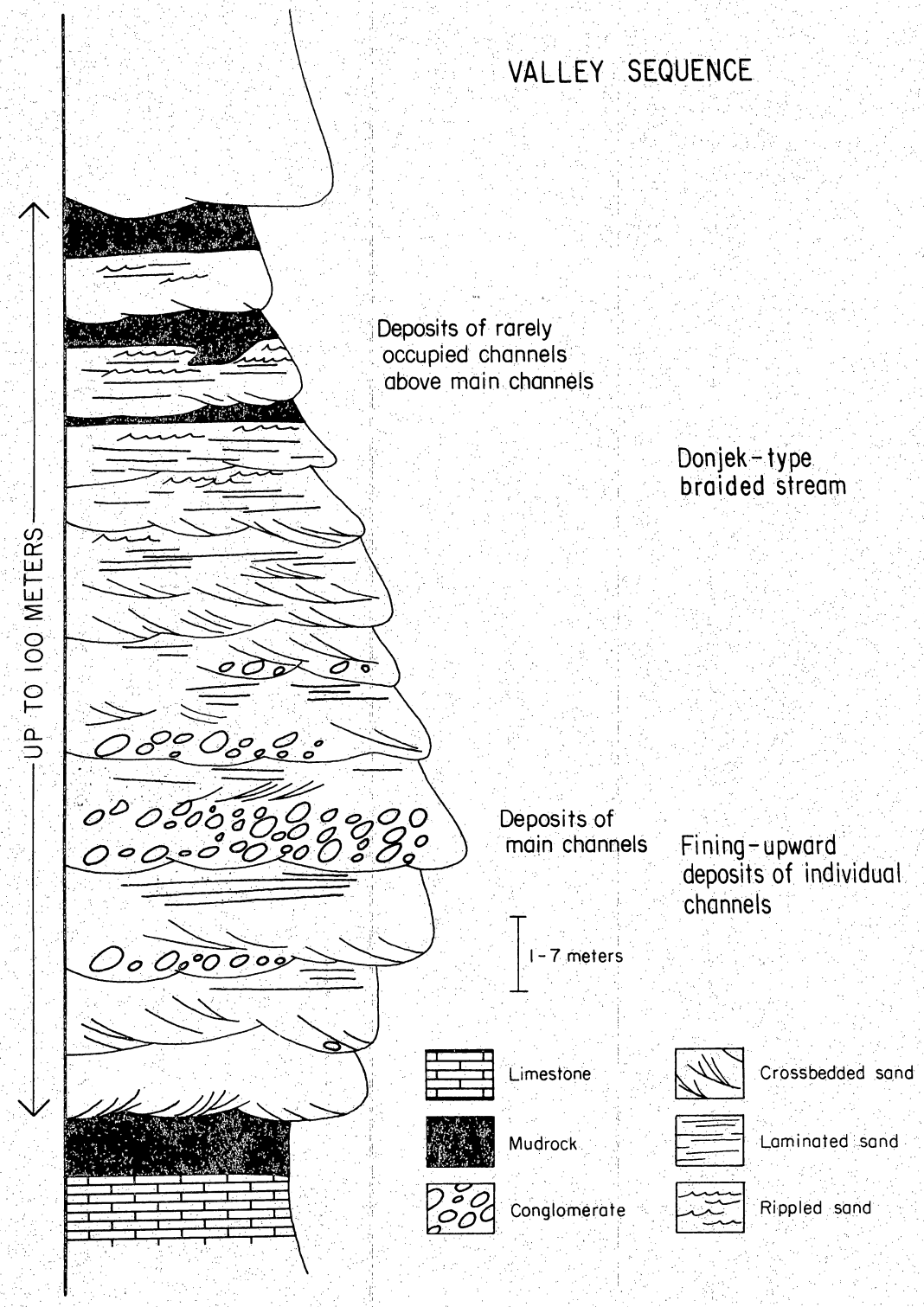
VALLEY SEQUENCE
UP TO 100 METERS
Deposits of rarely occupied channels above main channels
Donjek-type braided stream
Deposits of main channels
Fining-upward deposits of individual channels
1-7 meters
Limestone
Mudrock
Conglomerate
Crossbedded sand
Laminated sand
Rippled sand

Figure 9B

their load became dominated by pebbles and cobbles. With this load, the streams would have to increase their gradients to transport the debris. This increase probably occurred by building a wedge of material partly on the fan head and partly on the toe of the old source region of the active apron (Walton, in press).

The deposits of this phase of the Chinati volcano's history form part of the Perdiz conglomerate and the Perdiz member of the Tascotal (fig. 10). As described by Jordan in chapter VI, the Perdiz clearly was derived from the Chinatis and other highlands to the west and displays facies characteristic of braided streams common on alluvial fans. Jordan has also discovered lateral variations of facies with coarser sediments that include larger scale sedimentary structures close to the source and finer sediments with smaller sedimentary structures away from the Chinatis. Pebble counts, reported above, indicate separate fans of material from different parts of the source.

Intermediate Varieties

One of the individual fans of the Tascotal active apron facies displays some qualities of both the active- and inactive-phase aprons. This fan appears in sections from Cerro Boludo on the south to the Peñitas Ranch in the north and lies directly east of the Chinati Mountains, corresponding to Fan 2 defined by conglomerate clast types. In the lower Tascotal, its southerly extent is even greater, almost as far south as Wire Gap, but this early southern extent is overlain by more normal apron sediments in a section on San Jacinto Mountain and one on La Viuda.

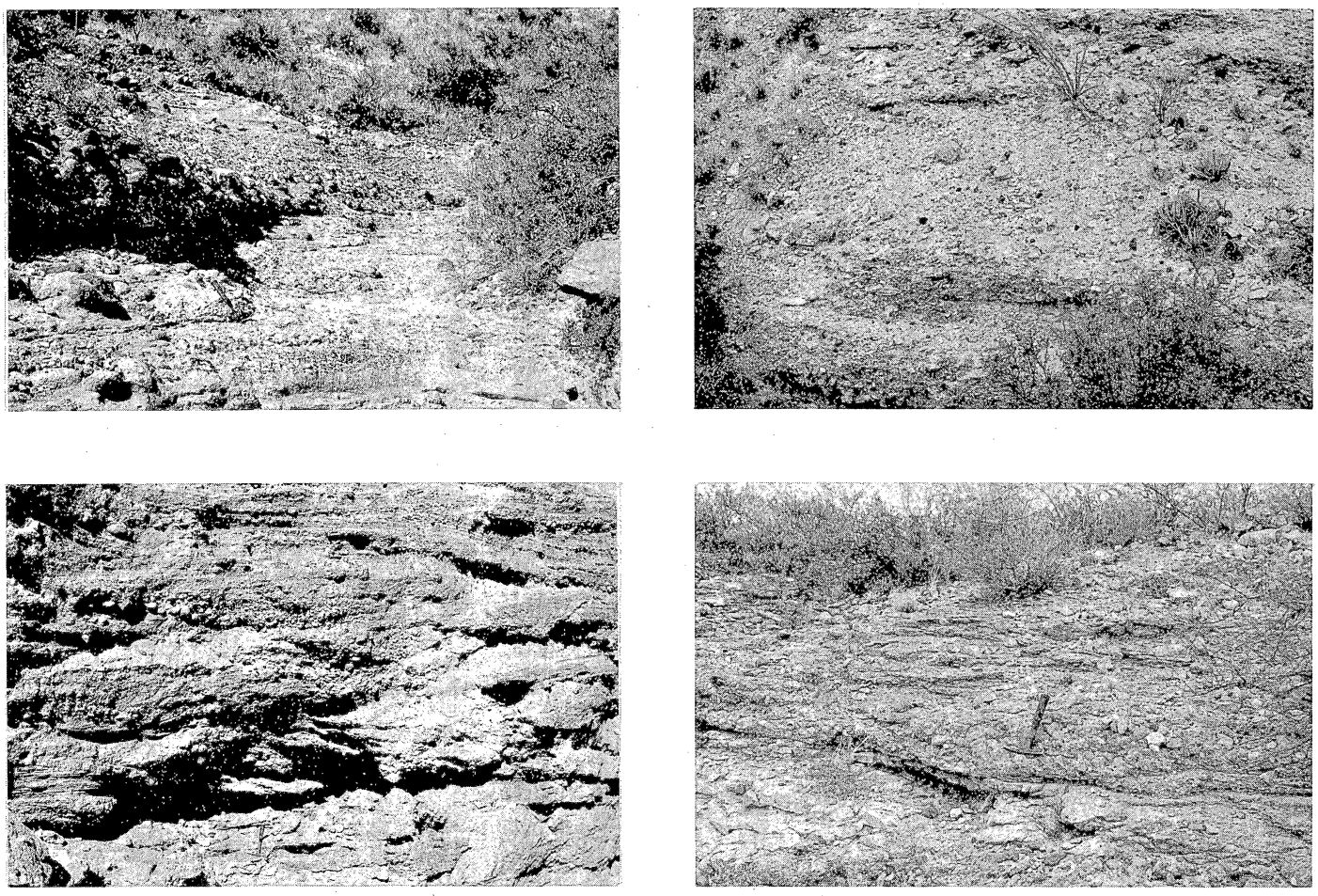

Figure 10. Conglomerate members of the Tascotal. A. Limestone clast-rich gravels and interbedded sands of the lower conglomerate member at the Murphy Bennett section. B. Conglomerates of the Solitario fan member contains clasts of Paleozoic cherts exposed in the core of the uplift. C and D, Perdiz gravels.

Most of the sediment in this Tascotal fan is similar to that in the other active-apron fans. This intermediate fan includes sheet-like beds of pebble and some cobble conglomerates that can be mapped as apparently continuous layers from one edge of the fan to the other. These conglomeratic intervals are up to 10 m thick, and include sandy conglomerates and sandstone intervals.

These beds contain clasts of blue amphibole rhyolite and a particular trachyte that, together with transport directions measured on imbricated pebbles, indicate derivations from the region of the Cienega Mountains and regions north and west of those mountains. This area is underlain by volcanic and intrusive rocks that are older than those exposed in the high Chinatis to the northwest (Rix, 1953; Cepeda, 1977). A plausible interpretation of this area is that it represents an extinct area of volcanism of a Chinati volcanic center larger than the caldera mapped by Cepeda (1977). If so, it might have been less completely covered by fine pyroclastic debris than were the source areas of the active-apron fans that lay north and south of it. Therefore, it should have a character intermediate between that of the active apron and that of an inactive apron.

Conglomerates are distinctly more common in the upper part of this fan than in the upper part of the other parts of the active apron member. In the area where it is present, furthermore, the eolian member is absent, suggesting that it did not have to adjust its gradient greatly when passing from active to inactive status. The passage from active apron member to inactive apron in the Perdiz Conglomerate appears to be quite gradational for this unit.

Eolian Member

Large-scale crossbedding early directed attention to the existence of eolian deposits in the Tascotal (McKnight, 1970; Dietrich, 1966). Some areas have sets of crossbeds up to 25 m thick, notably on the face of Tascotal Mesa due south of Casa Piedra. Because large scale crossbeds may be formed by processes other than eolian deposition, it is necessary to describe the bedding of the eolian member and to point out in it the features ascribed by several authors to eolian deposition (fig. 11).

On the scale of individual sedimentation units, features that can be interpreted with reference to the article by Hunter (1977) are fairly common. The eolian member consists of near-horizontal strata, especially near the top, and inclined strata that dip at angles of 20° to 30°. Most of the near-horizontal layers are millimeter-scale laminae in which slight size differences between adjacent laminae are visible. Only in exceptional cases can these laminae be seen to be individual coarsening-upward sequences a few grains thick. Hunter (1977) reports that this kind of laminae is formed by traction transportation of grains along horizontal or gently sloping surfaces. The bedform can either be ripples or plane bed, with ripples more common. Eolian ripples have the coarsest grains at their crests and commonly do not have interval cross stratification. Migration with accumulation of sediment leads to formation of thin, coarsening-upward laminae up to a few millimeters thick. The thickness depends on the angle of climb; the degree to which the upward-coarsening nature of the individual laminae is developed depends upon the angle of climb of the ripples and the degree of sorting of the sediment available.

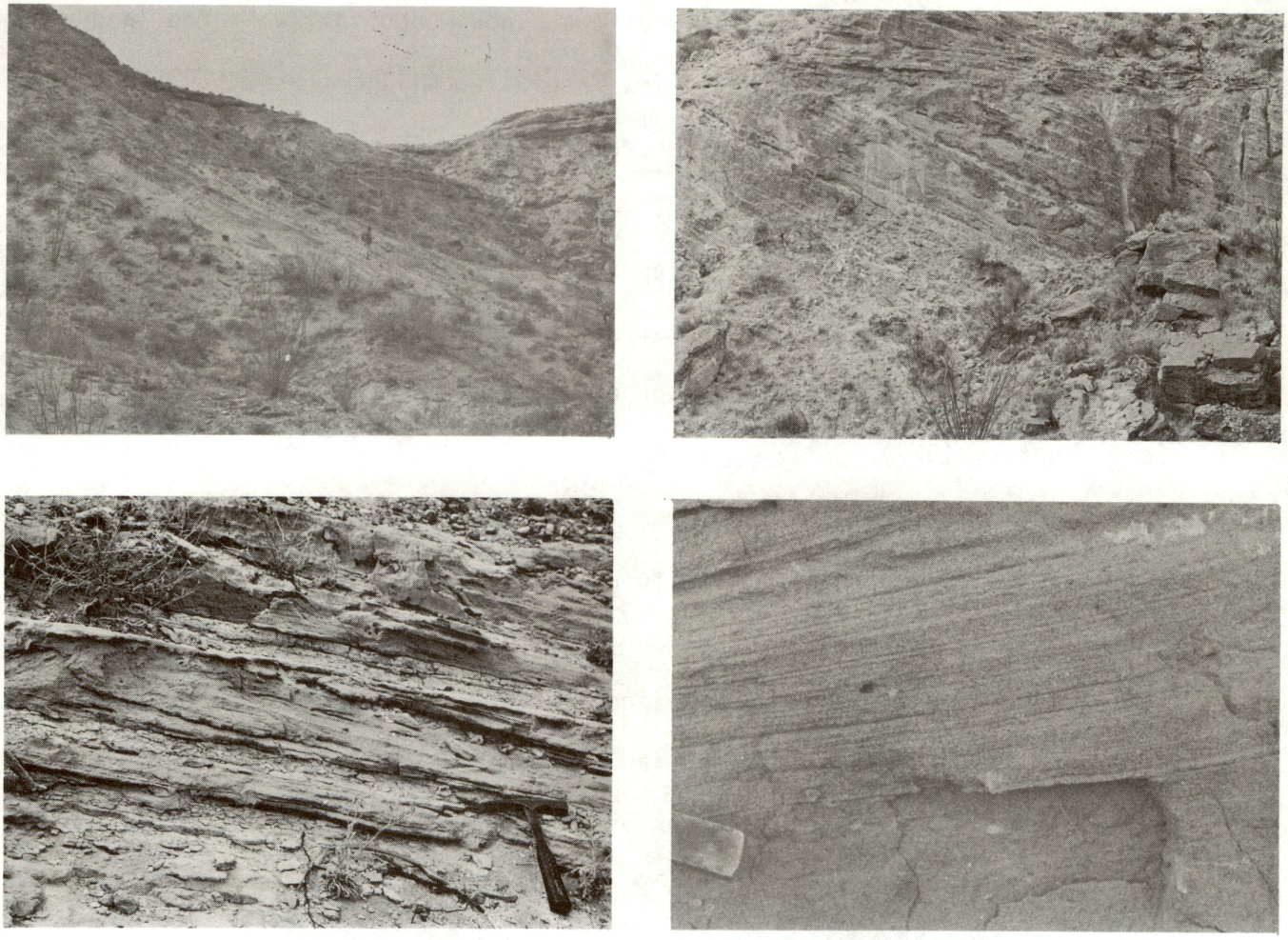

Figure 11. Eolian member of the Tascotal. A. Large-scale crossbeds dipping to the north (right). B. Large-scale crossbeds overlain by first-order bounding surface. Ocotillo bush in foreground is about 2 m tall. C. Second-order surfaces and crossbeds. D. Sub-critically climbing translatent strata (Hunter, 1977), the laminae formed by passage of wind ripples. E. Second-order surfaces (Brookfield, 1977) near the top of a dune in the Tascotal eolian member. Notice the rollover of the beds where the top of the dune is preserved.

The steeply dipping beds are of two kinds. Beds of laminated sand 2 to 10 cm thick in which the laminae are a few millimeters thick, are probably the result of what Hunter calls grainfall deposition, the deposition of bedload of wind at points of flow separation, such as dune crests. Structureless crossbeds up to 12 cm thick which form long (greater than 3 m) lenses, or are tabular at the scale of the outcrop exposures, are probably the results of avalanches of material down dune slipfaces (c.f. Hunter, 1977).

Brookfield (1977) has analyzed the larger scale bedding planes of eolian deposits and related them to activity of elements of the eolian bedform hierarchy proposed by Wilson (1972). Near horizontal surfaces that are 0.3 to 17 m apart are called first-order surfaces by Brookfield and are related to passage of eolian bedforms of the largest scale, draas, over an area. Second-order bounding surfaces, which are truncated by first-order ones, normally dip downwind and are commonly about 1 m apart. Commonly they are convex upwards because they are nearly horizontal at the top of sets and dip steeply in the lower parts of sets. Brookfield (1977) attributes them to passage of normal eolian dunes across draas. Crossbedding between these second-order surfaces dips downwind at an angle steeper than is characteristic of the surfaces, giving rise to the horsetail crossbedding described by McKee (1966) and visible in some outcrops of the Tascotal eolian member (fig. 11E). Brookfield (1977) equates third-order surfaces and reactivation surfaces and reports that they occur within crossbed sets.

Within the Tascotal Eolian member, first-order surfaces and cross-bedding are most common. First-order surfaces are nearly horizontal and several meters to a few tens of meters apart. Second-order surfaces are visible only under favorable circumstances (fig. 11).

Lower Conglomerate Member

The lower conglomerate member is well exposed at the Murphy Bennett section, near the south end of the northeast-facing escarpment of the Tascotal Mesa. Limestone-rich gravels, sandstones, and some tuff, mapped by Dietrich (1966) as the lower 150 to 200 feet of the Fresno Formation along the Rio Grande near the Boundary and Water Commission Gauging Station between Presidio and Redford, can probably also be assigned to this member. At the Murphy Bennett section, about 110 m of section can confidently be assigned to this member. Underlying rocks totaling about 35 m are rather poorly exposed and not easily attributable to any member. They do not seem to have the character of apron sediments, however, and are considered as part of the lower conglomerate unit even though they are mostly finer grained. All of the lower 146 m of the Murphy Bennett section will thus be assigned to this member. Unfortunately, the base of the Tascotal is concealed at this outcrop. This interval is laterally equivalent to most of the active apron facies of the Wire Gap section and lies only 5 km to the southeast of it.

The lower conglomerate consists mostly (80 percent) of sandstone; the remainder is conglomerate, some beds of pink clay, and one notable interval of limestone. The conglomerate contains clasts of carbonate rock, chert, and red siltstones and volcanic rock, including light and

dark felsitic rocks, scoria, and some Mitchell Mesa clasts, a mixture indicating a diversity of sources.

Conglomerates and sandstones are arranged in fining-upward units about 1 to 7 m thick. Conglomerate beds are structureless or contain imbricated clasts. Most sand-rich intervals contain low-angle crossbedding or horizontal bedding. Only a few display high-angle crossbeds. A few individual fine-grained beds display indications of desiccation such as mud cracks in some clay beds and bioturbation structures in some sands. The presence of fining-upward sequences of different thickness, the evidence of desiccation, and the abundance of coarse sediment suggest interpretation of this as the deposit of a braided rather than a meandering fluvial system.

Within the section, fining-upward sequences and other beds are arranged in groups in which all members of the group share common grain size character. The interval from 74 to 84 m above the base of the section is very conglomeratic, containing beds of pebble and cobble conglomerate but only a little sand. Above and below this, for example, at about 110 m above the base or at about 50 m, are fining-upward cycles of sand-rich sediment. Clay is common in the interval from 122 m to 133 m. This is suggestive of types of braided systems (Williams and Rust, 1969) in which different parts of the system occur at different topographic levels and are occupied by water flows with different current velocites at different times. The lowest parts of the system are occupied continuously, higher parts less and less commonly, with the highest parts active only during the most severe floods. The lowest

parts also have the greatest current velocity and are the sites of deposition of the coarsest sediment and largest scale sedimentary structures. Miall (1977) calls these Donjek-type braided systems (fig. 9).

The lower conglomerate interval of the Tascotal could be interpreted as a fan derived from a source to the west but south of the Chinatis or as a part of a valley system that was a regional drainage system for the area. Two features argue for its interpretation as a braided stream that was part of the regional drainage system. The first of these features is the variability of clast types (Walton, 1977a). It includes both chert from the Solitario Uplift to the south and felsic VRF's that certainly had to come from the west or northwest because few such rocks are known from the south that are old enough. Consequently, it appears to have come from a number of sources in contrast to individual fans in the Tascotal that came from small areas or single sources. Its grain size is more variable than that of other parts of the Tascotal, a feature accounted for most easily by reference to braided stream models. Sandstone-rich intervals are quite different from intervals of similar grain size in the active apron facies.

Finally, postulating a drainage axis north of the Solitario-derived fan and south of the active apron member fans allows a route by which water could flow out of the area near the present location of the Bofecillos Mountains. Thickness information (McKnight, 1970) and zeolite zonation both indicate that the Terlingua Monocline-Contrabando region was higher than the Bofecillos area. Similarly, paleocurrent and clast compositions indicate that highlands lay to the west of the Bofecillos. Water that

would flow from the west and east into this basin had to flow out either its north or south end. The lower conglomerate member may record that flow out the north end and around the flank of the Solitario, but south of the Chinati apron.

Other Members of the Tascotal

Three other members are recognized in the Tascotal: the Solitario fan, southern apron, and Fresno volcanic members. The Solitario fan member is poorly exposed, but appears to consist of gravel-rich deposits, displaying features similar to those of the Perdiz. The Fresno volcanic member is adequately described by McKnight (1970) and Dietrich (1966). The reader should bear in mind the differences in stratigraphic usage between their reports and that employed here.

Only the southern apron member merits comment. It superficially resembles the active-apron member of the Wire Gap region, consisting of zeolitized volcanic sandstones that contain very few interbeds of claystone or of conglomerate in a sequence over 100 m thick. The abundance of glass among its primary constituents argues for its formation as the sedimentary apron of an active volcano. In detail, however, it is different. Zeolitized intervals in it are commonly light green, especially in the lower part of the section. The green color arises from a green montmorillonite clay coating on each grain. This texture is similar to that in most Tascotal rocks, but why the clay layer is better developed in some places than in others is unclear.

More important differences characterize the sedimentary structures of the two members. At the sections examined, the southern apron member

contains few thin fining-upward sequences and few if any thick fining-upward sequences. Instead it consists mostly of crossbedded fine to medium sandstone similar to the medial part of the active-apron member and probably is the result of deposition on linguoid bars in a Platte-type braided stream (Miall, 1977). Some tendency for an upward increase in the abundance of crossbedding exists, similar to that in the active-apron member. Paleocurrent studies of this unit were not extensive, but several measurements of crossbedding made at outcrops south or southwest of the Bofecillos Volcano indicate a southwesterly or westerly source. Both the current indicators and the composition indicate that the southern apron member is not the active-phase apron of that volcano.

Which volcano was the source of sediment is not known. The only other volcano that is nearby is the Sierra Rica complex, which on the basis of reconnaissance studies is believed to be a volcanic center, but was most active late in the time period in which the Tascotal was deposited (Henry, oral communication, 1978). Sierra Rica lies almost due south, not southwest, of the southern apron member. Nevertheless, it is very tempting to relate this member and the growing Sierra Rica center. If this relationship exists, the southern apron member must be younger than the known history of the Chinatis and the active apron around the center.

URANIUM FAVORABILITY--GEOLOGICAL ANALYSIS

In order to form secondary uranium ore deposits, the metal must be released from a source, transported in ground water, and concentrated by

some trap. The abundance of silicic volcanic glass in four of the seven members of the Tascotal, the active-apron, southern apron, lower conglomerate, and the eolian members, implies that the whole formation is favorable, at first analysis, as a source of uranium. In addition, all sedimentary members of the Tascotal initially had excellent intergranular porosity and probably had good permeability. Even the Fresno volcanic member could have permeability zones developed along fractures and flow boundaries, and in vesicular zones.

Several factors must temper this favorable initial analysis: (1) The Tascotal contains virtually no organic matter, so conventional roll-front or other redox secondary deposits are unlikely. Deposits, if present, must have accumulated by some other means. Unfortunately, if no good model of ore deposit formation exists, exploring for those deposits is a hit-or-miss affair with little chance of success. (2) The analysis of diagenesis presented in chapter VI suggests that little uranium was actually released as glass altered in active apron sediments. (3) Diagenesis has reduced the permeability in sediments that initially contained glass.

The analysis of uranium potential in volcanic sediment sequences presented in the previous section of this report suggests that the valley facies, here represented by the lower conglomerate member, is the most likely host of deposits. Effective release of uranium is more likely in this member than in apron sediments, and permeability channels do exist in this member. But even the lower conglomerate contains little or no reducing material in exposures on Tascotal Mesa. If uranium traps

existed in the lower conglomerate member, they have been eroded away, or lie still buried under the Rawls Formation.

CONCLUSIONS

(1) The name "Tascotal" should be applied to the strata Maxwell and Dietrich (1970) called "Fresno" as well as to the white rocks on Tascotal Mesa and along Alamito Creek. In order to understand their mode of formation, the investigator should study rock intervals that have boundaries that are nearly time surfaces. By choosing such boundaries, lithologically diverse masses of rock will be grouped together, thus aiding attempts to reconstruct the geomorphology of the area at the time the rocks were formed.

(2) The Tascotal Formation so defined consists of seven members that correspond to the geomorphic entities where rock was forming during the period after the Mitchell Mesa Rhyolite formed and before the time that widespread outpouring of lava led to accumulation of the Rawls Formation.

(3) The active apron and Perdiz members record the history of the Chinati volcanic center during the period after collapse of the Chinati Caldera and emplacement of the Mitchell Mesa Rhyolite.

(4) The active-apron member formed mostly from sand-sized material produced by the Chinati Volcano during its period of activity after caldera collapse in the Chinatis led to emplacement of the Mitchell Mesa Rhyolite as an ash-flow tuff. The active apron consist of deposits of Platte-type braided streams that grade upward from distal fan to mid-fan.

Deposition was on and around linguoid bars in unconfined flow. The proximal part of the fan is represented by the overlying channel-fill deposits that accumulated in fanhead trenches.

(5) The eolian member accumulated after the active-apron member in a period during which streams on the apron around the Chinatis readjusted to the reduced sediment supply and coarser sediment caliber characteristic of the inactive phase of apron sedimentation. Eolian sediments include laminated beds formed by passage of eolian ripples over the sediment surface, beds that accumulated by grain fall from the air, and beds modified by avalanching on steep dune slopes.

(6) The Perdiz member accumulated after cessation of activity in the Chinati volcanic center forming the inactive phase apron around that center. In addition to sediments derived directly from the volcano, it includes clasts of limestone derived from south of the Chinatis. The Perdiz member of the Tascotal is continuous with the Perdiz Conglomerate.

(7) Activity at the Bofecillos volcanic center began late in the period during which the Tascotal formed. Lava flows from this center make up most of the Fresno volcanic member of the Tascotal. This member overlies or interfingers with three members of the southern area of the Tascotal, the southern apron member, the Solitario fan member, and part of the Perdiz member.

(8) The Solitario fan member occurs north and west of the Solitario Uplift. It consists of poorly exposed conglomerates containing abundant CRF's and chert fragments, including red or green fragments eroded from outcrops of Paleozoic rocks in the core of the uplift. Probably this

member formed as a series of alluvial fans.

(9) The southern apron is the active apron of a volcano, as yet unidentified, that was similar to the Chinatis in that it produced abundant glass. The southern apron is the result of deposition in Platte-type braided rivers.

(10) The lower conglomerate member occurs between the active-apron deposits of the Chinatis, on the north, and the Solitario fan and southern apron members to the south. It consists of sandstones and some conglomerates deposited in a Donjek-type braided river.

(11) The Tascotal was deposited between 31.5 and 26.2 million years ago. The active-apron member was probably deposited early in this period of time because the Chinati Mountain center was active until about 31 million years age (McDowell, 1978). Simultaneously, the Solitario fans and the valley system, represented by the lower conglomerate member, were active. The southern apron member also lies at the base of the Tascotal, but its period of formation may be later. The remaining 4 or 5 million years of the history of the Tascotal saw accumulation of the eolian member, the Perdiz member, and the Fresno volcanic member. Activity at the Bofecillos Volcano continued after formation of the Fresno flows to form some of the Rawls flows (McKnight, 1970). This implies that the Fresno volcanic member probably formed quite late in the history of the Tascotal, perhaps only 27 to 28 million years ago.

(12) The most favorable site for formation of secondary uranium deposits in the Tascotal is in the valley facies--the lower conglomerate member. The release, migration, and accumulation of uranium is more

likely in this member than in any of the others. Unfortunately, this member is poorly exposed and not well understood. Even in it, lack of reducing material prevents formation of oxidation-reduction deposits.

REFERENCES

Boothroyd, J. C., and Ashley, G., 1975, Process, bar morphology, and sedimentary structures on braided outwash fans, northeastern Gulf of Alaska: Society of Economic Paleontologists and Mineralogists Special Publication 23, p. 193-222.

Brookfield, M. E., 1977, The origin of bounding surfaces in ancient aeolian sandstones: Sedimentology, v. 24, p. 303-332.

Bull, W. B., 1968, Alluvial fans: Journal of Geological Education, v. 16, p. 101-106.

_____ 1972, Recognition of alluvial-fan deposits in the stratigraphic record: Society of Economic Paleontologists and Mineralogists Special Publication 16, p. 63-83.

Burt, E. R., 1970, Petrology of the Mitchell Mesa Rhyolite, Trans-Pecos Texas: The University of Texas at Austin, unpublished Ph.D. dissertation.

Cepeda, J. C., 1977, Geology and geochemistry of the Chinati Mountains, Presidio County, Texas: The University of Texas at Austin, unpublished Ph.D. dissertation.

_____ 1978, The Chinati Mountains caldera, Presidio County, Texas, in Walton, A. W., compiler, Cenozoic geology of the Trans-Pecos volcanic field of Texas, Walton, A. W., Lawrence, Kansas.

Clark, H. C., and Gilliland, M. W., 1978, Paleomagnetism of early Tertiary volcanics, Big Bend, Texas; in Walton, A. W., compiler, Cenozoic geology of the Trans-Pecos volcanic field of Texas, Walton, A. W., Lawrence, Kansas.

DeFord, R. K., 1958, Tertiary formations of Rim Rock County, Presidio County, Texas: Texas Journal Science, v. 10, p. 1-37.

Dietrich, J. W., 1966, Geology of Presidio area, Presidio County, Texas: University of Texas, Austin, Bureau of Economic Geology Quadrangle Map 28.

Eckis, R., 1928, Alluvial fans of the Cucamonga district; Southern California: Journal of Geology, v. 36, p. 224-247.

Erickson, R. L., 1953, Stratigraphy and petrology of the Tascotal Mesa quadrangle, Texas: Geological Society of America Bulletin, v. 64, no. 12, pt. 2, p. 1356-1386.

Fisher, R. V., 1961, Proposed classification of volcaniclastic sediments and rocks: Bulletin of the Geological Society of America, v. 72, p. 1409-1414.

Fisher, W. L., and McGowen, J. H., 1967, Depositional systems in the Wilcox Group of Texas and their relationship to occurrence of oil and gas: Gulf Coast Association of Geological Societies Transactions, v. 17, p. 105-125.

Folk, R. L., 1968, Petrology of sedimentary rocks: Austin, Texas, Hemphills.

Freeman, W. E., and Visher, G. S., 1975, Stratigraphic analysis of the Navajo Sandstone: Journal of Sedimentary Petrology, v. 45, p. 651-668.

Galloway, W. E., 1977, Catahoula Formation of the Texas Coastal Plain: Depositional systems, composition, structural development, ground water flow history, and uranium distribution: The University of Texas at Austin, Bureau of Economic Geology Report of Investigations 87.

Goldich, S. S., and Elms, M. A., 1949, Stratigraphy and petrology of the Buck Hill Quadrangle, Texas; Geological Society of America Bulletin, v. 60, p. 1133-1182.

Goldich, S. S., and Seward, C. L., 1948, Green Valley-Paradise Valley field trip: West Texas Geological Society Fall Field Trip Guidebook, October 29-31, 1948, p. 11-36.

Hunter, R. E., 1977, Basic types of stratification in small eolian dunes: Sedimentology, v. 24, p. 361-387.

Maxwell, R. V., and Dietrich, J. W., 1970, Correlation of Tertiary rock units, West Texas: The University of Texas at Austin, Bureau of Economic Geology Report of Investigations 70.

McDowell, F. W., 1978, Potassium-argon dating in the Trans-Pecos Texas volcanic field: in Walton, A. W., compiler, Cenozoic geology of Trans-Pecos volcanic field of Texas, Walton, A. W., Lawrence, Kansas.

McKee, E. D., 1966, Structures of dunes at White Sands National Monument, New Mexico: Sedimentology, v. 7, p. 1-69.

McKnight, J. R., 1970, Geology of Bofecillos Mountains area, Trans-Pecos Texas: The University of Texas at Austin, Bureau of Economic Geology Quadrangle Map 37.

Miall, A. D., 1977, A review of the braided-river depositional environment: Earth Science Review, v. 13, p. 1-62.

Parker, D. F., 1976, Petrology and eruptive history of an Oligocene trachytic shield volcano, near Alpine, Texas: The University of Texas at Austin, Ph.D. dissertation.

_____ 1978, The Paisano Volcano I: Stratigraphy, age, and petrogenesis: in Walton, A. W., compiler, Cenozoic geology of the Trans-Pecos volcanic field of Texas, Walton, A. W., Lawrence, Kansas.

Picard, M. D., and High, L. R., Jr., 1973, Sedimentary structures of ephemeral streams: New York, Developments in Sedimentology, v. 17.

Ramsey, J. W., 1961, Perdiz conglomerate, Presidio County, Texas: The University of Texas at Austin, M.A. thesis.

Ricci Lucchi, R., 1975, Depositional cycles in two turbidite formations of northern Apennines (Italy): Journal of Sedimentary Petrology, v. 45, p. 3-43.

Rix, C. C., 1953, Geology of Chinati Peak Quadrangle, Presidio County, Texas: The University of Texas at Austin, Ph.D. dissertation.

Schumm, S. A., 1977, The fluvial system: Wiley-Interscience, New York, John Wiley and Sons.

Walton, A. W., 1977a, Petrology of volcanic sedimentary rocks, Vieja Group, Southern Rim Rock Country, Trans-Pecos Texas: Journal of Sedimentary Petrology, v. 47, p. 137-157.

_____ 1977b, Oligocene volcanic sedimentary apron in Trans-Pecos Volcanic Field of Texas (abs.): AAPG-SEPM Program and Abstracts, Washington, D. C. meeting, June 12-16, 1977, p. 108.

_____ in press, Volcanic sediment apron in the Tascotal Formation (Oligocene?), Trans-Pecos Texas: Journal of Sedimentary Petrology.

Williams, P. F., and Rust, B. R., 1969, The sedimentology of a braided river: Journal of Sedimentary Petrology, v. 39, p. 649-679.

Wilson, I. G., 1972, Aeolian bedforms-their development and origins: Sedimentology, v. 19, p. 173-210.

Wilson, J. A., Stevens, J. B., and Stevens, M. S., 1978, New cross-section from southern Davis Mountains to northeast Solitario: in Walton, A. W., compiler, Cenozoic geology of the Trans-Pecos volcanic field of Texas: Walton, A. W., Lawrence, Kansas, p. 100-102.

Appendix I: Clast composition of Tascotal conglomerates.

	1*		2		3		4		5		6	
	P**	C**	P	C	P	C	P	C	P	C	P	C
Limestone	21	7	13	1	25	22	8	8	49	30	28	28
Chert - black	7	1	2		3	6		1				
white												
green									8	5	2	3
red												
Sandstone and conglomerate	4	3	1	1	3	7		1	4	5		
Siltstone		2										
Felsic VRF's (not included elsewhere)	7	13	77	65	76	50	53	29	37	49	41	22
Mafic VRF's	1	2		3				1			1	1
Mitchell Mesa	29	47	3	11	2	2	16	36		9	2	12
Blue amphibole rhyolite		1			1							
Scoria	17	23	2	9		9	22	25	2	7	9	22
Pumice												
Distractive trachyte												
Aenigmatite (?) trachyte												
Biotite-bearing rocks												
Intrusive rocks												
Intraclasts	14	1	2	10		4					12	2
TOTAL	100	100	100	100	110	100	100	100	100	105	95	90

Appendix I: Clast composition of Tascotal conglomerates. (Continued)

	7		8		9		10		11		12	
	P	C	P	C	P	C	P	C	P	C	P	C
Limestone	22	15	12	21	40	36				1	10	5
Chert - black	1	6	1	3	5	8					5	2
white												
green	1											
red	1	1										
Sandstone and conglomerate	4	4	1	1		1						2
Siltstone												
Felsic VRF's (not included elsewhere)	64	47	86	69	52	47	46	50	48	44	41	47
Mafic VRF's	1										15	13
Mitchell Mesa		16		1		1					6	9
Blue amphibole rhyolite			1	1	3	3	46	36	50	48	6	7
Scoria	4	8		4		4	8	14	2	7	16	14
Pumice												
Distractive trachyte												
Aenigmatite (?) trachyte												
Biotite-bearing rocks												
Intrusive rocks												
Intraclasts	3	5									1	1
TOTAL	101	102	101	100	100	100	100	100	100	100	100	100

Appendix I: Clast composition of Tascotal conglomerates. (Continued)

	13		14		15		16		17		18	
	P	C	P	C	P	C	P	C	P	C	P	C
Limestone											3	
Chert - black												
- white												
green												
red												
Sandstone and conglomerate										1		2
Siltstone												
Felsic VRF's (not included elsewhere)	48	19	30	30	59	50	44	48	94	81	39	29
Mafic VRF's			7	7					5	4		1
Mitchell Mesa	5	8								6	12	6
Blue amphibole rhyolite			65	60	12	14	32	40		5	28	53
Felsites					25	22	12	5				
Scoria	34	68	3	2	1	6	12	7			8	6
Pumice		1									6	3
Distractive trachyte												
Aenigmatite (?) trachyte					3	7						
Biotite-bearing rocks									1	3		
Intrusive rocks												
Intraclasts	8	4				1						
TOTAL	95	100	105	99	100	100	100	100	100	100	96	100

Appendix I: Clast composition of Tascotal conglomerates. (Continued)

	19		20		21		22		23		24	
	P	C	P	C	P	C	P	C	P	C	P	C
Limestone					67	34						
Chert - black					1	1						
white						1						
green												
red					1	1						
Sandstone and conglomerate					1	2						
Siltstone												
Felsic VRF's (not included elsewhere)	80	72	56	47	23	45	58	58	65	53	94	90
Mafic VRF's	6	2	18	24	5	7			1	1	2	4
Mitchell Mesa	3	3		1							1	
Blue amphibole rhyolite						4	17	19	10	14	1	2
Scoria	6	17	16	19	2	5			1	7	2	4
Pumice			7	7			18	17	23	26		
Distractive trachyte												
Aenigmatite (?) trachyte												
Biotite-bearing rocks			3	2								
Intrusive rocks	5	6					7	8				
Intraclasts												
TOTAL	100	100	100	100	100	100	100	102	100	101	100	100

Appendix I: Clast composition of Tascotal conglomerates. (Continued)

* Localities

1. Wire Gap Section, 127 m, active-apron member
2. Wire Gap Section, lower conglomerate of Perdiz member
3. Wire Gap Section, middle conglomerate of Perdiz member
4. Murphy Bennett Section, lowest conglomerate bed, lower conglomerate member
5. Murphy Bennett Section, about 50 m, lower conglomerate member
6. Murphy Bennett Section, about 80 m, lower conglomerate member
7. Murphy Bennet Section, lowest conglomerate bed of Perdiz member
8. Hill 4824 on Tascotal Mesa, northwest of Wire Gap, lowest conglomerate bed of Perdiz member
9. Elliott's Box Canyon, due south of Casa Piedra on escarpment of Tascotal Mesa, lowest bed of Perdiz member
10. Conglomerate bed, west of Casa Piedra Road, due west of Cerro Boludo, active-apron member (above #11)
11. Conglomerate bed, west of Casa Piedra Road, due west of Cerro Boludo, active-apron member (below #10)
12. Tascotal Mesa North Section, lowest conglomerate bed of Perdiz member
13. Base of thick fining-upward sequence at 40 m in the Tascotal Mesa North Section, active apron
14. Perdiz Conglomerate, on Big Bend Ranch, 4 miles WSW of Casa Piedra
15. Upper Tascotal, active apron, Soucada Creek, NNW of Casa Piedra
16. Perdiz Conglomerate, just north of Harper Ranch Headquarters
17. Penitas Ranch #1 section, 40 m
18. San Jacinto Ranch, at Road, due north of hill 4824, base of Tascotal, active-apron member
19. Bishop Ranch #1 Section, 31 m, active-apron member
20. Rock House Ranch, canyon north of Headquarters, uppermost exposed beds, Perdiz Conglomerate
21. Marfa-Redford Road, Perdiz Conglomerate
22. West foot of Cerro Boludo, base of active-apron member

Appendix I: Clast Composition of Tascotal conglomerate. (Continued)

* Localities (Continued)

23. Two miles south of Plata, just north of railroad crossing, active-apron member
24. Howard Ranch, northwest of headquarters, along road to Mellards; uppermost conglomerate of active apron

** P = pebbles - $^{-}4$ to $^{-}6\phi$ (5/8 - 2½ inches); C = cobbles - $^{-}6$ to $^{-}8\phi$ (2 ½ - 10 inches).

IV. PERDIZ CONGLOMERATE

by Jeffrey M. Jordan[1]

INTRODUCTION

The Perdiz Conglomerate, which crops out in Presidio County, Texas, consists of a series of (Oligocene?) volcaniclastic conglomerates and tuffaceous sandstones (fig. 1). North and west of the Chinati Mountains it unconformably overlies the Petan Basalt, and conformably overlies the Tascotal Formation to the east. The Perdiz pinches out against older volcanic and sedimentary rocks of the Chinati Mountains and in the area around Shafter, Texas. It is presently being dissected by eastward- and southward-flowing streams, exposing excellent outcrops in stream valley walls. Two major roads, U.S. Highway 67 and Texas Ranch Road 2810, cut through the Perdiz outcrop area, providing additional outcrops in the study area.

The Perdiz was deposited as a widespread alluvial fan system by high-gradient, short-duration peak-discharge streams flowing northward from the Chinati Mountains. Paleocurrent directions (to be discussed later) and field comparisons of clast rock types from the study area (fig. 2) with those of the Chinati Mountain volcanic sequence indicate the Chinati Mountains as the only possible source area. The Perdiz appears to be part of the last cycle of volcanic caldera activity in the area. The Perdiz represents the destructive and erosive cycle, after the volcanic center has ceased to produce volcanic ejecta (Walton, 1976, in review).

---

[1]Department of Geology, University of Kansas, Lawrence.

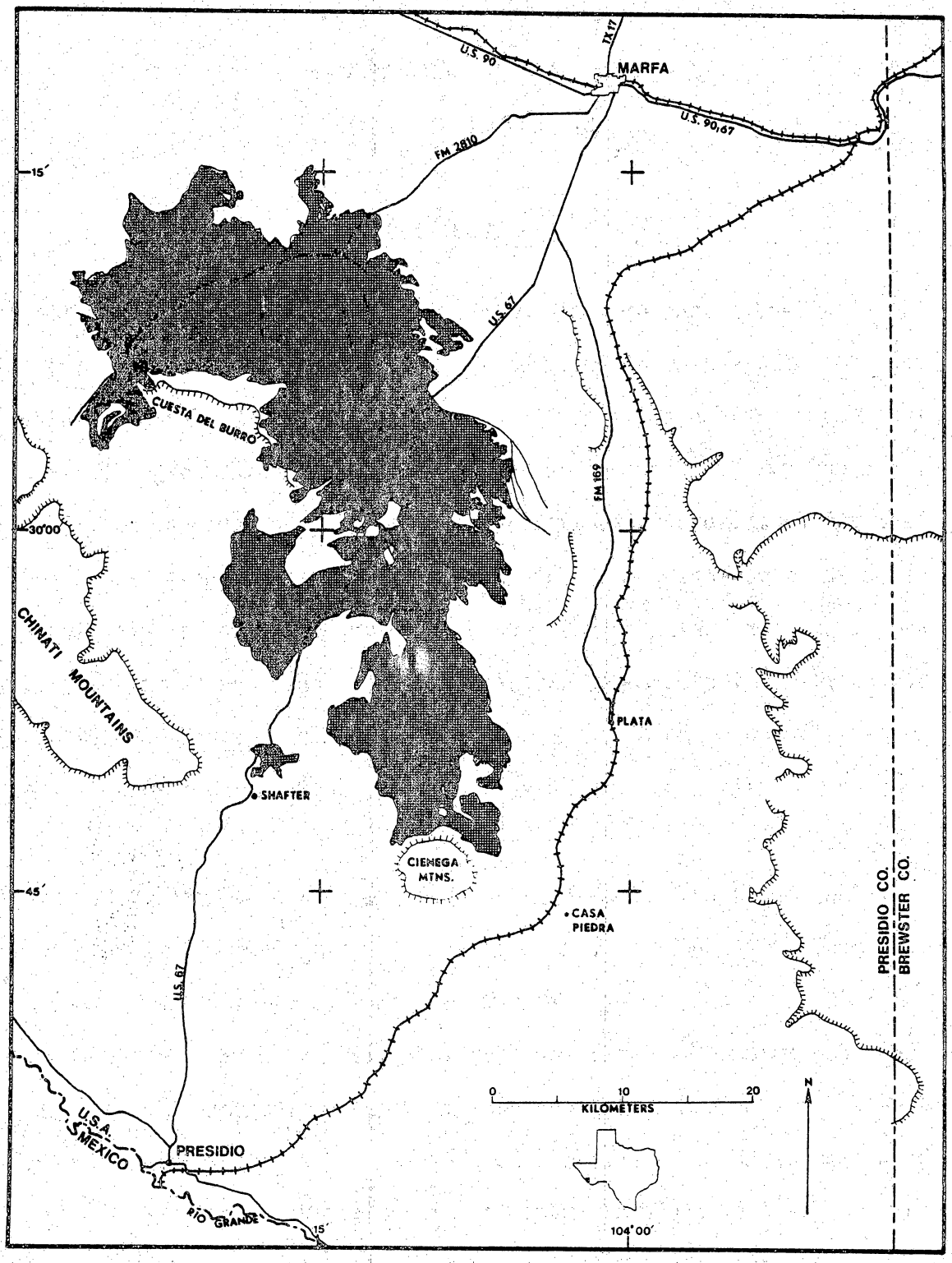

Figure 1. Approximate outcrop area of the Perdiz Conglomerate (after Barnes, in progress).

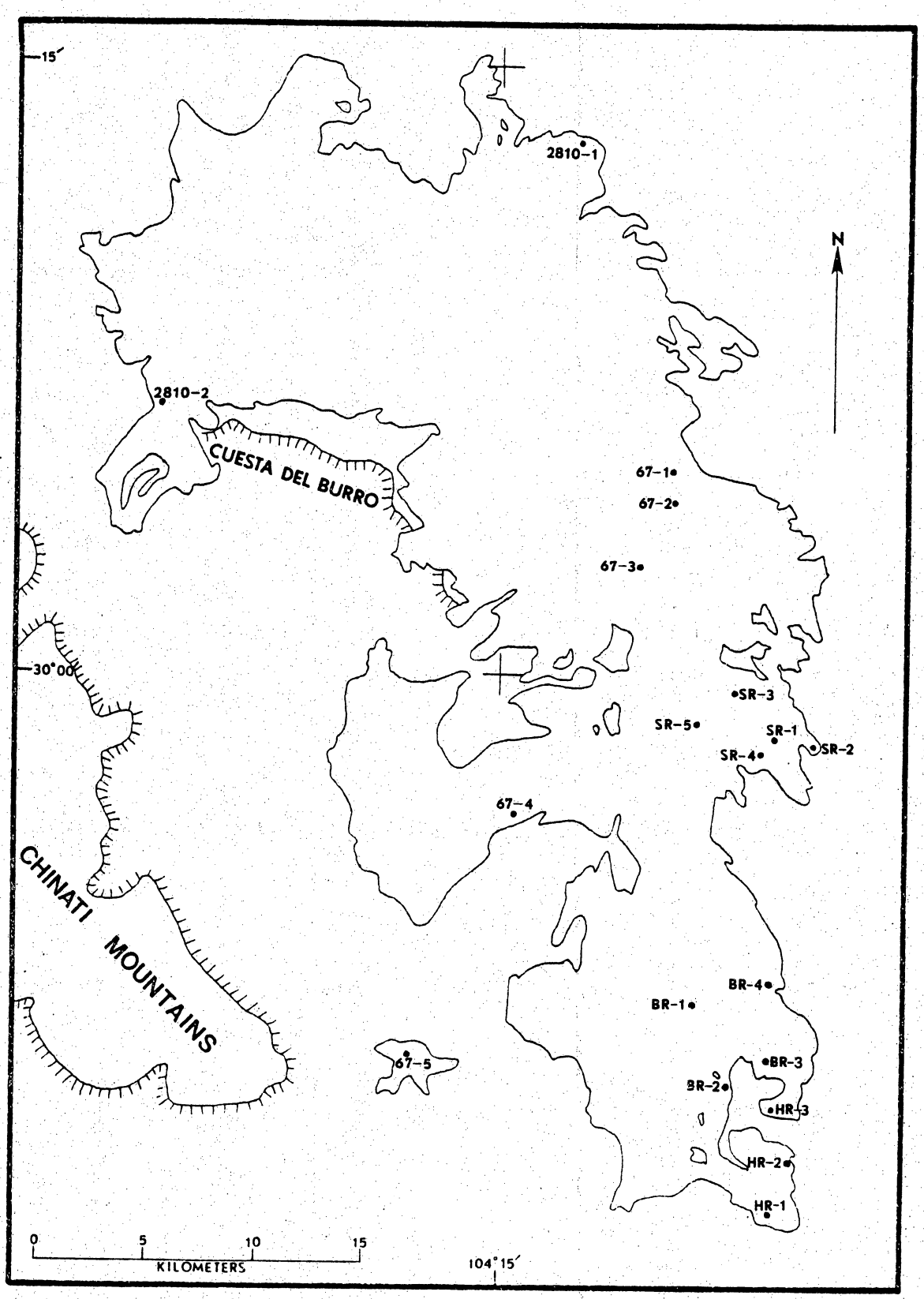

Figure 2. Locations of outcrops in study.

The Perdiz differs from the well-known arid-region fans (Blissenbach, 1954; Bull, 1963; Beaty, 1970; Denny, 1967; Hooke, 1967; Lustig, 1965) that are characterized by debris-flow and mud-flow deposits, and appears to be more similar to humid-region fans (Gole and Chitale, 1966), and to glacial outwash gravels (Boothroyd and Ashley, 1975; Church, 1972; Eyron and Walker, 1974; Gustavson, 1974; Ryder, 1971) that are characterized by braided-stream deposits. The Perdiz is also very similar to the Van Horn Sandstone, an ancient alluvial fan complex built largely by braided streams (McGowen and Groat, 1971). The Perdiz was deposited by water flowing across an alluvial fan complex. The different processes of deposition operating on a fluvially dominated alluvial fan complex should comprise a different model for the development of alluvial fan systems.

Facies of the Perdiz Conglomerate

The Perdiz may be divided into three main facies: proximal fan, mid-fan, and distal-fan facies. These facies relate primarily to the geometry of the deposit and characterize most alluvial fan deposits. The three main facies may be further subdivided into six subfacies which represent the fluvatile character of the Perdiz. These subfacies are:

(a) Massive conglomerate — (restricted to proximal fan)

(b) Channel fill

(c) Longitudinal bar — (primarily mid-fan)
   1. Bar core
   2. Bar front
   3. Bar stoss
   4. Bar top

(d) Sand lens

(e) Trough crossbedded — (mid-fan and distal-fan)

(f) Tabular crossbedded (restricted to distal fan)

The four "microfacies" (bar core, bar front, bar stoss, and bar top) listed under the longitudinal-bar subfacies are characteristic of bar growth in braided streams, and have been named in an earlier paper (Eyron and Walker, 1974).

Five subfacies correspond roughly to six facies typical of braided-river deposits described by Miall (1977). The massive conglomerate subfacies does not have an analogous braided-river counterpart, as this subfacies is interpreted to be deposited in entrenched channels (discussion later), which are not typical of a braided-river environment. The channel-fill subfacies is roughly analogous to Miall's "Gt" facies, which consist of stratified gravels displaying broad, shallow trough cross-stratification. The longitudinal-bar subfacies is similar to the "Gm" facies described by Miall (gravel, massive or crudely bedded, with minor sand, silt, or clay lenses). The sand-lens subfacies is similar to the "Ss" facies described by Miall (pebbly sands, with broad, shallow scours).

The trough-crossbedded subfacies is similar to Miall's "St" facies, which consist of pebbly sands displaying distinct cross-stratification. The tabular-crossbedded subfacies is similar to Miall's "Sp" facies (planar-bedded pebbly sands), and appears to be similar to the "Gp" facies (planar-bedded gravels) in coarser grained intervals.

Massive-Conglomerate Subfacies: Description

The massive-conglomerate subfacies has an overall channel-like appearance (fig. 3) and contains roughly lenticular, unstratified to faintly stratified gravel deposits. The deposits have concave-upward bases

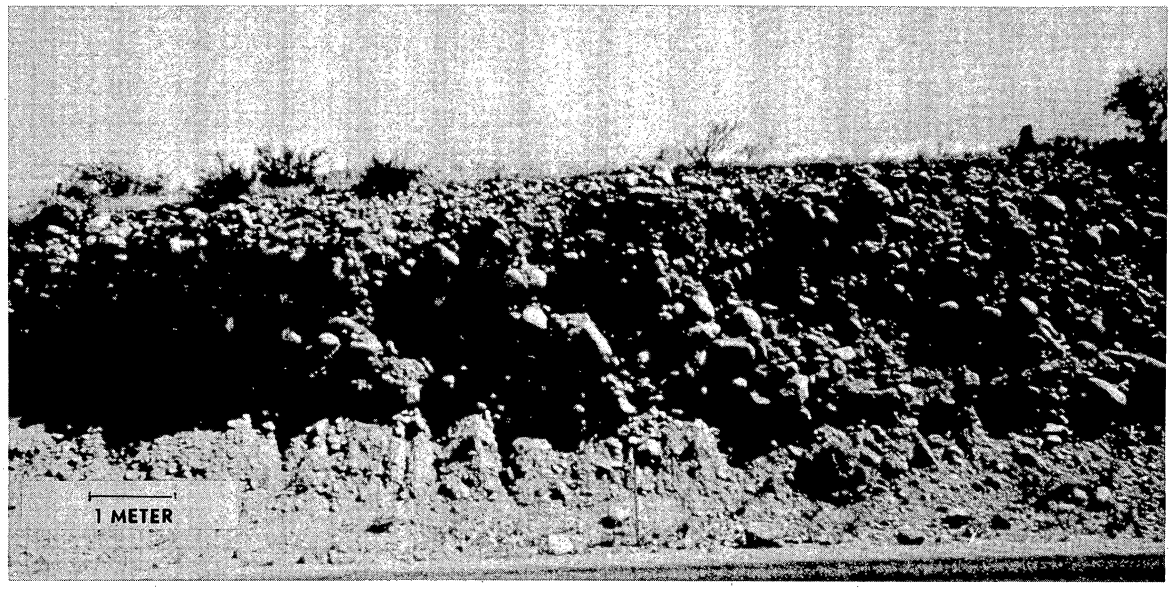

Figure 3. Massive conglomerate subfacies at outcrop location 67-5. Flow direction is into the picture.

which are erosively cut into the longitudinal bar subfacies underlying the massive conglomerate. Channels are normally 4 to 6 m thick and 16 to 20 m wide. The facies have flat tops and are overlain by the longitudinal bar subfacies. This subfacies, the coarsest in the Perdiz Conglomerate, contains isolated boulders over 120 cm in diameter and large boulder and cobble-sized clasts, with the matrix consisting of coarse sand and pebbles. Faint traces of stratification are defined by grain-size changes, as layers of coarser clasts are observed to run across the entire length of the outcrop. Imbrication is fairly well developed throughout the subfacies, although many of the larger bounders are imbricated contrary to the inferred

flow direction.

Channel-Fill Subfacies: Description

The channel-fill subfacies is composed of evenly bedded, lenticular bodies of pebbly sand. This facies displays a concave-upward erosive base overlying gravels in the longitudinal-bar subfacies and the trough-crossbedded subfacies (fig. 4). The top of the facies is flat and is overlain by gravels of the longitudinal-bar subfacies or the trough-crossbedded subfacies. Channels are up to 3 m deep and 10 m wide. Some channels display a channel lag composed of cobbles at the base up to 20 cm thick. Overall, the facies is composed of evenly bedded, parallel-laminated pebbly sands, with individual beds 10 to 20 cm thick. Individual beds thin and curve upward toward the sides of the channel in a concave manner. Grain size decreases toward the top of individual channel fills, with a distinct lack of pebbles in the top few centimeters.

Longitudinal-Bar Subfacies: Description

Bar-Core Microfacies

The bar-core microfacies has fairly flat bases, convex-upward tops, and roughly lenticular bodies of imbricated gravel displaying crude horizontal stratification. The gravels are primarily composed of cobble or small boulder clasts, with a matrix consisting of coarse sand. Grain size is greatest near the base of the core, or near the center of the core, and decreases upward from the center of the core. The lenses have a maximum thickness of 2 m and extend in a downcurrent direction for 3 to 6 m. They commonly contain thin, discontinuous horizons of matrix-

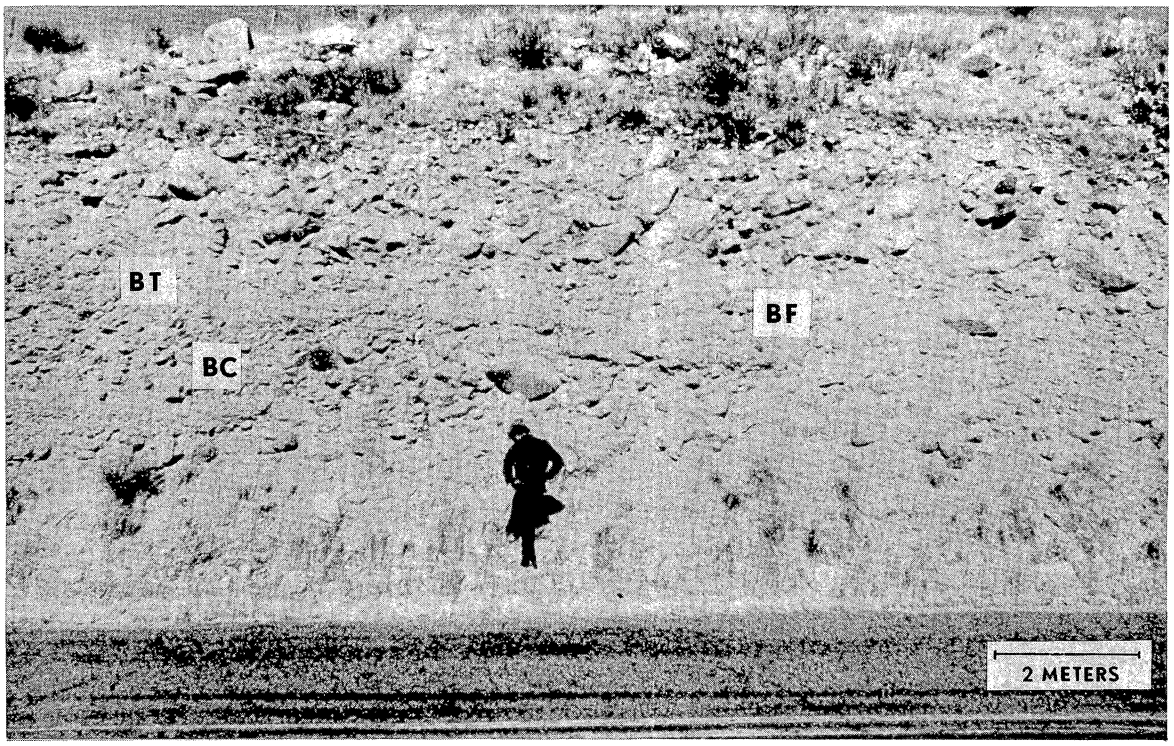

Figure 4. Longitudinal-bar subfacies at outcrop location 67-5. BC: Bar-core microfacies; BT: Bar-top microfacies; BF: Bar-front microfacies. The bar-stoss microfacies is not visible in this photograph. Flow direction is from left to right.

(sand-) rich gravel, 5 to 20 cm thick and 2 to 4 cm long, giving the facies a stratified appearance. Openwork gravels with very little matrix form the core of the lenses. Imbrication is well developed in the openwork core of the microfacies, although the best imbrication is generally found near the top of the lenses. Bar cores are often associated with nearby lenticular sand bodies of slightly smaller dimensions. These sand bodies probably represent smaller side channel development, with later sand fill-in under lower energy conditions than in the main channel.

Bar-Front Microfacies

The bar-front microfacies consists of trough crossbedded gravels and pebbly sands. It generally forms a wedge-shaped deposit which rests abruptly on and develops laterally from the bar-core microfacies, and passes gradationally upcurrent into the bar-top microfacies overlying the bar core. This microfacies is not well developed in most outcrops, and achieves a maximum thickness of only 1 m, with a maximum downstream length of 4 m. Individual foresets are 10 to 20 cm thick, with troughs up to 20 cm deep and 40 cm wide. The gravels are primarily composed of small cobble- to pebble-sized clasts with a sand matrix. The overall texture is heterogeneous, with little or no grain-size segregation. Pebble orientation is often unpredictable, as many clasts have their maximum planar surface oriented along the bedding planes which dip down-current.

Bar-Stoss Microfacies

The bar-stoss microfacies consists of tabular to nearly tabular trough crossbedded gravels and pebbly sands. The facies is very poorly developed, and is often very difficult to recognize in outcrop. It is developed upstream from the bar-core microfacies, and it grades laterally into the bar-top microfacies. The facies often appears to be a finer grained drape over the upstream sides of the bar-core microfacies and, where the facies thins rapidly at the top of the core, the facies grades into the bar-top microfacies. Maximum thickness reaches 75 cm, with a maximum length parallel to flow direction of 3 m. Individual beds are up to 15 cm thick, with troughs up to 10 cm deep. Fine cobble- to pebble-

sized clasts with a sand matrix make up this facies. Crossbedding is defined by pebble layers along the bedding planes. Imbrication throughout the facies is poorly developed.

Bar-Top Microfacies

This facies overlies the coarsest portion of the bar core, and achieves a maximum thickness of 50 cm. Stratification consists of discrete horizons of matrix- (sand-) rich gravel, 5 to 10 cm thick and 2 to 4 m long interbedded with matrix-poor gravel. The gravels are composed of small cobbles and pebbles, with a matrix of coarse sand. Imbrication is well developed.

Overall, this facies is very similar to the bar-core microfacies, except for finer grain size and the lack of openwork gravels (fig. 5).

Sand-Lens Subfacies: Description

The sand-lens subfacies contains lenticular to elongate bodies of laminated to slightly crossbedded sands. The sand bodies are characteristically 1 to 3 m thick, and may extend for over 30 m. Bedding is often difficult to observe in many outcrops, as this facies is commonly altered to caliche and displays calcite and caliche stringers. The facies commonly overlies the tabular-crossbedded subfacies and passes gradationally into the trough-crossbedded subfacies laterally. Tops of sand lenses are commonly very undulatory, and are overlain by the trough-crossbedded subfacies which displays troughs up to 1.3 m thick and 3 m wide. The size of the coarse to medium-sized sand grains is uniform throughout the sand-lens subfacies.

Trough-Crossbedded Subfacies: Description

This facies is always overlain by the tabular-crossbedded subfacies (although thin, discontinuous sand lenses may separate them), and it passes gradationally into the tabular-crossbedded subfacies horizontally. The trough-crossbedded subfacies consists of cobble, pebble, and coarse sand-sized grains arranged in a general coarsening-upward series. Individual crossbed sets are 20 to 60 cm thick, and comprise cosets with maximum thickness of 5 m. Trough depths reach a maximum of 130 cm, whereas trough widths reach 3 m (fig. 6). Cosets are often separated by thin (less than 50 cm), discontinuous sand lenses up to 4 m long. Imbrication is moderately developed in the coarser layers of the facies that do not display steep dips.

Tabular-Crossbedded Subfacies: Description

The tabular-crossbedded subfacies is composed of small cobbles, pebbles, and sands arranged in a coarsening-upward sequence. Individual crossbed sets are 20 to 40 cm thick, which make up cosets up to 3 m thick. Tabular cross-sets extend for distances up to 15 m and pass gradationally into the trough crossbedded subfacies. This facies always overlies the trough crossbedded subfacies (fig. 7). Crossbed sets often contain a pebble lag on top of the sequence. The sets of tabular crossbeds dip upcurrent, and appear to climb over the trough-crossbedded subfacies. Imbrication is poorly developed in this facies.

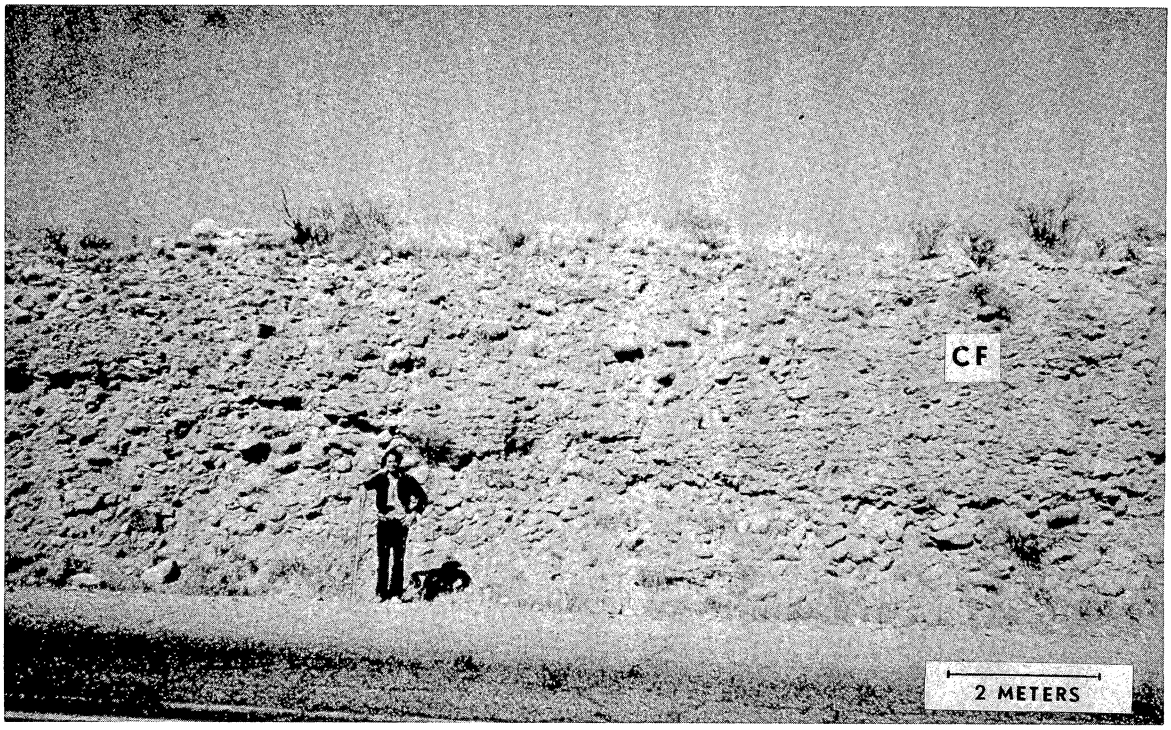

Figure 5. Channel-fill subfacies at outcrop location 67-5. CF: Channel-fill subfacies. Flow direction is towards viewer, slightly left to right.

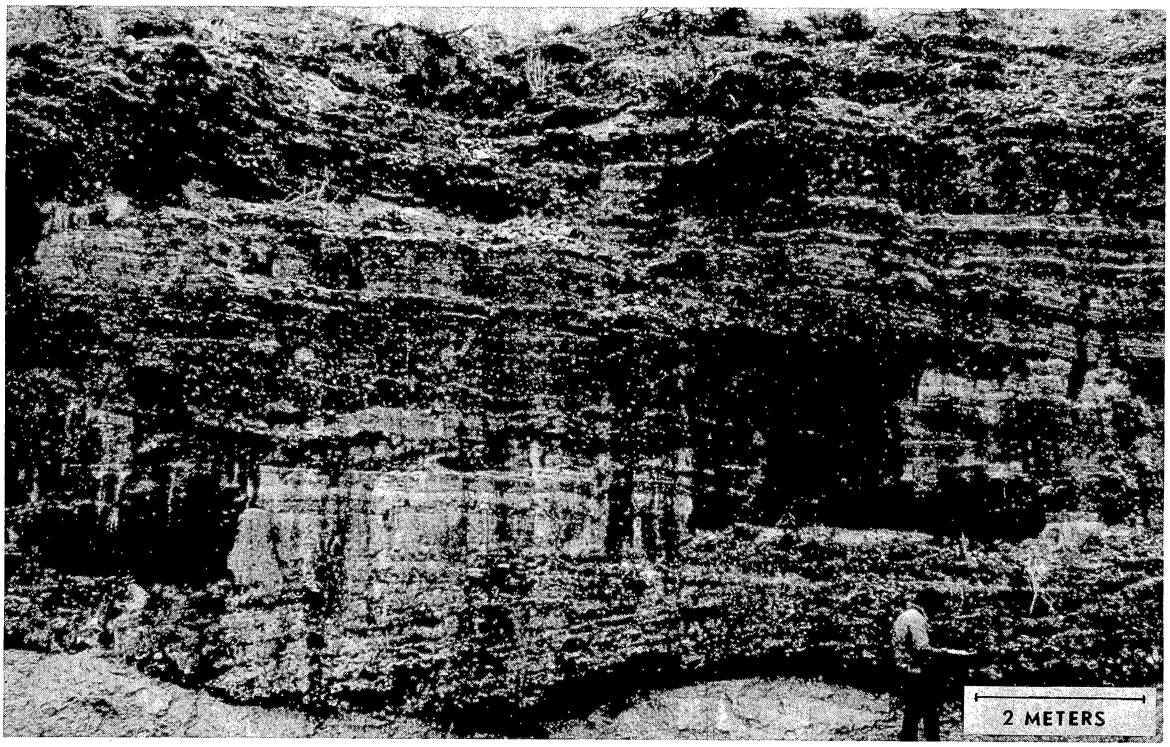

Figure 6. Trough crossbedded subfacies at outcrop location BR-4. Flow direction is right to left.

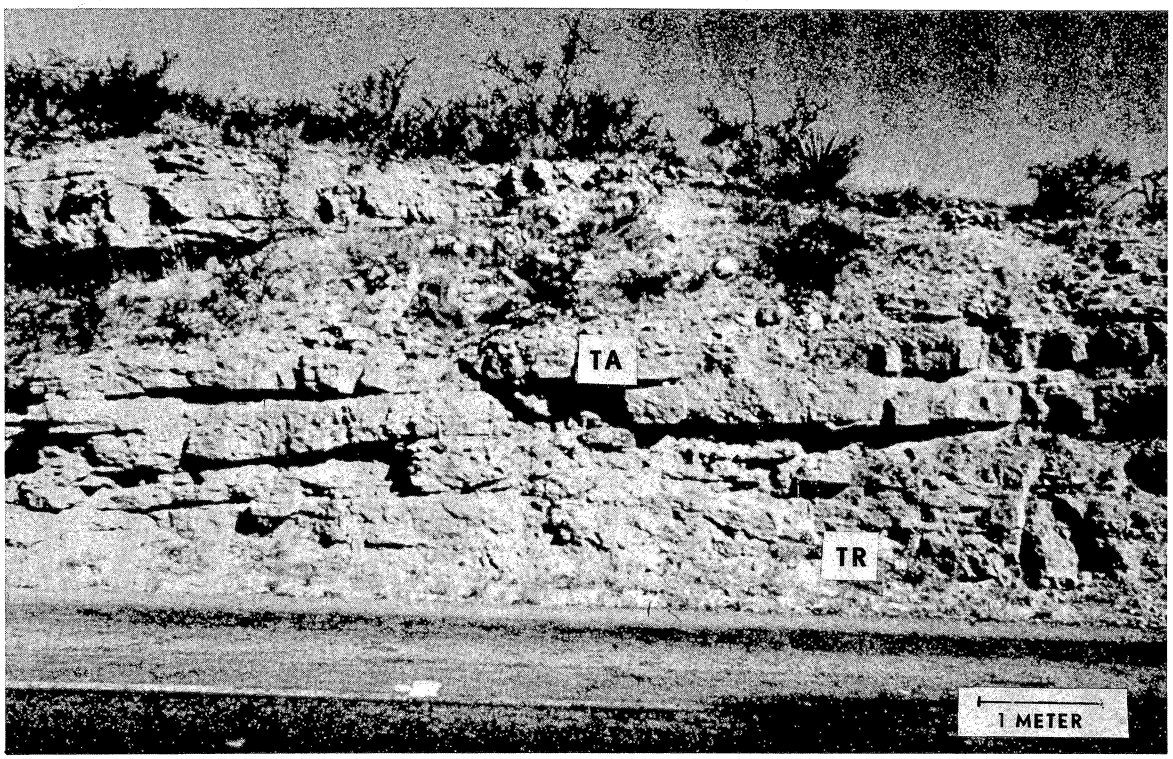

Figure 7. Tabular crossbedded subfacies at outcrop 67-1. TA: Tabular crossbeds; TR: Trough crossbeds. Flow direction is left to right.

Grain Size

Maximum grain size was measured at each outcrop by measuring 30 of the largest visible clasts, and recording the largest 10 clasts of that group. Figure 8 shows the range of the largest 10 clasts measured and the largest clast measured at each outcrop studied. There is an obvious decrease in maximum grain size measured from the proximal to distal facies. This would indicate a decreasing degree of competence in the fluvial processes moving sediment from the proximal to distal portions of the fan.

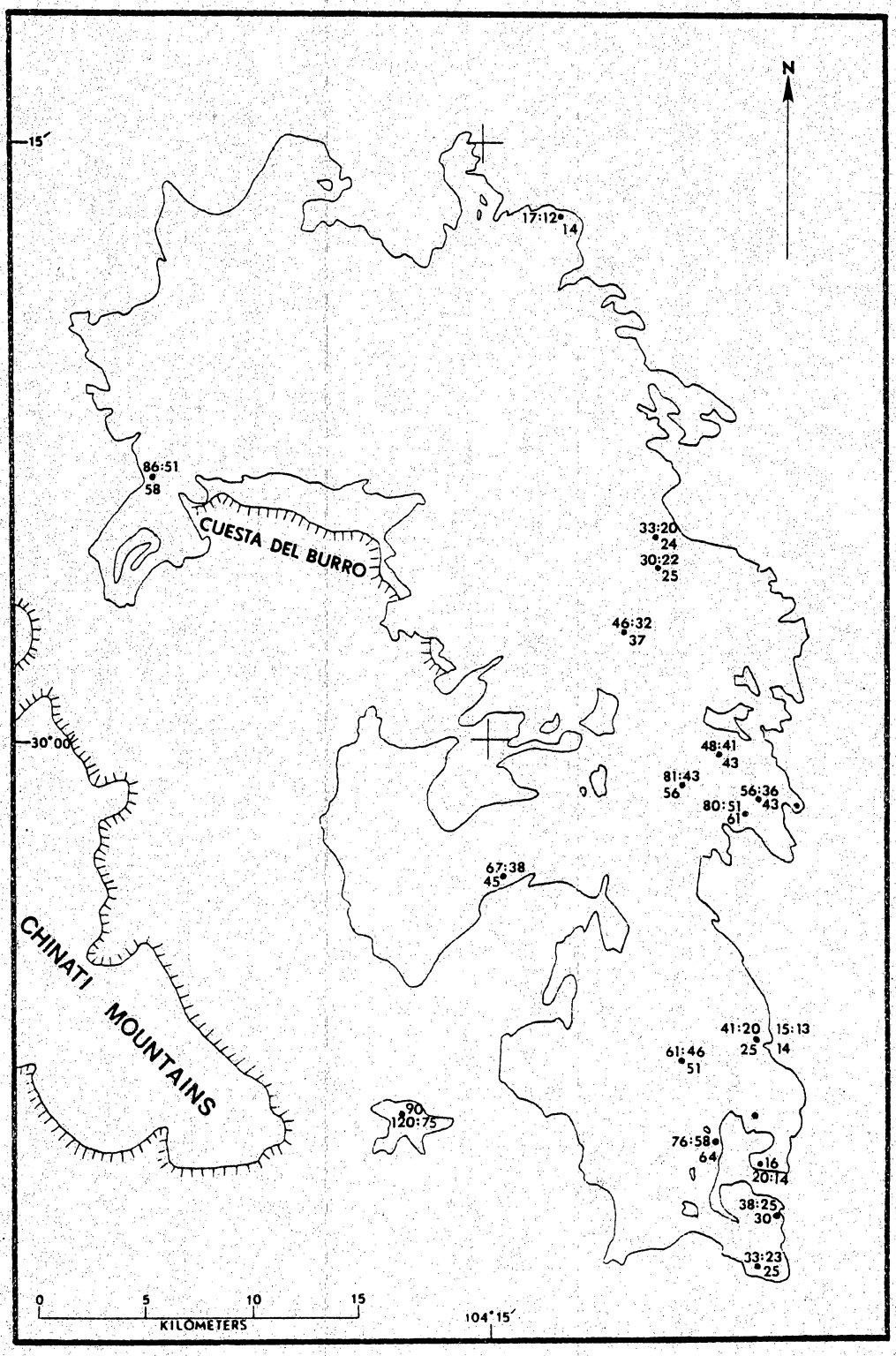

Figure 8. Diagram of largest 10 clasts measured at each outcrop locality. Double figure indicates range of largest 10 clasts measured (cm). Single figure indicates average size of largest 10 clasts measured (cm).

The individual facies also reflect major changes in grain size when mean grain size is observed in outcrop. The massive-conglomerate subfacies contains the coarsest clasts of all the subfacies. The longitudinal-bar subfacies contains the next coarser range of clasts, and also displays a finer grain size and smaller dimensions of bars in the lower mid-fan region than in the proximal-fan region. The trough-crossbedded subfacies contains material of the same grain size as does the tabular-crossbedded subfacies. The finest grain sizes are in the channel-fill and sand-lens subfacies.

Paleocurrents

Imbrications of 30 clasts were taken at each outcrop and plotted on rose diagrams. A statistical mean was then calculated from the rose diagrams in order to determine a mean current direction. The mean paleocurrent directions from each outcrop are plotted in figure 9. Almost all of the outcrops show the main current directions to be to the north and northeast, indicating the Chinati Mountains as the source area. The massive-conglomerate subfacies as well as the trough-crossbedded subfacies often yielded highly variable current directions, which may be due to the process of deposition. Crossbedding in most of the outcrops also indicates current directions to be in a northerly direction.

Geographic and Stratigraphic Distribution of Subfacies

Figure 10 shows the distribution of subfacies expressed in the outcrops studied. In general, the following subfacies pattern is evident.

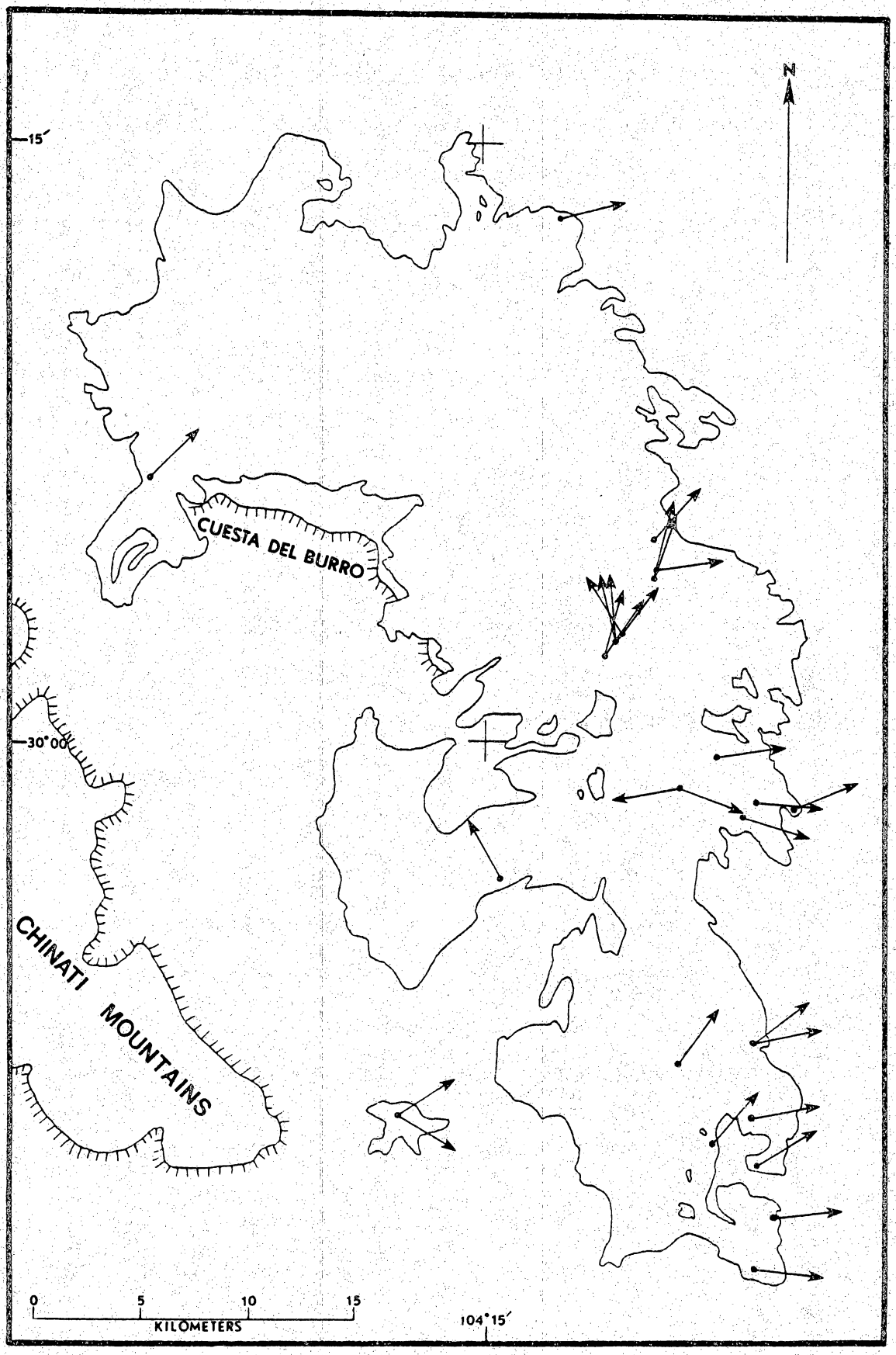

Figure 9. Diagram of mean flow directions as measured from pebble imbrications at each outcrop.

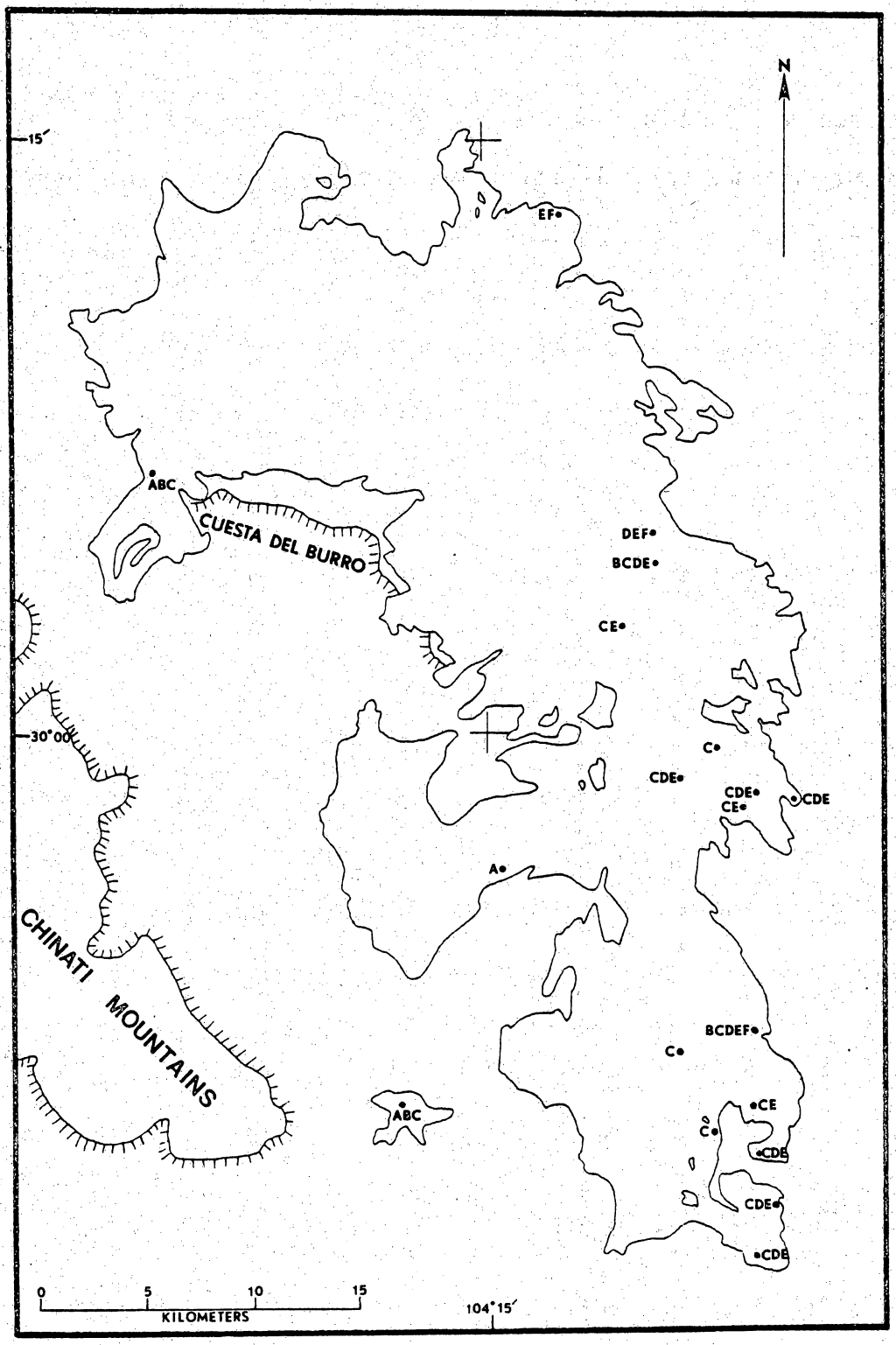

Figure 10. Diagram of geographic distribution of subfacies. Letters indicate facies found at each outcrop. (A) Massive conglomerate; (B) Channel fill; (C) Longitudinal bar; (D) Sand lens; (E) Trough crossbedded; (F) Tabular crossbedded.

The massive-conglomerate subfacies is restricted to the proximal-fan facies. The channel-fill and longitudinal-bar subfacies occur primarily in the mid-fan facies, although they are also present in the proximal facies but at a larger scale. The sand-lens and trough-crossbedded subfacies are present in the mid-fan and distal facies, although they do not make up the majority of the outcrops in the mid-fan facies. The tabular-crossbedded facies is restricted to the distal-fan facies.

Relations of the subfacies to each other in vertical sequence are much harder to ascertain because long sequences of strata are not exposed in the Perdiz. However, one outcrop (BR-4) exposes approximately 75 m of strata; consequently, stratigraphic relationships were largely based upon this outcrop. This outcrop exhibits a coarsening-upward sequence of sands and gravels which also displays an increase in scale of sedimentary features from the base of the section to the top of the sequence (fig. 11). The base of the section is dominated by trough-crossbedded and tabular-crossbedded gravels, which are overlain by some large-scale channel features and sand-lens units. The top of the sequence is dominated by the longitudinal-bar subfacies, with the scale of the bars becoming larger toward the top of the section.

The upper portion of this vertical sequence, consisting of the longitudinal-bar, sand-lens, and channel-fill subfacies, is very similar to the "Scott type" braided-river depositional profile described by Miall (1977). The lower portion of the vertical sequence, consisting of the trough-crossbedded and tabular-crossbedded subfacies is more similar to the "Platte type" braided-river profile (Miall, 1977), although the

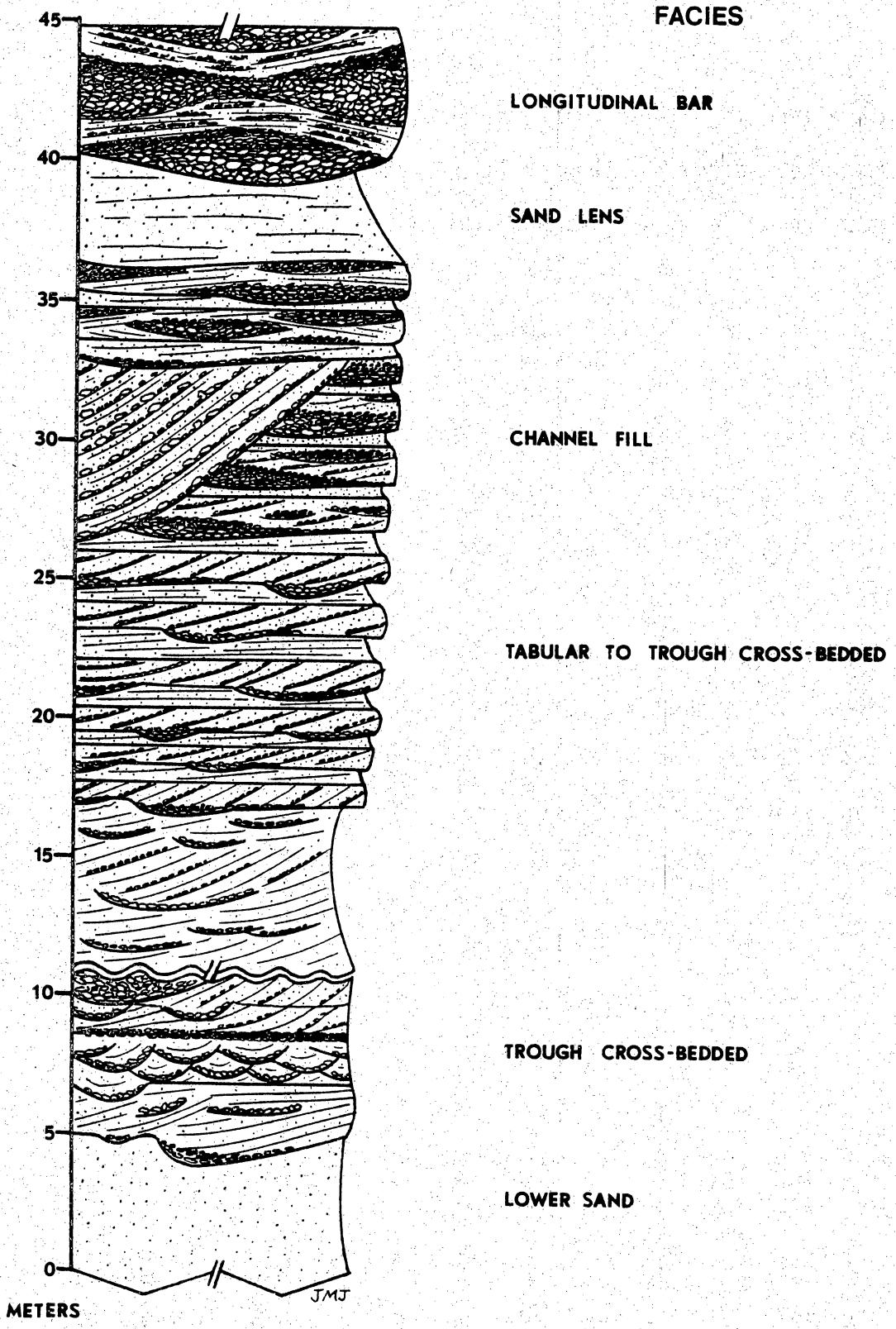

Figure 11. Stratigraphic distribution of subfacies at outcrop BR-4.

overall grain size in the Perdiz deposits are generally greater than those described in the Platte profile. The strong similarities between the vertical sequence of subfacies described in the Perdiz and the depositional profiles of two well-known braided-river systems strongly reinforce the braided-river type depositional character of the Perdiz.

The stratigraphic relationships seem to indicate a coarsening-upward, progradational sequence of sands and gravels. This is in contrast to the alluvial fan deposits described by McGowen and Groat (1971), in which they found a fluvially dominated alluvial fan sequence displaying regressional, fining-upward sequences. It may be that the Perdiz at this outcrop never attained a mature stage of development in which the deposits aggraded enough to decrease the slope and lessen the competence of the fluvial systems operating on the fan surface. There is also a strong possibility that a large portion of the upper stratigraphic sequences has been removed by erosion as drainage patterns have shifted and the area has been subjected to regional faulting.

Interpretation of the Subfacies

Massive Gravel Development

The massive gravel deposits resemble surge deposits similar to those of the Rubicon River of California (Scott and Gravlee, 1968). These deposits were probably formed in water several feet deep. Current velocities must have been substantial in order to move boulders greater than 120 cm in diameter. The channel-like shape of the deposits, along with indications that water depth and current velocities were substantial, indicate that the channels were entrenched in the fan-head or proximal facies of

the alluvial fan. Without confining banks, water depth and velocity could not be as great. The gravel probably moved along the channel floor in the form of large gravel waves (McGowen and Groat, 1971).

Longitudinal Bar Development

The longitudinal-bar subfacies represents the development of longitudinal bars in a shallow braided-stream system. The coarse bar-core microfacies represents the central portion of the longitudinal bars. The gravel probably moved in sheet flood during periods of high flood stage (Eyron and Walker, 1974), as indicated by its crude horizontal stratification, and formed coarse deposits on slight positive areas on the fan surface. The bar-front, stoss, and top microfacies were formed during periods of waning flood stage when the streams were not able to move the coarse material forming the bar cores. They also represent periods of net aggradation on the system. The bar-front microfacies represents material avalanched on the lee side of the bar core, while the stoss-side microfacies represents migration of smaller dunes up the back of the bar core. The bar-top microfacies represents aggradation during very low stages of flow.

Channel-Fill and Sand-Lens Development

The channel-fill and sand-lens subfacies formed during general aggradation of the fluvial system. As the sand and gravel deposits aggraded, filling the older channels, the fluvial system was diverted across new surfaces of higher gradient (McGowen and Groat, 1971). The new channels scoured into the older sediments soon after the flow was diverted. The new channels were then filled as the system continued to aggrade. The

finer grained sand-lens subfacies represents overbank or nonchannelized deposits formed during periods of high flood stage. The sands were deposited in a sheet-flood manner as indicated by their laminated texture.

Trough Crossbed and Tabular Crossbed Development

The trough crossbedded and tabular crossbedded subfacies represent development of lobate to transverse bars in a shallow water braided distributary system. The trough crossbedded sequences are very similar to those found in Irvine Creek, Ontario, Canada (Martini, 1977), and represent bar development during rising flood stage in the lower mid-fan to distal facies. The tabular crossbeds were formed by sheet-flood movement of gravels across the flat tops of low bars during peak periods of discharge (Eyron and Walker, 1974).

Summary

The proximal fan facies were characterized by incised channels in which large volumes of coarse gravel moved in sheet flood along channel bottoms, or formed large bar cores in a braided-stream manner within the channels. Debris-flow and mud-flow processes did not operate on this fan system, as the source area did not provide enough fine material to the system to produce these types of deposits. Rather, flowing water running over the surface of the alluvial fans provided the processes of deposition in this system. The mid-fan facies were characterized by shallow braided-stream channels, with large longitudinal bars formed within the channels. Stream channels rapidly shifted patterns in this area of the fan due to rapid aggradation of the system. The distal-fan facies were characterized by lobate to transverse bars formed in a system

of shallow braided distributary streams.

Cementation

The Perdiz exhibits two main zones of cementation. Carbonate cements (calcite) prevail in the proximal facies of the alluvial fan complex, while a variety of silicate cements (opal, clinoptilolite, and montmorillonite) characterize the distal facies. Calcite occurs as large, poikilitic, homogeneous crystals. Montmorillonite precedes the development of calcite in a few rocks. Opal occurs as laminate grain coats, botryoidal grain coats, small (5 micron) microspheres, and as indistinct polygonal meniscus cements. Montmorillonite occurs as very thin grain coats and pore linings. Chalcedony occurs as a pore filling cement in a few of the samples. Clinoptilolite occurs as indistinct polygonal meniscus cements, and is commonly the last stage of cementation to develop. The laminate or botryoidal texture of the silicate cements, and the poikilitic character of the carbonate cements indicate most of the cementation in the Perdiz took place in the phreatic zone. Some of the later stages of cementation may have occurred in the vadose zone, as indicated by the meniscus texture of some of the opal and clinoptilolite cements.

Possibility of Uranium Mineralization

The Perdiz represents a possible area of uranium mineralization because, as is the case with most highly permeable alluvial fans, large amounts of ground water appear to have moved through the Perdiz and because the source rocks of the Perdiz Conglomerate contain a fairly large

amount of uranium contained in glass shards of volcanic rocks. Studies in the area have shown that uranium is likely to be released in the ground water after the dissolution of the glass shards containing the uranium (Walton, personal communication, 1978). However, most uranium deposits in modern sandstones and conglomerates are associated with anoxic zones, or with rollfront deposits associated with anoxic ground waters moving through uranium-bearing strata. The Perdiz does not seem to contain any reduced zones, and in many places it exhibits highly oxidized zones as indicated by heavy iron staining. Ground waters moving through the area are not likely to be anoxic, as the Perdiz is the upper stratigraphic unit of the sedimentary sequence in the area, and is also high in structure. Therefore, the Perdiz does not seem to be a likely source of anoxic or rollfront uranium mineralization.

REFERENCES

Barnes, V. E., project director, in progress, Marfa and Emory Peak-Presidio Sheets: The University of Texas at Austin, Bureau of Economic Geology Geologic Atlas of Texas, scale 1:250,000.

Beaty, C. B., 1970, Age and estimated rate of accumulation of alluvial fan, White Mountains, California, U. S. A.: American Journal of Science, v. 268, p. 50-77.

Blissenbach, E., 1954, Geology of alluvial fans in semiarid regions: Geological Society of America Bulletin, v. 65, p. 175-189.

Boothroyd, J. C., and Ashley, G. M., 1975, Processes, bar morphology, and sedimentary structures on braided outwash fans, northeastern Gulf of Alaska: Society of Economic Paleontologists and Mineralogists, Special Publication No. 23, p. 193-222.

Bull, W. B., 1963, Alluvial fan deposits in western Fresno County, California: Journal of Geology, v. 71, p. 243-251.

Church, M., 1972, Baffin Island sandstones: a study of arctic fluvial processes: Geological Survey of Canada Bulletin 716.

Denny, C. S., 1967, Fans and pediments: American Journal of Science, v. 265, p. 81-105.

Eyron, G., and Walker, R. G., 1974, Facies relationships in Pleistocene outwash gravels, southern Ontario: a model for bar growth in braided rivers: Sedimentology, v. 21, p. 43-70.

Gole, C. V., and Chitale, S. V., 1966, Inland delta building activity of the Kosi River: Proceedings of American Society of Civil Engineers, Journal of the Hydraulics Division, HY2, v. 92, p. 111-122.

Gustavson, T. C., 1974, Sedimentation on gravel outwash fans, Malaspina Glacier Foreland, Alaska: Journal of Sedimentary Petrology, v. 44, p. 374-389.

Hooke, R. L., 1967, Processes on arid region alluvial fans: Journal of Geology, v. 75, p. 438-460.

Lustig, L. K., 1965, Clastic sedimentation in Deep Springs Valley, California: United States Geological Survey Professional Paper 352-F, p. 131-192.

Martini, I. P., 1977, Gravelly flood deposits of Irvine Creek, Ontario, Canada: Sedimentology, v. 24, p. 603-622.

McGowen, J. H., and Groat, C. G., 1971, Van Horn Sandstone, West Texas: An alluvial fan model for mineral exploration: The University of Texas at Austin, Bureau of Economic Geology, Report of Investigations, no. 72, 57 p.

Miall, A. D., 1977, A review of the braided-river depositional environment: Earth-Science Reviews, v. 13, p. 1-62.

Ryder, J. M., 1971, The stratigraphy and morphology of paraglacial alluvial fans in south-central British Columbia: Canadian Journal of Earth Sciences, v. 2, p. 270-277.

Scott, K. M., and Gravlee, G. C., 1968, Flood surge of the Rubicon River, California--hydrology, hydraulics, and boulder transport: United States Geological Survey Professional Paper 422-M, 40 p.

V. STRATIGRAPHY AND PETROGRAPHY OF THE LIMESTONE MEMBER OF THE PRUETT FORMATION

by Bob R. Robinson[1]

INTRODUCTION

Commercial uranium deposits may exist in basin-center lake sediments that accumulated in volcanogenic provinces. Uranium may be leached from surrounding alkaline igneous rocks or carried in hydrothermal waters ascending along basin-boundary faults, and transported toward the basin center either in surface run-off or ground water. Within the basin, uranium could be derived from the devitrification of glasses in water-laid tuffs. Uranium minerals carried in solution may be concentrated by organic debris associated with stagnant lake bodies and swampy coastal areas, or by the precipitation of authigenic silica minerals. These processes could result in the formation of uranium deposits of considerable size.

Potentially commercial uranium deposits are known from Tertiary lake deposits of West Texas, yet no detailed description of the sedimentological history of these strata or of the nature of the uranium is available. In this study, the environments of deposition, facies relations, and diagenetic hisotry of the strata are described, and these parameters are related to uranium mineralization.

---

[1]Department of Geological Sciences, The University of Texas at El Paso.

GEOLOGIC FRAMEWORK AND STRATIGRAPHY

The Pruett Formation (Eocene) (Goldich and Elms, 1949) crops out over an extensive area in the Big Bend country of West Texas. The Pruett consists principally of variegated water-laid tuffs, though locally tuffaceous sandstones, conglomerates, and nonmarine limestones are common. These deposits accumulated in a large shallow basin flanked by numerous active volcanic centers (fig. 1). In the northern exposures of the formation several volcanic flows are intercalated with the tuffs. The generalized physiography and stratigraphy of the area are shown in figures 1 and 2, respectively.

Lenticular fossiliferous limestones occur at various stratigraphic intervals within the Tertiary section but are generally restricted to the upper portion of the Pruett Formation or occur between flows of the Crossen Trachyte and Sheep Canyon Basalt. The thickest section of limestone crops out in the north-central part of the Buck Hill and southwestern part of the Cathedral Mountain Quadrangles (fig. 2). The detailed stratigraphy of these carbonate units is poorly understood because of a complex history of erosion and faulting, and the lack of biostratigraphic control or marker beds. Where the Crossen Trachyte is present the stratigraphic position of the underlying limestone can be readily established; however, in many areas this unit has been removed by erosion, and flows of the Sheep Canyon Basalt rest directly on nonmarine limestones. In such cases, the stratigraphic position of the underlying carbonate units cannot be positively established.

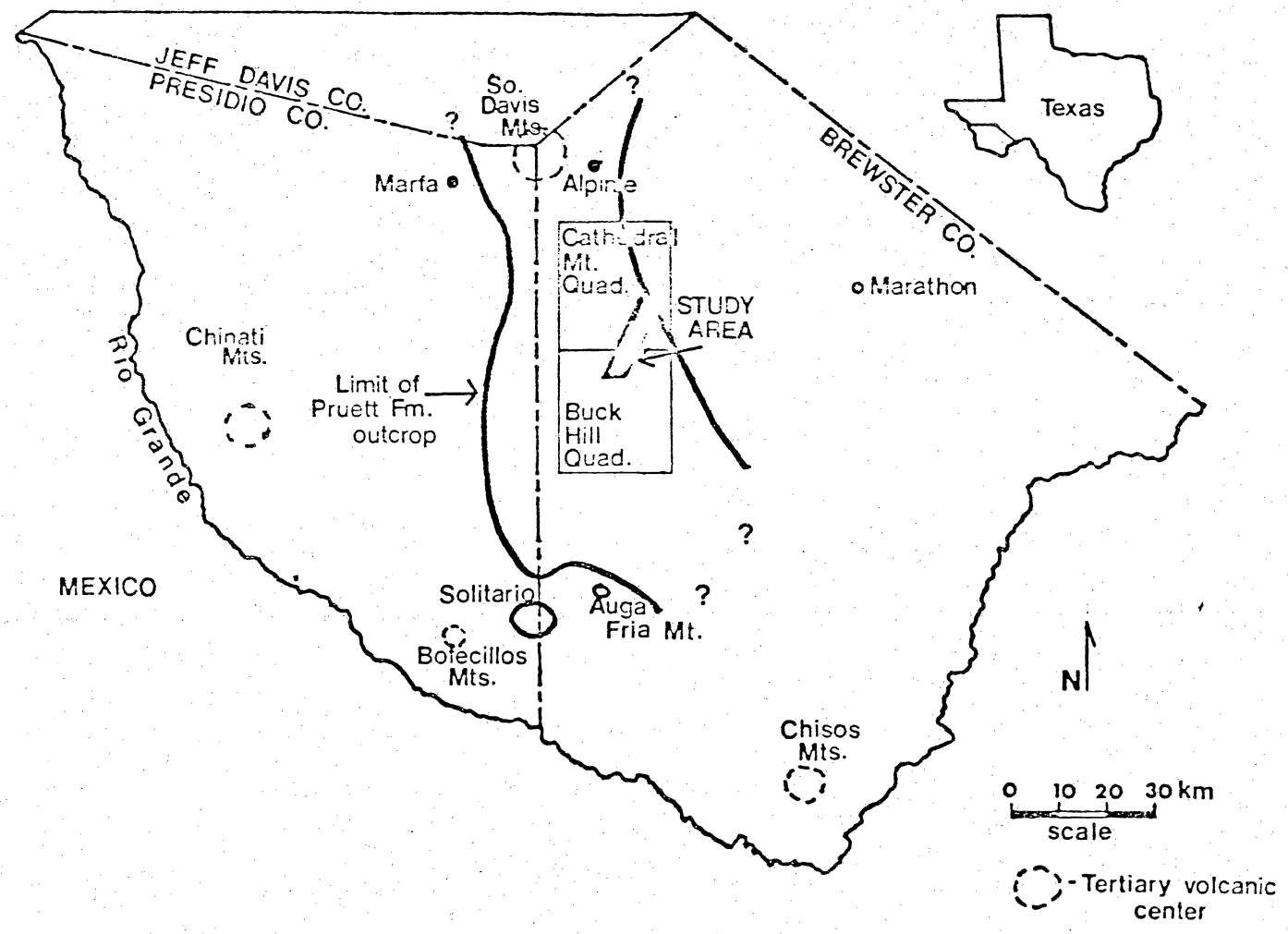

Figure 1. Generalized physiography of the study area and surrounding area.

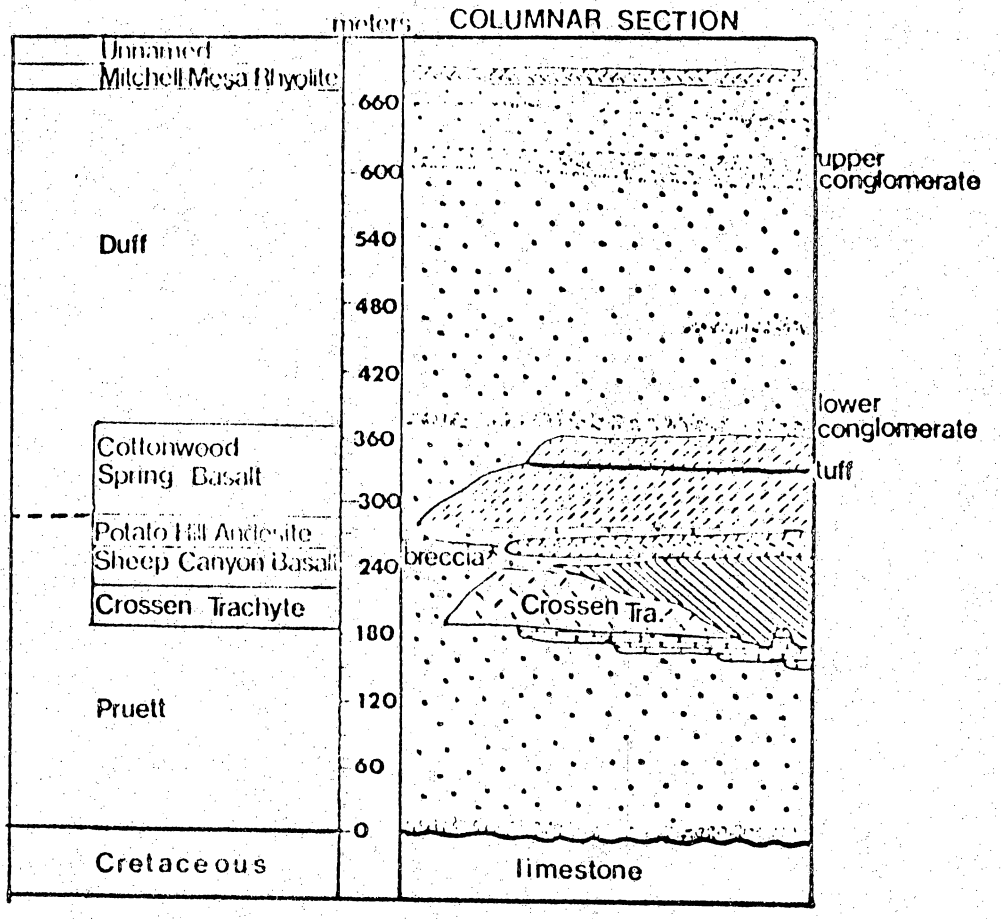

Figure 2. Generalized stratigraphy of study area (modified from Goldich and Elms, 1949).

In this study, the Sheep Canyon Basalt was used as a marker bed and only those limestones in which a pre-Sheep Canyon age could be demonstrated were examined. This is not to infer that these deposits are time-equivalent or genetically related, but only that they represent an environment of deposition that was recurring in the same area over considerable time.

Immediately north and west of Elephant Mountain as much as 60 m of limestone are exposed. These carbonate units can be traced northward toward Alpine where they pinch out in cross-bedded tuffaceous fluvial sandstones. Detailed studies to the south are lacking, and the depositional environments are poorly understood, with the exception of the area around Agua Fria Mountain where reworked fluvial tuffs dominate the section (Stevens, J.B., personal communication, 1977). In this study, I have concentrated on a relatively small area (fig. 3), in an attempt to adequately describe the petrographic fabric and facies relations of the sediments that accumulated at a single depositional site in which there are known uranium deposits.

Petrology

The carbonate rocks examined consist of allochemical, orthochemical, and terrigenous components, according to Folk's 1962 and 1968 classifications. The allochemical components are of three basic types: fossils, coated grains, and microcrystalline carbonate aggregates (usage after Williamson and Picard, 1974). Microcrystalline calcite and sparry calcite are volumetrically the most important orthochemical components,

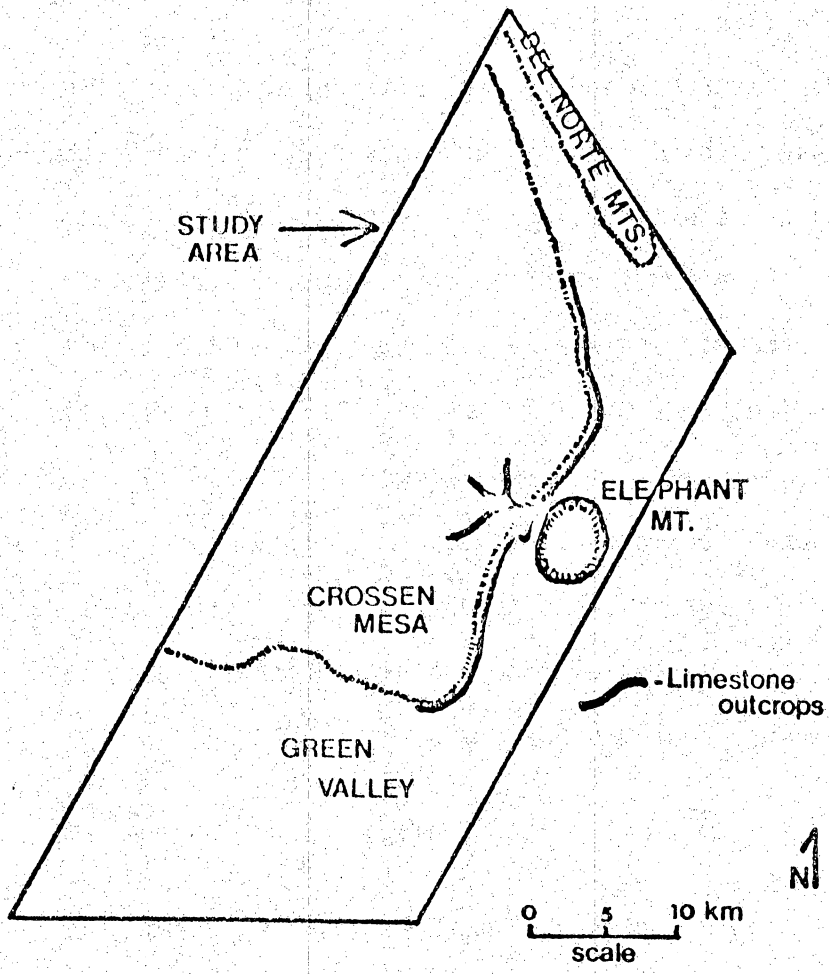

Figure 3. Major limestone outcrops in the study area.

though authigenic silica and various iron oxides are commonly present. In a few samples terrigenous mud is a major constituent, and sand-sized terrigenous grains are a minor constituent.

The limestones are dominantly light to medium gray, though shades of brown, orange, and tan also occur and form conspicuous ledges in the easily eroded tuffs. Bedding ranges from less than 5 cm to more than 3 m thick and forms accumulations up to 60 m thick, though most units are less than 3 m thick. On a weathered surface the rocks are rough and pitted, and silicified fossils and algal structures stand out clearly. The most common feature observed at the outcrop is algae-produced biogenic structures that occur as thin zones of near horizontal wavy laminae or as massive zones. Primary sedimentary structures including graded bedding, horizontal laminations, small scale cross-stratification, and bioturbation features are rarely observed.

Micritic rocks are the most common and widespread carbonate rock type; algal biomicrites are the most abundant. These units have undergone varying degrees of aggrading neomorphism to microspar or pseudospar and contain a high percentage of mud. Completely recrystallized rocks are not uncommon. Little petrologic information can be obtained from these recrystallized rocks.

Rocks with sparry calcite are composed of sorted, imbricated, and abraded algal plates, aggmicrites, or recrystallized ooliths. These sparite rocks crop out in a limited area and grade vertically and laterally into micrite units or algal biolithites. Biolithites are locally very extensive and are present in most exposed sections. Algal

forms within the biolithites are varied and include stromatolitic, digitate and several hemispheroidal types. These probably represent numerous algae genera that flourished on the lake bottom.

Petrography

Subenvironments of deposition (facies) were delineated on the basis of physical characteristics and biological components of the strata. The carbonate rocks are interpreted as having accumulated in three distinct lake microfacies that graded imperceptively into adjacent environs. The facies represented are (1) shallow open nearshore (shoal), (2) protected nearshore (lagoon), and (3) transitional.

Shallow Open Nearshore (shoal)

Carbonate strata interpreted as having accumulated in a shallow nearshore wave-agitated environment are a mixture of massive algal biolithites, algal biosparites, and oosparites. The later two rock types are grain supported and contain little mud-sized material.

The algal biolithites are composed of a variety of algal forms, and detailed work may further aid in the delineation of microfacies and the establishment of biologic zonations. Small algal plates and aggmicrites that may represent small rounded intraclasts ripped up from the lake floor, and/or recrystallized ooliths, are a common constituent between the algal framework.

Massive, structureless units composed entirely of in situ algae, are not common. In most areas the homogeneity of the units is broken by thin to thick interbeds of algal biosparites that are composed of small

imbricated algal plates, aggmicrites, and small rounded oncolites. Interbeds of oosparites are less common; however, this may only reflect the difficulty in distinguishing extensively recrystallized ooliths in thin section and hand specimen. West of Elephant Mountain, oosparite rocks comprise a 4.5 m thick unit that caps a thick sequence of interbedded algal biolithites and biosparites. The oosparites are composed of thin, graded beds of sorted ooliths that range from 0.3 to 7 mm in diameter. These beds may have formed as the algal structures grew vertically, causing the wave strength to increase over the shoal, or they may reflect the lateral migration of facies during fluctuation in the lake level.

Composite units of sparry-calcite-cemented rocks and biolithites often form mounds of considerable thickness and lateral extent. In one area discrete mound structures that must have obtained considerable relief (up to 4 to 5 m) above the lake bed are very well exposed. The cores of the mounds are composed of massive algal biolithites that grade laterally into thinly bedded algal biosparites and algal biomicrites, over a distance of 30 m. The depositional dips on the flanks of these mound structures are greater than 3°. A cross section of at least two superimposed structures is well exposed along a small creek west of Elephant Mountain. However, delineation of the mound geometry is not possible because of the lack of three dimensional exposures.

The wave-agitated deposits of the offshore shallow open-water environment seldom exhibit nonbiogenic primary sedimentary structures. This is probably the result of the abundance of in situ algae that bound the sediments and acted as a wave energy baffle, which inhibited the formation of current-produced sedimentary structures. Though rarely

observed at the outcrop, slabbed specimens and thin sections of algal biosparites and oosparites often exhibit primary sedimentary structures such as horizontal laminations, trough cross-stratification, and graded bedding.

Lagoonal Deposits

Irregularities along the lake margin formed a protected quiet-water environment in which the accumulation of fine-grained sediments was enhanced. The position of these small lagoons migrated laterally as the result of fluctuation in the lake level, and the resulting deposits are thin persistent micrite units that grade into shallow-water open nearshore deposits.

Horizontally laminated and disturbed algal biomicrites are the most common lagoonal deposits in the study area. Most contain considerable quantities of mud-sized tuffaceous material and minor occurrences of high spiraled gastropods. The strata are generally medium bedded and exhibit horizontal, wavy algal laminations, and occasionally small (approximately 7 cm diameter) isolated algal "cabbage heads" (type SH, mode V of Logan and others, 1964). Massive algal reefs are not present.

Occasionally interbedded with the micrites are thin beds of dark-brown horizontally laminated and cross-stratified waterlaid tuffs, and thin lignitic zones. Eight kilometers north of Elephant Mountain, several thin to medium-thick beds of limestone are interbedded with medium-thick beds of limestone are interbedded with medium- to dark-brown carbonaceous shale and lignite, and water-laid tuffs. The thickness of the carbonaceous unit varies from only a few centimeters to approximately

1 m and can be traced laterally for considerable distance along the outcrop. This "coal" unit is radioactive and is presently being drilled to delineate reserves.

Transition Zone

All gradations exist between shallow open nearshore and typical lagoon deposits. Rocks representing the transition zone possess characteristics of both environments, such as ooliths in micrite-supported rocks and cross-bedded, poorly washed algal biosparites that are interbedded with horizontally laminated biomicrites. Algal structures in the transition-zone strata occur as small isolated lenses and do not form massive mounds or "reef-like" structures that are common in the wave-agitated offshore environment.

Some of the transitional strata may represent sediments deposited below wave base in deeper water offshore of the shoal area. South of the study area a 15 m thick nonfossiliferous limestone crops out. These strata were not examined by the author, but the published descriptions of these deposits (Goldich and Elms, 1949) indicate that they could represent an anoxic basin center facies. However, the relation of these strata to those in the study area was not established, and there may exist no genetic relation between these widely separated carbonate units.

Diagenesis

The carbonate rocks of the Pruett Formation have undergone a complex history of diagenetic alterations that include cementation, recrystallization,

and replacement. An important point of this investigation is the determination of the mode of occurrence of authigenic minerals, as soluble uranium may be concentrated during the precipitation of silica.

Most rocks examined contain an appreciable amount (1 to 3 percent) of authigenic silica though no relations were noted between facies and the occurrence or degree of silicification. The most common occurrence of silica is a spherulitic chalcedony that has replaced calcium carbonate shells or calcified algae fragments. This silicification occurred early in the diagenetic history of the rock prior to cementation by sparry calcite.

Two other genetically unrelated modes of silicification were also noted, though neither should have affected the precipitation of uranium minerals. In one occurrence, silica replaces organic material exposed at the outcrop because of surface weathering. This silica has partially or totally replaced skeletal debris or occurs as blebs along bedding planes, often following algal structures. This replacement is only superficial and does not extend into the unweathered portion of the rock. Chafetz (1972) has reported similar occurrences of replacement of calcium carbonate by silica during surface diagenesis from the Morgan Creek Limestone of Central Texas. Late-stage silicification is widespread in the Pruett Formation but from a cursory examination of the outcrop the degree of silification could be overestimated. The other occurrence of silicification is related to volcanic flows. Where carbonate units directly underlie volcanic flows, the limestones are nearly always silicified. This silicified zone may extend from a few inches to several feet into the limestone.

The replacement silica deposited early in the diagenetic history of the rock was probably derived from the devitrification of volcanic glass within the Pruett Formation. Circulating ground water or downward percolating lake water saturated with silica may have resulted in the replacement of calcium carbonate material. Examination of these silicified zones for fluorescent uranium minerals proved negative, and a handheld scintillation counter showed no response when held over some of the more highly silicified areas. Uranium, if present, is probably not of commercial value because of the small amount of silicification. However, the presence of minute quantities of radioactive minerals could be used to establish whether these lake deposits were part of the "plumbing" through which uranium-rich ground waters that may have produced commercial deposits in other areas moved. Therefore, other tests for the presence of uranium in the silicified zones may be warranted.

SUMMARY--URANIUM OCCURRENCE, POTENTIAL, AND EXPLORATION

A uranium prospect currently under evaluation occurs approximately 8 km north of Elephant Mountain. The uranium minerals occur in silty-coal bed of variable thickness that is interbedded with micritic limestones. These limestones interfinger with fluvial tuffaceous sandstones and are overlain by flows of the Sheep Canyon Basalt. The uranium-bearing unit accumulated in a swampy coastal environment adjacent to the lake margin and is interfingered with lagoonal limestone, as a result of lateral migration of coeval depositional environments during fluctuations in the lake level.

The types of uranium minerals prevent have not been determined, and no other occurrences of uranium are known in the immediate area. However, the possibility of similar deposits existing in organic-rich lagoonal-swamp deposits or fluvial channels (Colorado Plateau type), which are buried under a thin cover of younger volcanic rocks, appears to warrant further exploration. Sediments that accumulated offshore in wave-agitated waters in an oxidizing environment do not appear to have contained enough organic matter to facilitate the precipitation of large quantities of uranium minerals.

Silicification of the limestone strata is not extensive enough and may have occurred too early in the diagenetic history of the sediments to have controlled the location of possible commercial uranium deposits. However, many similar basins exist in this part of Trans-Pecos Texas in which the diagenetic history may have varied enough to produce commercial deposits.

Though this paper deals with carbonate lake sediments, the information presented herein is applicable to clastic depositional regimes and may be useful in establishing preliminary working guidelines for the exploration of uranium minerals in volcanogenic basin-fill sediments.

REFERENCES

Chafetz, H. S., 1972, Surface diagenesis of limestone: Journal of Sedimentary Petrology, v. 42, p. 325-329.

Folk, R. L., 1962, Spectral subdivision of limestone types in Ham, W. E., ed., Classification of carbonate rocks: American Association of Petroleum Geologists Memoir no. 1, p. 62-84.

_____, 1968, Petrology of sedimentary rocks: Austin, Texas, Hemphills Press, 170 p.

Goldich, S. S., and Elms, M. A., 1949, Stratigraphy and petrology of the Buck Hill Quadrangle, Texas: Geological Society of America Bulletin, v. 60, p. 1133-1182.

Logan, B. W., Rezak, R., and Binsburg, R. N., 1964, Classification and Environmental significance of algae stromatolites: Journal of Geology, v. 72, p. 68-83.

McAnulty, W. N., 1955, Geology of Cathedral Mountain Quadrangle, Brewster County, Texas: Geological Society of America Bulletin, v. 66, p. 531-578.

Williamson, C. R., and Picard, M. D., 1974, Petrology of carbonate rocks of the Green River Formation (Eocene): Journal of Sedimentary Petrology, v. 44, p. 738-759.

VI. RELEASE OF URANIUM DURING ALTERATION OF VOLCANIC GLASS

by Anthony W. Walton[1]

ABSTRACT

Diagenesis of the Tascotal Formation in an open hydrologic system converted much of the primary glass to other minerals. The order of formation from first to last was clay, opal, calcite, clinoptilolote. During the process, the primary texture of the rock was preserved by growth of coatings on shards before they completely dissolved. Diagenetic textures indicate that diagenesis took place in a phreatic fresh-water environment where oxidizing to slightly reducing conditions prevailed.

Whole-rock uranium analyses of the Tascotal reveal no change of uranium content between the zone where glass is preserved and that where diagenetic minerals are present, indicating that uranium was not released to migrate long distances and to concentrate to form deposits of economic quality. The most common complexing agent, $CO_3^{=}$, was probably depleted by precipitation of calcite before the bulk of the glass dissolved and uranium was released. This suggests that only systems that are open to CO_2 or are not depleted in some other complexing agent are the most likely sites of release of uranium from volcanic glass. Soils are certainly open to CO_2 and would be excellent systems for uranium release. In the Trans-Pecos Volcanic Field, paleosoils are most common in valley facies rocks.

---

[1]Department of Geology, University of Kansas, Lawrence.

INTRODUCTION

Volcanic glass shards are the probable source of uranium in some sandstone uranium deposits, notably in South Texas. Glass is at least a potential source of uranium in many other areas: the Wyoming Tertiary basins; Tallahassee Creek, Colorado; and the Sierra Peña Blanca. In fact, most sandstone uranium occurrences are associated with volcanic material that could be a source of the uranium. The shards may occur as minor constituents of normal sandstones in which the uranium deposits occur, or they may be concentrated into sequences of volcanic sediment or tuff that either are the host of the uranium deposit or overlie the host.

In order to release the uranium they contain, shards must undergo some reaction with ground water. The purpose of this chapter is to describe the results of the reaction between ground water and glass and, from this, to extrapolate the processes that must have occurred. One conclusion is that the uranium that was in the glass shards when they were deposited to form the Tascotal was not released to form uranium deposits but was simply recombined with other elements to form impurities in authigenic silicate minerals or disseminated uranium minerals. Some reasons why this might have occurred and a list of criteria that will help identify systems where the same phenomenon has taken place follow. Finally, the report includes speculations on what kinds of diagenetic systems are most likely to release uranium for migration and where these systems probably occur in volcanic terrains.

This section describes alteration of glass in the glass-rich members of the Tascotal, chiefly the active-apron member; little alteration occurs in the eolian member and thin sections of the southern apron member display textures similar to those in the active apron. The analysis follows the open hydrologic model of zeolite formation (Hay, 1963; Walton, 1975; Hay and Sheppard, 1977). Although this model may be the best to account for the features of glass alteration in the Tascotal, it may not be an accurate description of the way the alteration happened, but that caveat applies to any interpretation that too closely follows an established conceptual model. The observations--mineralogy, textures, paragenesis--are not controvertible; their interpretation is (fig. 1).

OBSERVATIONS OF DIAGENESIS

Mineralogy

Volcanic Glass

Volcanic glass is the most abundant phase that was active in diagenesis. It is the most common primary phase in the active-apron member, but it now shows the most comprehensive degree of alteration and contains glass only in certain horizons. Unaltered volcanic glass is present in most of the eolian members and in the uppermost part of the active-apron member at Wire Gap and along the escarpment of Tascotal Mesa at least as far northwest as Casa Piedra. It also occurs in some sections in the Bofecillos Mountains, notably near Big Hill on the Rio Grande and in some domes in the southwestern Bofecillos, and near Lajitas, along the Rio Grande. Gen-

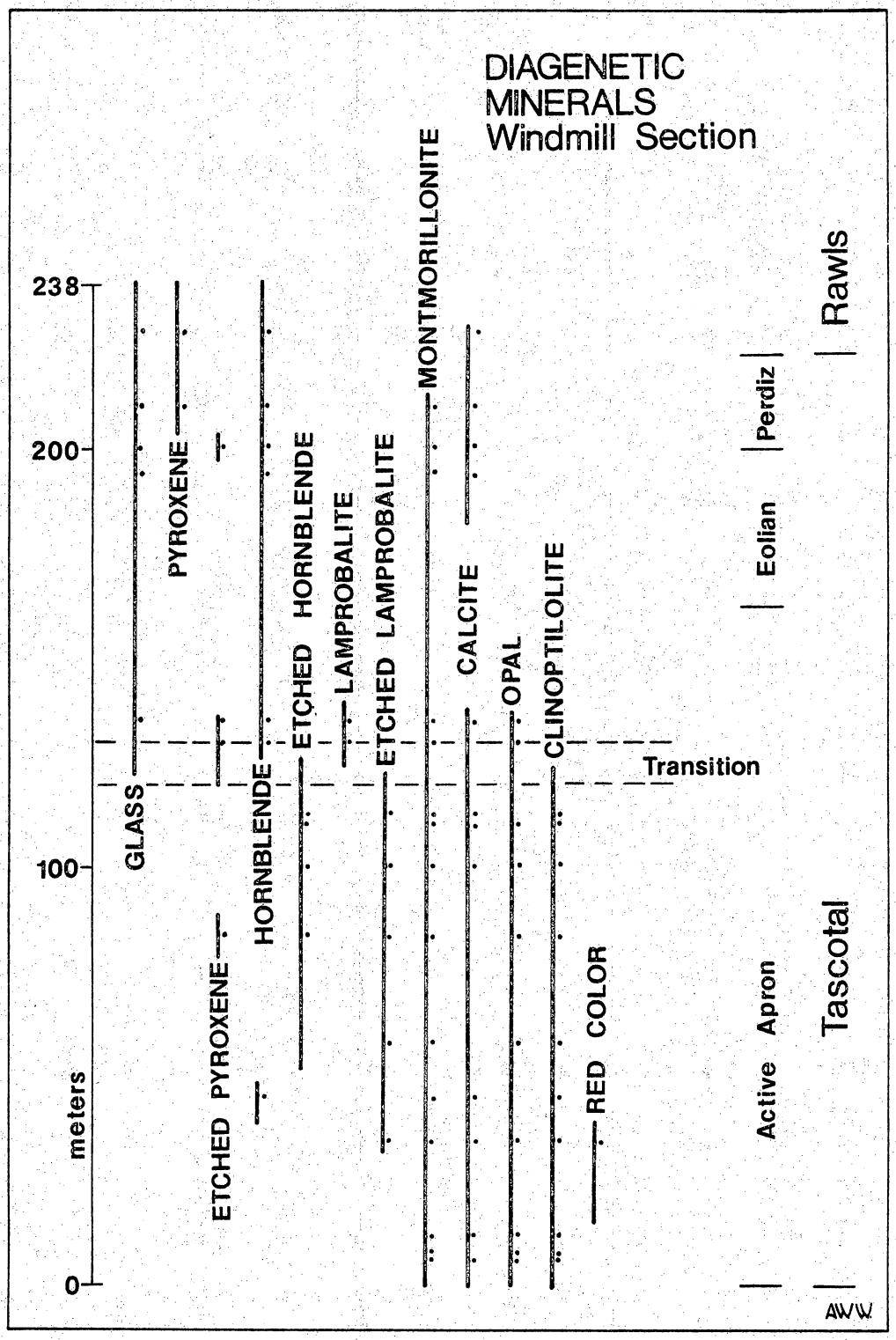

Figure 1. Occurrence of phases active in diagenesis in the Windmill section of the Tascotal. Dots represent thin-section control; lines indicate the inferred interval in which the indicated minerals occur. Six samples in the transition interval are not shown nor are the interbedding and concretions of that zone.

erally, unaltered glass occurs in the upper parts of glass-rich sections or in places where the section is thin. In the rest of the active-apron member and southern apron member, and in the lowermost part of the eolian member at La Viuda, volcanic glass has dissolved, and its constituent elements have reprecipitated as a variety of minerals including clay, opal, calcite, and clinoptilolite. This process has minutely preserved the outline of the shards so that areas where these minerals occur can be unequivocally recognized as either primary voids or pseudomorphs after glass.

Shards apparently dissolved rapidly, but adjacent shards dissolved at slightly different times. Even in samples a considerable distance above the level at which all glass is dissolved, some shards are completely dissolved. Pumice fragments, especially long tube pumice with large surface area, are particularly vulnerable to early dissolution. The dissolution process of massive shards begins by the formation of hemispherical pits on the surface of the grains. The number of these pits grows as their size increases, eventually leading to complete dissolution of the glass. All stages of this process can be observed in thin section and by scanning electron microscopy (fig. 2).

The textures are those one would expect of congruent dissolution: no secondary phases line the hemispherical pits in grain surfaces. The voids produced are for the most part devoid of dissolution products. Glass grains, even those close to the zone of alteration, are isotropic and give no evidence of internal crystallization. Even the earliest stages do not show evidence of incongruent reaction because the first

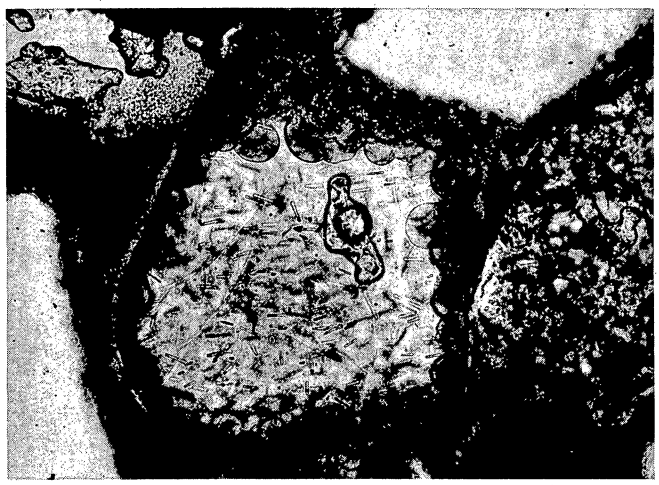

Figure 2. Photomicrographs of etched glass shards. Hemispherical pits are the first sign of solution. Glass remains isotropic until entirely dissolved.

product of diagenesis, a thin clay coat, lines both glass shards and grains of quartz, feldspar, and volcanic rock fragments as though it forms by precipitation from solution, not by partial solution of glass. All constituents of all authigenic phases, therefore, appear to have migrated distances of several tens of micrometers or more from the point at which they were freed from glass to the point where they accumulated as new mineral grains.

Chemically, this assertion of congruent dissolution is harder to maintain because partial electron probe analyses for SiO_2, Al_2O_3, Fe_2O_3,

Na_2O, K_2O, and CaO total only 90 to 92 percent of these oxides (appendix I; methods of analysis are outlined in appendix II). It is unlikely that constituents other than water could form 8 to 10 percent of these glasses that are mostly 69 to 71 percent silica. This water might have been introduced since deposition and the introduction could have been accompanied by considerable release of constituents, especially mobile ones such as alkali elements. The relative importance of congruent versus incongruent dissolution remains to be determined. Rosholt and others (1971) and Zielinski (1978), however, maintain that little uranium is leached from glass during hydration.

Clay

Clay is the first product of diagenesis. It is a very pale green to green clay with a low refractive index, probably montmorillonite (fig. 3). The clay forms coatings up to a few microns thick on all grains in nearly all rocks. The coatings closely follow the outline of all grains in the sample; they are not thicker near grain contacts nor do they have "gravity" textures, geopetal structures, or masses on lower surfaces of the grains.

Within the coatings, individual clay grains are arranged in such a way that their slow optic direction is tangential to the grain surfaces. In contrast, scanning electron microscopy (SEM) indicates that the clay occurs in a frothy texture, similar to that described by Wilson and Pittman (1977) as honeycomb texture, and believed to be characteristic of authigenic montmorillonites. The apparent contrast between the SEM texture in which the clays seem to be mostly perpendicular to the grain

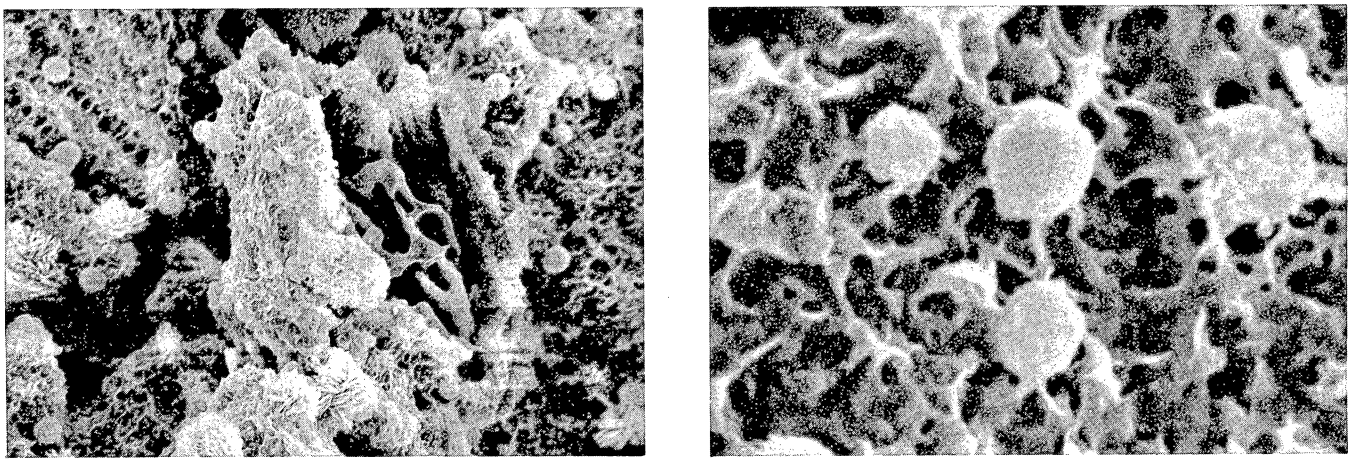

Figure 3. Scanning electron microscope (SEM) photographs. A. Frothy clay with opal rosettes and opal spheres coating a partially dissolved glass shard. B. Frothy clay with opal spheres.

surface, and the optic orientation in which they are tangential to it, is unresolved.

Clay coatings in unaltered rocks collected from high in the interval in which glass is preserved are commonly very thin, visible in thin section only with the aid of a first-order red plate, which enhances their birefringence so that isotropic glass fragments appear to have yellow or blue boundaries. Farther down the section, the clay coatings reach thicknesses of several micrometers, and point counts indicate that clay coatings

form 4 to 22 percent, by volume, of rocks that contain little carbonate.

Opal

The second diagenetic silicate to form is opal. X-ray diffraction of whole-rock and light-mineral concentrates yields a diffraction maximum at about 4.0 Å, confirming the presence of opal in these rocks. Unfortunately, pure separates cannot be prepared, and the form of the opal cannot be determined according to the scheme of Jones and Segnit (1971) because of interference with zeolite peaks. The lack of distinctive peaks other than the single large one at 4.0 Å, however, suggests opal CT as the major form present. Electron probe analyses of opal, identified on the basis of low refractive index and distinctive habit, confirm that the material is hydrous and about 90 percent silica (appendix I).

Opal occurs in several textures (fig. 4). The first opal to form occurs as apparently structureless spheres, a few micrometers across, that lie on the clay coating of grains. Actually these dots are not conclusively identified as opal, but their low refractive index (they are noticeably pink in plane polarized light) and spherical habit suggest few other possibilities.

Associated with the spheres in samples near the base of the rock interval containing unaltered glass are rosettes of opal. Rosettes consist of bladed crystals arranged in masses up to 30 to 40 microns across that have an irregularly hemispherical overall shape. The rosettes are similar to the spherical aggregates of silica described by Weaver and Wise (1972), but are several times larger. In any section of the Tascotal, at about the same level at which glass is completely dissolved,

the rosettes have coalesced into a nearly complete, irregular layer, grossly paralleling and overlying the clay coating on grains and shards. Opal rosettes do form within voids left by dissolution of glass, but they are not common nor do they form the continuous coating that overlies the clay layer. In the continuous coating, precipitation of opal between blades of the rosette causes it to merge into a continuous coating several micrometers thick. After completion of this continuous coating, the system ceases to form opal. In one sample, taken from a concretion at 126 m up the Windmill section, opal occurs as a continuous lining of the void left by the solution of a glass shard. The coating is 10 to 20 micrometers thick. Opal has formed in some other rocks as a result of recent processes.

Fully developed opal rinds, like those of clay, are marked by their continuous nature; layers of opal are not thicker at points of grain contact, nor are they better developed on one side of a grain than on the other. Though neither dots nor rosettes forms a continuous layer, individual opal precipitates are uniformly distributed over the outside of clay coating on shards or voids left where shards dissolved.

Clinoptilolite

The last silicate material to form during diagenesis of the Tascotal is clinoptilolite, which both partially to completely fills the primary pore space left after formation of clay and opal coats and partially fills voids left by dissolved glass shards (fig. 5). It forms bladed crystals ranging from about 10 by 3 by 1 micrometers to 30 by 15 by 5 micrometers. These crystals show asymmetric pointed terminations when

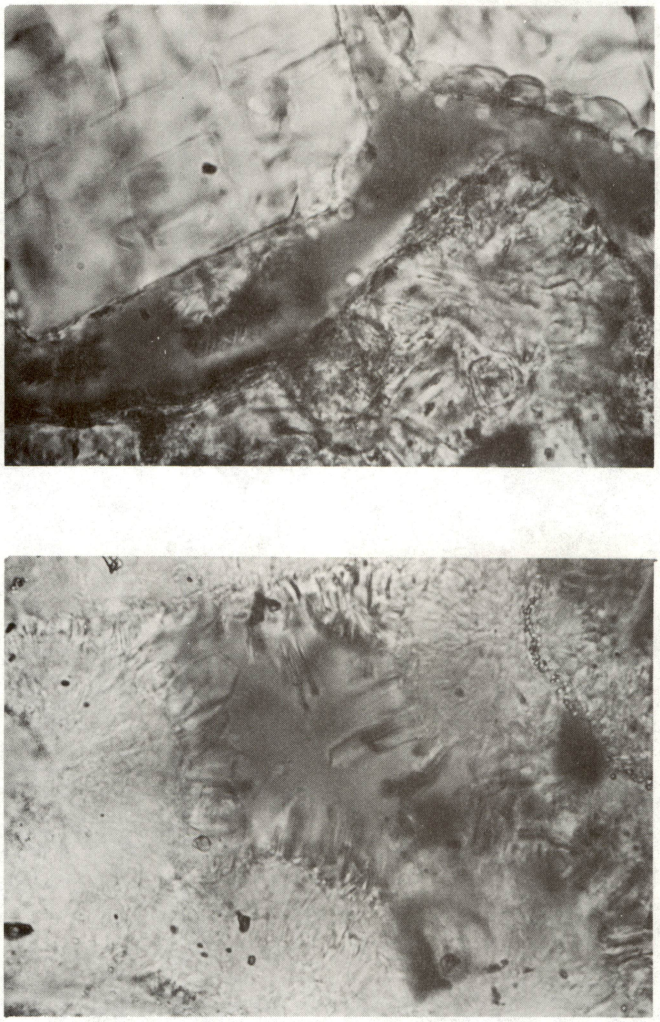

Figure 4. Photomicrographs of diagenetic textures. A. Etched glass shard, feldspar grain, and volcanic rock fragments (VRF), some opal rosettes. B. Large opal rosettes, with small zeolite crystals grown on them.

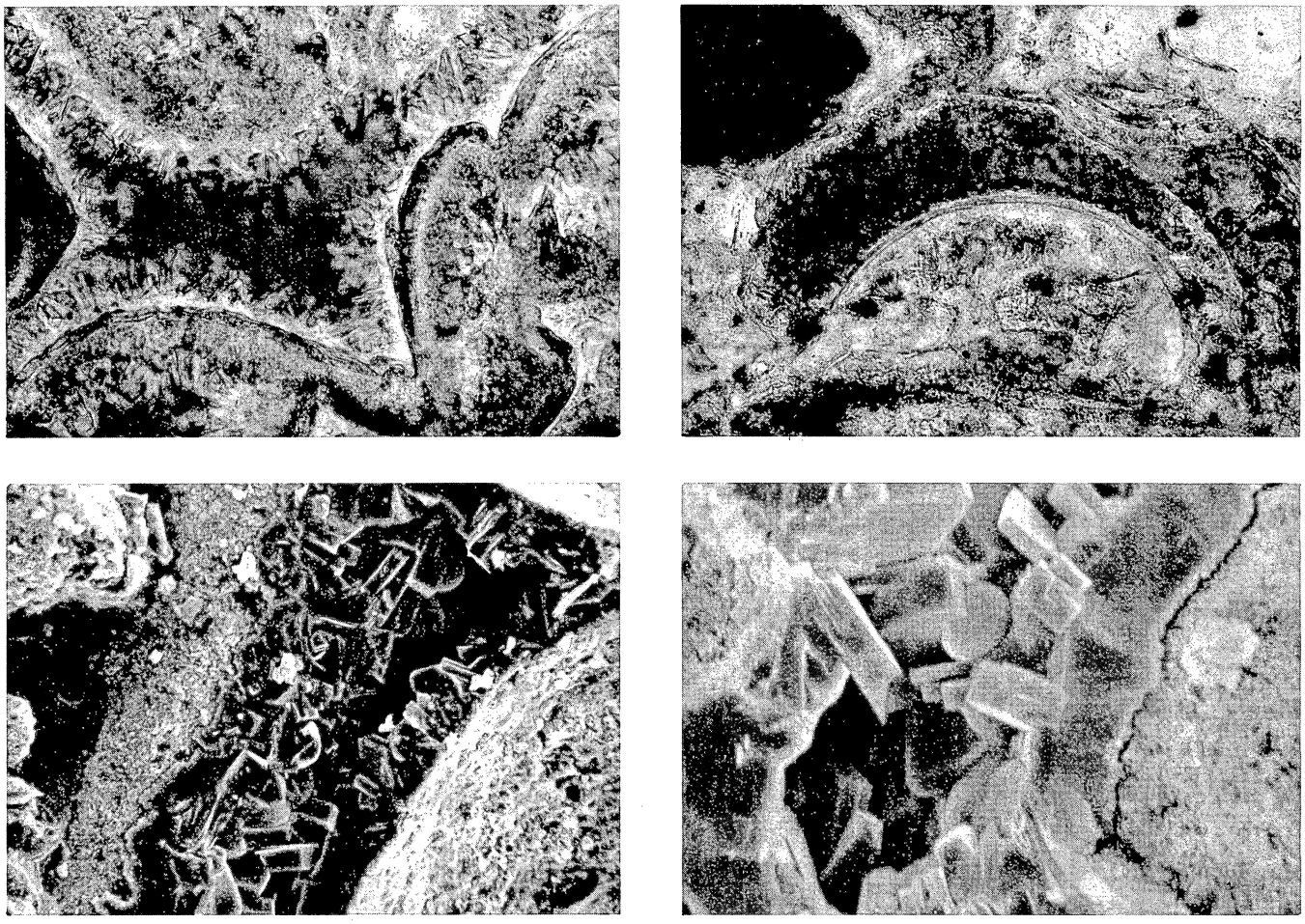

Figure 5. A. Photomicrograph of pseudomorph of glass shard filled with druse of clinoptilolite crystals. Shape of shard is preserved by a clay layer and a diaphanous opal layer. Centers of pores are partially filled by clinoptilolite. B. Photomicrograph of a similar shard pseudomorph with a better developed opal layer on the outside of the shard. C. Scanning electron microscope (SEM) photograph of a pore lined by clinoptilolite. Adjacent grains have frothy clay coatings. D. SEM views of a pore with massive opal and drusy clinoptilolite.

viewed parallel to the b crystallographic axis, that is, perpendicular to their largest cross section; the terminations are probably indications of the monoclinic symmetry of the crystals. Identification as clinoptilolite is based on habit of the crystals as viewed in the petrographic and scanning electron microscopes (Mumpton and Ormsby, 1976), x-ray diffraction traces, and electron probe microanalyses. The probe studies indicate that ratios of sodium to calcium range from 2 to 1 to 1 to 4 (appendix I).

Only in one sample were both clinoptilolite and glass present. For the most part, zeolite occurs only in a zone below that in which glass remains undissolved. The boundary between the occcurrence of zeolite and that of glass is not a simple, planar surface because zeolite-bearing concretions occur above the general level at which clinoptilolite becomes predominant. Elsewhere, particularly permeable beds are cemented by zeolite before beds above and below are cemented.

Clinoptilolite is found in most of the active-apron members and in parts of the southern apron member. Jordan (this report, chapter IV) reports clinoptilolite in the Perdiz Conglomerate. Clinoptilolite also occurs in the Perdiz member of the Tascotal along Tascotal Mesa. Because this zeolite is separated by 50 m or so of unzeolitized active-apron and eolian members from the altered part of the lower Tascotal, the Perdiz probably acted as a separate diagenetic system.

The crystals of zeolite that occur in primary pore space are smaller than those that line the voids left by dissolved shards, but they fill the space more completely. Like both opal and clay, the zeolite coatings

form continuous layers of nearly constant thickness. No evidence of increasing thickness near points of grain contact was observed.

Calcite

The most common nonsilicate diagenetic mineral is calcite. Unlike the other minerals, calcite has two distinct zones of occurrence in several sections of the shard-rich part of the Tascotal Formation: it occurs as cement at the top of the eolian member, and it occurs as cement and concretions throughout the interval where opal or clinoptilolite occur. Calcite can be either in poikilitic habit or as sparry pore-filling cement. The relative time of formation of calcite in zeolitized rocks can be determined rather precisely. It began to form after opal, but before most of the glass was dissolved and before the clinoptilolite formed. Calcite rarely replaces shards, but it clearly fills pores that are rimmed by opal. Calcite, like the silicate authigenic minerals, shows no evidence of preference for points of grain contact nor for gravity-influenced textures.

Other Minerals

Pyroxenes, hornblende, and lamprobolite have altered to provide materials to the diagenetic system. The process begins just above the level where the glass disappears. There, pyroxenes have been attacked along cleavage planes to form the characteristic coxcomb texture (fig. 6). At a slightly lower level, hornblende and lamprobolite have been etched to the same texture, but their coxcomb spires are sharper than the stubby peaks of dissolved pyroxene. Coxcomb inosilicates occur throughout the

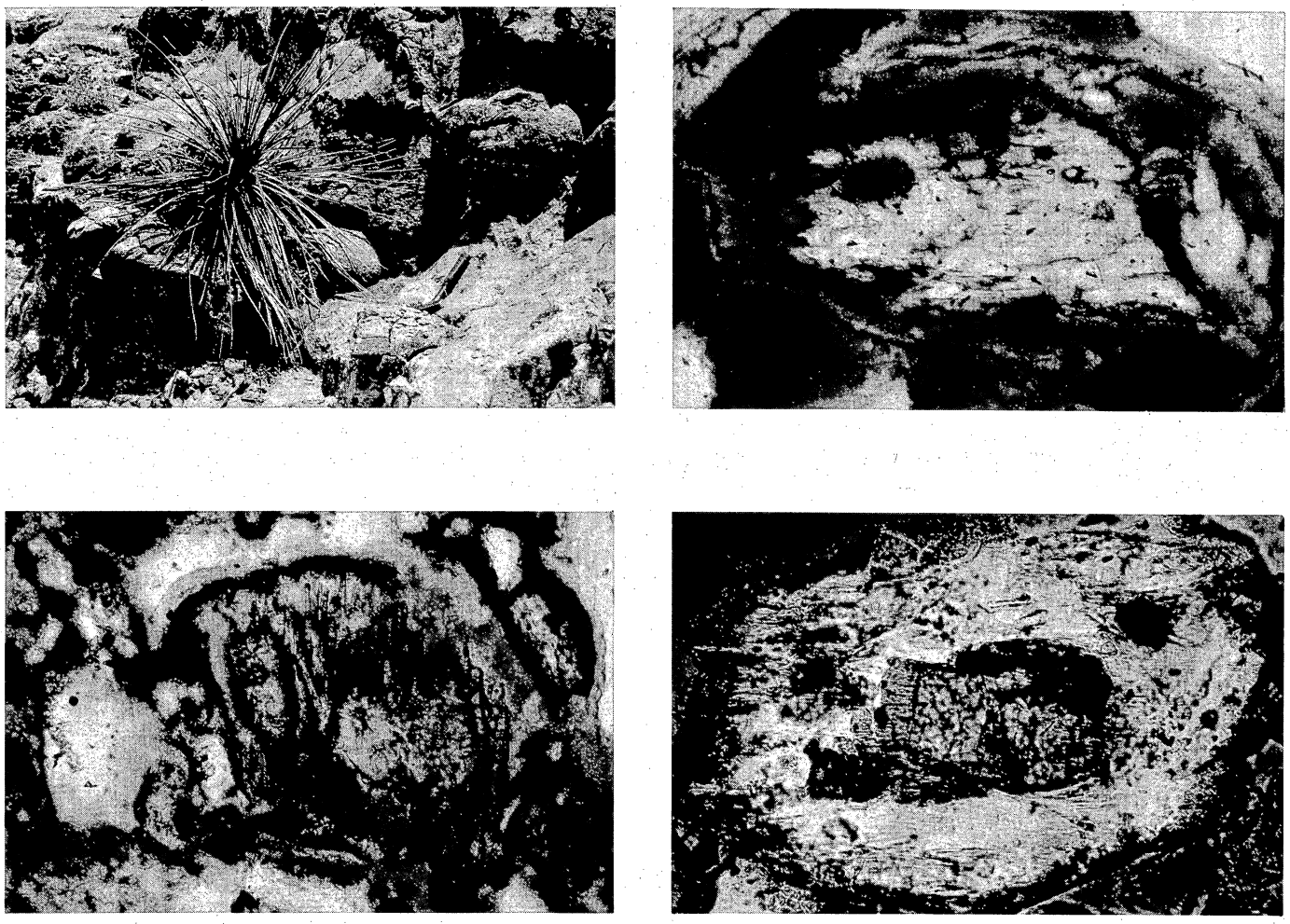

Figure 6. A. Photograph of large spherical or irregular concretions in the transition interval between the glass assemblage above and the zeolite assemblage below. These concretions contain zeolite cement and opal pseudomorphs of glass shards; calcite concretions also present at this level. Other rocks contain no zeolite, but have preserved glass. B. Coxcomb pyroxene with diaphanous clay partially filling the void left by solution of the pyroxene grain. The empty pores indicate that this sample is from the glass assemblage. C. Coxcomb lamprobolite grain. D. Olivine grain, partially converted to clay.

clinoptilolite-containing part of the Tascotal. The space left by their partial solution outlined by a rim of clay and opal like that of the shards and may be partially filled with a diaphanous membrane of clay. Some contain opal rosettes and zeolite crystals.

Other solution voids that contain no fragment of the mineral that once filled them are present in the lower part of the Tascotal. Such voids commonly contain clay, opal, or zeolite like those of the voids left after solution of inosilicates, and they do not have the characteristic shape of shards or pumice. These voids are presumed to represent mafic heavy minerals, probably amphibole or pyroxene, but possibly olivine.

Biotite and magnetite are common heavy minerals that undergo little or no change. Both undergo some oxidation and may be surrounded by a rim of red iron oxide, but are generally well preserved and easily recognizable.

Color

Observations of alteration sequence do little to explain the occurrence of iron coloring matter in the Tascotal or in other volcanic sedimentary units of the Trans-Pecos Volcanic Field: the Duff and Pruett Formations, which together with the Tascotal make up the volcanic sedimentary units of the Buck Hill Volcanic Series (Goldich and Elms, 1949), and the formations of the Vieja Group (DeFord, 1958; Walton, 1972). In both of these sequences, color development is the same. The upper part of the sequence is white or very pale shades of gray, blue, or tan.

Rocks just below the level at which zeolite appears are very pale tan. Below these are white, zeolitic rocks of the type characteristic of the Tascotal. Some distance below the appearance of zeolite and the disappearance of volcanic glass, the rocks become stained with pink along bedding planes and in finer grained beds. The coloring becomes more pervasive deeper in the stratigraphic sequence with red-browns, grayish pink, and similar colors replacing the pale shades of the upper part. The lower parts of the Tascotal are stained pink around Wire Gap, La Viuda, and San Jacinto Mountain. Much of the Duff Formation, which is beneath the Mitchell Mesa Rhyolite and farther down the diagenetic sequence than the Tascotal, is red or pink.

This change of color is related to the appearance of microscopic dots of red pigment in the clay layer of the diagenetic coating on grains and shards. These dots must form from the clay because the iron is released much higher in the section where the mafic heavy minerals and glass dissolve, and none of the other diagenetic phases should contain much iron, a supposition supported by electron probe analyses (appendix I). Iron must be released from the heavy minerals and shards, precipitated with the clay, then released farther down the system.

Conditions of Diagenesis

The minerals and textures of diagenesis can be interpreted to reveal much about the conditions under which this diagenesis took place. The information is generally qualitative or at best semi-quantitative. Nevertheless, from these conclusions, an understanding of the uranium geology

of the system can be developed.

(1) The textures of clay, opal, zeolite, and calcite indicate that diagenesis took place below the water table, in the phreatic zone. Among carbonate workers, "isopachous" cements, those which uniformly coat all grains, are routinely assigned to the phreatic zone (Bathurst, 1976). Carbonate cements that selectively form at points of grain contact, or that form as discontinuous, gravity-influenced coatings on grains are believed to form in the vadose zone. To conclude that isopachous silicate textures are formed below the water table is an extension, but a reasonable one, of the logic of carbonate petrologists. Their reasoning is not based on peculiarities of carbonate minerals but on the location of water in pore spaces; that is, in the vadose zone it is held by capillary forces at points of grain contact or as drops on undersides of grains when the rest of the pore space is empty. Water stays in contact with all of the grain surface in the phreatic zone.

(2) Carbonate textures also indicate that the waters of diagenesis were not concentrated brines. Folk (1973) pointed out that coarsely crystalline, blocky, or sparry carbonate cements form in rather fresh water, but fine-grained cements are the common result of precipitation from concentrated solutions like sea water. Investigations of carbonate systems are not sufficiently advanced to permit a quantitative distinction between the fields of concentrations where coarse and fine crystals form, but the Tascotal carbonate cements clearly lie on the low ionic strength side of the boundary between them.

(3) The sequence of minerals indicates that the pH of the system was rising as glass was dissolved. This is to be expected because hydrolysis of silica and alumina as they are released from the glass consumes hydrogen ion, which is replaced in solution by alkali and alkaline earth ions, and leaves hydroxyl ion to accumulate. The sequence from clay to opal to zeolite can also be interpreted in terms of increasing activity of the four-fold aluminate ion with increase of pH and a concomitant decrease in the availability of six-fold coordinated, gibbsite-like platlets of aluminate hydroxide that can form templates for formation of clay minerals (Hem and Roberson, 1967; Walton, 1975). The values of pH reached are likely to be about 9 or greater, according to results of Mariner and Surdam (1970). For natural systems, this pH is remarkably alkaline but it is similar to the pH achieved by other ground-water systems in volcanic regions, including warm springs in the Trans-Pecos Volcanic Field where the discharge may be exclusively water that has flowed long distances through volcanic rocks or altered volcanic sediments (Henry, oral communication). Because the rise of pH is dependent on hydrolysis of glass, it ceases when the supply of glass is exhausted.

(4) The effect of this increasing pH on the mineralogic reactions involving iron is not clear, and simple conclusions cannot be drawn about whether the system was oxidizing or reducing. Diagrams in Garrels and Christ (1965, p. 178-197) indicate that at high pH, hematite or iron hydroxides are likely to form even in slightly reducing circumstances. These are the minerals most likely to be found in the red pigment of parts of the lower Tascotal. Conversely, the oxidized rims on magnetite,

if they formed during diagenesis, indicate that the Eh was -0.2 to -0.3 or greater at pH 9 or 10.

Diagenetic Assemblages

It is convenient to divide this system into two assemblages, each of which is characterized by particular minerals that participate in the diagenetic reactions or are otherwise distinctive. These are the glass assemblage and the clinoptilolite assemblage. The boundary between the two assemblages is gradational, and one may recognize a transition interval between the assemblages. This division scheme indicates that the diagenetic system in the preserved remnant of the Tascotal is not as complete as certain diagenetic systems in volcanic sediment sequences elsewhere (Hay and Sheppard, 1977).

The glass assemblage, which encompasses the upper part of the active-apron member and nearly all of the eolian member, totals up to 100 m of section. Unaltered glass is present in all samples from it; normally glass is coated by clay, though the films of clay may be extremely thin. In the lower part of this zone, opal rosettes became common, and the glass is visibly etched. Rocks of this assemblage are light gray and almost completely friable unless cemented by calcite. Unaltered glass shards in it are clear or may appear greasy in hand specimens if the clay coating is thick enough.

The clinoptilolite assemblage forms most of the active-apron member and contains no unaltered glass. Instead it contains pseudomorphs of glass shards and pumice fragments outlined by opal and clay and filled

or partially filled by clinoptilolite. Spaces in primary pores left after clay and opal forms are similarly filled by clinoptilolite or by calcite. Rocks of the clinoptilolite zone of the Tascotal are characteristically pure white, though pink volcanic sandstones occur low in the section, but not at the bottom. Pink clays occur at various levels, but, as pointed out above, only as parts of particular depositional sequences. In the upper part of the interval containing clinoptilolite, colors may be pale yellow or tan, instead of white. This reflects a greater relative abundance of opal. These rocks are moderately indurated, with the calcite-cemented intervals and concretions in them being noticeably less cemented. Hand specimen inspection shows that the white appearance of the rock derives from the fine-grained pore-filling opal-zeolite cement, and the shards in some specimens can be seen to be microscopic druses of crystals.

The transition interval reflects the fact that the alteration takes place over a thin but discrete interval of rock. In this assemblage, brown, opal-rich, zeolite-containing areas--spherical concretions, fracture linings or individual beds--alternate with or are surrounded by light-gray, almost blue-gray, sediments containing unaltered glass and some calcite concretions. This zone is less than 10 m thick in most places; its top is at the top of the first bed or concretion containing zeolite and opal; its base is the lowest level at which glass is present. Exact definition requires careful study, and only use of x-ray diffraction or the petrographic microscope leads to confident identification of its upper and lower boundaries.

Bodies of rock where clinoptilolite has replaced glass do occur isolated within the glass assemblage. Some of these are in zones of coarse sediment, such as the one in the lower part of a thick fining-upward sequence at the Wire Gap section. Some calcite concretions up to a few tens of meters below the top of the zeolite assemblage still contain glass. Apparently they are isolated lenses of rock rendered impermeable by precipitation of calcite.

DIAGENESIS IN OPEN HYDROLOGIC SYSTEMS

Hay (1977) divides models of zeolite formation at low temperature into four types: (1) closed hydrologic system models, (2) burial metamorphic models, (3) open hydrologic system models, and (4) deep-sea diagenetic models. The burial metamorphic models require greater depths of burial than have affected the Tascotal, and the accompanying higher temperatures would produce chlorite or illite clay, not montmorillonite. Deep-sea diagenetic models do not apply to the continental sediments of Tascotal. Surdam (1977) makes clear that closed hydrologic systems, which might better be termed ground-water discharge systems, are features of playas and closed basin lakes in arid or semiarid regions. It is unlikely that fluvial sediments of the Tascotal were altered according to this model.

Only the open hydrologic system model of Hay (1963), Walton (1975), and Hay and Sheppard (1977) remains. This conclusion is supported by several lines of evidence. The textures and structures of alteration are similar to those encountered in other open hydrologic systems such

as the John Day Formation (Hay, 1963) or the Vieja Group (Walton, 1975). The observed sequence of formation of minerals is also the sequence of their occurrence with increasing depth. Finally, the stratigraphic position of the boundary between the glass assemblage and the clinoptilolite climbs stratigraphically through some outcrop belts of the Tascotal, just as it does in other sequences where zeolites have formed in open hydrologic systems. The best example of this stratigraphy is in the southern apron member of the Tascotal which contains zeolite only at its base near Big Hill and throughout its thickness at Tapado Canyon.

The Course of Diagenesis

Open-system diagenesis occurs as the sediment accumulates and is driven by the reactions between unstable constituents of the sediment and the water that flows through it. In the Tascotal, the reactions took place in the phreatic zone. The open system requires that a critical thickness of sediment lie beneath the water table before extensive mineral reactions begin because water flowing past a certain point in the rock must reach a certain composition before each of the series of reactions can occur there (fig. 7, Walton 1975). The initial formation of clay probably occurs shortly after a particular increment of sediment passes beneath the water table. As more sediment accumulates and the water table rises through it, the water reaching each increment of sediment in the phreatic zone has been in contact with volcanic glass for a longer period of time and is more concentrated in constituents it has dissolved from the glass. Presumably, the water table

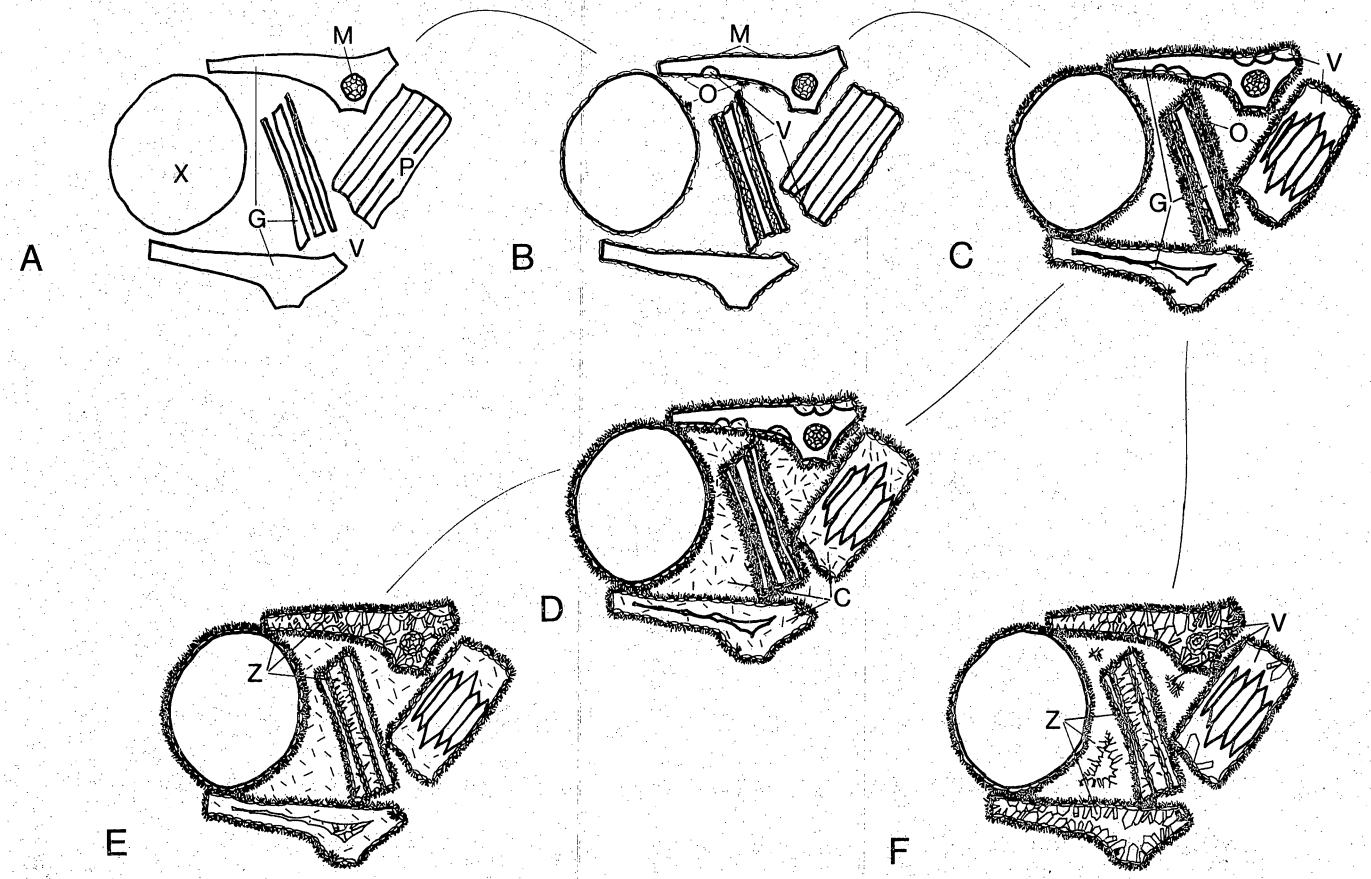

Figure 7. Paths of diagenesis and the textures that result. A. Initial condition--glass shards (G), a crystal of quartz or feldspar (X) and a pyroxene or hornblende grain (P). This composition is characteristic of fine sandstones of the active apron. Voids (V) between grains. Montmorillonite (M) fills a bubble in a shard. B. A clay coating (M) covers all surfaces. Opal spheres and rosettes (O) are present. A hemispherical etch pit has formed on the glass shard and the inosilicate grain is beginning to dissolve. Note clay filling pumice tubes. C. Dissolution of the glass and inosilicate grains has continued--one shard is reduced to a small fiber near the center of the shard pseudomorph, which has not been filled with anything--yet. The opal rim is now complete, but pores are still large. From this point, either of two paths can be followed: directly to F or through D to E. D. Precipitation of calcite (C) in all pores of the previous sketch. E. This is followed by dissolution of remaining glass and precipitation of zeolite (Z). F. The other route occurs outside calcite concretions where the glass dissolves and zeolite forms druses in pores, shard pseudomorphs, and inosilicate pseudomorphs. Crystal size of the clinoptilolite is smaller in the pores than in pseudomorphs, and voids remain.

rises because the accumulation of sediment in the active apron and valley raise the level at which discharge can occur. It may also rise because permeability restriction caused by precipitation of clay, opal, and zeolite during diagenesis forces the flow of ground water to remain near the surface and not to reach deep into the system.

As the reactions with glass proceed, silica and alumina are precipitated first as clay and then as opal, keeping the level of those components in solution below saturation with respect to glass, but raising the pH by hydrolysis. With increasing pH, in the range from neutrality to about pH 9, aluminate becomes more soluble, but silica solubility remains rather constant. Consequently, the ratio of aluminate to silicic acid in solution increases: the composition of the precipitated phase changes from clay, which contains six-fold alumina but not four-fold aluminate, to opal, which contains some aluminate having an Si/Al atomic ratio of 20 to 1 to 70 to 1, to clinoptilolite, in which the proportion of silica to aluminate is about 3 to 1 to 5 to 1 (appendix I, Hem and Roberson, 1967; Mariner and Surdam, 1970; Walton, 1975).

The final solution of glass must be quite rapid compared to the earlier course of the reaction, both because the pH is quite high, perhaps high enough for silicic acid to dissociate and the solubility of silica consequently to increase, and because silica and alumina are being removed from the solution in a proportion similar to that in which they are being released from glass. Consequently, the accumulation of neither silica nor alumina takes place in solution, and no limit exists on the amount of glass solution. This condition develops because the solubilities

of aluminate and of silica are greater with respect to glass than they are with respect to clinoptilolite. Solution continues until all glass is consumed.

At any time an accumulation of volcanic sediment undergoing diagenesis in an open hydrologic system can be divided into a number of zones separated by surfaces at which the percolating water has reached a particular composition. Thus, a certain diagenetic reaction occurs only at that level and below it. As the water table rises through each increment of sediment, these surfaces move upstream in the water flow because the water takes longer to reach each point in the sediment. The flow of water may be downward, laterally, or, conceivably, upward toward a zone of discharge. This movement of the surfaces continues until the process is interrupted by a cessation of sediment accumulation, sealing of the ground-water system by a lava flow or welded ash-flow tuff, or interruption of the flow by faulting or erosion.

Reactions Involving Carbonate and Uranium

The glass shards of the Tascotal contained about 9 ppm uranium when deposited, and during dissolution all of this uranium, presumably, was released into the solution as the glass dissolved (table 2). The volume of glass in the Tascotal is so great that had this amount of uranium been free to migrate through ground water, uranium deposits of immense proportion could have been formed. But whole-rock uranium analyses indicate that such deposits are not formed (table 1): the average of 12 analyses of rocks from the glass assemblage is 4.2 ppm; the average of

Table 1: Uranium content of Tascotal rocks (in ppm)*

Diagenetic Assemblage	Wire Gap Section Sample - #	Wire Gap Section U content	Windmill Section Sample - #	Windmill Section U content	Tascotal Mesa North Section Sample - #	Tascotal Mesa North Section U content	La Viuda Section Sample - #	La Viuda Section U content	Manny Howard Section Sample - #	Manny Howard Section U content
			187	3.2						
			163.8	3.3						
Glass Assemblage	687	6.5	137	3.0	118	5.2				
	640	2.2	135.5	3.0	727	5.7				
	476	6.2	130	3.0	63	2.9	264	6.2		
			127.5	0.9	42.1	5.8				
			126NZ	4.1	42	7.7				
Transition			126 Z	2.3						
			124.5	1.2	41.8	5.6				
			122.5	2.7						
			111	1.4			220	11.3	364	4.2
			109	2.6	31.2	4.6			274	25.8
	418	5.6	60.9	3.1					227	5.0
Zeolite Assemblage			42	3.5	8	5.8			180	5.0
			33.5	3.4					65	6.8
			33	3.9					10	7.8

*Analysis methods outlined in appendix II.

Table 2: Uranium content of glass or zeolite-opal fraction of Tascotal rocks*

Fraction	Windmill Section		Tascotal Mesa North		Manny Howard Section	
	Sample # -	U-content	Sample # -	U-content	Sample # -	U-content
Glass	135.5	9.4	118	8.0		
	127.5	9.1	727	11.0		
	126NZ**	8.2	63	9.8		
	124.5**	5.4	42.1**	9.4		
			41.8**	10.3		
Zeolite + Opal	113.5	1.8	37.1	4.4	364	4.4
	111	6.6	8	4.5	274	35.4
	101	5.4			227	2.9
	12.3	6.8			180	4.9
	8	6.2				
	7	5.3				

*Methods outlined in appendix II.
**These samples may contain appreciable amounts of opal in addition to the glass.

16 analyses of rocks of the zeolite assemblage is 6.2 ppm; and the average of 8 analyses from the transition interval is 3.8 ppm. Sample MH 274 is clearly anomalous (25.8 ppm), and elimination of this value from the average of zeolite assemblage rocks reduces their average to 4.8 ppm. A very slight enrichment of uranium in the zeolite assemblage is implied; perhaps this balances the slight depletion in the transition interval, or it may not even be significant. Whole-rock analyses indicate that the uranium has simply moved from one phase to another, migrating distances measured in micrometers or meters, but not being concentrated into economic deposits.

Table 2, which lists uranium content of mineral fractions separated by density, shows that the glass fraction contains about 9 ppm uranium, and therefore probably contains most of the uranium available for migration. Samples containing only zeolite-opal intergrowths average 6.8 ppm, but elimination of the anomalous MH 274 sample reduces this to 4.4 ppm. Clearly, the uranium does not simply migrate from glass to zeolite-opal, but must go elsewhere in the rock; perhaps some goes into clay, but most clay forms before the glass dissolves and uranium is released. Nor is the uranium absorbed into the zeolite as an exchangeable action. Zielinski (oral communication) points out the importance of iron-manganese oxide specks in zeolite as a host of uranium. It is unlikely that the preparation procedures (grinding, sieving, separation by heavy liquids and washing with acetone) would disturb the uranium content of these specks, if they are present in Tascotal samples, any more than outcrop exposure did. The fate of uranium in this system is a major unresolved question.

Why Did Uranium Not Migrate?

On the other hand, it is important to analyze the system in order to determine the reasons why uranium did not migrate in this alteration system. By understanding why this system was ineffective at releasing uranium for concentration, it is possible to suggest alternative kinds of systems in which uranium release could be effective. Recognition of diagenetic systems that produced uranium-rich solutions could be a valuable key to evaluating volcanic sedimentary or tuffaceous intervals as potential uranium deposits.

Initially the diagenetic system was slightly reducing to slightly oxidizing. In such circumstances, uranium can migrate only if it is complexed by some ligand in solution (Hostetler and Garrels, 1962). Most common of these ligands is carbonate ion. Although other complexes are possible, this analysis will treat carbonate ion first, then mention phosphate, a possible alternative. The analysis presented here hinges on observations of calcite distribution in the rock and on understanding this system as an open hydrologic system that operated in the phreatic zone. In an open leaching system, water entering the phreatic zone will contain a certain amount of CO_2, and the partial pressure of CO_2 will depend on the history of the water; if it is recharged from rivers, it should contain CO_2 in equilibrium with the atmosphere, a partial pressure of $10^{-3.5}$ atmospheres. If the water passed through the soil on its way to the water table, it could have a higher pCO_2, perhaps 10 to 100 times atmospheric partial pressures. The amount of total dissolved carbonate species is a function of the pH of the system as well as the controlling pCO_2, if the pH is

fixed independently of CO_2-water reactions.

Probably, the pCO_2 with which waters entering the Tascotal diagenetic system came to equilibrium was about that of the atmosphere. Water recharge into alluvial fan-like systems would likely be through channel bottoms. There is no evidence of paleosoil development in the Tascotal, which would imply that the high pCO_2 associated with some soil atmospheres probably did not develop. Finally, vertebrate remains from older and younger rocks indicate that the climate was that of a steppe or other region with rather small or seasonal amounts of rainfall--though clearly greater than the amounts characteristic of deserts (Wilson, oral communication, 1978). Generally, the pCO_2 of the soil atmosphere increases with rainfall (Hunt, 1972) because the productivity of plants, the amount of organic matter, and the rates of decay are higher in wet climates. On the other hand, the initial pCO_2 controlled the initial pH of the ground water until the process of hydrolyzation of silica became important because no other pH controlling factors, such as accumulation of organic matter, occurred in the Tascotal.

Dissolution of glass, however, had two effects on this water that are relevent to the CO_2 concentration. One is the increase of pH mentioned before. Increasing pH converts a fraction of the dissolved carbon dioxide to bicarbonate ion and eventually to carbonate ion, according to the dissociation constants of these species. The second effect was that solution of glass released to ground water the CaO contained in the Tascotal glass, about 0.5 to 0.6 percent by weight (appendix I). The combined result of these two effects was that the solution became saturated with $CaCO_3$. Petrographic evidence indicates that precipitation of calcite began when only

a small amount of glass had dissolved, about the same time that opal formed (fig. 7). Precipitation continued as glass dissolved and released calcium, until virtually no CO_2 remained in solution in any form. The high calcium content of the ground water is confirmed by the abundance of Ca in the clinoptilolite (appendix I).

Only after the CO_2 was depleted did most of the glass dissolve. Calcite replaces glass only in uncommon situations in the Tascotal. Instead, it forms a cement, filling voids that lie in primary pores. If glass had been dissolved at the time calcite formed, there would be little reason to expect the carbonate cement to be restricted to the primary pores; it should fill the secondary pores formed by solution of glass as well. In fact, the relatively rapid solution of glass alluded to before may have taken place because the depletion of dissolved carbon dioxide species leaves little buffer capacity in the ground water solution. The pH may rise, uninhibited, to levels at which silica is very soluble and the aluminate ion to silicic acid in the solution is such that clinoptilolite forms. With no CO_2 present in any form, the most likely complexing agent for uranium released from glass is removed, and the uranium will precipitate as uranophane or uraninite, as an impurity in opal, or in iron-maganese oxide specks (Zielinski, oral communication).

Several other complexing agents might act to keep uranium in solution. One which could be important, but which was probably not important in this system, is phosphate. Phosphate compounds have a solubility pattern similar to that of carbonate in that a calcium-bearing phase, apatite, dahllite or collophane, becomes less soluble with increasing pH.

The effectiveness of phosphate as a complexing agent in this system can be understood by considering the fact that the pH was quite high by the time most of the glass dissolved and the fact that none of the apatite in the system shows evidence of solution. In fact, phosphate occurs mostly as rod-like apatite crystals in plagioclase. Some plagioclase has suffered dissolution during diagenesis and left a pile of unaffected apatite crystals in void formed by its solution. The lack of phosphate solution, the high concentrations of calcium inferred above, and the high pH of the system indicate that although the ground water was saturated with apatite or other phosphate phases, it contained little phosphate ion, apparently not enough to complex uranium.

SYSTEMS THAT CAN RELEASE URANIUM: HYPOTHETICAL

The key reason that dissolving glass in the Tascotal apparently did not release uranium for long distance migration is that the high pH and large amounts of calcium released during diagenesis used up the likely complexing agents. Systems that should release uranium, then, are those in which complexing agents are available and have not been removed by reactions in the system itself. This discussion will concentrate on systems in which carbonate is the most likely complexing agent.

Two kinds of systems in which consumption of CO_2 could be prevented are buffered systems, in which some mechanism prevents the increase of pH that characterized the Tascotal, and systems open to CO_2. Buffering could result from the lack of volcanic glass in the system, but that would be an uninteresting system if the glass were the only source of uranium.

More likely, it could occur in a diagenetic situation in which organic matter or other sources of acid are abundant. Organic matter is an excellent material in some respects because it not only provides acid, but its oxidation can also provide CO_2 to the system. Unfortunately, organic matter may also absorb some of the uranium itself and slow or prevent its release and migration.

Systems open to CO_2 are probably the most suitable ones for release of uranium for long distance migration. Of these kinds, the simplest and most reliable are soil systems in which plant-root respiration and decay of organic matter provides excellent, renewable supplies of CO_2. Such systems generally are acid, though they may be alkaline in arid regions and are zones of intense leaching. Attacks of organisms, especially plants, on soil material, and active leaching solutions would remove certain constituents of the glass, converting it to a mixture of aluminum- and silicon-rich materials like allophane or clay. Downward infiltrating water would erode these materials high in the soil column and deposit them lower down, where they form alluviated clay features such as cutans. The result would be a soil in which the glass was dissolved and nothing remained to preserve its primary texture. Soils could exist that were developed exclusively on pure volcanic glass, but they would contain no trace of that material. They would consist only of clay, some resistant oxide phases, and either bauxite or calcite, depending on the climate. In such a circumstance the glass is completely dissolved and the uranium released, just as was true in the Tascotal. But after release the uranium could be complexed by carbonate ion and transported to a distant site of

precipitation. Because of a constant replenishment of CO_2, soil systems can yield solutions rich in uranium.

In evaluating sequences of sediment that originally contained volcanic glass for their potential as uranium deposits, one should look for evidence that the system could have released uranium. Such evidence could be any of the following: (1) extensive development of paleosoil horizons; (2) alteration of glass or clay or its replacement by calcite, and; (3) evidence of buffering materials such as organic matter in the system.

The presence of early calcite, precipitated only before extensive dissolution of glass, and indicators of high pH such as zeolites, suggest that uranium, though released from the glass, could not migrate to form deposits. These differences are easily recognizable in thin section and might be detected by careful field observation. In any case, chemical analyses should be used, if possible, to substantiate any conclusions.

FAVORABLE ENVIRONMENTS FOR URANIUM IN VOLCANIC SEDIMENTS

None of the informal members of the Tascotal contains recognized paleosoils. Consequently, none is known to have released uranium during solution of glass. Soil development can occur in almost any continental depositional environment if sedimentation is slow enough and the climate promotes growth of vegetation. Generally, the most favorable environment for release of uranium among those in volcanic sediment terrains is the valley environment, because broad areas of slow sedimentation on parts of the floodplain are subject to soil formation, and a relatively high water table there is favorable for growth of plants and higher pCO_2 in

the soil atmosphere. Walton (1977a) describes a valley facies in the Chambers and Capote Mountain Formations of the Vieja Group along the western margin of the Trans-Pecos Volcanic Field. The rocks consist of interbedded fluvial channel deposits and floodplain deposits, including calcite-rich, shard-free horizons interpreted as paleosoils. These horizons did contain some ghosts of shards replaced by calcite and they probably have effectively released any uranium they originally contained. Becuase the beds contain few ghosts of shards, however, they may or may not have contained substantial amounts of uranium initially.

CONCLUSIONS

(1) Diagenesis of the Tascotal occurred in an open hydrologic system. Glass was dissolved, perhaps congruently, and its constituents precipitated as clay, opal, clinoptilolite, calcite, and perhaps hematite. Mafic silicate heavy minerals also were dissolved.

(2) Diagenesis occurred below the water table in an oxidizing to slightly reducing milieu in which hydrolization of silica and alumina raised the pH to values of 9 or greater.

(3) Precipitation of calcite before most of the glass dissolved removed carbonate species from the diagenetic system.

(4) Uranium was present in glass shards in amounts averaging about 9 ppm. When the shards were dissolved, this uranium was released to solution. A lack of complexing agents in solution prevented long distance migration of uranium and its concentration into deposits of economic

grade.

(5) Diagenetic or alteration systems in which complexing agents are not depleted are more efficient at releasing uranium than are systems where complexing agents are not present, even though large amounts of uranium may initially have been present in the systems depleted by the complexing agent. Soil systems are the best examples of systems in which carbonate complexing agents are not depleted.

(6) Of the depositional environments in volcanic terrains, the ones most suitable for release of uranium from volcanic glass are the valley systems, where soils are more likely to occur and high water tables promote growth of vegetation. Paleosoils have not, however, been recognized in the lower conglomerate member of the Tascotal Formation.

REFERENCES

Bathurst, R. G. C., 1976, Carbonate sediments and their diagenesis: 2nd ed., Amsterdam, Elsevier.

DeFord, R. K., 1958, Tertiary formations of Rim Rock Country, Presidio County, Texas: Texas Journal of Science, v. 10, p. 1-37.

Folk, R. L., 1973, Carbonate Petrography in the post-Sorbian age, in Ginsburg, ed., Evolving concepts in sedimentology: Baltimore, Johns Hopkins University Press, p. 118-158.

Garrels, R. M., and Christ, C. L., 1965, Solutions, minerals, and equilibria: New York, Harper and Row.

Goldich, S. S., and Elms, M. A., 1949, Stratigraphy and petrology of the Buck Hill Quadrangle, Texas: Geological Society of America Bulletin,

v. 60, p. 1133-1182.

Hay, R. L., 1963, Stratigraphy and zeolitic diagenesis of the John Day Formation of Oregon: Berkeley, University of California Publications in Geological Sciences, v. 42, p. 199-262.

Hay, R. L., 1977, Geology of zeolites in sedimentary rocks: in Mumpton, F. A., ed., Mineralogy and geology of natural zeolites: Mineralogical Society of America, Short Course Notes no. 4, p. 53-64.

Hay, R. L., and Sheppard, R. A., 1977, Zeolites in open hydrologic systems: in Mumpton, F. A., ed., Mineralogy and geology of natural zeolites: Mineralogical Society of America, Short Course Notes, no. 4, p. 93-102.

Hem, J. D., and Roberson, C. E., 1967, Form and stability of aluminum hydroxide complexes in dilute systems: U.S. Geological Survey Water-Supply Paper, 1827-A.

Hostetler, P. B., and Garrels, R. M., 1962, Transportation and precipitation of uranium and vanadium at low temperatures, with special reference to sandstone-type uranium deposits: Economic Geology, v. 57, p. 137-167.

Jones, J. B., and Segnit, E. R., 1971, Nature of opal I, nomenclature and constituent phases: Journal of the Geological Society of Australia, v. 18, p. 57-68.

Mariner, R. H., and Surdam, R. C., 1970, Alkalinity and formation of zeolites in saline alkaline lakes: Science, v. 170, p. 977-980.

Mumpton, F. A., and Ormsby, V. C., 1976, Morphology of zeolites in sedimentary rock by scanning electron microscopy: Clays and Clay Minerals, v. 24, p. 1-23.

Rosholt, J. N., Prijana, and Noble, D. C., 1971, Mobility of uranium and thorium in glassy and crystallized silicic volcanic rocks: Economic Geology, v. 66, p. 1061-1069.

Surdam, R. C., 1977, Zeolites in closed hydrologic systems: in Mumpton, F. A., ed., Mineralogy and geology of natural zeolites: Mineralogical Society of America, Short Course Notes no. 4, p. 65-91.

Walton, A. W., 1972, Sedimentary petrology and zeolite diagenesis of the Vieja Group (Eocene-Oligocene), Presidio County, Texas: The University of Texas at Austin, Ph.D. dissertation.

Walton, A. W., 1975, Zeolitic diagenesis in Oligocene volcanic sediments, Trans-Pecos Texas: Geological Society of America Bulletin, v. 86, p. 651-724.

Walton, A. W., 1977a, Petrology of volcanic sedimentary rocks, Vieja Group, southern Rim Rock Country, Trans-Pecos Texas: Journal of Sedimentary Petrology, v. 47, p. 137-157.

Weaver, F. M., and Wise, Jr., S. W., 1972, Ultramorphology of deep sea cristobalitic chert: Nature, Physical Sciences, v. 237, p. 56-57.

Wilson, M. D., and Pittman, E. D., 1977, Authigenic clays in sandstones: Recognition and influence of reservoir properties and paleoenvironmental analysis: Journal of Sedimentary Petrology, v. 47, p. 3-31.

Zielinski, R. A., 1978, Uranium abundances and distribution in associated glassy and crystalline rhyolites of the western United States: Geological Society of America Bulletin, v. 89, p. 409-414.

Appendix I: Electron probe analyses of diagenetically active phases.

Mineral	Sample*	Analysis**	SiO_2	Al_2O_3	FeO Total	CaO	Na_2O	K_2O
Clinoptilolite	WM 58.7	140400	64.77	12.68	.08	---	---	---
	WM 58.7	140410	61.37	12.17	.06	---	---	---
	WM 58.7	140420	64.50	12.69	.09	---	---	---
	WM 58.7	140430	65.79	12.79	.18	---	---	---
	WM 58.7	140440	65.16	13.07	.13	---	---	---
	WM 58.7	140450	63.64	12.63	.08	---	---	---
	WM 58.7	140460	65.18	13.05	.14	---	---	---
	WM 58.7	140470	63.15	12.84	.18	---	---	---
	WM 58.7	140480	62.00	12.82	.12	---	---	---
	WM 58.7	140490	64.79	13.12	.14	---	---	---
	WM 122.5	141400	66.97	15.34	1.69	4.94	1.87	1.42
	WM 122.5	141410	66.46	14.58	.05	4.61	.44	1.58
	WM 122.5	141420	66.92	14.68	.24	4.67	.47	1.38
	***WM 122.5	141430	91.99	1.31	.13	2.41	.29	.90
	WM 122.5	141440	74.25	11.81	.05	2.53	.27	.74
	WM 122.5	141450	70.03	12.02	<0.01	4.51	.39	1.52
	WM 122.5	141460	70.33	12.90	.05	4.90	.55	1.42
	TM 42	142400	70.35	14.51	.12	2.31	2.50	2.94
	TM 42	142411	68.25	14.11	.21	2.89	2.16	2.14

* WM = Wind mill section; TM = Tascotal Mesa north section; LV = La Viuda section; B-3 = Bishop Ranch #3 section; G = Godbold-Jap section; RR = Rawls road section.

** Each analysis is the average of three or more counts on one or more points within a grain or an area of a thin section.

*** Analysis considered suspect because it does not indicate a likely composition for this phase.

Appendix I: Electron probe analyses of diagenetically active phases. (Continued)

Mineral	Sample*	Analysis**	SiO_2	Al_2O_3	FeO Total	CaO	Na_2O	K_2O
Clay	*** TM 42	142567	62.93	3.38	3.80	----	----	----
	TM 42	142586	57.10	13.74	2.93	2.06	1.05	2.35
	TM 42	142570	57.17	17.72	6.91	2.58	3.20	2.56
	***G 103	158500	36.78	6.32	2.21	3.54	2.24	1.67
	G 103	158501	53.14	23.49	.68	1.88	1.02	.73
	G 103	158502	55.62	9.90	2.90	1.29	.62	.61
	G 103	158503	66.47	13.21	3.40	.39	.26	5.79
	***G 103	158504	36.35	3.91	4.27	.73	.69	2.41
	G 103	158505	49.97	8.03	.04	.34	.34	.26
	G 103	158506	59.59	10.91	4.29	.22	.08	.73
	G 103	158507	59.60	8.73	5.65	.94	.26	1.43
	G 103	158508	48.27	6.67	5.88	.96	.24	1.35
	G 103	158509	57.53	13.40	6.25	.60	2.34	6.20
Opal	WM 122.5	141200	76.47	3.58	2.87	.95	.09	.37
	***WM 122.5	141210	48.58	10.47	9.82	1.25	.11	.99
	WM 122.5	141230	80.06	1.35	.69	.46	.25	.44
	***WM 122.5	141240	41.25	10.18	5.05	2.58	1.38	2.50
	***WM 122.5	141250	36.06	2.65	.55	1.71	.10	.92
	***WM 122.5	141260	37.40	4.78	.87	.79	.17	.49
	TM 42	142200	87.44	2.14	.46	.78	.03	1.00
	TM 42	142221	84.96	1.96	.47	.77	.54	1.07
	***TM 42	142262	37.20	5.28	6.65	.60	.35	.69
	***TM 41.8	143200	39.08	2.90	1.11	----	----	----
	***TM 41.8	143210	46.75	3.90	2.43	----	----	----

Appendix I: Electron probe analyses of diagenetically active phases. (Continued)

Mineral	Sample*	Analysis**	SiO_2	Al_2O_3	FeO Total	CaO	Na_2O	K_2O
Clinoptilolite	TM 42	142434	72.87	14.43	.27	2.42	2.19	2.75
	TM 42	142445	69.61	13.13	.15	2.25	3.34	2.76
	TM 42	142478	66.77	13.01	.12	2.56	2.92	2.60
	TM 42	142420	68.79	13.80	.14	2.57	2.85	2.62
	TM 42	142450	71.05	13.73	.12	2.10	2.98	2.75
	TM 42	142460	69.92	13.62	.12	2.40	2.73	2.67
	TM 42	142480	60.44	11.53	.17	2.14	2.85	2.86
	WM 126Z	144400	66.45	12.95	.05	4.52	.65	1.26
	WM 126Z	144422	65.61	11.98	.24	2.66	.63	.81
	WM 126Z	144433	69.94	10.74	.25	3.12	.42	.87
	WM 126Z	144444	70.94	13.50	.28	4.33	.61	1.09
	WM 126Z	144410	70.11	10.82	.14	2.30	.35	.64
	WM 126Z	144450	68.93	12.70	.10	4.71	1.99	1.03
	WM 126Z	144460	67.67	11.66	.20	4.27	.38	.70
	WM 126Z	144470	74.30	6.26	.03	4.39	.56	1.09
	WM 126Z	144480	64.58	12.71	.18	4.42	.52	1.09
	WM 126Z	144490	67.63	12.70	.25	3.03	.45	.82
	WM 101	146400	68.10	13.48	.54	4.38	1.47	.98
	WM 101	146401	65.85	14.29	<0.01	3.52	2.94	1.32
	WM 101	146402	64.77	13.53	.10	3.51	3.34	1.24
	WM 101	146403	64.01	13.76	.10	3.51	3.08	1.06
	WM 101	146404	-----	-----	----	3.21	3.30	1.02
	WM 113.5	155410	68.45	13.66	<0.01	----	----	----

Appendix I: Electron probe analyses of diagenetically active phases. (Continued)

Mineral	Sample*	Analysis**	SiO_2	Al_2O_3	FeO Total	CaO	Na_2O	K_2O
Clinoptilolite	***WM 113.5	155400	53.28	10.68	< 0.01	----	----	----
	WM 113.5	155420	72.32	13.07	< 0.01	----	----	----
	WM 113.5	155430	69.19	13.85	< 0.01	----	----	----
	WM 113.5	155440	68.95	13.65	< 0.01	----	----	----
	WM 113.5	155450	68.64	13.26	0.01	----	----	----
	WM 113.5	155460	69.12	13.54	< 0.01	----	----	----
	WM 113.5	155470	71.55	12.52	< 0.01	----	----	----
	WM 113.5	155480	68.72	13.61	< 0.01	----	----	----
	WM 113.5	155490	66.38	13.69	.02	----	----	----
	LV 163.5	156400	68.17	13.51	.20	----	----	----
	LV 163.5	156410	69.76	12.83	.17	----	----	----
	LV 163.5	156420	70.08	13.12	.05	----	----	----
	LV 163.5	156430	68.73	13.15	< 0.01	----	----	----
	LV 163.5	156440	68.52	13.50	.01	----	----	----
	LV 163.5	156450	70.44	13.30	.09	----	----	----
	LV 163.5	156460	70.41	13.23	< 0.01	----	----	----
	LV 163.5	156470	71.72	12.87	.14	----	----	----
	LV 163.5	156480	71.22	13.08	.07	----	----	----
	LV 163.5	156490	71.34	13.64	.09	----	----	----
	B3 11.5	157400	63.61	17.30	< 0.01	----	----	----
	B3 11.5	157410	64.92	16.11	.03	----	----	----
	B3 11.5	157420	65.60	15.80	.08	----	----	----
	B3 11.5	157430	68.16	15.43	.02	----	----	----
	B3 11.5	157440	61.51	15.44	< 0.01	----	----	----

Appendix I: Electron probe analyses of diagenetically active phases. (Continued)

Mineral	Sample*	Analysis**	SiO_2	Al_2O_3	FeO Total	CaO	Na_2O	K_2O
Clinoptilolite	B3 11.5	157450	64.26	16.60	< 0.01	----	----	----
	B3 11.5	157460	64.00	17.30	< 0.01	----	----	----
	B3 11.5	157470	64.30	16.45	< 0.01	----	----	----
	B3 11.5	157480	65.48	14.06	.61	----	----	----
	B3 11.5	157490	65.91	15.84	< 0.01	----	----	----
	G 103	158400	71.20	13.24	< 0.01	2.93	2.62	2.43
	G 103	158401	69.05	13.10	.09	2.15	3.26	2.69
	G 103	158402	69.46	13.05	< 0.01	2.29	3.21	2.41
	G 103	158403	64.60	12.23	.02	3.55	2.19	1.85
	G 103	158404	68.82	11.88	.21	3.21	1.95	1.76
	G 103	158405	68.82	12.61	< 0.01	2.58	3.56	2.71
	G 103	158406	69.92	13.09	.25	2.82	2.17	1.99
	G 103	158407	68.90	12.70	< 0.01	1.93	3.74	2.72
	G 103	158408	69.00	13.23	< 0.01	3.05	2.48	1.98
	G 103	158409	68.02	13.71	.12	2.22	2.65	2.47
	LV 220	159433	-----	-----	-----	3.32	1.77	1.70
	LV 220	159400	-----	-----	-----	3.66	1.57	1.12
	LV 220	159410	-----	-----	-----	3.67	1.97	1.31
	LV 220	159420	-----	-----	-----	3.88	2.18	.80
Clay	WM 58.7	140500	42.81	7.30	9.14	----	----	----
	WM 58.7	140510	40.26	8.21	10.66	----	----	----
	WM 58.7	140520	51.99	10.67	15.24	----	----	----
	TM 42	142500	61.28	9.63	2.41	1.61	1.20	2.35
	TM 42	142511	48.40	13.74	9.74	.70	.60	1.07

Appendix I: Electron probe analyses of diagenetically active phases. (Continued)

Mineral	Sample*	Analysis**	SiO_2	Al_2O_3	FeO Total	CaO	Na_2O	K_2O
Opal	***TM 41.8	143220	53.80	4.41	2.92	----	----	----
	WM 126Z	144200	89.08	1.60	.15	.79	.28	.45
	WM 126Z	144210	87.20	1.42	.08	.75	.24	.41
	WM 126Z	144220	85.08	1.31	.06	.62	.27	.12
	WM 126Z	144230	90.74	.33	.14	.10	.15	.14
	WM 126Z	144240	86.91	1.47	.06	.66	.13	.17
	WM 126Z	144250	88.68	.38	.08	.50	.13	.04
	WM 126Z	144260	90.13	1.34	.19	.66	.12	< .01
	WM 126Z	144270	89.62	1.13	.25	.45	.17	.24
	WM 126Z	144280	89.33	1.40	.14	.60	.21	.06
	WM 126Z	144290	87.65	1.66	.13	1.26	.27	.24
Glass	TM 41.8	143100	70.14	11.10	.68	.48	2.62	5.40
	TM 41.8	143110	68.39	12.21	1.82	.73	2.59	5.23
	TM 41.8	143120	73.55	11.72	.67	.32	2.88	5.98
	TM 41.8	143130	71.54	11.22	.77	.29	2.73	5.39
	TM 41.8	143140	70.79	11.39	1.13	.39	2.68	5.63
	TM 41.8	143150	71.11	11.29	.64	.63	2.55	5.40
	TM 41.8	143160	67.70	12.44	2.62	1.31	2.58	5.69
	TM 41.8	143170	69.60	11.03	.85	.36	2.39	5.21
	TM 41.8	143180	70.56	10.81	.50	.33	2.59	5.18
	TM 41.8	143190	71.00	12.46	.55	.33	2.70	5.85
	TM 118	147100	70.18	11.65	.87	.47	2.15	6.33
	TM 118	147110	70.07	11.17	.80	.39	2.13	6.42

Appendix I: Electron probe analyses of diagenetically active phases. (Continued)

Mineral	Sample*	Analysis**	SiO_2	Al_2O_3	FeO Total	CaO	Na_2O	K_2O
Glass	TM 118	147120	70.48	11.37	.93	.36	2.30	6.29
	TM 118	147130	68.47	11.08	.92	.40	2.08	6.55
	TM 118	147140	68.18	10.94	1.03	.53	1.80	5.96
	TM 118	147150	70.93	11.09	1.30	.67	1.99	5.85
	TM 118	147160	70.37	11.14	1.28	.42	2.23	6.25
	TM 118	147170	69.46	10.98	1.17	.73	2.00	5.87
	TM 118	147180	69.24	11.12	1.25	.63	2.26	5.80
	TM 118	147190	70.12	10.72	1.02	.37	2.34	6.08
	WM 194.5	148100	67.59	10.94	1.05	.47	2.38	5.69
	WM 194.5	148110	69.33	10.91	1.05	.59	2.20	5.70
	WM 194.5	148120	70.89	11.44	1.38	.53	3.30	4.86
	WM 194.5	148130	71.07	12.43	1.34	.84	3.11	5.16
	WM 194.5	148140	67.38	11.67	1.20	1.03	2.13	5.28
	WM 194.5	148150	70.27	11.06	1.45	.63	2.04	5.66
	WM 194.5	148160	68.67	11.99	1.61	1.17	1.84	4.26
	WM 194.5	148170	71.35	10.61	1.08	.55	2.97	5.49
	WM 194.5	148180	68.71	11.35	.95	.45	2.42	5.93
	WM 194.5	148190	69.91	10.47	.66	.50	2.26	5.86
	LV 345	149100	69.63	10.94	1.30	.60	2.52	5.30
	LV 345	149110	71.71	10.78	1.10	.51	2.77	5.94
	LV 345	149120	69.31	11.09	1.01	.55	2.80	5.33
	LV 345	149130	70.50	11.04	1.32	.62	2.66	5.26
	LV 345	149140	69.03	10.80	1.94	.97	2.50	4.87
	LV 345	149150	72.10	11.25	1.34	.52	2.43	5.08

Appendix I: Electron probe analyses of diagenetically active phases. (Continued)

Mineral	Sample*	Analysis**	SiO_2	Al_2O_3	FeO Total	CaO	Na_2O	K_2O
Glass	LV 345	149160	71.58	11.18	1.28	.54	2.62	5.49
	LV 345	149170	57.90	9.44	3.08	.42	2.74	5.31
	LV 345	149180	72.38	10.95	1.14	.49	2.80	5.80
	LV 345	149190	71.19	11.33	1.00	.45	2.87	5.34
	RR 165	150100	70.90	11.18	1.95	.86	1.88	5.61
	RR 165	150110	70.69	11.63	1.03	.29	2.23	6.42
	RR 165	150120	71.47	11.42	1.07	.31	2.24	6.40
	RR 165	150130	71.68	11.36	.84	.60	2.18	6.16
	RR 165	150140	66.82	11.89	1.70	.96	2.16	5.92
	RR 165	150150	68.71	11.32	.83	.46	2.11	6.32
	RR 165	150160	69.36	10.93	1.26	.48	1.99	6.15
	RR 165	150170	70.71	11.41	.91	.42	2.22	6.29
	RR 165	150180	69.46	11.48	.84	.41	2.13	6.31
	RR 165	150190	70.99	11.00	.83	.46	2.37	6.57
	WM 130	151100	73.49	11.05	.79	.34	1.96	5.54
	WM 130	151110	69.01	10.92	.75	.35	2.49	5.76
	WM 130	151120	72.10	11.32	.24	.25	2.14	6.16
	WM 130	155130	69.86	11.38	.81	.63	2.30	5.70
	WM 130	151140	59.29	9.08	1.24	.66	2.29	5.35
	WM 130	151150	71.27	11.68	.93	.32	2.80	5.90
	WM 130	151160	71.81	11.35	.42	.50	2.37	5.86
	WM 130	151170	58.14	14.00	10.87	5.43	3.74	1.69
	WM 130	151180	71.02	11.35	.81	.31	2.26	5.66
	WM 130	151190	58.01	13.88	10.06	4.60	3.91	2.75

Appendix I: Electron probe analyses of diagenetically active phases. (Continued)

Mineral	Sample*	Analysis**	SiO_2	Al_2O_3	FeO Total	CaO	Na_2O	K_2O
Glass	WM 135.5	152100	71.64	11.20	.53	.54	2.25	5.39
	WM 135.5	152110	72.56	11.26	.76	.61	2.13	5.49
	WM 135.5	152120	65.90	11.64	2.14	1.01	1.71	4.63
	WM 135.5	152130	70.21	10.77	.59	.61	1.96	4.88
	WM 135.5	152140	70.87	11.11	.63	.58	2.14	5.39
	WM 135.5	152150	72.63	11.24	.64	.58	2.21	5.50
	WM 135.5	152160	71.21	11.47	.70	.61	2.20	5.26
	WM 135.5	152170	70.87	11.21	.75	.53	2.05	5.28
	WM 135.5	152180	72.44	11.19	.79	.69	1.99	5.05
	WM 135.5	152190	71.21	11.68	.80	.70	1.74	4.74
	TM 63	153100	71.03	11.55	1.27	.44	2.22	5.90
	TM 63	153110	69.28	11.56	.98	.60	1.88	5.33
	TM 63	153120	71.72	11.49	.65	.31	2.04	5.75
	TM 63	153130	70.46	11.79	1.27	.65	1.85	5.28
	TM 63	153140	71.63	12.07	.88	.92	2.49	5.29
	TM 63	153150	58.14	15.00	8.39	5.37	3.60	2.33
	TM 63	153160	71.48	11.50	.50	.32	2.14	5.63
	TM 63	153170	71.34	12.27	.84	.59	2.29	5.82
	TM 63	153180	73.23	11.62	.73	.62	1.71	5.21
	TM 63	153190	74.01	11.32	.80	.36	2.20	5.83

Appendix II

Samples collected during field studies of outcrop sections were used for chemical analysis. Samples were given a designation that indicates the section from which they were collected and the elevation above the base of the section in feet or meters. Fragments of selected samples were ground with a mortar and pestle to pass a 125 mesh sieve. These were analyzed for uranium by the Bureau of Economic Geology using a fluorometric technique. Precision is estimated at ± 1 ppm for concentrations less than 10 ppm and ± 10 percent for concentrations greater than 10 ppm.

The 125- to 230-mesh fraction of some samples was separated into a light and heavy fraction using bromoform adjusted to a specific gravity of 2.40 with dimethylsulfoxide. The light fraction contained glass shards or pseudomorphs of opal and clinoptilolite after glass shards. These concentrates were analyzed for uranium by the Bureau of Economic Geology using a fluorometric technique. Estimated precision is ± 1 ppm.

Samples for electron probe microanalysis were selected to include large crystals or specimens of the diagenetic phases. Circular thin sections were then cut from the hand specimen especially for probe studies. These samples were polished and then coated with carbon. Analysis was performed using the Applied Research Laboratory microprobe owned by the Department of Geological Sciences of The University of Texas. Acceleration potential was 15 kv and sample currents were kept very low, 0.0016 to 0.002 microamps, to prevent vaporization of the sample. Spot size was adjusted to the maximum that would fit on the grain of interest. During analysis, when count rates for volatile elements such as sodium began

to drop, analysis of that spot was terminated and the values for that point accepted as valid only if three iterations of the count on the point had been completed before the count rate droped noticeably. Count rates of samples were compared to those of intralaboratory standards in use at The University of Texas. Probe data were corrected for background, deadtime, and matrix effects and converted to oxide weight percent using computer programs available at The University of Texas at Austin. Precision of the analysis is not known; however, the low sample currents necessary to keep the volatile elements from vaporizing prevented accumulation of large numbers of X-rays from the samples and kept the precision low.

VII. ALTERATION AND URANIUM RELEASE FROM RHYOLITIC IGNEOUS ROCKS: EXAMPLES FROM THE MITCHELL MESA RHYOLITE, SANTANA TUFF, CHINATI MOUNTAINS GROUP, AND ALLEN COMPLEX, TRANS-PECOS TEXAS

By Christopher D. Henry[1] and G. Nell Tyner[2]

INTRODUCTION

The Mitchell Mesa Rhyolite, Chinati Mountains Group, Allen Complex, and Santana Tuff of Trans-Pecos Texas represent a spectrum of mostly rhyolitic igneous rock types including ash-flow tuffs, lava flows, and intrusions. The Mitchell Mesa Rhyolite and Chinati Mountains Group are genetically related volcanic rocks erupted from a caldera in the Chinati Mountains (fig. 1). The Allen Complex includes a group of shallow intrusions at the northern end of the Chinati Caldera; the intrusions may be part of an older cycle of caldera activity. The Santana Tuff, although not genetically related to the other rock types, is an ash-flow tuff chemically similar to the Mitchell Mesa Rhyolite. This report shows that all of these rock types have high background concentrations of uranium. A variety of mechanisms acting on these rocks could release or redistribute uranium. The first section of this chapter, Mechanisms of

---

[1]Bureau of Economic Geology, The University of Texas at Austin.

[2]Department of Geological Sciences, The University of Texas at Austin.

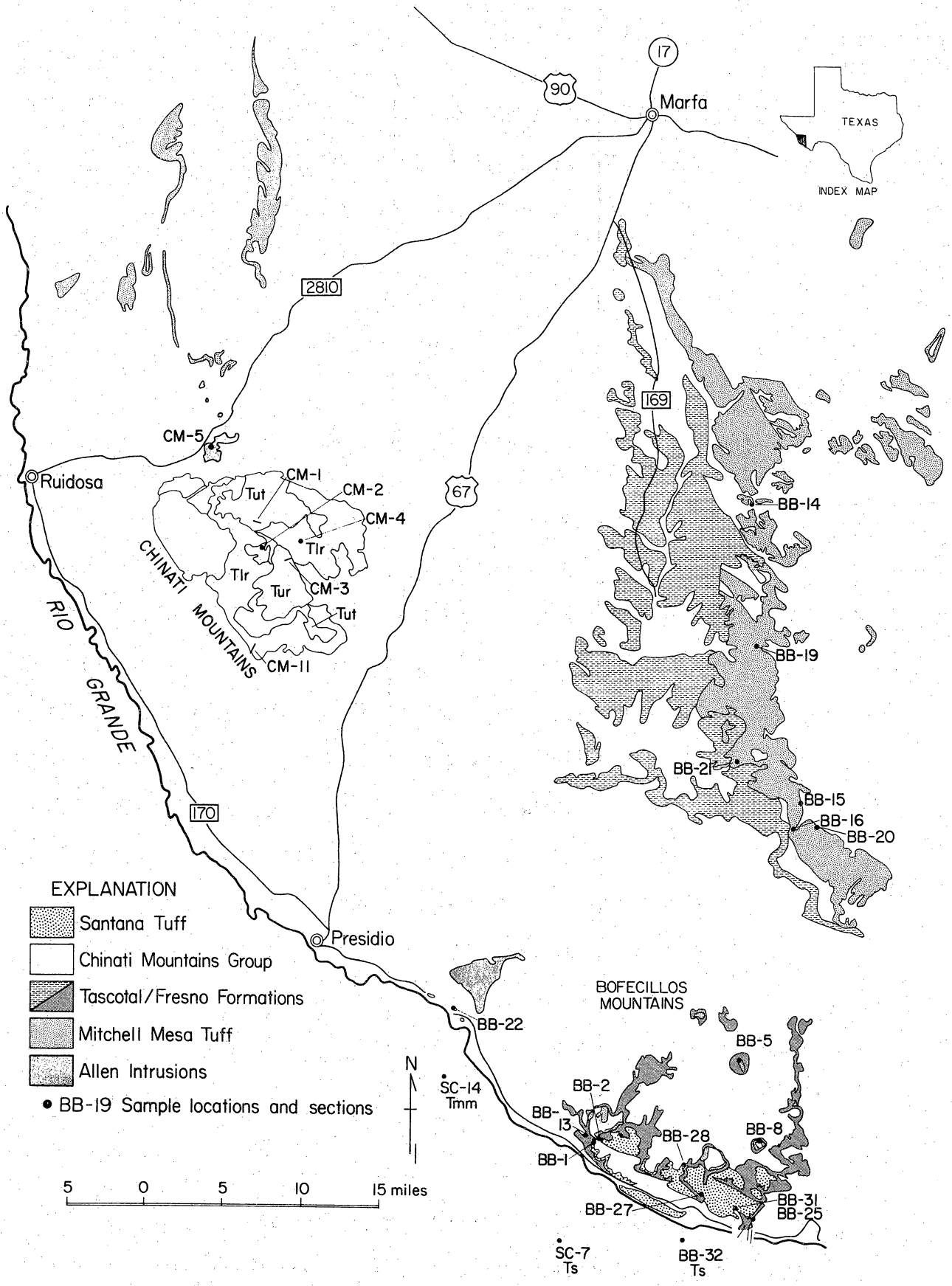

Figure 1. Generalized geologic map of part of Trans-Pecos Texas showing distribution of formations discussed in text and sample locations.

Uranium Release and Redistribution, discusses general processes bearing on uranium mobility in rhyolitic igneous rocks. The following sections give examples of how these processes have affected uranium in the various rock types. Figure 1 is a generalized geologic map showing sample locations.

MECHANISMS OF URANIUM RELEASE AND REDISTRIBUTION

Introduction

Rhyolitic igneous rocks commonly undergo several types of changes from glassy to crystalline and from one crystalline assemblage to another. All these changes can cause the release of uranium. In many respects the processes are similar for initially glassy rocks whether they are ash-flow tuffs, lava flows, or intrusions. However, differences in processes can arise from the differences in formation of each rock type, including eruption or emplacement processes, conditions of crystallization, mineral assemblages formed, permeability, and separation of a volatile phase. For example, ash-flow tuffs have a unique mechanism of eruption and are always initially glassy whereas thick lava flows or intrusions could crystallize directly from a magma without going through a glassy stage. This discussion will first consider processes occurring in ash-flow tuffs and then discuss lava flows and intrusions.

The alteration processes can be subdivided in two ways: (1) high-temperature and low-temperature processes and (2) processes that convert glass to crystalline rock or from one crystalline assemblage to another.

High-temperature processes include devitrification, hydrothermal (aqueous) or vapor phase separation and crystallization, granophyric crystallization and fumarolic alteration (Smith, 1960b). Low-temperature processes include alteration of glass by ground water through a variety of stages that can generally be termed weathering and diagenesis. Low-temperature alteration of already crystalline rocks can also occur.

High-Temperature Processes

Ash-Flow Tuffs

The first potential mechanism for uranium release from an ash-flow tuff is in the eruption process itself. An ash-flow tuff erupts because the confining pressure on the magma chamber has been reduced sufficiently so that dissolved volatiles can no longer be retained within the magma resulting in rapid vapor separation and vesiculation. Uranium can be fractionated into the vapor phase, probably as a uranium-fluoride complex (Rosholt and others, 1971). During eruption some of the vapor is released to the atmosphere and some is adsorbed on the surfaces of glass shards (Taylor and Stoiber, 1973). The proportion of vapor released to the atmosphere and vapor adsorbed on shards is not known. However, Taylor and Stoiber (1973) demonstrated that a large proportion of volatiles is adsorbed. They did not report on uranium, but Taylor (personal communication, 1978) believed that much uranium would be similarly adsorbed. Whatever proportion of volatiles and uranium is released to the atmosphere would likely be so dispersed as to be

unavailabe for concentration in ore deposits.

Thus after it has been deposited, an ash flow will contain uranium in two distinctly separate sites--dissolved (probably homogeneously) in glass shards and adsorbed with other volatiles on shard surfaces. The uranium dissolved in glass can only be released by complete breakdown of the glass, whereas uranium adsorbed on the shards can be removed easily, for example, by washing by rainfall. The distribution of uranium to two sites and to the atmosphere may be controlled by several factors including the overall chemistry of the initial magma, particularly its volatile content, and by the temperature of eruption.

Immediately after they come to rest, ash flows have porosities as high as 50 percent (Smith, 1960a). Compaction of the ash flow should expel much of the entrapped gas, probably through fumaroles such as occurred on the surface of the ash flow in the Valley of Ten Thousand Smokes, Alaska (Fenner, 1923). Expulsion of entrapped gas ought to cease after compaction ceases. The continuation of fumarole activity at the Valley of Ten Thousand Smokes for many years indicates that an additional source of gas exists (Smith, 1960a). This additional source, gas dissolved in glass and released during devitrification, is discussed below.

High temperature devitrification of rhyolitic ash-flow tuffs occurs after compaction and most commonly produces alkali feldspar and cristobalite or tridymite in axiolitic or spherulitic intergrowths. In many older rocks the high-temperature silica polymorphs have been replaced by quartz. Simple devitrification occurs in rocks too impermeable or

compacted to allow volatile-phase crystallizations including the most densely welded parts of ash-flow tuffs. High-temperature devitrification is largely a solid state process with minor diffusion of ions over short distances. Studies of major element chemistry of glass and devitrified rock indicate that devitrification is largely isochemical (Lipman, 1965).

Vapor-phase formation and release from densely welded rocks with little porosity or permeability seems unlikely. However, depletion of fluorine and chlorine from devitrified rocks compared to glass suggests that a vapor phase does form from volatiles dissolved in glass and separates from the rock (Noble and others, 1967). Noble and others did not describe the petrography of their samples, but from their discussion it is apparent that most had undergone devitrification without vapor-phase crystallization. Possibly fracturing of the rock attendant to volume decrease during devitrification provides avenues for volatile escape. Whether or not vapor-phase separation occurs from all devitrified rocks is not known. It is noteworthy, however, that vapor-phase separation could occur without leaving petrographic evidence such as vapor-phase crystallization.

Vapor-phase crystallization occurs in rocks with sufficient porosity so that a vapor phase cannot only separate during devitrification, but also collect and precipitate vapor-phase minerals. The upper partially welded part of an ash-flow tuff is a typical site for such conditions. The vapor collects in cavities in which alkali feldspar and tridymite crystallize from the vapor, or the vapor may escape entirely from the rock as in fumaroles.

If uranium is fractionated into the vapor-phase it could be significantly redistributed through the rock. Uranium could be depleted

from part of the rock and concentrated in the zone of vapor-phase crystallization or it could be lost to the atmosphere through fumaroles. However, if vapor simply collects in nearby cavities and precipitates, little concentration could occur. By either process of devitrification or vapor-phase crystallization uranium initially dissolved in glass would be relocated. Uranium would likely be excluded from the major mineral phases and localized in minor phases that may be more susceptible to later leaching.

Granophyric crystallization as a devitrification process occurs only in exceptionally thick ash-flow tuffs, probably on the order of 180m (600 ft) thick (Smith, 1960). The products are graphically intergrown quartz and alkali feldspar; granophyric crystallization is the only type of devitrification process that produces primary quartz. Like other forms of devitrification, granophyric crystallization could release or redistribute uranium.

Fumarolic alteration occurs where vapors released during devitrification react with the upper parts of an ash flow. Uranium fractionated into the vapor phase could be precipitated along the walls of the fumaroles, a possible mechanism for concentrating uranium from the vapor-phase.

Lava Flows and Intrusions

Processes affecting lava flows and intrusions are in many respects similar to processes affecting ash-flow tuffs. The following discussion will emphasize differences and discuss similarities only briefly.

Both lava flows and shallow intrusions may crystallize directly from a magma without going through a glassy stage. However, many of the lavas and intrusions studied here are still glassy, and most of the crystalline ones have textures which show that they devitrified from glass. Either process, direct crystallization or devitrification, would have similar results. Uranium in the magma would be dispersed through the rock on a large scale, but on a smaller scale would be concentrated in minor minerals or intergranular films. The major phases, alkali feldspar and quartz (or tridymite or cristobalite), would largely exclude uranium except possibly as inclusions of uranium-bearing minerals.

Granophyric crystallization, which is rare except in very thick ash-flow tuffs, is much more common in thick lava flows or shallow intrusions, where cooling is slower. Granophyric crystallization should produce a uranium distribution similar to that produced by devitrification. However, the specific sites for uranium may not be the same for different kinds of crystallization.

A volatile phase (either a vapor phase or a hydrothermal fluid) may separate during crystallization or devitrification. However, the volatile content of a magma forming a lava flow or intrusion may be distinctly lower than the volatile content of a magma producing an ash-flow tuff. Clearly a magma that flows quietly out as a lava must be less likely to produce vapor than an ash flow. The lavas of this study are dominantly from caldera-related, post-ash-flow magmatism. Such magmas would likely have lower volatile concentration than the earlier ash-flow magmas either because the residual magmas had been depleted

in volatiles during eruption or because the erupted magma came from the more differentiated volatile-rich cap of a magma chamber.

Shallow intrusions examined in this study could also be lower in volatile content because they too are post-ash-flow magmas. However, shallow intrusions are under greater confining pressure than are either ash flows or lava flows; a volatile phase might not separate even if the volatile content were relatively high. Thus volatile separation may be less likely or less pervasive in lavas and intrusions than in ash flows.

Provided that a volatile phase does separate, it could be either a vapor phase similar to the vapor phase formed during eruption or devitrification of an ash-flow tuff or a hydrothermal fluid. The chemical composition might be similar for each, but their physical properties would be a function of temperature and pressure.

Fluorite deposits commonly form from hydrothermal fluids enriched in fluorine. According to Lamarre and Hodder (1978), SiF_4 in the vapor phase reacts with meteoric water to form HF + SiO_2; HF in turn reacts with calcium bearing wall rocks, dominantly carbonates, to form fluorite. Uranium complexed with the fluorine could precipitate with the fluorite as its complexing agent is lost or, if additional complexing agents are available, could be further transported. Fluorite deposits at Spor Mountain, Utah, contain as much as 0.33 percent uranium (Staatz and Carr, 1964); some fluorite deposits in Trans-Pecos Texas are also enriched in uranium (Daugherty and Fandrych, 1978).

Low-Temperature Processes

Introduction

Low-temperature processes can affect both crystalline rocks devitrified by high-temperature processes and glassy rocks. Low-temperature processes can be considered as different stages of weathering and diagenesis involving ground water. Without the catalyzing effect of water, low-temperature devitrification is a slow process (Marshall, 1961), unlikely to be significant in geologically reasonable times. Once cooled, all glassy rocks respond in similar ways to ground-water alteration, with differences largely a function of permeability as it controls movement of water. Thus diagenesis of an ash-flow tuff or lava flow is analogous to diagenesis of tuffaceous sediment, except that unfractured massive lava flows, densely welded tuffs, and even porous partially welded tuffs that have unconnected lithophysal cavities may be largely impermeable. Also they should have greatly reduced ratios of surface area to volume in comparison to sediments.

Washing of Adsorbed Uranium

Before any chemical or mineralogical alteration of the glass can occur, rain and surface water contacting glass can wash off the coating of adsorbed volatiles. The top of an ash-flow tuff immediately after deposition consists of loose, nonwelded and undevitrified glass shards and pumice. This material is permeable, and water passing through it will remove the volatile coating left from the eruptive gases (Taylor and Stoiber, 1973). Any uranium incorporated in the coating will like-

wise be removed with several possible end results. If the tuff is in a throughgoing drainage, the water and uranium may be transported completely out of the system. If it is in a closed basin, the uranium will be trapped within the basin; the exact location will depend upon solubility controls in the basin.

Some uranium may simply be transported downward to be concentrated in underlying parts of the ash flow, probably just at or above the zone in which partial welding and devitrification becomes significant. At this level, compaction and crystallization will have so reduced permeability that the water will not be able to pass rapidly through the tuff. Dissolved uranium could conceivably be precipitated--again dependent upon available solubility controls. Possible mechanisms of uranium deposition are precipitation of uranium silicates or adsorption of uranium by secondary silica such as opal.

Unless somehow protected from erosion, the loose ash will shortly be eroded away. The Mitchell Mesa Rhyolite of this study is commonly eroded down to a relatively resistant layer of poorly welded but devitrified tuff. This layer is also commonly silicified, probably from deposition of silica derived from the glassy material present before erosion.

Diagenesis

In the diagenetic process ground water moves through glassy rock, dissolving glass with a concomitant rise in dissolved solids and pH. At appropriate concentrations various minerals precipitate, either directly from solution or by replacement of previously formed minerals. The

diagenetic mineral assemblages observed in tuffaceous sediments in Trans-Pecos Texas (Walton, 1975 and this report) are listed in order of increasing degree of alteration:

1. Hydration of glass without mineralogical change
2. Montmorillonite - opal - glass
3. Montmorillonite - opal - clinoptilolite
4. Montmorillonite - quartz - clinoptilolite
5. Montmorillonite - quartz - analcime
6. Quartz - analcime

Hydration of glass, the first step in this process, is not a mineralogical change; however, hydration can produce significant chemical changes. An additional mineral assemblage, quartz and potassium feldspar, can form as an alternative to quartz and analcime in diagenetic systems with different chemical compositions. In particular, highly saline, alkaline brines seem to favor formation of potassium feldspar over clinoptilolite or analcime because such waters have very high pH, high K^+/H^+, high SiO_2 concentration, and low activity of H_2O (Surdam, 1977). All these factors favor formation of potassium feldspar. The assemblage of quartz and potassium feldspar can also be produced by high-temperature devitrification. It is necessary to recognize the origin of the particular assemblage to interpret chemical changes properly. For reasons discussed below, none of the rocks studied here should have quartz and alkali feldspar produced by low-temperature devitrification.

During the diagenetic process glass undergoes congruent dissolution, thus all chemical constituents of the glass initially enter into

solution, into ground water. This should be a favorable process for formation of uranium deposits if conditions exist for transport and concentration of uranium.

Crystalline devitrification products are more resistant to weathering than is glass. However, quartz and alkali feldspar, the major devitrification products, incorporate very little uranium in their crystal lattices. Uranium originally contained in glass will probably wind up in either accessory minerals, minor secondary minerals such as iron-titanium-manganese oxides (Zielinski, 1978), or as intergranular films between quartz and feldspar grains. These sites ought to be more susceptible to minor weathering by a process analogous to uranium leaching from crystalline granitic rocks (Stuckless and others, 1977). This kind of leaching leaves little easily observable evidence. Thus uranium could be released from devitrified rocks by low-temperature weathering that does not significantly affect the rock's major mineral components and is not recognizable by common petrographic techniques.

Alteration by Geothermal (Hot Spring) Water

An additional mechanism for uranium release occurs at temperatures intermediate between those of high-temperature devitrification and low-temperature ground-water diagenesis and shares characteristics of both. Alteration of glass or crystalline rock by circulating geothermal (hot spring) waters could occur within a caldera where continued igneous activity and slow cooling of underlying magma chambers set up convective geothermal flow.

Water temperature would range from average surface temperatures to as high as 200°C. Although the water is in a sense hydrothermal, minerals found in ash-flow tuff and tuffaceous sediment altered by geothermal water at Yellowstone National Park (Honda and Muffler, 1970 and Keith and Muffler, 1978) are the same minerals (opal, quartz, montmorillonite, clinoptilolite, and analcime) that occur in rocks altered by ground-water diagenesis. In most respects the processes are similar. Alteration is by solution of glass by ground water, but the geothermal water has a much higher temperature. Distinction of occurrence is difficult, but may be possible on the basis of geologic setting, textural relations, or mineral zonation. Because, as in diagenesis, hot spring water dissolves glass and can leach crystalline rocks, the resultant alteration should be favorable for uranium release.

Previous Studies of Uranium Leaching

Several studies have addressed the problem of uranium loss from glassy rhyolitic volcanic rocks. In addition, several other studies have examined the effects of devitrification and hydration on other chemical constituents that are relevant to understanding the behavior of uranium. Most of the studies, however, have considered only hydration and crystallization without distinguishing high-and low-temperature processes or different kinds of devitrification.

Rosholt and others (1971) determined uranium concentrations and related chemical contents of three welded ash-flow tuffs and four lava flows including nonhydrated and hydrated glasses and crystalline (by

primary high-temperature devitrification and granophyric crystallization) rocks. Uranium concentrations of hydrated and nonhydrated glass were identical when corrected for water content of hydrated glass. Uranium concentrations of crystallized rocks were only 20 to 80 percent of uranium concentrations of glass. Rosholt and others (1971) noticed a general correspondence between uranium depletion and fluorine depletion in the same rocks, although two crystalline rocks that have experienced uranium depletion were enriched in fluorine. Several other studies (Lipman and others, 1969; Noble and others, 1967) have shown a similar loss of fluorine and other halogens in crystalline felsites relative to glass. Isotopic studies demonstrated uranium mobility in some of the rocks within the last 100,000 years. For these reasons Rosholt and others postulated that uranium loss occurred by volatilization of the UF_6 complex during primary devitrification and by ground-water leaching of devitrified rock. They did not, however, specify the exact process of leaching and indicated that there was no evidence for secondary alteration.

Comparing glassy, perlitic, and crystalline samples, Zielinski and others (1977) determined the concentration of uranium and several other minor elements of four rhyolite lava flows. Uranium concentration of obsidian and perlite were identical within analytical precision. However, uranium and the geochemically associated element, molybdenum, were depleted in felsites with relative depletion increasing with age. Fluorine was also depleted in felsite but did not correlate with age. Zielinski and others interpreted this to mean that fluorine was lost at about the time of crystallization; at that time some uranium could also

have been lost but most uranium loss was due to slow weathering over millions of years.

Zielinski (1978) examined uranium concentration and distribution in calc-alkaline (nonperalkaline) and peralkaline lava flows and ash-flow tuffs. He found that uranium in glassy rocks was uniformly distributed through the glass. In undepleted (relative to glass) crystalline rocks, uranium was either concentrated in accessory minerals (zircon, sphene, or apatite) or associated with, but not necessarily in, iron-titanium-manganese oxides. In depleted crystalline rocks uranium occurred with secondary iron-manganese-titanium oxides as fissure fillings and grain coatings. The amount of uranium depletion was a function of time and composition with older peralkaline rocks showing the greatest loss. This suggests that weathering rather than high-temperature volatile transport controlled uranium loss and that peralkaline rocks are more susceptible to depletion than calc-alkaline rocks.

Several studies have shown that hydration leads to depletion of sodium and increase in potassium but produces no change in halogens (Lipman, 1965; Lipman and others, 1969). Alkalis in calc-alkaline felsites are unchanged compared to glasses (Lipman and others, 1969), but are depleted in many peralkaline felsites relative to glass (Noble, 1970).

Together these studies indicate that uranium is homogeneously distributed in glass. Uranium can be released, probably as a UF_6 complex, during initial high-temperature devitrification but, in most rock suites studied, uranium has not been significantly depleted by this process. Slow low-temperature weathering of devitrified rocks better explains most

uranium depletion. Hydration of glass does not release uranium even though some other elements are removed from glass by hydration.

Anderson (1975) examined uranium mineralization in the Buckshot Ignimbrite of Trans-Pecos Texas. He found uranophane, a potassium uranium silicate, in lithophysal cavities, pore spaces in rock fragments, and in pumice fragments in the partly welded zone. Although this could be interpreted as resulting from degassing and vapor-phase crystallization, Anderson thought otherwise. He noted that fumaroles in the Buckshot, where vapor-phase alteration might be concentrated, were not enriched in uranium and that the lithophysal zone of the Buckshot was strongly altered (to a crumbly yellow-brown mass of quartz and sanidine) only at the uranium occurrence.

URANIUM GEOLOGY OF THE MITCHELL MESA RHYOLITE AND SANTANA TUFF

Introduction

The following discussions of the Mitchell Mesa Rhyolite, Santana Tuff, Chinati Mountains Group, and Allen Complex use a repeated pattern. First, the primary characteristics including texture, mineralogy, and major element and uranium chemistry are discussed. Then the types and degrees of alteration are described. Finally the effect of the different kinds of alteration on uranium is discussed. Sample locations are shown in figure 1.

Prealteration Characteristics

Texture and Mineralogy

Descriptions of the primary characteristics of the Santana Tuff are derived from observations of three samples of vitrophyre (fig. 2). However, predevitrification characteristics of the Mitchell Mesa Rhyolite cannot be observed directly because no undevitrified samples have ever been found either in this study or in previous studies. For the Mitchell Mesa primary characteristics are inferred from available devitrified samples (fig. 3) and from comparison with other ash-flow tuffs, including the Santana Tuff. Because both the Mitchell Mesa and the Santana are ash-flow tuffs they share many characteristics. They are composed of phenocrysts, pumice fragments, and foreign rock fragments in a mass of glass shards and fine dust. Differences exist in specific populations of each of these. Petrographic descriptions are also derived in part from Burt (1970) for the Mitchell Mesa Rhyolite and from McKnight (1969) for the Santana Tuff.

Phenocrysts in the Mitchell Mesa Rhyolite consist primarily of subequal amounts of alkali feldspar and quartz, with a slight preponderance of alkali feldspar. Densely welded samples contain as much as 20 percent by volume of the two minerals. Quartz is generally bipyramidal and sanidine is irridescent, a characteristic feature of the Mitchell Mesa best developed in the most welded parts. Mafic phenocrysts consist of oxyhornblende, augite, magnetite, and rare biotite. Minor accessory minerals that also occur in the Santana Tuff include zircon, sphene, and apatite.

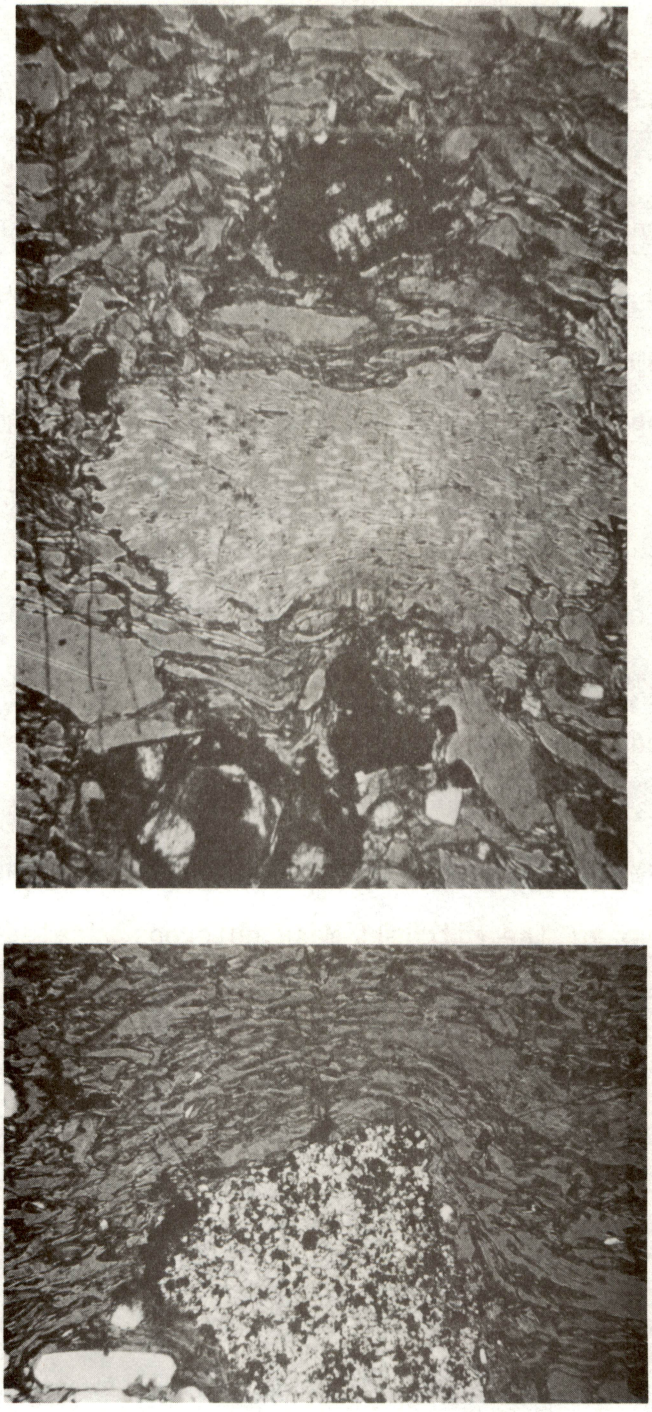

Figure 2. BB-32f. Densely welded vitrophyre of Santana Tuff showing flattened pumice fragment and olivine phenocrysts (top) and rock fragment (bottom). Long dimension of each photograph 2 mm.

The dominant phenocryst mineral in the Santana Tuff is sanidine. However, minor amounts (less than a few percent) of quartz, plagioclase, augite, oxyhornblende, and fayalitic olivine are also present. Phenocrysts compose as much as 10 percent of the Santana Tuff.

Rock fragments in the Santana Tuff are entirely from other volcanic rocks including welded tuff and flow rocks. Rock fragments in the Mitchell Mesa also include welded tuffs and intermediate-composition lava-flow rocks and possibly some tuffaceous sediments. Abundant pumice fragments are characteristic of both the Mitchell Mesa and the Santana. The ground masses are composed of glass shards and a fine dust composed of finely ground shards, phenocrysts, and rock fragments. Together, shards, pumice, and fine dust make up most of any of the samples.

Both the Mitchell Mesa and Santana range from densely welded to nonwelded. Most of the Mitchell Mesa outcrops visited in this study are in distal parts, so densely welded rocks were found mostly in the lower parts of the ash flow close to the base. The Santana was observed mostly in thicker sections close to its source area, and is densely welded throughout much of its thickness. Densely welded rocks contain flattened pumice in which all the pore space has been removed, and flattened and distorted glass shards. Because of compaction, phenocrysts and rock-fragment concentrations are greatest and porosity lowest in welded rocks.

Whole-Rock Chemistry

All previous chemical analyses of the Mitchell Mesa Rhyolite are from devitrified rocks that have undergone some chemical modification from originally glassy rock (Burt, 1970). The analysis listed in table 1

Table 1. Chemical analyses of rocks discussed in text

	Mitchell Mesa Rhyolite B32D[a]	Santana Tuff Sant-2[b]	Chinati Mountains Volcanic Group[c]				Black Perlite Allen Complex[b]	Devitrified Rhyolite Allen Complex[b]
			Middle Trachyte	Lower Rhyolite	Upper Trachyte	Upper Rhyolite		
iO_2	76.1	76.0	61.97	70.88	55.97	75.52	73.00	75.90
iO_2	0.22	0.11	1.23	0.60	1.87	0.20	0.29	0.10
l_2O_3	11.6	12.18	15.29	14.74	15.64	11.58	12.15	13.15
e_2O_3	1.76	1.99	4.57	2.30	4.57	2.05	1.12	0.33
eO	--	<0.10	0.90	0.35	3.40	1.33	0.75	0.35
nO	0.11	0.04	0.14	0.05	0.16	0.13	0.08	0.01
gO	0.28	0.03	1.42	0.24	2.05	0.08	0.07	0.13
aO	0.22	0.52	2.68	0.55	4.70	0.12	0.47	0.49
a_2O	3.84	3.75	4.51	4.26	4.02	4.73	3.79	3.82
$_2O$	4.90	5.12	4.43	5.57	3.68	4.44	5.18	4.40
$_2O^+$	0.43	0.31	1.01	0.54	1.36	0.18	3.26	0.89
$_2O^-$	0.15	0.07	0.37	0.26	0.92	0.06	0.28	0.51
$_2O_5$	0.02	0.34	0.53	0.18	0.78	0.04	0.00	0.00
O_2	0.10	0.01	0.01	0.02	0.02	0.02	0.00	0.00
otal	99.76	100.47	99.06	100.54	99.14	100.48	100.44	100.08

[a] From Burt, 1970.

[b] Chemical analysis provided by Daniel S. Barker.

[c] From Cepeda, 1977.

was chosen as most representative of primary chemistry because it has the highest sodium content and has probably experienced the least sodium loss. However, it has suffered some alteration, and almost all iron is in the ferric form, probably as a result of oxidation during high-temperature devitrification.

The analysis shows that the Mitchell Mesa is high-silica rhyolite, rich in alkalis and low in aluminum, calcium, magnesium, and iron. Two of four analyses listed by Burt contain normative acmite and are peralkaline with a molar Na + K/Al greater than 1. The sample listed does not contain acmite and has Na + K/Al almost exactly equal to 1. Thus it is almost peralkaline. It is possible that all analyzed samples have experienced some sodium loss and that the Mitchell Mesa is peralkaline. Certainly it is a highly alkaline rhyolite.

Only one whole rock analysis of the Santana Tuff exists (table 1). It is also a devitrified sample. It is chemically similar to the Mitchell Mesa in that it is a high-silica, alkali rhyolite low in aluminum, calcium, magnesium, and iron. Molar Na + K/Al is 0.96, so it is not peralkaline. Like the Mitchell Mesa it may have experienced sodium loss or other alteration.

Primary Uranium Concentration

Introduction

All comparisons of depletion and enrichment of uranium must be made relative to a known primary concentration. Typically the uranium concentration in unaltered glassy rock is used as the primary concentration. Unfortunately glassy samples are rare in many of the rock types of this

study. No samples of glass were obtained for the Mitchell Mesa Rhyolite; in fact no glass has ever been found in the Mitchell Mesa. Also, prior to this study glass had not been found in the Santana Tuff and only two occurrences were found during this study. Chemical analyses of both rock types had been made on devitrified, welded tuffs for which gross changes in major element chemistry should not have occurred. These samples are not adequate for determining primary uranium concentration, however, if one of the purposes of the study is to determine the effect of devitrification on uranium concentration. Nevertheless, if the rocks studied were completely homogeneous with respect to primary uranium concentration, then analysis of any single unaltered sample would provide a reference. However, both the Mitchell Mesa and the Santana are composed of several separate ash flows. Each ash flow is a heterogeneous mixture of phenocrysts, rock fragments, and glass or devitrification products, so it is likely that they are heterogeneous in uranium concentration.

Uranium concentration in three samples of vitrophyre of Santana Tuff illustrates the problem. Sample BB-32f (table 2; fig. 2) contains 7.6 ppm; two other samples (SC-7c-1 and SC-7c-2) from float but probably derived from the same outcrop approximately 9 km from BB-32f contain 12 and 11 ppm. The latter two concentrations are not statistically different. All three samples are petrographically identical. Although the Santana Tuff is apparently relatively homogeneous in uranium concentration at the scale of a single outcrop, at a larger scale it is clearly heterogeneous. No one sample can be considered representative of the Santana Tuff or other ash-flow tuffs.

Table 2a. Uranium concentrations--Mitchell Mesa Rhyolite

Sample	Degree of Welding	Mineral Assemblage[a]	Alteration[b]	Uranium (ppm)	
				Total	HNO_3 leach
BB-2c	Slightly welded	Alk Feld, Qtz, minor Cc	D + major VP	11	
BB-2b	Slightly welded	Alk Feld, Qtz, minor Cc	D + major VP	12	
BB-2a	Densely welded	Alk Feld, Qtz	D + moderate VP	12	
BB-8c	Nonwelded, silicified	Alk Feld, Qtz	D + minor VP	7.7	
BB-8b	Slightly welded	Alk Feld, Qtz	D + minor VP	6.2	
BB-8a	Densely welded	Alk Feld, Qtz, Crist	D	6.8	
BB-14c	Moderately welded	Alk Feld, Qtz, Cc	D + major VP	6.7	<1
BB-14b	Moderately welded	Alk Feld, Qtz	D + moderate VP	3.8	<1
BB-14a	Moderately welded	Alk Feld, Qtz, Cc	D + moderate VP	1.3	<1
BB-15b	Nonwelded	Alk Feld, Qtz	D + major VP	6.0	
BB-15a	Moderately welded	Alk Feld, Qtz	D + moderate VP	5.5	
BB-16e	Nonwelded	Alk Feld, Qtz, Cc	D + major VP	3.5	
BB-16d	Slightly welded	Alk Feld, Qtz	D + major VP	7.0	
BB-16c	Moderately welded	Alk Feld, Qtz	D + major VP	5.1	<1
BB-16b	Moderately welded	Alk Feld, Qtz, Cc	D + major VP	5.5	
BB-16a	Slightly welded	Alk Feld, Qtz, Cc	D + major VP	5.3	<1

Table 2a. Continued

Sample	Degree of Welding	Mineral Assemblage[a]	Alteration[b]	Uranium (ppm)	
				Total	HNO_3 leach
BB-19f	Nonwelded	Alk Feld, Qtz	D + major VP	8.5	
BB-19e	Calcified pumice	Cc, Alk Feld, Qtz		4.4	1
BB-19d	Slightly welded	Alk Feld, Qtz, minor Mont	D + major VP, Diag	7.5	<1
BB-19c	Moderately welded	Alk Feld, Qtz, minor Mont	D + moderate VP, Diag	5.2	1.3
BB-19b	Moderately welded	Alk Feld, Qtz, minor Mont	D, Diag	6.3	1.2
BB-19a	Nonwelded	Mont, Qtz	Diag	<1	
BB-22b	Nonwelded	Alk Feld, Qtz	D + major VP	7.1	
BB-22a	Slightly welded	Alk Feld, Qtz	D + moderate VP	4.8	
BB-25c	Slightly welded	Alk Feld, Qtz, Cc	D + moderate VP	4.3	
BB-25b	Densely welded	Alk Feld, Qtz	D + minor VP	3.2	
BB-25a	Nonwelded	Alk Feld, Qtz	D + moderate VP	4.4	
SC-14f	Nonwelded pumice	Alk Feld, Qtz, Cc	D + major VP	12.4	2.5
SC-14e	Nonwelded	Alk Feld, Qtz, Cc	D + major VP	7.2	1.6
SC-14d-2	Slightly welded pumice	Alk Feld, Qtz, Cc	D + major VP	12.4	<1
SC-14d-1	Slightly welded	Alk Feld, Qtz, Cc	D + major VP	9.1	<1
SC-14c	Moderately welded	Alk Feld, Qtz, Cc	D + moderate VP	7.6	1.2
SC-14b	Moderately welded	Alk Feld, Qtz, Cc	D + moderate VP	9.5	2.3

Table 2a. Continued.

Sample	Degree of Welding	Mineral Assemblage[a]	Alteration[b]	Uranium (ppm)	
				Total	HNO_3 leach
BB-5a	Moderately welded	Alk Feld, Qtz	D + major VP	7.0	
BB-20a	Moderately welded	Alk Feld, Qtz	D + major VP	12	
BB-21b	Nonwelded	Mont, Alk Feld, minor Qtz	Diag	1.4	

[a] From thin-section and x-ray analysis; Alk Feld = Alkali Feldspar; Qtz = Quartz; Cc = Calcite; Mont = Montmorillonite; Crist = Cristobalite.

[b] D = Devitrification; VP = Vapor-Phase Crystallization; Diag = Diagenesis.

[c] Ash-flow boundary.

Table 2b. Uranium concentrations--Santana Tuff

Sample	Degree of Welding	Mineral Assemblage[a]	Alteration[b]	Uranium (ppm)	
				Total	HNO_3 leach
BB-32f	Welded vitrophyre	Glass and phenocrysts	None	7.6	
SC-7c-1	Welded vitrophyre	Glass and phenocrysts	None	12	
SC-7c-2	Welded vitrophyre	Glass and phenocrysts	None	11	
BB-1h	Nonwelded	Alk Feld, Qtz, minor Cc	D + major VP	10	
BB-1g	Slightly welded	Alk Feld, Qtz, minor Cc	D + major VP	4.8	
BB-1f	Nonwelded	Alk Feld, Qtz, minor Cc	D + major VP	5.5	
BB-1e	Nonwelded	Alk Feld, Qtz, minor Mont	D + major VP, Diag	12	
BB-1d	Slightly welded	Alk Feld, Qtz	D + major VP	11	
BB-1c	Densely welded	Alk Feld, Qtz, minor Cc	D + major VP	9.3	2.2
BB-1b	Densely welded	Alk Feld, Qtz	D + moderate VP	9.5	2.2
BB-1a	Moderately welded	Alk Feld, Qtz, minor Cc	D + moderate VP	7.0	2.5
BB-13e	Nonwelded	Alk Feld, Qtz	D + major VP	5.1	
BB-13d	Slightly welded	Alk Feld, Qtz, minor Cc	D + major VP	8.6	1.5
BB-13c	Slightly welded	Alk Feld, Qtz, minor Cc	D + major VP	9.8	<1
BB-13b	Moderately welded	Alk Feld, Qtz, minor Cc	D + moderate VP	6.6	1.2
BB-13a-2	Moderately welded	Alk Feld, Qtz, Crist	D + moderate VP	9.0	<1
BB-13a	Slightly welded	Alk Feld, Qtz, Crist	D + minor VP	4.5	

Table 2b. Continued.

Sample	Degree of Welding	Mineral Assemblage[a]	Alteration[b]	Uranium (ppm)	
				Total	HNO_3 leach
BB-25h	Slightly welded	Alk Feld, Qtz	D + major VP	5.2	
BB-25g-2	Slightly welded pumice	Alk Feld, Qtz, Cc	D + major VP	8.7	
BB-25g-1	Slightly welded	Alk Feld, Qtz	D + major VP	7.1	
BB-25f	Densely welded	Alk Feld, Qtz	D + major VP	7.2	
BB-25e	Slightly welded	Alk Feld, Qtz, Crist	D	5.6	
BB-25d	Nonwelded	Mont, minor Alk Feld, Qtz	Diag	3.7	
BB-27f	Nonwelded	Alk Feld, Qtz	D + major VP	5.9	<1
BB-27e	Moderately welded	Alk Feld, Qtz	D + major VP	7.1	<1
BB-27d	Densely welded	Alk Feld, Qtz	D + moderate VP	6.9	1
BB-27c	Densely welded	Alk Feld, Qtz, minor Crist	D + minor VP	7.8	<1
BB-27b	Densely welded	Alk Feld, Qtz, Crist	D	4.2	<1
BB-27a	Densely welded	Alk Feld, Qtz, Crist	D	3.7	<1
BB-31c	Nonwelded	Alk Feld, Qtz, Cc	D + major VP	5.9	<1
BB-31b	Nonwelded	Alk Feld, Qtz, Crist	D + major VP	4.6	1
BB-31a	Nonwelded	Alk Feld, Qtz	D + major VP	6.4	<1

Table 2b. Continued.

Sample	Degree of Welding	Mineral Assemblage[a]	Alteration[b]	Uranium (ppm)	
				Total	HNO_3 leach
BB-28d	Nonwelded	Alk Feld, Qtz	D + major VP	6.6	
BB-28c	Moderately welded	Alk Feld, Qtz, minor Mont	D + moderate VP	6.4	
BB-28b	Densely welded	Alk Feld, Qtz, Crist, Mont	D, Diag	5.7	
BB-28a	Nonwelded	Cc, Clin, Qtz, minor Mont	Diag	2.4	

[a] From thin-section and x-ray analysis; Alk Feld = Alkali Feldspar; Qtz = Quartz; Cc = Calcite; Mont = Montmorillonite; Crist = Cristobalite; Clin = Clinoptilolite.

[b] D = Devitrification; VP = Vapor-Phase Crystallization; Diag = Diagenesis

[c] Ash-flow boundary.

Sources of Variation

Two types of variations that can lead to sample-to-sample inhomogeneity are (1) variations in the proportions of different uranium-bearing phases (for example, glass, phenocrysts or rock fragments) and (2) variations in the uranium concentration of the different phases. An assumption that almost all uranium in undevitrified rocks is bound up homogeneously in glass removes some possible sources of variation. This assumption is valid because other phases that are major constituents are unlikely to have significant uranium concentration and because in general all nonglass constituents are relatively minor components of the rocks. Other major phases besides glass are phenocrysts of quartz, alkali feldspar, and mafic minerals and rock fragments. None of the major phenocrysts have significant uranium concentrations; the uranium concentration in them should be considerably less than 1 ppm (Dostal and Capedri, 1975). Xenoliths of silicic volcanic rocks probably have uranium concentrations comparable to the silicic volcanic rocks being analyzed. However, rock fragments commonly make up only a few percent of the total rocks. Fission-track mapping of silicic volcanic rocks by Zielinski (1978) demonstrates that uranium is homogeneously distributed in glass with other major phases containing negligible amounts. Similar fission-track studies to determine uranium distribution in these samples would be useful.

Some minor phenocrysts such as zircon, sphene, or apatite can have very high uranium concentrations. For example, zircons can contain from several hundred to several thousand ppm uranium. However, they are extremely minor constituents of the rocks studied. A population of zircons

that contains 1000 ppm uranium and makes up 0.1 percent of a rock contributes only 1 ppm uranium to the total rock. Although they have been observed in many thin sections, zircons probably constitute much less than 0.1 percent of the rocks studied. Point counts averaging 350 counts per section of more than 60 sections totaled 6 zircons, or approximately 0.03 percent.

Thus the variations discussed above reduce to two factors: (1) variations in the primary uranium concentration of glass and (2) variations in the proportions of glass to other components. Variations in uranium content of glass arise from fractionation within a magma chamber. A single ash flow erupted from the top of a differentiated magma chamber could have glass with a wide range of uranium concentrations. Turbulence within an ash flow ought to sufficiently mix shards so that any one section through a flow should have a homogeneous population of shards although individual shards might differ. However, the same ash flow several kilometers or tens of kilometers away, which was erupted at the same time from a different part of the same magma chamber, could have a measurably different uranium concentration. Also, if uranium is fractionated during eruption into the volatile phase, then the amount of fractionation and volatile separation and the efficiency with which the volatile phase is adsorbed into shard surfaces could lead to significant regional variations in uranium concentrations.

How much variation in the uranium concentration should be expected in the magmas that produced the Santana Tuff and Mitchell Mesa Rhyolite? Both are relatively crystal poor--the Mitchell Mesa contains no more than 20 percent phenocrysts and the Santana Tuff, commonly less than 10 percent.

Also, petrographic variation between different ash flows is relatively minor. If magmatic variations in uranium concentration are due primarily to residual concentration in a crystallizing magma in which the crystals contain negligible uranium, then the variation in concentration should be small as long as there is not extensive fractionation. For example, a magma that initially contains 10 ppm uranium and experiences 20 percent crystallization would have a residual magma with 12.5 ppm uranium. Because the Santana and Mitchell Mesa are crystal-poor, variation in uranium concentration within individual ash flows should not be large. Variation between successive ash flows would also be a result of fractionation and could be greater than either local or regional variations within individual flows. Ash-flow sheets in New Mexico (Smith and Bailey, 1966) and Nevada (Lipman and others, 1966) show progressive upward changes in phenocryst proportions, phenocryst compositions, and groundmass compositions. Uranium concentration in the New Mexico sheet varies by a factor of 2. The chemical differences in both sheets were attributed to eruption of zoned, differentiated magma chambers.

This hypothesis can be tested by comparing uranium concentration of vitrophyre samples from the Chinati Mountains, two from the Upper Trachyte and one from the Upper Rhyolite of Cepeda (1977). Cepeda determined that these rocks were part of a continuous differentiation chain of a a single magma and that 100 parts of Upper Trachyte would produce about 25 parts of Upper Rhyolite. Thus if uranium were entirely concentrated in the residual magma the concentration in the rhyolite ought to be 4 times the concentration in the trachyte. Concentrations are in

fact 4.6 and 7.4 ppm in the trachyte and 13 ppm in the rhyolite; the rhyolite is enriched by a factor of about 2. Some uranium may have been incorporated in crystallizing minerals, and some may have been lost by volatile separation during eruption of the Upper Rhyolite. However, the concentrations may not be representative of either all the Upper Trachyte or all the Upper Rhyolite. Nevertheless it suggests that uranium, although concentrated in the residual magma, is not totally excluded from crystallizing minerals.

Variation in the proportion of glass relative to other phases that could result from differences in effectiveness of transport by an ash flow can be dealt with from point-count data. In general the variation in proportion of originally glassy material is small and much less than the measured variation in uranium concentration.

Although analyses of vitrophyres are available for the Santana Tuff, another method must be used to establish some reliable estimate of primary concentration for each sample of Santana or Mitchell Mesa. Uranium analyses are available for more than one sample from a total of nine sections through the Mitchell Mesa Rhyolite, and from six sections through the Santana Tuff. Many of the sections seem to have a maximum "plateau" value which is different for different sections. For the Mitchell Mesa a plateau between 5 and 8 ppm is the most common plateau value, but two sections (BB-2 and SC-14) have plateaus possibly as high as 12 ppm. These concentrations could result in three different ways: (1) they are primary concentrations, (2) they have been uniformly depleted, or (3) they are uniformly enriched. Although either of the latter two is possible,

it is difficult to imagine alteration producing uniform enrichment or depletion unless depletion led to near total removal of uranium. It seems more likely that these concentrations are primary and that the lower values that occur within these sections result from depletion. In the following discussion the uranium concentration of samples from each section is used to determine the primary uranium concentration for that section.

The best estimate then for the primary uranium concentration in most of the Mitchell Mesa is about 6 to 8 ppm, but both higher and lower plateaus occur. A similar range of primary uranium concentrations exists in the Santana Tuff.

Alteration

Introduction

Various parts of the Mitchell Mesa and Santana Tuff have undergone devitrification and vapor-phase crystallization at high temperature, and alteration by ground water at low temperature. Table 2 and the following discussion relate the uranium concentration of various samples of Mitchell Mesa and Santana to the type of alteration they have undergone. The criteria used to distinguish the kinds of alteration of each sample are discussed here.

High-Temperature Alteration

Devitrification without vapor-phase crystallization occurs only in the lowest parts of the Mitchell Mesa and Santana. High-temperature devitrification during initial cooling converted glass to a combination

of alkali feldspar and cristobalite (or rarely tridymite). X-ray analysis shows that in most samples the high-temperature silica polymorph has since been converted to quartz. The devitrification products occur in two textural forms, axiolites, parallel intergrowths within individual shards (figs. 3 and 4), and spherulites, spherical intergrowths originating from a central nucleus. Axiolitic structures probably result from progressive crystallization of the shard from the boundary inward. Some shards have a central line where the waves of crystallization met. In other shards the parallel structure crosses completely from one side to the other. The original texture has largely been preserved by devitrification; shard textures in the groundmass and in pumice fragments are still clearly recognizable. However, many pumice fragments devitrified as a unit with spherulitic structures (which are more common in pumice than in groundmass shards) and axiolitic structures extending across the entire fragment (fig. 5). Under crossed nicols the devitrification products obscure the shard structure. Adjacent but separate shards, even in densely welded samples, devitrified as separate units, and the devitrification products mimic the shards.

Devitrification has had no observable effect on quartz or feldspar phenocrysts. Mafic minerals, including olivine, augite, and oxyhornblende, have undergone little or no oxidation. The textures and lack of alteration of phenocrysts suggest that maximum distances of chemical transport were approximately the same as the width of individual shards. Lack of transport is consistent with the observation of Lipman (1965) that devitrification is largely isochemical.

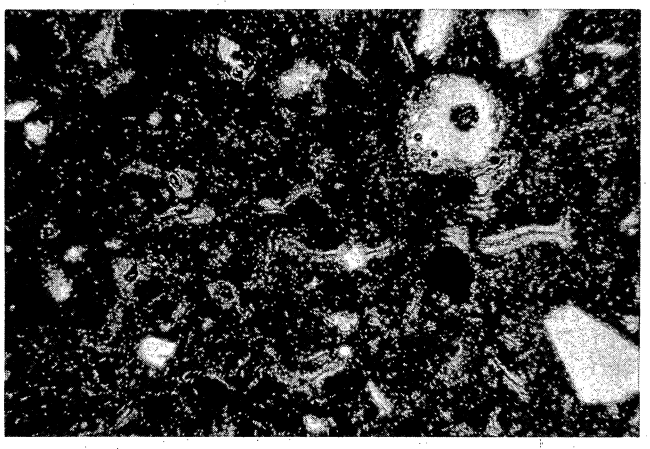

Figure 3. BB-8a. Axiolitically devitrified Mitchell Mesa Rhyolite. Long dimension 2.5 mm.

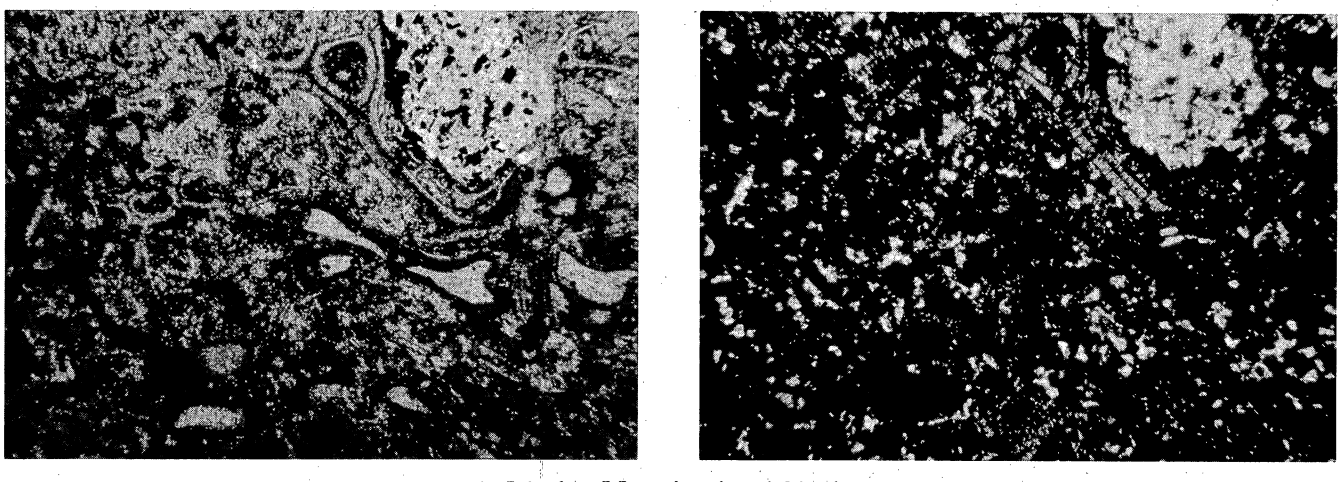

Figure 4a. BB-13a. Axiolitically devitrified Santana Tuff. Uncrossed (left) and crossed nicols (right). Long dimension 2 mm.

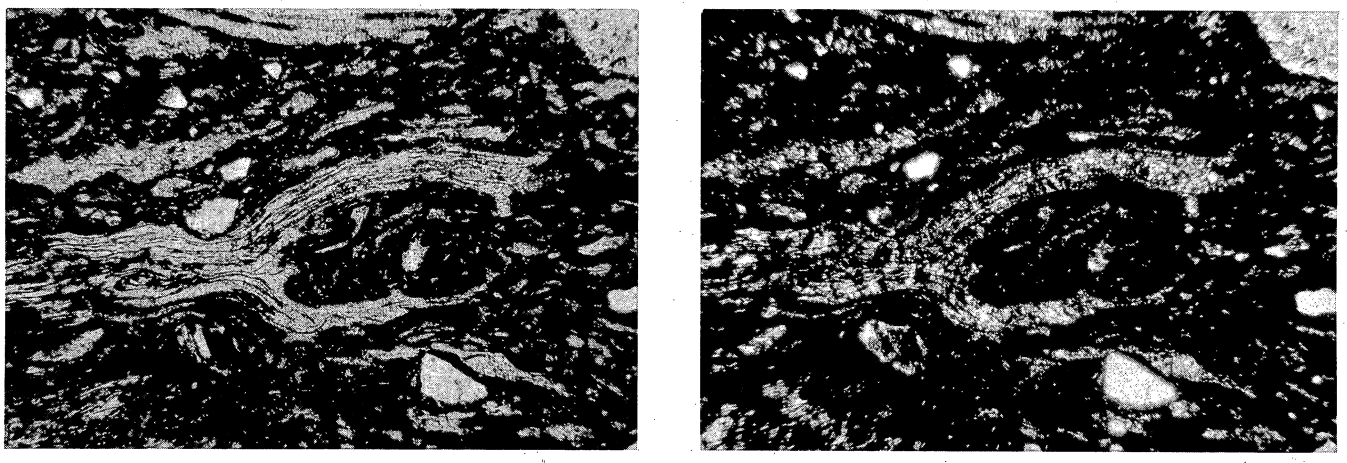

Figure 4b. BB-27a. Axiolitically devitrified shards and pumice, Santana Tuff. Uncrossed (left) and crossed nicols (right). Long dimension 3 mm.

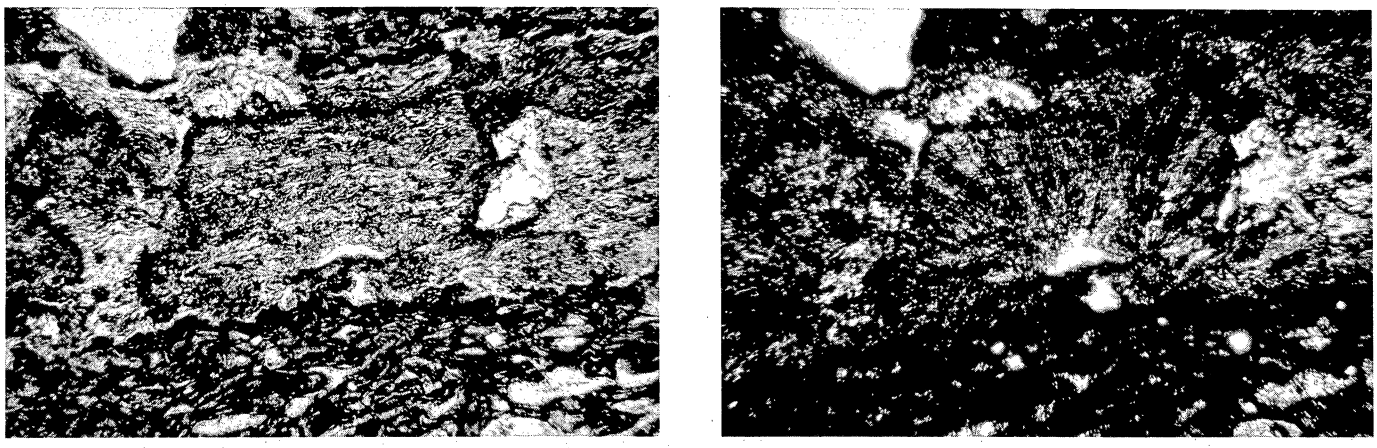

Figure 5. BB-27c. Devitrification of pumice fragment obscuring shard structure, Santana Tuff. Uncrossed (left) and crossed nicols (right). Long dimension 3 mm.

Vapor-phase crystallization is pervasive throughout the Mitchell Mesa and Santana. Only a few Mitchell Mesa samples have not undergone vapor-phase crystallization, probably because most samples were collected from thin nonwelded distal sections. Many of the sampled Santana tuff secions are much thicker; however, in these sections vapor-phase crystallization was first noticed within a few tens of meters of the base and is extensive throughout the major part of the section. For example, in a 180 m thick section of the Santana Tuff (BB-27) two samples from near the base have well-preserved devitrification features, but all higher samples

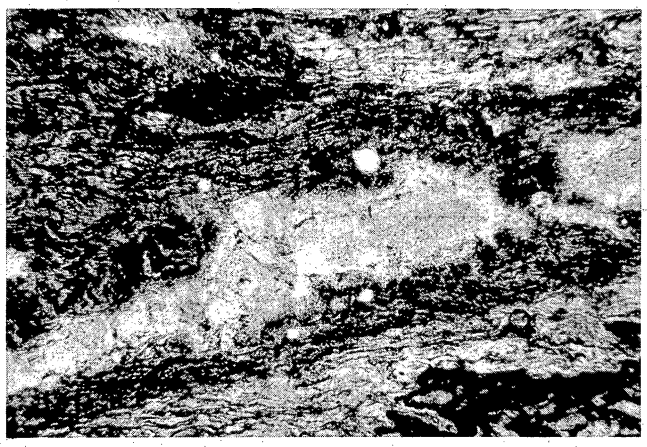

Figure 6. BB-27b. Vapor-phase crystallization in pumice fragment in axiolitically devitrified Santana Tuff. Long dimension 3 mm.

have discernible vapor-phase features (fig. 6). In samples from about the middle of the section upward, vapor-phase crystallization has totally obliterated the devitrification features.

The transition from devitrification alone to devitrification with vapor-phase crystallization is gradational. Incipient vapor-phase crystallization is marked by coarse aggregates of alkali feldspar and quartz or cavities lined with vapor-phase minerals in pumice fragments (fig. 6). In fact in rocks that have undergone all stages of vapor-phase crystallization, pumice fragments have been more extensively

altered than the groundmass, probably because volatiles were concentrated in pumice. With increase in vapor-phase crystallization, extensive crystallization of the groundmass occurred. Initial groundmass crystallization formed fine irregular aggregates dotted through an otherwise dark but devitrified groundmass. Crystallization in the groundmass was more extensive and aggregates are coarser higher in the ash flow. Samples which have undergone major vapor-phase crystallization are composed of coarse irregular mosaics of alkali feldspar and quartz in which the shard texture may have been totally destroyed (fig. 7). Cavities are common in these rocks not only because of vapor-phase formation but also because these rocks are from the uppermost, least welded parts of the ash flows. The cavities are lined with vapor-phase minerals, most commonly alkali feldspar and tridymite. Vapor-phase crystallization has also produced optically continuous overgrowths on alkali feldspar phenocrysts (fig. 8).

Mafic minerals are totally oxidized to opaque aggregates in samples with extensive vapor-phase crystallization. This change is also gradational with the least oxidation having occurred in samples with the least vapor-phase crystallization. Some oxidation also occurred in samples that are devitrified but have not undergone vapor-phase crystallization.

In general, the petrographic features resulting from vapor-phase crystallization imply much more extensive chemical transport than that which has occurred in rocks that have experienced only devitrification.

No evidence of fumarolic alteration was found in either the Mitchell Mesa or Santana. Because vapor-phase crystallization was extensive in both, fumaroles undoubtedly did occur. Evidence for them may not have been

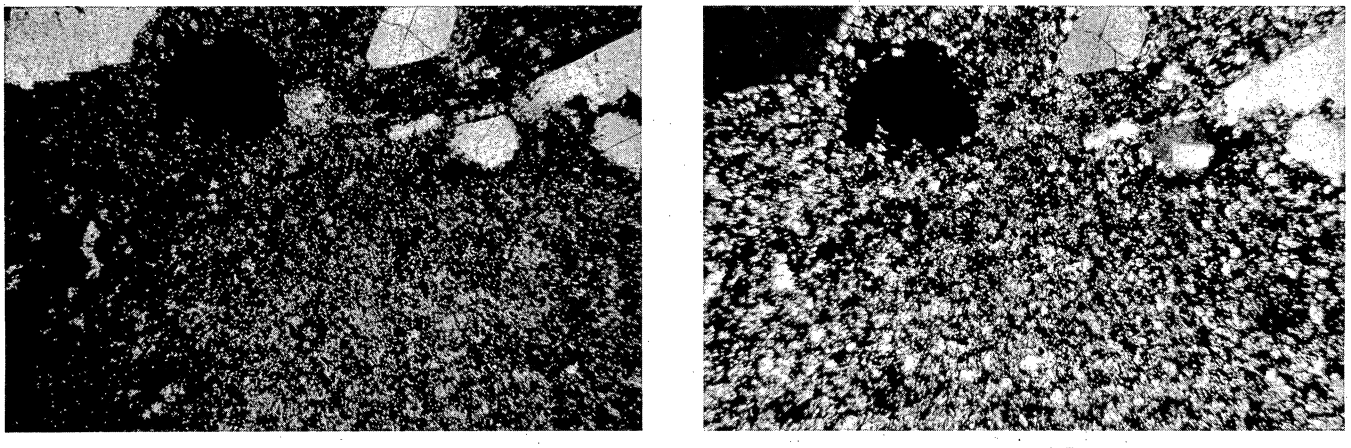

Figure 7a. BB014a. Vapor phase-crystallization in Mitchell Mesa Rhyolite. Note coarse mosaic of quartz and alkali feldspar, and lack of shard structure. Uncrossed (left) and crossed nicols (right). Long dimension 2.5 mm.

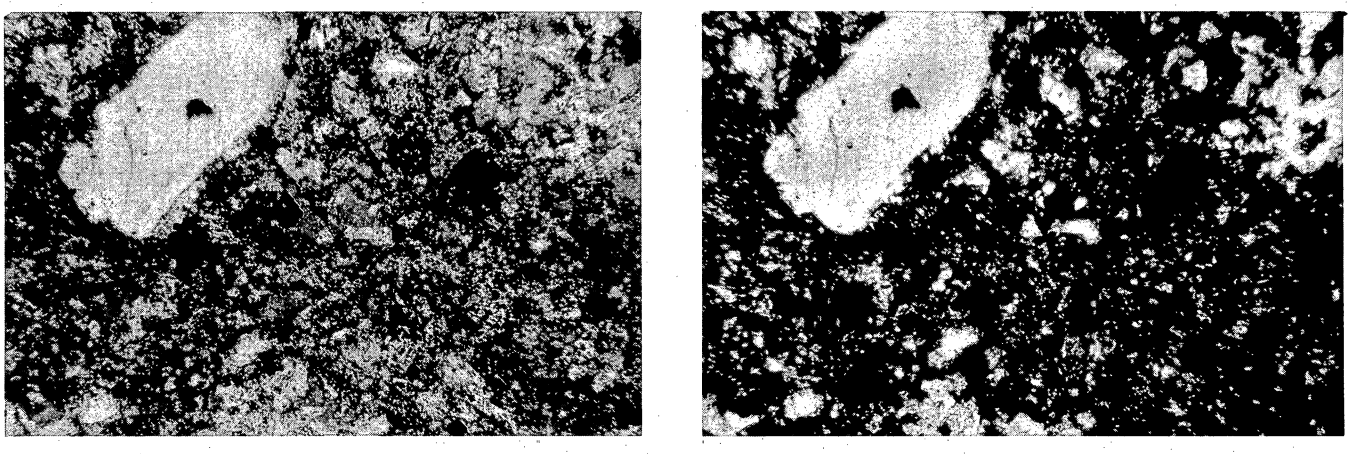

Figure 7b. BB-27f. Vapor-phase crystallization in porous, nonwelded top of Santana Tuff. Uncrossed (left) and crossed nicols (right). Long dimension 2 mm.

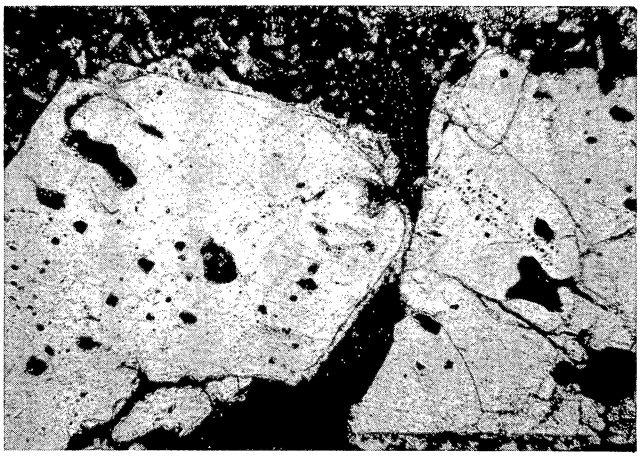

Figure 8. BB-31b. Optically continuous overgrowths forming rim on alkali feldspar phenocrysts. Long dimension 3 mm.

found for the following reasons: (1) the fumaroles produced little or no noticeable alteration; (2) fumarolic alteration was restricted to the upper parts of the Mitchell Mesa and Santana that have since been stripped away; and (3) fumarolic alteration was probably not widely distributed and was not actively sought, so it simply was not discovered in this study.

Only one thin section shows arguable evidence for granophyric crystallization. Granophyric crystallization is apparently restricted to very thick ash flows, 180 m (600 ft) or thicker (Smith, 1960 b). The Santana approaches this thickness in one sampled section (BB-27). BB-27b from

this section has granophyric-looking clots that occupy no more than 5 percent of the area of the thin section. Granophyric crystallization thus could not be a major factor in uranium release in either the Santana or the Mitchell Mesa.

Low-Temperature Alteration

Rocks which from field characteristics could be determined to have undergone alteration at low temperature were not extensively sampled. In general, very little of either of the Mitchell Mesa or Santana remained glassy after initial cooling. Available samples include several basal ash layers (not devitrified at high temperature) and one upper nonwelded and undevitrified part of the Mitchell Mesa. The undevitrified basal layers of the Mitchell Mesa and Santana are covered with rubble over most of the outcrop area, are thin (less than a few meters thick), and are volumetrically only a minor part of either ash flow.

Outcrops of upper undevitrified layers are rare in the Mitchell Mesa and absent in the Santana because each was eroded down to layers that were indurated by devitrification, and thus resistant to erosion. In the Mitchell Mesa most such erosion occurred before deposition of the Tascotal Formation and reworked Mitchell Mesa ash was incorporated into lower parts of the Tascotal. Recent erosion also has removed remaining nonresistant parts of the Mitchell Mesa.

Some other samples show mineralogical or textural evidence for low-temperature alteration that could not be detected in the field. All of these samples had also been devitrified at high temperature, and the high-temperature characteristics dominate the appearance of the rocks.

Observed mineralogic products of low-temperature alteration of glass include montmorillonite, clinoptilolite, and calcite. Three samples (BB-19a, BB-21b, and BB-25d) are composed almost entirely of montmorillonite; the only other minerals present are residual phenocrysts of quartz and alkali feldspar (fig. 9). One sample (BB-28a) contains abundant calcite and clinoptilolite along with minor montmorillonite and residual phenocrysts (fig. 10). In all four samples the only quartz and feldspar present are the residual phenocrysts. No high-temperature devitrification products or vapor-phase minerals occur. Either alteration converted glass to montmorillonite or clinoptilolite or alteration converted quartz and feldspar completely to the observed assemblages. The latter possibility is obviously unlikely because quartz, at least, is extremely resistant to chemical alteration and would be preserved. Also, evidence of intermediate stages of alteration was not found. Thus, these samples were probably glassy after cooling and were altered by ground water at low temperature.

In the Tascotal Formation the alteration mineral assemblage of montmorillonite, clinoptilolite, and calcite results from diagenesis. The same process was responsible for alteration of the glassy Mitchell Mesa and Santana samples, but for the reasons discussed below neither the Mitchell Mesa nor the Santana was part of the diagenetic system which altered the Tascotal glass.

Clinoptilolite was not found in the Mitchell Mesa. Upper porous nonwelded parts of the Mitchell Mesa directly beneath the Tascotal Formation could be expected to contain clinoptilolite if the diagenetic

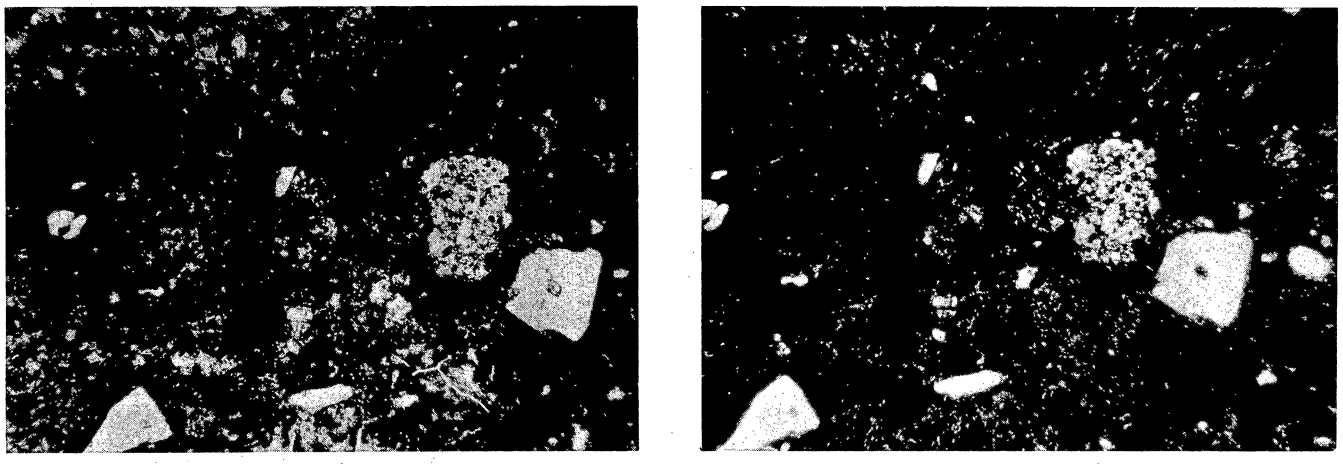

Figure 9a. BB-19a. Formerly glassy Mitchell Mesa Rhyolite altered to montmorillonite by ground water. Uncrossed (left) and crossed nicols (right). Long dimension 3 mm.

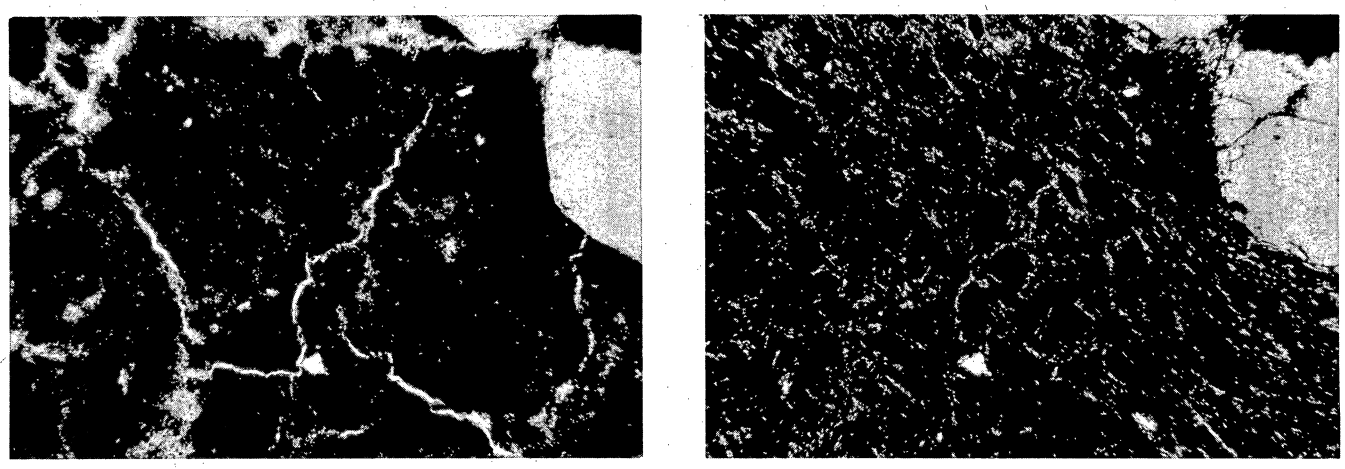

Figure 9b. BB-25d. Formerly glassy basal ash of Santana Tuff altered to montmorillonite by ground water. Uncrossed (left) and crossed nicols (right). Long dimension 3 mm.

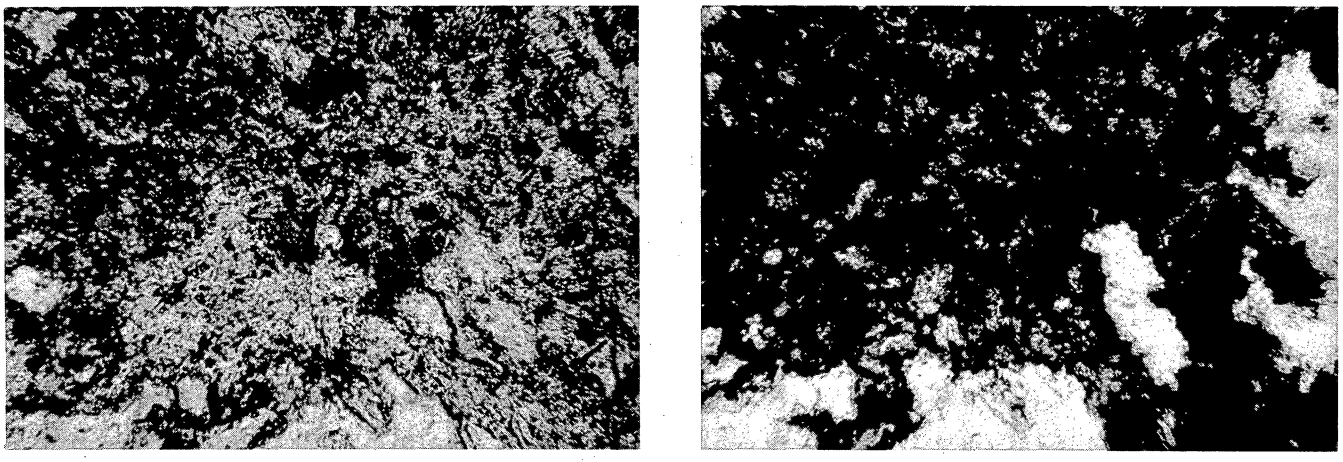

Figure 10. BB-28a. Formerly glassy basal ash of Santana Tuff altered to calcite (high birefringence) and clinoptilolite. Uncrossed (left) and crossed nicols (right). Long dimension 1 mm.

solution could penetrate into the Mitchell Mesa and even if the Mitchell Mesa had devitrified at high temperature. Quartz and feldspar within the Mitchell Mesa would probably not contribute significantly to the diagenetic solution. However, the Tascotal immediately above the Mitchell Mesa is altered to clinoptilolite. A solution saturated with respect to clinoptilolite entering the top of the Mitchell Mesa should have continued to precipitate at least some clinoptilolite. A thin, topmost layer may in fact contain clinoptilolite, but no such samples were discovered in this

study. Evidently the nonwelded Mitchell Mesa was too impermeable, even though highly porous, to allow passage of the diagenetic solution.

Another line of evidence shows that the Mitchell Mesa did not participate in the diagenesis that affected the Tascotal. Sample BB-21b, a rare example of upper undevitrified Mitchell Mesa, was altered at low temperature to montmorillonite but does not contain clinoptilolite. Sample BB-19a from the base of the Mitchell Mesa contains montmorillonite with partly altered residual phenocrysts (fig. 9). Both samples must have been altered to montmorillonite before deposition or alteration of the Tascotal. If they had remained glassy before alteration of the Tascotal, they would have been permeable ash and would have altered to clinoptilolite as did all the glass in the Tascotal and in the underlying Duff Formation. However, because they had been altered to montmorillonite before deposition of the Tascotal, they were impermeable and were not affected by diagenesis.

Sample BB-25d from the base of the Santana Tuff probably had an origin similar to that of BB-19a. It contains montmorillonite and overlies a mostly glassy section of the Fresno Formation that shows only minor alteration near the base (fig. 9). It is curious that only glass in the tuff is altered.

Sample BB-28a from the base of Santana Tuff contains clinoptilolite, calcite, and montmorillonite altered from glass (fig. 10). At that location the Santana fills a channel cut into Fresno Formation lava flows along the edge of the Bofecillos Volcano. The Fresno Formation at this location contains no tuffaceous sediment or tuff of any kind. Nevertheless the

diagenetic solution that altered the Santana glass was sufficiently evolved to produce clinoptilolite in addition to montmorillonite. The history of this solution is not known but may have involved alteration of overlying lavas and tuffs in the Rawls Formation.

Thus all low-temperature alterations of glass observed in the Mitchell Mesa and Santana are parts of separate, small diagenetic systems, restricted to glassy and highly permeable parts of the ash flows.

Ground water has also altered parts of the Mitchell Mesa and Santana which had devitrified at high temperature. Because the devitrification products, quartz and alkali feldspar, are far more resistant to alteration than glass, ground-water alteration of devitrified rocks is not extensive. The observed alteration products are montmorillonite and calcite but neither makes up more than about 5 percent of any sample. Calcite in particular is extremely common in both the Mitchell Mesa and Santana where it fills cavities and was probably introduced by ground water.

Montmorillonite indicates more extensive chemical reaction with the rock. Because the devitrification products are so resistant to alteration, extensive ground-water alteration must have occurred for montmorillonite to be present in detectable amounts.

Effect of Alteration on Uranium Concentration

Samples collected from various sections through the Mitchell Mesa Rhyolite and Santana Tuff (fig. 1; table 2) are discussed section by section. In table 2 samples are grouped by section, and within each section samples are arranged in stratigraphic order. Most sections are composed

of a single ash flow. Where more than one ash flow was sampled in a single section, the separate flows are indicated in table 2.

All uranium analyses are by fluorometry. Total uranium was obtained by lithium borate fusion, whereas "soluble" uranium was extracted by hot HNO_3 leach. All analyses are $\pm$ 1 ppm up to 10 ppm and $\pm$ 10% above 10 ppm.

Total uranium by the fusion method should include all uranium in the rock regardless of its mineral form. Even minerals such as zircon which are resistant to acid attack are fused. "Soluble" uranium is extracted by leaching a ground sample with HNO_3 at 90^{o} C for two hours. The acid leach is an attempt to determine how much of the total uranium can be easily removed by natural weathering. The HNO_3 dissolves secondary uranium minerals and should extract absorbed uranium. The acid leach has no effect on uranium structurally bound within most silicate minerals including the major rock-forming minerals. However, the method is at best only an approximation of weathering. Moreover, it is not known whether HNO_3 will remove uranium in oxyhydroxides which have been identified as important sites for uranium in devitrified rocks (Zielinski, 1978).

Mitchell Mesa Rhyolite

Section BB-2

Three samples from a single ash-flow tuff in section BB-2 have undergone moderate to major vapor-phase crystallization and have uniform uranium concentrations of 11 to 12 ppm. The uniformity of concentration indicates that they are primary concentrations unaffected by vapor-phase crystallization. Minor calcite in samples BB-2b and BB-2c suggests possible groundwater interaction, but it has apparently not affected uranium either.

Nitric-acid-soluble uranium is low and may show why ground water has not reached uranium. Devitrification and vapor-phase crystallization has apparently placed uranium in a relatively insoluble phase.

Section BB-8

Three samples from a single ash-flow tuff at section BB-8 have undergone axiolitic devitrification and some minor vapor-phase crystallization. Vapor-phase crystallization is expressed by recrystallized pumice only in BB-8a from the lowest part of the section and by recrystallized pumice and slight recrystallization of the groundmass in BB-8b and BB-8c. Uranium concentrations vary slightly from 6.2 to 7.7 ppm but are equal within analytical uncertainties. They are probably primary concentrations but are distinctly lower than the presumed primary concentrations in BB-2.

Section BB-14

Three samples from a single ash-flow tuff in section BB-14 have undergone devitrification with moderate to major vapor-phase crystallization. Axiolitic textures are not preserved in any of the three samples, but the groundmasses in BB-14a and BB-14b have not been as coarsely recrystallized as those in BB-14c and are composed of fine mosaics of quartz and alkali feldspar. Uranium concentrations are 1.3, 3.8, and 6.7 ppm. The primary concentration is not obvious from these analyses, but 6.7 ppm is closer to estimated primary concentrations in other sections than are the lower values. Whatever the primary concentration, the low values suggest significant uranium depletion. HNO_3-soluble uranium is less than 1 ppm in all three samples. Either vapor-phase crystallization has released uranium or ground water (as indicated by minor amounts of calcite in thin section)

has leached uranium placed in soluble form by vapor-phase crystallization. However, the latter possibility is not supported by other samples.

Section BB-15

Two samples from the same ash flow have undergone moderate and major vapor-phase crystallization. Uranium concentrations are 5.5 and 6.0 ppm and do not indicate any mobilization of uranium.

Section BB-16

All 5 samples from a single ash-flow tuff have undergone major vapor-phase crystallization, and all contain minor amounts of calcite. Three samples have uranium concentrations of 5.1 to 5.5 ppm, whereas two other samples have slightly higher (7.0 ppm) and slightly lower (3.5 ppm) concentrations. The high and low values are not statistically different, however. HNO_3-soluble uranium in two of the intermediate samples is less than 1 ppm. No demonstrable uranium mobilization has occurred and like some other samples devitrification and vapor-phase crystallization has evidently left uranium in a relatively insoluble form in the rock.

Section BB-19

Samples from section BB-19 have undergone a wide variety of types of alteration, including devitrification, vapor-phase crystallization, calcification of pumice, and ground-water alteration of glass. The samples come from two different ash flows. Three devitrified samples from the lower ash flow contain between 5.2 and 7.5 ppm uranium. The scatter of these values does not allow precise estimation of the primary concentration of uranium, but it may be within the range of these values. Of the three samples, one has undergone devitrification and displays excellent

preservation of axiolitic textures. The other two samples have undergone moderate to major vapor-phase crystallization. The different processes have not obviously had a major effect on uranium concentration or distribution. A single sample from the upper ash flow contains 8.5 ppm uranium and has undergone major vapor-phase crystallization. Its uranium concentration cannot be compared to a primary concentration; however, it cannot have been either leached or enriched to any great extent. HNO_3-soluble uranium in these four samples and in a sample of calcified pumice is low.

A sample of basal ash (BB-19a) composed almost entirely of montmorillonite contains less than 1 ppm uranium. As discussed previously, the sample had remained glassy following cooling and was converted to montmorillonite by ground-water alteration. Its primary concentration was probably in the range of 5 to 7 or 8 ppm, similar to that of the devitrified samples. The low-temperature alteration has clearly depleted the rock of almost all its original uranium. Samples BB-19b, BB-19c, and BB-19d are devitrified but also contain minor amounts of montmorillonite probably resulting from alteration by ground water. Uranium concentrations in the three samples have not obviously been affected, however. Evidently low-temperature alteration of devitrified rock does not release uranium even though alteration of glass does.

Section BB-22

Two samples from a poorly exposed section representing only the upper nonwelded part of the Mitchell Mesa Rhyolite have undergone moderate to major vapor-phase crystallization. Sample BB-22a has undergone moderate vapor-phase crystallization and has a uranium concentration of 4.8 ppm;

sample BB-22b has undergone major vapor-phase crystallization and has a uranium concentration of 7.1 ppm. It is impossible to establish a primary concentration from these data, but samples from section SC-14, the nearest sampled section of Mitchell Mesa, have considerably higher uranium concentrations. Although extrapolating uranium concentrations from section SC-14 is tenuous, it may indicate that uranium loss or mobility has occurred in samples from section BB-22. The difference in uranium concentration between samples BB-22a and BB-22b is slightly greater than the limits of analytical precision, so some uranium mobility is definitely implied.

Section BB-25

Three samples from a single ash flow have undergone devitrification with minor to moderate vapor-phase crystallization. Samples BB-25a and BB-25c have undergone moderate vapor-phase crystallization, but some axiolitic textures are preserved and not all mafic minerals have been oxidized. The two samples contain 4.4 and 4.3 ppm uranium, respectively. Sample BB-25b has undergone minor vapor-phase crystallization with well-preserved axiolitic devitrification and unoxidized mafic minerals; uranium concentration in it is 3.2 ppm. The uranium concentrations of all three are the same within analytical precision; they are probably primary concentrations although they are lower than primary concentrations in other sections.

Section SC-14

Six samples from a well-exposed section of Mitchell Mesa Rhyolite in Mexico just south of section BB-22 contain the highest uranium

concentrations of any Mitchell Mesa samples. Four samples are whole rock samples, and two are samples of pumice fragments. Samples SC-14b and SC-14c have experienced only moderate vapor-phase crystallization with most mafic minerals unoxidized and much of the axiolitic textures preserved; all other samples have undergone major vapor-phase crystallization with complete destruction of axiolitic textures. All samples contain abundant calcite either as coarse, poikilitic concretions scattered irregularly through the rock or as fine aggregates disseminated through the rock.

The whole rock samples have uranium concentrations of 7.2, 7.6, 9.1, and 9.5 ppm. The differences are not large and may simply indicate a primary concentration around 8 to 9 ppm. However, there seems to be two distinct clusters (about 7.5 and 9.5 ppm) suggesting that some alteration and uranium mobility may have occurred. The two highest values (both 12 ppm) are from the two pumice fragments, SC-14f and SC-14d-2. Point counts for the pumice fragments are similar to point counts for the rock samples and show that the difference in uranium concentration is not a result of differential dilution. The pumice samples may be enriched in uranium because of entrapment of a uranium-rich volatile phase either during eruption or during devitrification and vapor-phase crystallization. If so, this enrichment implies that uranium is fractionated into the vapor phase and transported. The mechanism could be important even though most samples show no evidence of uranium mobility during vapor-phase crystallization.

HNO_3-soluble uranium is generally low and shows no correlation with type of sample (pumice or whole rock), extent of devitrification, or total uranium concentration.

Other Sections

Only one sample was collected from each of three other sections. Samples BB-5a and BB-20a contain 7.0 and 12 ppm uranium, respectively. Both samples have undergone major vapor-phase crystallization. Sample BB-20a was collected only 3 km from section BB-16, yet it has a distinctly higher uranium concentration. Either large variations in concentration can occur over short distances, the most likely explanation, or uranium has been mobilized at one location or the other.

Sample BB-21b was collected from the nonwelded upper part of the Mitchell Mesa and is composed of montmorillonite with minor residual phenocrysts of alkali feldspar and quartz. The rock must have been glassy following cooling but was altered to clay before diagenesis of the Tascotal Formation. The sample's uranium concentration of 1.4 ppm shows that considerable uranium has been removed from the rock.

Santana Tuff

Section BB-1

Eight samples were taken from two ash flows with possibly a slight cooling break between them. All have undergone devitrification with moderate to major vapor-phase crystallization. Five of eight samples (4 from the lower flow, one from the upper flow) contain between 9.3 and 12 ppm uranium. Three samples contain distinctly less uranium. Sample BB-1a from the base of the lower flow contains 7.0 ppm; samples

BB-1f and BB-1g from the upper flow contain 5.5 and 4.8 ppm uranium.

The range in concentrations can be explained in several ways. The primary concentration may be approximately 12 ppm with most samples moderately to slightly depleted by vapor-phase crystallization or low-temperature ground-water leaching. The latter possibility is unlikely because the only sample with evidence for ground-water alteration (BB-1e contains minor montmorillonite) has the highest uranium concentration. Vapor-phase transport may have mobilized uranium with lower parts of each flow depleted and upper parts enriched by precipitation from rising vapor. In this case 12 ppm may not be the primary concentration.

Section BB-13

Six samples from section BB-13 contain 4.5 to 9.8 ppm uranium. Three samples seem to define a plateau at 8.6 to 9.8 ppm which is probably the primary concentration. Three samples contain lower concentrations, 4.5 to 6.6 ppm. Two of these samples are from the very top and the very bottom of the flow where vapor-phase loss or ground-water leaching might occur more easily than in the interior of the flow. Ground-water leaching is unlikely because one of the low-concentration samples (BB-13e; 5.1 ppm uranium) does not contain calcite, whereas all the other samples do. Possibly different mechanisms of loss have operated on the different samples. HNO_3-soluble uranium in the four analyzed samples is low.

Section BB-25

Five of six samples from two ash flows from section BB-25 are devitrified; one of these (sample BB-25c; 5.6 ppm uranium) has experienced devitrification only; the other four have also undergone major vapor-

phase crystallization and have uranium concentrations ranging from 5.2 to 8.7 ppm. The low value of 5.2 ppm is from a single sample from the upper ash flow. The primary concentration of the lower flow is probably 6 to 7 ppm; the one higher value of 8.7 ppm is from a pumice fragment (BB-25g-2) contained within sample BB-25g-1. The higher concentration is not statistically different from the 7.1 ppm of BB-25g-1, but it fits the pattern of high uranium concentration established with other pumice fragments. Vapor phase collects in pumice fragments and vapor-phase crystallization is most extensive in pumice. Possibly uranium is being fractionated into the vapor phase and is therefore concentrated in pumice to a minor extent. However, none of the devitrified samples provides any evidence for significant vapor-phase transport of uranium.

A sample from the base of the ash flow (BB-25d) is made up of montmorillonite with minor quartz and feldspar from residual phenocrysts. The sample apparently remained glassy after initial cooling and then was altered by ground water to montmorillonite. Its uranium concentration of 3.7 ppm is moderately depleted from the estimated primary concentration although it is no lower than some other samples from other sections which have not been similarly altered (for example BB-27a).

Section BB-27

Section BB-27 is the same as measured section MS-5 of McKnight (1970); McKnight determined a total thickness of 170 m (559 ft). The section is composed of at least six separate ash flows, composing one cooling unit, of which four ash flows were sampled. Two samples, BB-27a and BB-27b, from the lowermost ash flow contain 3.7 and 4.2 ppm uranium.

These values are distinctly lower than concentrations in ash flows higher in the section. However, they may be primary concentrations for this flow, as interflow variation seems significant. Both samples have undergone devitrification with only slight vapor-phase crystallization in pumice fragments; BB-27a also has a few granophyric intergrowths, but they make up only a few percent of the total rock. The primary concentration is probably 4 ppm and there has been no uranium depletion.

Two samples, BB-27c, and BB-27d, from the second lowest ash flow show considerably more vapor-phase crystallization, but some evidence of axiolitic devitrification is preserved in both. Uranium concentrations are 7.8 and 7.9 ppm, suggesting a primary concentration of about 8 ppm and no evidence of depletion.

One sample each, BB-27e and BB-27f, was collected from two higher ash flows. Because they are single samples no intraflow comparisons can be made, but their uranium concentrations (7.1, 5.9 ppm) are within the normal range observed in other flows. They probably have not been significantly depleted in uranium.

HNO_3-soluble uranium in all six samples is 1 ppm or less, including sample BB-27f which has undergone major vapor-phase crystallization. Devitrification and vapor-phase crystallization has apparently not placed uranium in an easily leachable site.

Section BB-31

At section BB-25 and BB-27 the top of the Santana Tuff had been removed by erosion and could not be sampled. However, at section BB-31, approximately half way between the two sections, the Santana Tuff is

protected from erosion by overlying lava flows. Three samples of the two topmost ash flows were collected there. All three have undergone major vapor-phase crystallization. Two samples, BB-31a and BB-31b, from the lower flow contain 6.4 and 4.6 ppm uranium. The difference is not statistically significant. A single sample from the upper flow contains 5.9 ppm. Although the 4.6 ppm value is lower than the approximately 7 ppm that seems to be characteristic of some lower flows, it is consistent within its own flow. There certainly is no evidence of major uranium depletion. HNO_3-soluble uranium is again low.

Section BB-28

At section BB-28 the Santana Tuff fills a channel eroded into the side of the Bofecillos Volcano. Three of four samples have undergone devitrification, and two of these samples have experienced moderate to major vapor-phase crystallization. These three samples have uranium concentrations ranging from 5.7 to 6.6 ppm, probably representing the primary concentration. A fourth sample of basal ash (BB-28a) contains calcite, clinoptilolite, and minor montmorillonite and quartz. As discussed above, it remained glassy after initial cooling and was altered by groundwater diagenesis to the observed assemblage. All minor quartz is probably from residual phenocrysts, although it can form from diagenesis. The sample's uranium concentration of 2.4 ppm shows that it has been significantly depleted. Samples BB-28b and BB-28c (5.7 and 6.4 ppm uranium) from above sample BB-28a contain minor montmorillonite but are composed largely of quartz and alkali feldspar devitrification products. Possibly a minor amount of glass remained after cooling and was altered to

montmorillonite. Alternatively montmorillonite resulted from diagenetic alteration of the feldspar devitrification products. By either method the normal uranium concentration shows that later ground-water alteration of devitrified rock does not release uranium.

Summary and Conclusions

A number of significant conclusions can be drawn from the pattern of uranium concentrations and correlation with alteration.

(1) The Mitchell Mesa Rhyolite and Santana Tuff have relatively high uranium concentrations, equal to or greater than the generally accepted 4 ppm average for rhyolite and granite (Rogers and Adams, 1969). From the standpoint of uranium concentration alone, both rocks would be considered good source rocks.

(2) Within individual ash flows at any one section uranium concentrations are fairly uniform and imply homogenization of any heterogeneous populations of glass. There is, however, some interflow variation even at a single section. Such variation should be expected because successive ash flows probably tap different parts of a differentiated magma chamber. Uranium concentrations also vary geographically by as much as a factor of 3. This variation was also shown by the different samples of vitrophyre of Santana Tuff. Again the variation should be expected because flows at different sections also probably came from different parts of the magma chamber. Variation in the uranium concentration in glass may also result from differential uranium loss by volatile loss during eruption. Estimates of depletion and enrichment are necessarily

compared to a primary concentration. The results of this study show that considerable care must be taken in estimating the primary concentration.

(3) Within a single flow, pumice samples contain more uranium than the host rock. To a lesser degree the same pattern also appears in undevitrified pumice from an ash flow from Virgin Valley, Nevada (this report). Enrichment in pumice could result from lack of dilution with phenocrysts and rock fragments, although this was not true for pumice from section SC-14, or from concentration of uranium-enriched volatiles during eruption of vapor-phase crystallization. This suggests that some fractionation of uranium into the vapor phase is occurring.

(4) Little clearcut depletion of uranium has occurred from either the Mitchell Mesa Rhyolite or the Santana Tuff. The lack of glass samples makes comparisons to primary concentrations tenuous and is one of the major deficiencies of this study. Nevertheless most devitrified samples of Santana Tuff have uranium concentrations similar to concentrations in the analyzed vitrophyres. It is unlikely that large-scale depletion has occurred in most of the devitrified samples. Also corroboration of nonrelease of uranium by devitrification is available from comparison of uranium concentrations of vitrophyres and devitrified rocks from the Allen Complex (Trans-Pecos Texas) and from Virgin Valley, Nevada (Henry, this report).

A few samples from the Mitchell Mesa and Santana that devitrified at high temperature apparently experienced depletion, but there is no clearcut reason for or pattern to the depletion. Depletion in these samples may have resulted from devitrification or from later alteration

by ground water that had little or no detectable effect on the rock.

Ground-water alteration of devitrified rocks, as evidenced by minor montmorillonite, clearly has not removed uranium. Calcite is present in many samples but shows no correlation with depletion.

Lack of depletion in samples which have undergone extensive vapor-phase crystallization is surprising. Vapor-phase crystallization clearly implies chemical transport, but evidently either uranium is not fractionated into the vapor phase or vapor-phase transport is minor and consists only of small scale coalescence of vapor.

This conclusion is not in accord with the results of Noble and others (1967) which show considerable fluoride and chlorine depletion in devitrified rocks compared with vitrophyres. However, the lack of volatile transport of uranium is consistent with the results of Zielinski and others (1977) and Zielinski (1978). Uranium can possibly be transported in the vapor phase, but there are additional factors, such as whole rock chemistry, total volatile content, or volatile composition, which control whether or not vapor transport of uranium occurs. Obviously identifying these factors is important.

(5) Depletion that can clearly be documented is due to alteration of glass by ground-water diagenesis, a process which seems particularly efficient at removing uranium.

(6) The concentration of HNO_3-soluble uranium is uniformly low; HNO_3-soluble uranium makes up a fraction of total uranium in all analyzed samples. Evidently devitrification and vapor-phase crystallization do not put uranium into a form that can be dissolved by hot, concentrated

HNO_3. This observation is consistent with the lack of depletion by groundwater alteration of devitrified samples. Devitrification must put uranium in relatively insoluble phases such as stable accessory minerals. Incorporation of uranium in major silicate phases is highly unlikely but remains a possibility until the distribution of uranium can be determined. Fe-Ti-Mn oxyhydroxides have been identified as major uranium bearing phases in devitrified rocks (Zielinski, 1978). Because of the mineralogical complexity of the oxyhydroxides and the uncertainty as to how uranium is incorporated in them, it is not certain whether or not leaching by HNO_3 removes uranium in oxyhydroxides. Uranium is probably incorporated by adsorption. The low concentration of acid-soluble uranium implies that either uranium in devitrified Mitchell Mesa Rhyolite and Santana Tuff is not associated with oxyhydroxides or uranium is somehow tightly bound within them.

(7) Lack of depletion contrasts with the correlation of age and depletion found by Zielinski (1978). Zielinski found that depletion increased with age and that at any given age peralkaline rhyolites were more depleted than were calcalkaline rhyolites. Whether or not the Mitchell Mesa Rhyolite and Santana Tuff are peralkaline is uncertain because of the lack of analyses of vitrophyre; nevertheless chemical analyses of devitrified samples show that they are highly alkaline rocks more similar to Zielinski's peralkaline suite than to the calcalkaline suite. Also, the Mitchell Mesa Rhyolite and Santana Tuff are as old as any of the samples studied by Zielinski, yet they are markedly undepleted.

(8) Depletion of uranium from the one zeolitized sample is also surprising. Katayama and others (1974) found that zeolitized tuff in Japan

was concentrated in uranium, even to ore grade, and that the uranium occurred in zeolite. Furthermore, they found that zeolite adsorbed almost all uranium from solution over a pH range of 4.5 to 8.5 with some uranium adsorbed at pH greater than 9. The pH of water in contact with the volcanic rocks of this study could range from near neutral to greater than 9. Possibly the pH of ground water that precipitated clinoptilolite in sample BB-28a was too high for uranium adsorption. Alternatively, leaching of uranium may have occurred, and the uranium may have flushed out of the system before clinoptilolite precipitated. Dissolution of glass is the important step in uranium release, and samples altered to montmorillonite without clinoptilolite are depleted in uranium. Clearly the actual precipitation of clinoptilolite is irrelevant to uranium depletion. However, the evidence of diagenesis in the Tascotal Formation shows that solution of glass, precipitation of montmorillonite, and precipitation of clinoptilolite is a continuous, progressive process. There is no evidence to suggest that alteration is a series of discrete, separate events by which uranium could be removed before precipitation of clinoptilolite. Another possible explanation is that the zeolite in BB-28a (clinoptilolite) is not the same zeolite as that which occurs in the Japanese tuffs. Katayama and others (1974) were uncertain about whether their zeolite was clinoptilolite or heulandite, a similar zeolite.

(9) The Mitchell Mesa Rhyolite and Santana Tuff could be considered good source rocks based on their high uranium concentrations. However, this study shows that they are in fact poor source rocks. High-temperature processes have resulted in little apparent uranium depletion.

Significant depletion has occurred by low-temperature alteration of glass, but so little of the Mitchell Mesa or Santana remained glassy after cooling that the total quantity of uranium released by alteration of glass is probably not large. Also devitrification has placed uranium in insoluble forms in the rock so that later leaching by ground water cannot release uranium. Probably uranium could only be released from devitrified rocks by weathering that completely broke down the rock. Although even small concentrations of uranium from a large enough volume of rock could supply enough uranium to form a minable ore deposit, concentration of uranium would have to be particularly efficient. Clearly the more uranium released, the easier it is to concentrate enough uranium to form a deposit. At most a tiny fraction of the uranium originally in the Mitchell Mesa and Santana has been released. It is extremely unlikely that significant uranium deposits have formed from uranium released from the Mitchell Mesa or Santana.

No attempt has been made to evaluate uranium loss by volatile separation before ash-flow deposition. Uranium concentrations in the devitrified rocks are compared with known or estimated concentrations in glass. Glass samples could be depleted relative to magma concentrations, however. Uranium lost during eruption and transport of the ash flow would likely be dispersed in the atmosphere and become unavailable for ore formation.

CHINATI MOUNTAIN GROUP

Geologic Setting

The most thorough work on the Chinati Mountains Group is by Cepeda (1977) who drew heavily on earlier work by Rix (1953), Amsbury (1958), and Burt (1970). Rix and Amsbury mapped the southern and northern parts respectively of the Chinati Mountains; Burt studied the Mitchell Mesa Rhyolite. The stratigraphy of the Chinati Mountains Group as determined by Cepeda is shown in table 3. The Chinati Mountains Group consists of five separate formations, four of which are composed of rhyolite or trachyte lava flows; one formation is a rhyolite ash-flow tuff. According to Cepeda all fill the Chinati caldera, the source of the Mitchell Mesa Rhyolite; the Mitchell Mesa is nowhere exposed in the caldera, however. Presumably, a thick caldera filling of Mitchell Mesa Rhyolite is buried beneath the oldest lava flows of the Chinati Mountain Group.

The oldest caldera fill is the Lower Trachyte which is only poorly exposed in the northern part of the caldera and was not investigated for this report. The second oldest unit is the Middle Trachyte, composed of several flows of porphyritic trachyte with a total thickness of about 150 m. The Lower Rhyolite overlies the Middle Trachyte and is the most widespread of the volcanic units, filling a central depression or secondary collapse structure within the Chinati caldera. The Lower Rhyolite consists of several thick porphyritic rhyolite lava flows (fig. 11). The Upper Trachyte overlies the Lower Rhyolite and is subdivided into two subunits, a lower series of flows with a few, small phenocrysts and

Table 3. Stratigraphy--Chinati Mountains Group.

Chinati Mountains Group	Upper Rhyolite		Ash-flow tuff
	Upper Trachyte	Upper unit	Coarsely porphyritic lavas
		Lower unit	Finely porphyritic lavas
	Lower Rhyolite		Porphyritic lavas
	Middle Trachyte		Porphyritic lavas
	Lower Trachyte		Porphyritic lavas
	Base not exposed		
	Mitchell Mesa Rhyolite (inferred in subsurface)		Ash-flow tuff

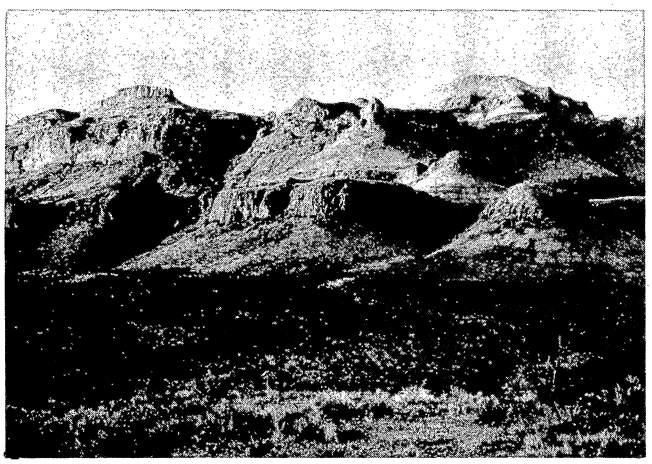

Figure 11. Massive lava flows of Lower Rhyolite with overlying Upper Trachyte in background.

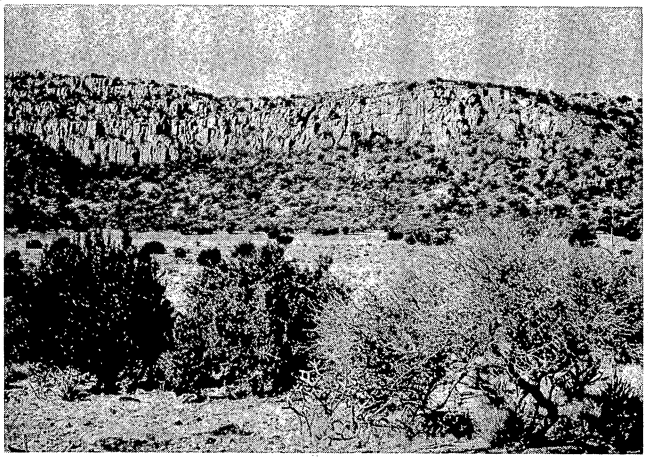

Figure 12. Upper Rhyolite in thick caldera fill.

an upper set of flows containing many large phenocrysts. It is as much as 400 m thick in the northern part of the Chinati caldera where it evidently built up a major shield volcano. The youngest unit, the Upper Rhyolite, is an ash-flow tuff that filled a third collapse feature in the central part of the Chinati caldera. The collapse was probably induced by withdrawal of the magma that makes up the Upper Rhyolite; thus, most of the Upper Rhyolite is intracaldera facies. Within the approximately 5 km diameter depression the Upper Rhyolite is more than 180 m thick

(fig. 12); it extended slightly outside the depression where it occurs in thin (30 m), scattered outcrops.

Tuffaceous sediment or air-fall tuff occurs in thin scattered lenses throughout the section and is a minor component of the total caldera fill. The Chinati caldera was filled almost entirely by volcanic rocks and in this respect is unlike some other calderas that commonly have thick sequences of volcaniclastic sediments interbedded with more subordinate volcanic rocks (Smith and Bailey, 1968).

Uranium Geology

Upper Rhyolite

Primary Characteristics

Vitrophyre of the Upper Rhyolite occurs only at the base of the thin outcrops that lie just outside the edge of its collapse structure. Sample 77001 provided by Daniel S. Barker and Joseph Cepeda contains abundant anorthoclase and quartz phenocrysts, green, flattened pumice fragments, and rhyolite rock fragments in a groundmass of green densely welded, undevitrified glass shards (fig. 13). Laminar flow features which obscure ash-flow textures in some samples of vitrophyre indicate relatively low viscosity of the ash flow after deposition. Cepeda (1977) implied that a high volatile content may have been responsible for the lowered viscosity. High alkali and iron concentrations, low Al concentration (Scarfe, 1977), and high temperature due to the proximity to the source may also have been important.

Figure 13. 77001. Densely welded vitrophyre of Upper Rhylite. Long dimension 3 mm.

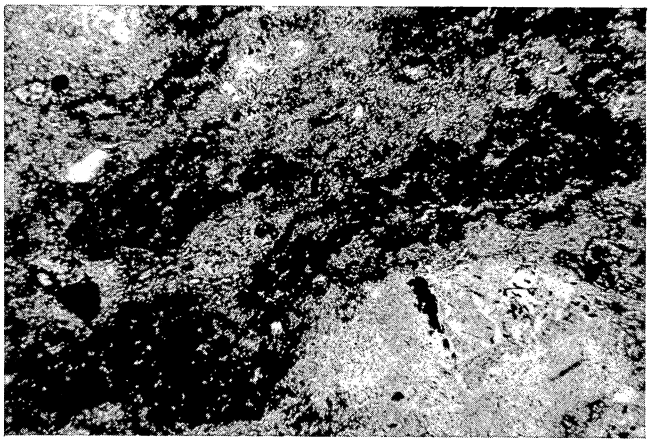

Figure 14. CM-3c. Devitrification of Upper Rhyolite with preservation of pumice but loss of all shard structure. Long dimension 3 mm.

No chemical analysis is yet available for the vitrophyre, but an analysis of a devitrified sample (table 1) is similar to analyses of Mitchell Mesa Rhyolite and Santana Tuff except that the Upper Rhyolite is richer in sodium and iron. It is peralkaline with a molar Na + K/Al greater than 1. Uranium concentration of the vitrophyre is 13 ppm (table 4).

Table 4. Uranium concentrations--Chinati Mountains Group.

Sample			Uranium concentration (ppm)	
			Total	HNO_3 leach
77001	Upper Rhyolite	Vitrophyre	13	<1
CM-3h	Upper Rhyolite	"Granophyric" crystallization	5.8	<1
CM-3g	Upper Rhyolite	"Granophyric" crystallization	7.2	<1
CM-3f	Upper Rhyolite	"Granophyric" crystallization	7.4	<1
CM-3e	Upper Rhyolite	"Granophyric" crystallization	5.2	<1
CM-3c	Upper Rhyolite	Devitrified	12	<1
CM-3b	Upper Rhyolite	"Granophyric" crystallization	8.7	<1
CM-3a	Upper Rhyolite	"Granophyric" crystallization	8.7	<1
CM-1k	Upper Trachyte (upper)	Primary crystallization	6.3	
CM-1j	Upper Trachyte (upper)	Glassy, vesicular	5.2	
CM-1i	Upper Trachyte (upper)	Glassy, partial alteration to montmorillonite	3.2	
CM-1d	Upper Trachyte (lower)	Primary crystallization, vesicular	6.4	
CM-1c	Upper Trachyte (lower)	Primary crystallization	5.1	
CM-1b	Upper Trachyte (lower)	Glassy, vesicular	4.6	
CM-1a	Upper Trachyte (lower)	Primary crystallization	4.5	
C-172	Upper Trachyte (lower)	Glassy	7.4	

Table 4. Continued.

Sample			Uranium concentration (ppm)	
			Total	HNO_3
CM-11i	Lower Rhyolite	Primary crystallization, deuteric alteration	5.2	
CM-11h	Lower Rhyolite	Primary crystallization, deuteric alteration	4.6	
CM-11f	Lower Rhyolite	"Granophyric" crystallization, deuteric alteration	6.0	
CM-11e-2	Lower Rhyolite	"Granophyric" crystallization, deuteric alteration	6.6	
CM-11e-1	Lower Rhyolite	"Granophyric" crystallization, deuteric alteration	6.6	
CM-11c	Middle Trachyte	Primary crystallization, deuteric alteration	4.4	
CM-11b	Middle Trachyte	Primary crystallization, deuteric alteration	4.1	
CM-11a	Middle Trachyte	Primary crystallization, deuteric alteration	4.6	

Alteration and Effect on Uranium Concentration

All other samples were collected from a thick section of the Upper Rhyolite within the collapse structure approximately 3 km from the vitrophyre locality. All other samples are devitrified. The style of devitrification falls into two general categories. The least altered category is composed of only one sample (CM-3c, fig. 14). This sample has aziolitic devitrification similar in some respects to devitrification shown by the Mitchell Mesa Rhyolite and Santana Tuff. In hand specimen and thin section outlines of pumice fragments are well preserved, but the internal structure of pumice is at most only faintly preserved in a few fragments. Shard structure in the groundmass has been totally destroyed, and only a faint banding suggests an original welded ash-flow texture. Mafic minerals are totally oxidized. A few small pockets contain intergrown alkali feldspar and quartz; the quartz in these pockets consists of a single optically continuous grain that partially encloses the feldspar and that is suggestive of granophyric textures. All these features are in contrast with devitrification features seen in other ash-flow tuffs that commonly preserve the shard and pumice structures.

All other samples have undergone moderate to extensive vapor-phase crystallization. Several samples show much more extensive areas of irregular intergrown quartz and feldspar, similar to the texture described above. In all these samples the groundmass has been converted to a mosaic of quartz and alkali feldspar with abundant grains of highly pleochroic clinopyroxene, possibly aegirine. No evidence of ash-flow tuff textures is preserved; pumice fragments, shard textures, and even

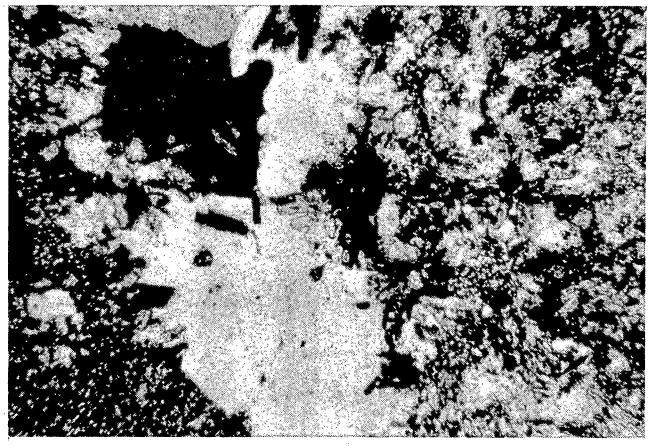

Figure 15. CM-3f. "Granophyric" crystallization of Upper Rhyolite with radial alkali feldspar aggregates (center) and final filling of quartz. Crossed nicols. Long dimension 2 mm.

the faint banding observed in sample CM-3c have been destroyed. Cavity fillings that may be analogous to vapor-phase cavities in other ash flows contain a unique mineral and textural assemblage. Finely intergrown quartz and alkali feldspar, which have a texture similar to that of the groundmass, occur at the contact, but clinopyroxene is much less abundant at the contact than it is in the groundmass and it occurs as large isolated grains. Stubby laths of kaolinitized alkali feldspar 2 mm long are scattered through the rest of the cavity; many occur in radial aggregates (fig. 15). Coarsely crystalline quartz fills the rest of the

space, poikilitically enclosing the feldspar. Overgrowths occur on both quartz and anorthoclase phenocrysts, yet in one sample the anorthoclase has been extensively dissolved with development of coxcomb textures as seen in mafic minerals in the Tascotal Formation (Walter, this report). These features are also in contrast with samples of Mitchell Mesa Rhyolite or Santana Tuff which, even in samples which have undergone extensive vapor-phase crystallization, have recognizable shard structures and other features characteristic of ash-flow tuffs.

Uranium concentration in the devitrified samples ranges from 5.2 to 12 ppm with all but one below 8.7 ppm (table 4). All but the sample with 12 ppm contain considerably less uranium than the vitrophyre. HNO_3-soluble uranium is <1 ppm for all devitrified samples.

These results can be interpreted in several ways. The first is that the uranium concentration of the vitrophyre is not representative of the primary uranium concentration of the devitrified samples. This interpretation makes further speculation on uranium release meaningless but for the following reason is unlikely. The least altered, axiolitically devitrified sample (CM-3c) contains 12 ppm uranium. Among the devitrified samples it is least likely to have undergone uranium mobilization. The similarity in uranium concentration between vitrophyre (77001) and the devitrified sample (CM-3c) suggests that the other, more altered samples also had primary concentrations near 12 to 13 ppm.

A second interpretation, assuming a primary concentration of 12 to 13 ppm, is that gound water has leached uranium placed in an easily soluble form such as intergranular films or in iron oxides by devitrification and vapor-phase crystallization. This explanation requires that

all soluble uranium be removed from all analyzed samples without any of the samples showing detectable effects of ground-water leaching. The mineral assemblage of quartz and feldspar is resistant, but it seems unreasonable to expect such complete depletion without noticeable effects such as alteration of less resistant vapor-phase mafic minerals.

The best explanation is that depletion of uranium has occurred in these samples during devitrification. All the depleted samples show the intense and extensive alteration just described. Sample CM-3c has experienced only normal devitrification and has a uranium concentration almost identical to that of the vitrophyre. The key to understanding this depletion is in understanding the origin of the alteration assemblage.

Origin of Alteration of the Upper Rhyolite

Why should the Upper Rhyolite, an ash-flow tuff, suffer extensive uranium loss during devitrification when the Mitchell Mesa Rhyolite and Santana Tuff, which are also ash flows and have considerable vapor-phase crystallization, have not? The answer to this question lies in the style and intensity of the crystallization. Important features are complete destruction of ash-flow textures, growth of coarse alkali feldspar including radial aggregates, and crystallization of primary quartz.

According to Smith (1960), silica phases produced by devitrification and vapor-phase crystallization include cristobalite and tridymite only; although quartz occurs in many ash-flow tuffs, it is probably a secondary product formed by inversion of the high-temperature silica minerals.

Smith stated that primary quartz occurred only in granophyrically crystallized ash flows and speculated that very hot, gas-rich, and thick ash flows would experience slow cooling, extended periods of deuteric alteration, development of granophyric textures, and complete obliteration of ash-flow textures. Keith and Muffler (1978) found primary quartz suggestive of granophyric crystallization in the Lava Creek Tuff of Yellowstone National Park. They attributed the presence of primary quartz to slow, complex cooling of the thick caldera filling ash-flow tuff. Cepeda (1977) noted the presence of granophyric textures in the Upper Rhyolite; quartz and alkali feldspar in samples of this study are intergrown in textures similar to those of granophyres. However, the classic micrographic textures most characteristic of granophyre were not found. Nevertheless the characteristics of the Upper Rhyolite generally do fit Smith's model.

Results of experimental work bear on the origin of the granophyric-like texture. Lofgren (1971) devitrified natural rhyolite glass at a variety of temperatures and fluid compositions. Many of his devitrification experiments produced textures. These resemble textures in the Upper Rhyolite that he considered similar to granophyric textures. The silica phase produced was quartz in all tests because all tests were made on a system oversaturated with water. Fenn (1977) and Swanson (1977) studied nucleation and rates of crystal growth in hydrous granitic melts. They found that small amounts of undercooling below the liquidus temperature leads to a low nucleation density and rapid crystal growth. They also found that as the water content of the melt is increased,

nucleation density further decreases and rate of growth increases. Fenn (1977) also indicated that tabular faceted feldspar crystals developed at low undercooling, whereas spherulitic textures were produced by greater undercooling. Tabular feldspars in radial aggregates shown by Fenn are remarkably similar to the feldspars in figure 15. In devitrified natural glasses spherulitic textures should occur because undercooling is large and the volatile concentration is low. The assemblage of coarse, tabular alkali feldspars and coarse quartz in the Upper Rhyolite thus implies little undercooling and crystallization in a fluid-rich environment.

The distinctive form of crystallization may have occurred for several reasons. First, granophyric crystallization, which it resembles, is restricted to very thick ash-flow tuffs approximately of 180 m (600 ft) thick (Smith, 1960b). The Upper Rhyolite is at least 180 m thick. However, the Santana Tuff in section BB-27 was almost as thick, but vapor-phase crystallization was not as intense; nothing suggestive of granophyric crystallization occurred and little uranium depletion occurred. The second reason, then, is that the Upper Rhyolite was lower in viscosity and enriched in volatiles (which should also lower viscosity) compared with either the Mitchell Mesa Rhyolite or Santana Tuff. Lower viscosity is indicated by several factors: (1) the peralkaline composition (low aluminum, high sodium, potassium, and iron) leads to much lower viscosities than those found in most rhyolitic glasses (Scarfe, 1977); (2) laminar flowage features in some vitrophyres indicate low viscosity (Cepeda, 1977); (3) the setting of the Upper Rhyolite filling a caldera provides a mechanism by which volatiles and heat can be

concentrated. The Upper Rhyolite accumulated almost entirely within a small collapse structure produced by removal of the Upper Rhyolite. Because it was not transported far, the Upper Rhyolite should not have lost much heat or volatile content during transport. All sampled Mitchell Mesa Rhyolite and Santana Tuff sections are distant from their source calderas, and significant volatile and heat loss probably occurred during transport. Volatiles released during initial vesiculation that accompanied eruption of the Upper Rhyolite were probably all trapped within the rhyolite within the caldera.

Thus after eruption and settling of the Upper Rhyolite a caldera had formed filled with a hot, volatile-rich ash-flow tuff. Cooling was slow and devitrification at this point released large amounts of volatiles that reacted with the rock to form the distinctive mineral and textural assemblage.

The volatile phase may have been more nearly a hydrothermal fluid than the vapor phase of most ash-flow tuffs. Another difference is in apparent amount of movement of the volatile phase. Vapor-phase movement, except for vapor lost through fumaroles, may be no more than a few centimeters and may consist mostly of the local accumulation of volatiles released by devitrification. Volatile movement in the Upper Rhyolite may have been over much greater distances. If the low uranium concentration of devitrified samples compared to the uranium concentrations of the vitrophyre and sample CM-3c does indicate large-scale depletion of uranium, and if depletion has occurred because uranium was fractionated into the volatile phase, then transport had to be sufficiently great so that

the uranium was removed from the Upper Rhyolite. It is possible that the depleted uranium was concentrated somewhere in the Upper Rhyolite, but, if so, it was not sampled. The uranium could also have been either lost to the atmosphere or deposited in wall rocks adjoining the caldera. The uranium that remained in the devitrified rocks was evidently tied up in relatively insoluble sites unaffected by HNO_3 leaching, similar to uranium in the Mitchell Mesa Rhyolite and Santana Tuff.

The Upper Rhyolite is volumetrically a very small ash-flow tuff, even though it is exceptionally thick within its caldera. Total volume is approximately 15 to 20 km^3. In contrast, the Mitchell Mesa Rhyolite may have had a total volume of as much as 150 km^3. The Mitchell Mesa within the Chinati caldera may be similarly thickened in comparison to outcrops outside the caldera. Alteration of a several hundred meters or more thick Mitchell Mesa within the caldera could conceivably have been even more intense than alteration of the Upper Rhyolite.

Upper Trachyte

Primary Characteristics

The Upper Trachyte consists of two lithologically distinct subunits each made up of several individual lava flows. The lower subunit contains 5 to 15 percent wormeaten plagioclase phenocrysts rarely up to 5 mm long; augite and opaque minerals occur as minor but ubiquitous phenocrysts. A few percent anorthoclase is present in some samples. The groundmass varies from glassy to totally crystalline with small intergrown grains of plagioclase, clinopyroxene, and opaques. Samples with glassy groundmasses

have microphenocrysts of plagioclase in light-to dark-brown glass. The upper subunit is similar, except that it contains as much as 25 percent plagioclase phenocrysts up to 1 cm long. Flows in both subunits have massive bases and vesicular tops. The vesicles are lined with quartz, chalcedony, and chabazite (?).

A chemical analysis (table 4) of a totally crystalline sample of the lower subunit shows that it is far more mafic than are the rhyolitic units. The trachyte contains much less silica, more calcium, magnesium, and iron; alkali concentrations, however, are almost as high as they are in the Upper Rhyolite, testifying to the general alkalic nature of Trans-Pecos rocks.

Two glassy samples from the lower subunit have been analyzed for uranium. Sample CM-1b contains less than 10 percent total phenocrysts of plagioclase, augite, and opaque in a vesicular flow top with quartz and chabazite lining vesicle walls; it contains 4.6 ppm uranium. Sample C-172 (supplied by Joseph Cepeda) is from a different flow but is lithologically similar to CM-1b except that it is not vesicular. It contains 7.4 ppm uranium.

Alteration and Effect in Uranium Concentration

The kinds of processes that could release uranium from a mafic lava flow are different from those that could release uranium from silicic ash-flow tuffs. Samples collected from the Upper Trachyte were selected to determine whether it has sufficient uranium for it to be a significant source rock and also to evaluate several possible release mechanisms. Thus samples were collected from glassy and crystalline samples

and from massive and vesicular samples to see whether crystallization and formation of a vapor phase could extract uranium. Unlike the Upper Rhyolite, totally crystalline samples of Upper Trachyte probably resulted from direct crystallization from a magma rather than devitrification of glass. Additionally partly weathered samples were collected to determine if weathering could release uranium, for example, from intergranular films or accessory phases where uranium was concentrated during crystallization.

Three pairs of samples were analyzed from the Upper Trachyte--two from the lower subunit and one from the upper subunit. Sample CM-1b is a glassy, vesicular sample from the top of a flow; sample CM-1a is a crystalline nonvesicular sample from the base. They have nearly identical uranium concentrations of 4.6 and 4.5 ppm, respectively. The results could be explained in two ways. The concentrations are equal to magmatic concentrations, and crystallization does not exclude uranium from the total rock. Alternatively, both samples have been equally depleted, one by crystallization and one by separation of a volatile phase. The former interpretation seems more likely.

Samples CM-1c and CM-1d are from a flow directly above the flow represented by samples CM-1a and CM-1b. Both are totally crystalline with phenocrysts of plagioclase, augite, and magnetite in a fine-grained groundmass of the same minerals; CM-1d is vesicular with fillings of quartz, and sample CM-1c is nonvesicular. The uranium concentrations are similar; certainly CM-1d has not experienced any uranium loss.

Samples CM-1i and CM-1j are from the same flow in the upper subunit. Sample CM-1j is vesicular with cavity fillings of chabazite. Sample

CM-1i is partly weathered to montmorillonite. Both were originally glassy. The differences in uranium concentration suggest that weathering is releasing uranium tied up in glass, but the differences are just at the limits of analytical precision.

Sample CM-1k is also from the upper subunit. It is totally crystalline. Its uranium concentration of 6.3 ppm cannot be compared to any primary concentration, but because it is one of the higher values in the Upper Trachyte it probably does not indicate significant depletion.

The uranium concentrations of the various samples do not indicate any significant depletion of enrichment. The Upper Trachyte is, however, a potentially good source rock. Its range of uranium concentrations (3.2 to 7.4 ppm) is comparable to uranium concentrations in the Mitchell Mesa Rhyolite and is remarkably high for mafic lavas. Weathering of CM-1i may have released uranium. Large amounts of Upper Trachyte have been eroded, and much of the eroded material is now incorporated in the Tascotal Formation, Perdiz Conglomerate, and other sedimentary units derived from the Chinati Mountains. Additional alteration of clasts of Upper Trachyte could release uranium for potential deposits in some of these sediments.

Lower Rhyolite

Primary Characteristics

Lava flows of the Lower Rhyolite contain abundant phenocrysts of anorthoclase ranging in size from less than 1 to 5 mm and contain a few percent quartz phenocrysts (Cepeda, 1977). Biotite and clinopyroxene or their alteration products are minor constituents of most thin sections. Observed rocks are totally crystalline with two types of groundmass

textures. In one flow the groundmass is made up of interlocking quartz, alkali feldspar, and opaques; in another flow all samples have granophyric textures.

No samples of glassy Lower Rhyolite were found in this study or by Cepeda (1977). Groundmass textures suggest crystallization from a magma rather than devitrification. Possibly vitrophyres could be found at the top or bottom of some flows, but it appears that most of the Lower Rhyolite never went through a glassy state. The chemical analysis listed in table 1 is from the freshest crystalline sample found by Cepeda, but he indicated that even that sample showed some evidence of alteration. The analysis shows that the Lower and Upper Rhyolites have comparable alkali, calcium, and iron concentrations, but the Lower Rhyolite has lower silica and higher aluminum concentrations than does the Upper Rhyolite. It is not peralkaline.

Primary uranium concentration of the magma that formed the Lower Rhyolite is unknown. Three of five analyzed samples from a section of the Lower Rhyolite in the western Chinati Mountains are from the lowest exposed flow, and two are from the highest exposed flow. All five samples are totally crystalline, and within each flow uranium concentrations are fairly constant at approximately 6.5 ppm and 5 ppm, respectively. The consistency of the uranium concentrations suggests that they are primary concentrations. Because of its genetic relation to, and chemistry intermediate between, the Upper Trachyte and Upper Rhyolite it seems likely that the Lower Rhyolite should have an intermediate uranium concentration. However, the entire range of uranium concentrations falls within

the range of concentrations of the Upper Trachyte.

Alteration and Effect on Uranium Concentration

Samples from the lower flow (CM-11e-1, CM-11e-2, CM-11f) have undergone extensive alteration. The groundmass in each sample consists of 1 to 2 mm patches of intergrown, optically continuous quartz and alkali feldspar; this texture is more like established granophyric textures than are any of the textures observed in the Upper Rhyolite. Minor mafic minerals are totally altered to opaque clusters but were probably clinopyroxene originally. Anorthoclase phenocrysts are partly altered to sericite with alteration decreasing inward. Sericite also occurs sparsely in the groundmass. Apparently the flow underwent granophyric crystallization plus a deuteric or hydrothermal alteration that converted some feldspar to sericite.

Two samples from the upper flow are less altered than samples from the lower flow. Anorthoclase phenocrysts are altered to sericite but to a lesser degree, and in one sample abundant grains of clinopyroxene are almost unaltered. In the other sample many clinopyroxene grains are altered to serpentine or to opaque clusters. The groundmass consists of interlocking quartz and alkali feldspar in a nongranophyric texture. However, sericite is abundant in the groundmass. This flow evidently underwent the same kind of deuteric alteration that affects the other flow.

Although samples from both flows show considerable evidence of alteration, uranium does not seem to have been mobilized in either. The lower, granophyrically crystallized flow has uranium concentrations of

6.0, 6.6, and 6.6 ppm uranium. It seems unlikely that alteration that caused significant uranium mobility would have left such uniform concentrations. In the Upper Rhyolite, which also has granophyric-like textures, evidence for uranium mobility includes the wide range in the analyzed uranium concentrations. Why granophyric crystallization should cause extensive uranium mobility in the Upper Rhyolite and not in the Lower Rhyolite, even when accompanied by an additional alteration, is unknown.

The upper flow is less altered than the lower flow but has lower and uniform uranium concentrations. It is doubtful that alteration has depleted uranium, so the difference between the two flows is probably due to primary differences.

Although alteration has not obviously affected uranium concentration in the Lower Rhyolite, the analyses do show that the Lower Rhyolite has a moderately high uranium concentration. The Lower Rhyolite has been extensively eroded and incorporated in adjacent sedimentary deposits, similar to the Upper Trachyte. Also, the Lower Rhyolite makes up most of the western edge of the Chinati Mountains where it is bordered by Presidio Bolson, a deep fault-bounded basin. Long-term weathering of the uranium-rich Lower Rhyolite or other rocks could have supplied uranium-enriched ground water for secondary enrichment in bolson sediments.

Middle Trachyte

Primary Characteristics

The Middle Trachyte is lithologically similar to the Upper Trachyte but more extensively altered. Phenocrysts include plagioclase, augite,

and opaques in a crystalline, fine-grained groundmass of the same minerals. No glassy samples are available, and textures indicate primary crystallization. The analysis of Middle Trachyte shown in table 1 shows that it contains more silica and alkalis and less calcium, magnesium, and iron than does the Upper Trachyte, but it is more like the Upper Trachyte than either of the rhyolites. The uranium concentrations (4.6, 5.2, and 7.4 ppm) of vitrophyres of Upper Trachyte are probably representative of the primary uranium concentration of the Middle Trachyte.

Alteration and Effect on Uranium Concentration

The Middle Trachyte has been extensively altered. In all three samples examined, plagioclase phenocrysts are wormeaten and partly altered to montmorillonite. All clinopyroxene grains have been destroyed in CM-11b and partly altered in CM-11a, CM-11c. Alteration products are opaques and montmorillonite. Secondary cavity fillings of quartz or chalcedony are common in outcrop and were found in thin section in CM-11a. The Middle Trachyte was collected from the same section as the Lower Rhyolite and has probably been altered by the same event that affected the Upper Rhyolite.

Uranium concentrations of the three samples range from 4.1 to 4.6 ppm. Because of poor exposures, it was impossible to determine how many different flows are represented by the samples. The uniformity of concentration indicates little uranium mobility; however, like the Lower Rhyolite and Upper Trachyte, the Middle Trachyte contains sufficient uranium so that it would be a good source rock for deposits in sediments derived from the Chinati Mountains.

Conclusions

Volcanic rocks of the Chinati Mountain Group contain high primary concentrations of uranium. Analyzed samples contain between 3.2 and 13 ppm. Primary concentrations are highest for the Upper Rhyolite (13 ppm); primary concentrations in the Upper Trachyte, Lower Rhyolite, and Middle Trachyte are apparently between 4 and 7 ppm. Concentrations in the trachytes are remarkably high for mafic rocks and are probably related to their alkalic nature. The Upper Rhyolite experienced granophyric-like devitrification, probably due to slow cooling of the thick, high-temperature, volatile-rich ash flow within its source caldera. Crystallization has apparently released about 50 percent of the original uranium contained within glass. The released uranium could have been concentrated or dispersed through other parts of the Upper Rhyolite or adjacent wall rocks. Alternatively the uranium could have vented to the atmosphere if the granophyric crystallization is at all analogous to vapor-phase crystallization. The Mitchell Mesa Rhyolite is believed to have erupted from the Chinati Mountains and may occur as an exceptionally thick caldera fill beneath the exposed Chinati Mountain Group. If the process that acted on the Upper Rhyolite also acted on the Mitchell Mesa Rhyolite, then major amounts of uranium could have been released from the Mitchell Mesa. Uranium remaining in the Upper Rhyolite is insoluble by HNO_3 leaching and probably would be released only by weathering that completely breaks down the rock.

Available evidence indicates little or no mobility of uranium in the Middle Trachyte, Lower Rhyolite, or Upper Trachyte by the observed

processes of crystallization and alteration, even though most of the rocks are highly altered. The Lower Rhyolite has also experienced granophyric crystallization which, in contrast to crystallization of Upper Rhyolite, has not mobilized uranium. If HNO_3-leaching studies of the Upper Rhyolite can be applied to the other rocks, only extensive weathering will release uranium. However, the Chinatis have been deeply eroded. Large amounts of the volcanic rocks are now incorporated in adjacent sedimentary deposits.

Exploration for uranium in the Chinati Mountains should focus on two areas: (1) around the Upper Rhyolite where possible hydrothermal deposits could occur within the Upper Rhyolite or in adjacent wall rocks or (2) in sediments derived from or adjacent to the Chinati Mountains, where ground water could have concentrated uranium released by erosion and weathering of volcanic rocks of the Chinati Mountains.

ALLEN COMPLEX

Introduction

The Allen Complex is a group of shallow intrusions and lava flows occurring along the north boundary of the Chinati caldera (fig. 16). They are intruded into and contemporaneous with the Shely Group, a sequence of ash-flow tuffs, lava flows, and tuffaceous sediment older than either the Chinati Mountain Group or the Mitchell Mesa Rhyolite. The Shely Group and Allen Complex may be part of an older caldera cycle, the evidence of which is buried beneath and largely destroyed by activity

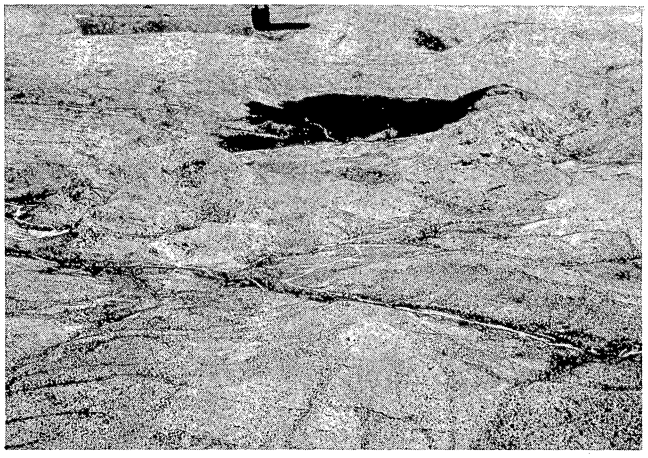

Figure 16. Intrusions of Allen Complex form irregular line of knobby domes in middle ground.

of the Chinati caldera. Rock types of the Allen Complex include abundant vitrophyre, perlite, rhyolite, porphyry, and breccia.

The Allen Complex was selected for examination as a part of this study because, in contrast to the other units studied, it contains several uranium anomalies. Understanding the processes that produced mineralization in the Allen Complex should aid in understanding how uranium mineralization could form in the other rocks. Also in contrast to the other rocks, the rocks of the Allen Complex contain abundant vitrophyre

and are largely intrusive. Thus two potential sources of uranium mineralization are immediately apparent that are not available or are less available from the largely devitrified volcanic rocks that make up the Mitchell Mesa Rhyolite, Santana Tuff, and Chinati Mountain Group. Low-temperature alteration of glass is a known way to provide uranium for mineralization, and hydrothermal processes should be more intense in an area of intrusions. Also, because vitrophyre is abundant, a better knowledge of primary uranium concentrations and the effect of various types of alteration can be obtained.

Shely Prospect

The best known of the uranium anomalies in the Allen Complex is the Shely Prospect, discovered in the 1950's by a ground radioactivity survey. It is described briefly by Amsbury (1958) and Reeves and others (1978). The description here is derived from those reports, from personal communications from Pat Kenney, Jr. (1978), and from observations made during this study.

Uranium mineralization consisting of autunite, metatorbernite, and tyuyamunite (Reeves and others, 1978) occurs in a fracture zone within oligoclase rhyolite of Amsbury's unit Ta_2. Amsbury (1958) reported that 200 tons of ore averaging 0.34 percent U_3O_8 were extracted in the 1950's and stockpiled nearby. The rhyolite is moderately brecciated along the fracture zone, and manganese oxide veins fill many of the fractures. The rhyolite contains phenocrysts of quartz, sanidine, and plagioclase in a fine crystalline groundmass of quartz and alkali feldspar. Textures

in the groundmass show that it devitrified from glass at high temperature. Additionally, the rock is partly altered to montmorillonite and kaolinite.

The fracture zone strikes N 80° E and dips 50° N. A drilling program by Wyoming Minerals and Meeker and Company aimed at the possibility of discovering larger and higher grade, unoxidized pitchblende veins at depth was able to follow the fracture zone to a depth of about 90 ft. Everywhere encountered it was similarly mineralized with yellow, oxidized uranium minerals. Several deeper holes that should have encountered the fracture zone did not, either because the zone steepened or because it did not propagate below 90 ft. According to Kenney, several other fracture systems occur around the oligoclase rhyolite and other intrusions of the Allen Complex, and many are mineralized. However, drilling by Wyoming Minerals and Meeker and Company has failed to discover any economic deposits.

Uranium Geology

Primary Characteristics

The igneous rocks of the Allen Complex can be grouped into two distinct rock types--nonporphyritic glassy rocks and porphyritic crystalline or devitrified rocks. In major-element chemistry (table 1), the two groups are similar to each other and to other rhyolites of this study. The glassy rocks include Amsbury's (1958) unit Ta_6 vitrophyre, black flow banded or massive glass with at most a few percent small sanidine phenocrysts and unit Ta_7 perlite, composed of black, gray, or green hydrated

vitrophyre without phenocrysts. Both contain microphenocrysts, probably of alkali feldspar. They occur together in several places and are probably related subgroups of the Allen Complex being distinguished only by extent of hydration. Even the black vitrophyres show some effects of hydration such as mild perlitic cracking.

Uranium concentration of the glassy rocks ranges from 7.0 to 9.6 ppm (table 5). The highest values are from perlite. The range of values is significant because it shows how much variation in primary uranium concentration can exist even for closely related rocks.

The porphyritic rocks include Amsbury's units Ta_1, Ta_2, and Ta_3. They contain phenocrysts of quartz and sanidine with or without plagioclase in a crystalline groundmass. Some samples have spherulitic textures indicating devitrification of glass during cooling. Other samples have groundmasses composed of fine mosaics of quartz and alkali feldspar. These may have devitrified from glass or they may have crystallized directly from a magma. Because all of the intrusions of the Allen Complex are small and shallow, it may be that all were initially glassy. However, this suggestion cannot be proven with the available evidence.

Uranium concentration in these rocks ranges from 4.6 to 78 ppm. The sample from the Shely prospect (CH-4) has clearly been enriched in uranium. The others may have been depleted. The devitrified porphyritic rocks are chemically similar to the perlites; the range of uranium concentrations of the glassy rock is probably indicative of the range in the crystalline rocks.

Table 5. Uranium concentrations--Allen Complex.

Sample		Uranium concentration
CM-5a-1	Perlite	9.1
CM-5a-2	Perlite	9.6
CM-5a-3	Perlite	8.2
CM-5b-1	Devitrified porphyritic rhyolite	4.6
CM-5b-2	Devitrified porphyritic rhyolite	5.1
CM-5c	Vitrophyre	7.6
CM-5d	Devitrified rhyolite	7.4
CM-5d-S	Devitrified rhyolite with opal and chalcedony	15
CM-5g	Vitrophyre	7.0
CM-5i	Devitrified porphyritic rhyolite	14
CM-5j	Perlite with clinoptilolite and montmorillonite	8.6
CM-5k	Perlite with clinoptilolite and montmorillonite	8.0
CH-4	Devitrified porphyritic rhyolite with kaolinite and montmorillonite	78

Alteration and Its Effect on Uranium Concentration

Observed processes which could have affected the uranium concentration of rocks of the Allen Complex are high-temperature devitrification (and probably crystallization), hydration, and low-to intermediate-temperature alteration or diagenesis by ground water. Based on previous studies that show that hydration has no effect on the uranium concentration of glass, the uranium concentrations of perlites are taken to be primary concentrations. The assumption appears confirmed by the fact that the perlite samples contain as much or more uranium than nearby vitrophyre (for example CM-5a-1 vs. CM-5c). There is certainly no evidence that hydration has significantly depleted uranium. It is not known under what conditions the hydration occurred or if all hydration occurred at the same conditions. At least some of the perlites are intruded into breccias probably sedimentary in origin. If the breccias contained interstitial water at the time of intrusion, hydration may have occurred at relatively high temperature during cooling. However, crystallization might be expected to be more extensive under these conditions. Hydration may also have occurred from interaction with low to moderate (up to 100^{o}C) temperature ground water.

Sample CM-5d is a devitrified equivalent of CM-5c vitrophyre collected less than a meter from CM-5c. They are petrographically identical except that CM-5d is devitrified with small spherulites and contains a few cavities lined with vapor-phase minerals (fig. 17). Vapor phase crystallization was restricted to the cavities. Uranium concentration of the two samples are nearly identical showing that devitrification has

Figure 17a. CM-5c. Vitrophyre of Allen Complex showing flow bands and minor perlitic cracks. Long dimension 3 mm.

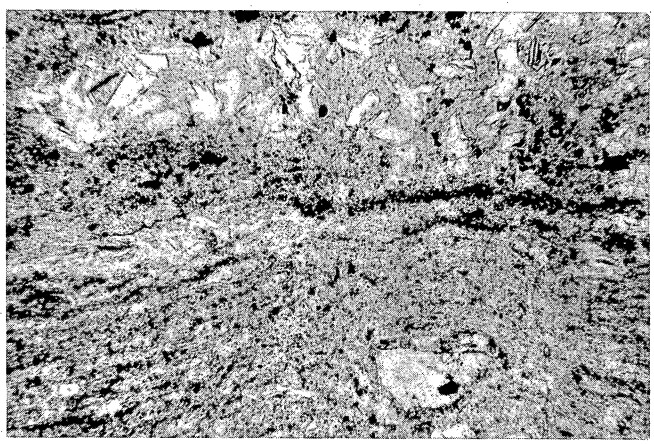

Figure 17b. CM-5d. Devitrified version of CM-5c showing flow bands and vapor-phase crystallization in cavity.

not mobilized uranium.

All the porphyritic group samples are totally crystalline. Of the crystalline samples, one (CH-4) is clearly enriched in uranium, one (CM-5i) is either unchanged or enriched, and two samples (CM-5b-1 and CM-5b-2) are either unchanged or depleted (table 5). No clear pattern arises from this information. Because uranium concentration of sample CM-5d was not affected by devitrification, it may be that these were also unaffected. However, it is at least possible that devitrification has mobilized uranium.

All the crystalline samples also contain montmorillonite and/or kaolinite which is interpreted here to indicate alteration by ground water. Several glassy samples have also undergone alteration by ground water. Two related samples (CM-5j and CM-5k) contain montmorillonite and clinoptilolite in perlite. The uranium concentration of these samples is 8.6 and 8.0 ppm, which falls within the range of glassy samples and indicates that they have not been depleted. However, neither is extensively altered; both are still composed primarily of hydrated glass with montmorillonite and clinoptilolite simply lining perlitic fractures (fig. 18). Probably not enough glass has been altered to deplete the uranium concentration measurably.

Sample CM-5d-S contains 15 ppm uranium, twice that of either CM-5c or CM-5d to which it is related. All are from the same outcrop within a meter of each other. CM-5d-S is identical to CM-5d (devitrified non-porphyritic rhyolite) except that it also contains abundant opal and chalcedony lining cavities (fig. 19). Clearly the enrichment in uranium is related to the silicification either because uranium is within the opal or chalcedony or because the same process introduced both uranium and the silica minerals into the rock. Volcanic rocks in Virgin Valley, Nevada, and the Thomas Range, Utah, contain similar opal and chalcedony coatings and are enriched in uranium; at both locations the uranium is apparently contained within the opal (Henry, this report, chapter X). Uranium in CM-5d-S is probably also within opal. The opal consists of thin, lightly colored coatings of radial fibers. It is not isotropic but is distinguished from chalcedony by its high negative relief. Low relief

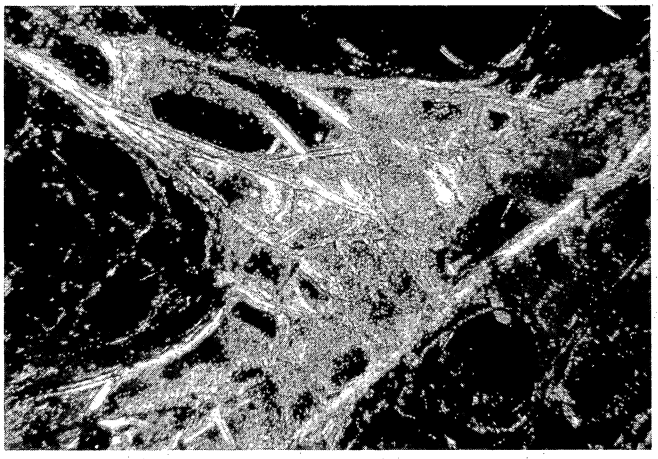

Figure 18. CM-5j. Perlite of Allen Complex slightly altered to clinoptilolite and montmorillonite within perlitic fractures. Crossed nicols. Long dimension 3 mm.

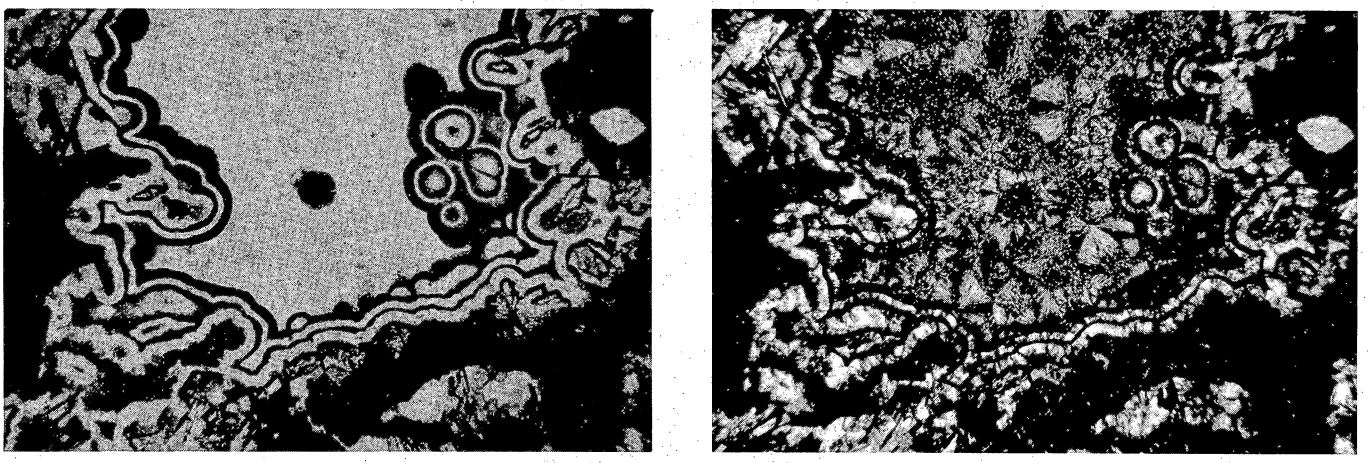

Figure 19. CM-5d-S. Silicified version of CM-5d with alternating bands of non-isotropic opal (high relief, dark under uncrossed nicols) and chalcedony (low relief, colorless under uncrossed nicols). Uncrossed (left) and crossed nicols (right). Long dimension 3 mm.

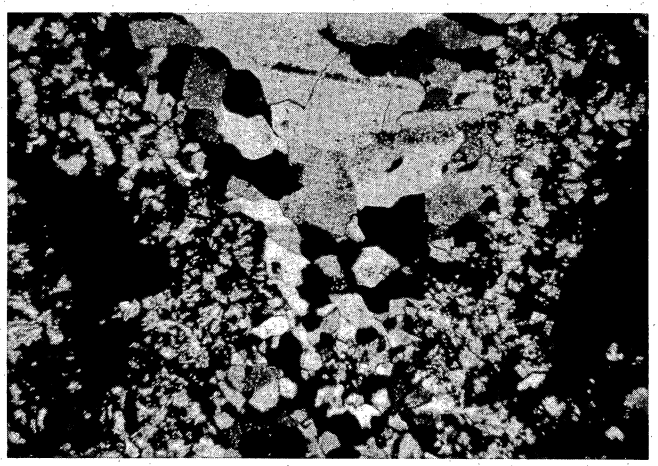

Figure 20. CM-5d-S. Megaquartz filling cavity partially filled by fibrous chalcedony. Crossed nicols. Long dimension 3 mm.

and higher birefringent chalcedony occurs interlayered with the opal and as a final filling of fibrous masses. Megaquartz occurs as a final filling after chalcedony in one cavity in CM-5d-S (fig. 20). Isotropic opal also occurs in cavities in CM-5d but is such a minor component that it has no effect on the uranium concentration. A more complete discussion of the association of uranium and opal is given in the chapter on "Origin of Uraniferous Opal."

Conclusions and Origin of Shely Prospect

Two obvious possible mechanisms to form the Shely Prospect and other similar uranium anomalies in the Allen Complex are (1) release of uranium by crystallization of magma or devitrification of glass and transport by hydrothermal fluids, or (2) release of uranium by alteration of glass and transport by either hot or cold ground water. Mineralization should be expected within fracture zones because they would concentrate fluids formed by either mechanism. The reason for precipitation of uranium minerals is unknown and is an uncertainty for either mechanism.

The second mechanism of alteration and transport by ground water is favored for the following reasons:

1. Diagenesis of glass has occurred in the area of the Allen Complex. Some samples are partly altered to clay and clinoptilolite, and much of the glass is hydrated--a preliminary step in ground-water alteration preceding complete solution of glass. Abundant formerly glassy material must have existed above the present level of outcrop, and at standard temperature and pressure would be altered rapidly rather than being transported out

of the area before alteration.

2. Although no glassy samples show evidence of uranium depletion, none of the rocks sampled were sufficiently altered so that measurable uranium release should have occurred. Complete alteration of formerly glassy samples of Mitchell Mesa Rhyolite and Santana Tuff has definitely released uranium, however.

3. At the Shely prospect and other anomalies, uranium is associated with montmorillonite and kaolinite. Montmorillonite has been produced by diagenesis of glass in the Tascotal Formation to the south and east (Walton, this report, chapter VI). Ground water exclusively in contact with volcanic rocks in the area has high pH and high Na^{+}/H^{+} and Ca^{++}/H^{+} activity ratios (Henry, 1978) and falls within the stability field of montmorillonite. Formation of kaolinite requires lower pH and lower Na^{+}/H^{+} and Ca^{++}/H^{+} activity ratios than does formation of montmorillonite. Cretaceous carbonates in the area of the Allen Complex would buffer ground water to lower pH's. Analyzed cold and thermal ground water that has been in contact with both volcanic and carbonate rocks has the appropriate chemistry (Henry, 1978). Thus both montmorillonite and kaolinite should be in equilibrium with ground water in contact with rocks known to occur around the uranium mineralization. Although this does not prove that uranium was deposited by the same fluids that precipitated montmorillonite and kaolinite, disequilibrium between the observed alteration assemblage and ground water would be a strong argument against ground-water transport. The significance of the association with manganese oxide is uncertain.

4. Although devitrification and crystallization have also occurred extensively in the Allen Complex, there is no evidence that these processes have released uranium. In one sample pair (CM-5c and CM-5d) devitrification has clearly not released uranium, and extensive study of the Mitchell Mesa Rhyolite and Santana Tuff indicates that significant uranium release does not occur during devitrification and vapor-phase crystallization. Although the geologic setting of the Mitchell Mesa Rhyolite and Santana Tuff is not identical to that of the Allen Complex, the processes affecting each are similar. However, a conclusion based on a single pair of samples is clearly arguable.

To evaluate more thoroughly the processes releasing uranium and creating uranium mineralization in the Allen Complex and to evaluate the favorability for additional uranium deposits in the area, additional sampling is needed. Analysis of more thoroughly altered formerly glassy samples would show if uranium is truly released by the alteration. A search for glassy parts of the devitrified porphyritic rocks to determine primary uranium concentrations and the effect of devitrification would also be useful.

The question also remains as to the precise conditions under which the alteration that produced opal, chalcedony, montmorillonite, kaolinite, and clinoptilolite occurred and whether or not they all were formed by the same process. Both cold and hot ground water with temperatures form near $0^{o}C$ up to about $150^{o}C$ could produce the observed minerals (Walton, 1975; Keith and Muffler, 1978). The geologic setting of the Allen Complex allows either. Hot spring activity associated with initial

cooling of the intrusions could have been important but circulation of purely cold ground water at any time after intrusion would be sufficient. A more thorough discussion of this question is given in the chapter on "Origin of Uraniferous Opal."

SUMMARY OF CONCLUSIONS

Conclusions about uranium mobility during various processes acting on the Mitchell Mesa Rhyolite, Santana Tuff, Chinati Mountains Group, and Allen Complex have been presented. However, it is worthwhile to restate the conclusions briefly and to speculate on how broadly the conclusions can be applied.

High-temperature processes of crystallization, devitrification, and vapor-phase crystallization acting on all the rocks studied have not significantly released uranium. Additionally, the processes have placed uranium in apparently insoluble sites where later leaching by ground water also cannot remove uranium. Thus, for example, the Mitchell Mesa Rhyolite and Santana Tuff cannot have supplied a significant amount of uranium to the Tascotal Formation or other sedimentary sequences either at the time of ash-flow deposition and initial cooling or later during weathering.

One high-temperature process apparently has released a significant proportion of uranium. The Upper Rhyolite of the Chinati Mountains Group accumulated in a small caldera where the combination of entrapped heat and volatiles and slow cooling lead to granophyric-like crystallization. Samples of the Upper Rhyolite average about 50 percent depletion

in uranium compared to a sample of vitrophyre.

Low-temperature alteration (diagenesis) of glass releases uranium. Four samples of Mitchell Mesa Rhyolite and Santana Tuff altered to montmorillonite or clinoptilolite have all been depleted in uranium. However, very little of the Mitchell Mesa or Santana remained glassy after initial cooling so only a very small fraction of the total uranium of either unit was released.

Abundant glass remained in the Allen Complex after initial cooling, and several samples show evidence of diagenesis such as hydration and presence of montmorillonite, kaolinite, and clinoptilolite. The presence of several small areas of uranium mineralization in fracture zones is probably due to release of uranium by solution of glass. Among the sites investigated in this part of the study, the Allen Complex is the most favorable for finding additional uranium mineralization. Whether or not mineable grade deposits occur depends on how much glass has undergone solution and how efficiently the released uranium was concentrated.

Several of the conclusions should be tested. Analysis of other elements, for example fluorine and thorium, and correlation with uranium could indicate whether or not uranium was depleted and by what mechanism it was depleted. An association with fluorine would indicate volatile transport as a uranous-fluoride complex. High Th/U ratios (compared with ratios in vitrophyres) would indicate depletion of uranium by a process involving oxidation.

The process by which uranium is depleted during solution of glass requires additional study. Similar solution of glass in the Tascotal

Formation did not remove uranium, possibly because of a lack of suitable complexing agents to transport uranium (Walton, this report, chapter VI). Identification of differences between diagenesis of the Tascotal Formation and diagenesis of glassy parts of the volcanic rocks could show under what circumstances uranium is transported and concentrated.

The location of uranium in devitrified rocks is important. Most of the initial uranium of all rock types studied is still tied up in devitrified rocks. The comparison of total and HNO_3-soluble uranium gives only an indication of uranium distribution and the analogy of HNO_3 leaching to weathering is arguable. More specific chemical-solution methods along with fission-track mapping could identify uranium sites precisely and indicate whether uranium in devitrified rocks really cannot be released by low-temperature alteration.

The conclusions that high-temperature processes do not release uranium and in fact put uranium in insoluble sites in devitrified rocks and that low-temperature diagenesis of glass does release uranium seem broadly applicable to the volcanic rocks of Trans-Pecos Texas.

How applicable are these results to other volcanic and volcaniclastic rocks? Investigation of volcanic rocks of Virgin Valley, Nevada (Henry, this report, chapter VIII), shows an identical pattern of nonrelease of uranium by high-temperature processes and release by low-temperature diagenesis. The Mitchell Mesa and Santana Tuff are alkali-rich rhyolites similar in major-element chemistry to many of the rhyolites of the western United States. The total group of rocks studied is also broadly similar to the volcanic rocks of the western United States. The high- and low-

temperature processes that have affected the rocks and the mineralogical and textural assemblages produced by the different processes are identical. For these reasons it seems likely that the results of this study can be broadly applied to other volcanic and volcaniclastic provinces in the western United States.

REFERENCES

Amsbury, D. L., 1958, Geologic map of Pinto Canyon area, Presidio County, Texas: University of Texas, Austin, Bureau of Economic Geology, Geologic Quadrangle Map 22.

Anderson, W. B., 1975, Cooling history and uranium mineralization of the Buckshot Ignimbrite, Presidio and Jeff Davis Counties, Texas: Unpublished Master's thesis, The University of Texas at Austin, 135 p.

Burt, E. R., 1970, Petrology of the Mitchell Mesa Rhyolite, Trans-Pecos Texas: Unpublished Ph.D. dissertation, The University of Texas at Austin, 94 p.

Cepeda, J., 1977, Geology and geochemistry of the igneous rocks of the Chinati Mountains, Presidio County, Texas: Unpublished Ph.D. dissertation, The University of Texas at Austin, 153 p.

Daugherty, F. W., and Fandrych, J. W., 1978, Geology of the Christmas Mountains fluorspar district, Brewster County, Texas: in Walton, A. W., ed., Cenozoic geology of the Trans-Pecos volcanic field of Texas, p. 85.

Dostal, J., and Capedri, S., 1978, Partition coefficients of uranium for some rock-forming minerals: Chemical Geology, v. 15, p. 285-294.

Fenn, P. M., 1977, The nucleation and growth of alkali feldspar from hydrous melts: Canadian Mineralogist, v. 15, p. 135-161.

Fenner, C. N., 1923, The origin and node of emplacement of the great tuff deposit in the Valley of Ten Thousand Smokes: National Geographic Society Contributed Technical Papers, Katmai Series, v. 1, no. 1, 74 p.

Henry, C. D., in press, Geologic setting and geochemistry of thermal water and geothermal assessment, Trans-Pecos Texas: University of Texas, Austin, Bureau of Economic Geology Report of Investigations.

Honda, S., and Muffler, L. J. P., 1970, Hydrothermal alteration in core from research drill hole Y-1, Upper Geyser Basin, Yellowstone National Park, Wyoming: American Mineralogist, v. 55, p. 1714-1737.

Katayama, N., Kubo, K., and Hirono, S., 1974, Genesis of uranium deposits of the Tono Mine, Japan, in Formation of uranium ore deposits: International Atomic Energy Agency, p. 437-451.

Keith, T. E. C., and Muffler, L. J. P., 1978, Minerals produced during cooling and hydrothermal alteration of ash flow tuff from Yellowstone drill hole Y-5: Journal of Volcanology and Geothermal Research, v. 3, p. 373-402.

Lamarre, A. L., and Hodder, R. W., 1978, Distribution and genesis of fluorite deposits in the western United States and their significance to metallogeny: Geology, v. 6, p. 236-238.

Lipman, P. W., 1965, Chemical comparison of glassy and crystalline volcanic rocks: U. S. Geological Survey Bulletin 1201-D, 24 p.

Lipman, P. W., Christiansen, R. L., and Van Alstine, R. E., 1969, Retention of alkalis by calc-alkalic rhyolites during crystallization and hydration: American Mineralogist, v. 54, p. 286-291.

Lipman, P. W., Christiansen, R. L., and O'Connor, J., 1966, A compositionally zoned ash flow sheet in southern Nevada: U. S. Geological Survey Professional Paper 524-F, 47 p.

Lofgren, G., 1971, Experimentally produced devitrification textures in natural rhyolitic glass: Geological Society of America Bulletin, v. 82, p. 111-124.

Marshall, R. R., 1961, Devitrification of natural glass: Geological Society of America Bulletin, v. 72, p. 1493-1520.

McKnight, J. F., 1969, Geologic map of Bofecillos Mountains area, Trans-Pecos Texas: University of Texas, Austin, Bureau of Economic Geology Geologic Quadrangle Map 37.

Noble, D. C., 1970, Loss of sodium from crystallized comendite welded tuffs of the Miocene Grouse Canyon member of the Belted Range tuff, Nevada: Geological Society of America Bulletin, v. 81, p. 2677-2688.

Noble, D. C., Smith, V. C., and Peck, L. C., 1967, Loss of halogens from crystallized and glassy silicic volcanic rocks: Geochimica et Cosmochimica Acta, v. 31, p. 215-223.

Reeves, C. C., Kenney, P., and Wright, E., 1978, Known radioactive anomalies and uranium potential of Cenozoic sediments, Trans-Pecos Texas: in Walton, A. W., ed., Cenozoic geology of the Trans-Pecos volcanic field of Texas, p. 86-99.

Rix, C. C., 1953, Geology of Chinati Peak quadrangle, Trans-Pecos Texas: Unpublished Ph. D. dissertation, The University of Texas, 188 p.

Rogers, J. J. W., and Adams, J. A. S., 1969, Uranium: in Wedepohl, K. H., ed., Handbook of Geochemistry, v. 2, no. 4, p. 92-B to 92-O.

Rosholt, J. N., Prijana, and Noble, D. C., 1971, Mobility of uranium and thorium in glassy and crystallized silicic volcanic rocks: Economic

Geology, v. 66, p. 1061-1069

Scarfe, C. M., 1977, Viscosity of a pantellerite melt at one atmosphere: Canadian Mineralogist, v. 15, p. 185-189.

Smith, R. L., 1960a, Ash flows: Geological Society of America Bulletin, v. 71, no. 6, p. 795-842.

Smith, R. L. 1960b, Zones and zonal variations in welded ash flows: U. S. Geological Survey Professional Paper 354-F, p. 149-159.

Smith, R. L., and Bailey, R. A., 1966, The Bandelier Tuff: A study of ash-flow eruption cycles from zoned magmas: Bulletin of Volcanology, v. 29, p. 83-104.

Smith, R. L., and Bailey, R. A., 1968, Resurgent cauldrons, in Coats, R. R., Hay, R., and Anderson, C., eds., Studies in volcanology: Geological Society of America Memoir, 116, p. 613-662.

Staatz, M. H., and Carr, W. J., 1964, Geology and mineral deposits of the Thomas and Dugway Ranges, Juab and Tooele Counties, Utah: U. S. Geological Survey Professional Paper 415, 188 p.

Stuckless, J. S., Bunker, C. M., Bush, C. A., Doering, W. P., and Scott, J. H., 1977, Geochemical and petrological studies of a uraniferous granite from the Granite Mountains, Wyoming: U. S. Geological Survey Journal of Research, v. 5, p. 61-81.

Surdam, R. C., 1977, Zeolites in closed hydrologic systems, in Mumpton, F. A., ed., Mineralogy and geology of natural zeolites: Mineralogical Society of America Short Course Notes, v. 4, p. 65-92.

Swanson, S. E., 1977, Relation of nucleation and crystal-growth rate to the development of granitic textures: American Mineralogist, v. 62,

p. 966-978.

Taylor, P. S., and Stoiber, R. E., 1973, Soluble material on ash from active Central American volcanoes: Geological Society of America Bulletin, v. 84, p. 1031-1042.

Walton, A. W., 1975, Zeolitic diagenesis in Oligocene volcanic sediments, Trans-Pecos Texas: Geological Society of America Bulletin, v. 86, p. 615-624.

Zielinski, R. A., 1978, Uranium abundances and distribution in associated glassy and crystalline rhyolites of the western United States: Geological Society of America Bulletin, v. 89, p. 409-414.

Zielinski, R. A., Lipman, P. W., and Millard, H. T., 1977, Minor-element abundances in obsidian, perlite, and felsite of calc-alkalic rhyolites: American Mineralogist, v. 62, p. 426-437.

VIII. GEOLOGY AND URANIUM POTENTIAL, VIRGIN VALLEY, NEVADA

by Christopher D. Henry[1]

GEOLOGIC SETTING OF VIRGIN VALLEY, NEVADA

Introduction - Previous Work and Problems

Virgin Valley is in northwestern Nevada (fig. 1). In Miocene time it was an active volcanic center, producing silicic lava flows, ash-flow and air-fall tuff, and tuffaceous sediment. Abundant uneconomic uraniferous opal beds in the sediments have aroused interest in ascertaining how the uranium was concentrated and whether economic deposits could be formed by the same mechanism.

Previous work on the geologic setting of Virgin Valley includes studies by (1) Merriam (1910), who first described the stratigraphy of the area and assigned most of the currently used nomenclature; (2) Willden (1964), who included the area in a regional study of Humboldt County; (3) Fyock (1963) and Wendell (1970), who studied in detail the stratigraphy and structure of the Virgin Valley area; and (4) Noble and others (1970), who described the regional volcanic stratigraphy of northwestern Nevada. Work specifically on uranium mineralization includes that by Staatz and Bauer (1951), who investigated the extensive opal beds of Virgin Valley; Garside (1973), who cataloged uranium deposits in the opal beds; and Cupp and others (1977), who evaluated favorability

---

[1]Bureau of Economic Geology, The University of Texas at Austin.

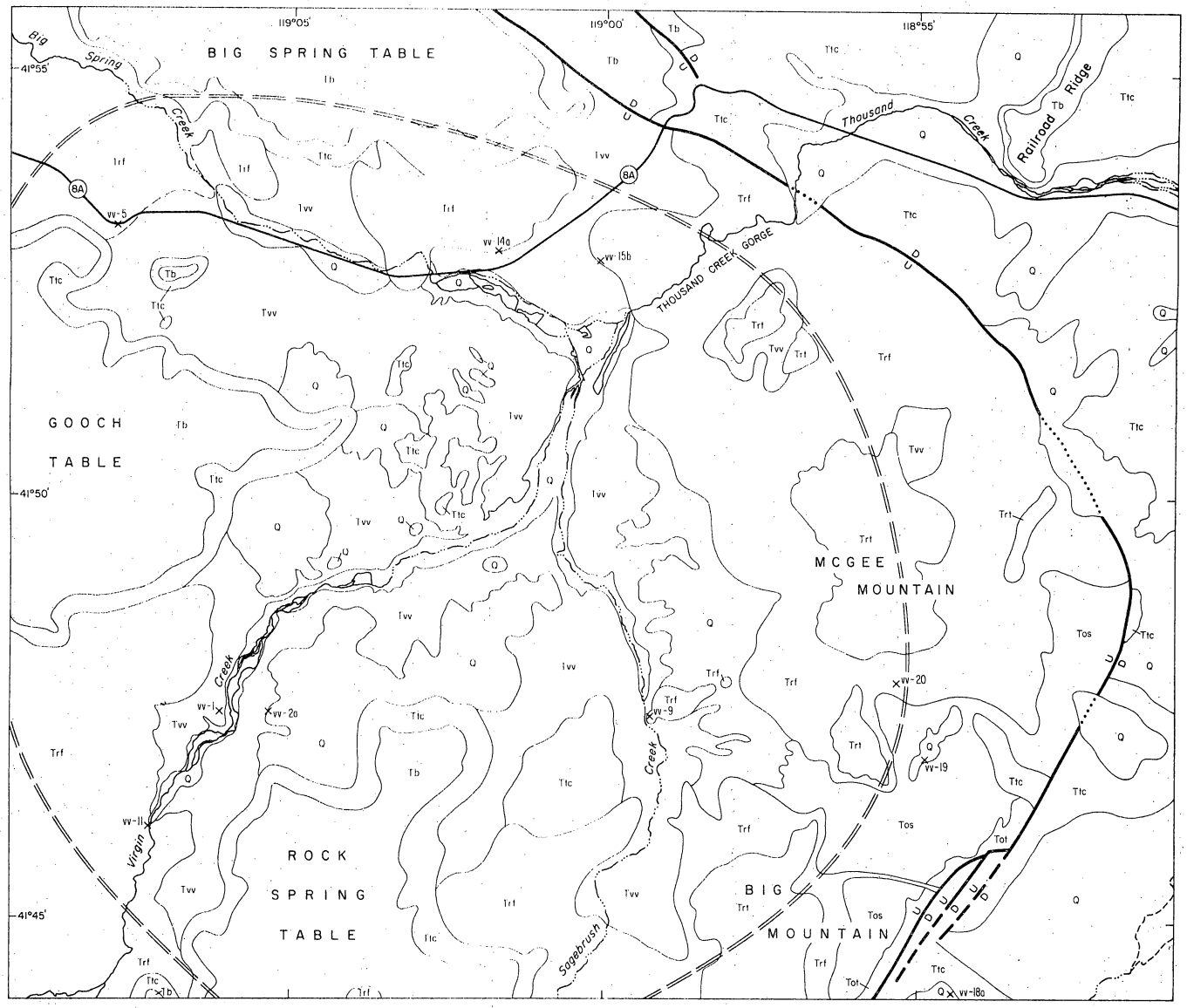

EXPLANATION

- Q — Quaternary alluvium and landslide deposits
- Tb — Mesa Basalt
- Ttc — Thousand Creek Formation
- Tvv — Virgin Valley Formation
- Trt — Canyon Rhyolite – ash flow tuff
- Trl — Canyon Rhyolite – lava flow
- Tos — Pre-Canyon Rhyolite – tuffaceous sediment
- Tot — Older ash flow tuff (Idaho Canyon Tuff)
- D U — Normal fault with sense of displacement
- Inferred caldera boundary
- ×vv-16 — Locations discussed in text and sample locations

INDEX MAP (NEVADA)

SCALE: 0 1 2 3 4 5 miles; 0 1 2 3 4 5 kilometers

Geology from Wendell (1970), Fyock (1963), Willden (1964), and this study.

Figure 1. Geologic map of Virgin Valley area.

for uranium deposits in the Virgin Valley area. Several early Atomic Energy Commission reports which also described uranium mineralization and were referred to in Cupp and others (1977) were not available to us.

Merriam (1910), Fyock (1963), Wendell (1970), and Cupp and others (1977) all discuss in detail the stratigraphy of the Virgin Valley area. Table 1 summarizes the stratigraphic interpretation of each. The previous works agree in a general sense that the Virgin Valley area contains a thick sequence of tuffaceous sediments with a sequence of rhyolitic lava flows and ash-flow tuffs either at the base of or within the sedimentary sequence. It is also generally agreed that the Mesa Basalt, a distinctly younger basalt lava flow, caps the entire sequence. As noted by Cupp and others (1977), lithologic map boundaries of different studies are generally in agreement, but stratigraphic relationships are not. The major difference in interpretation is largely in assignment of relative ages to the Virgin Valley Formation and Canyon Rhyolite. Fyock (1963) and Cupp and others (1977) believed that the Canyon Rhyolite overlies the Virgin Valley Formation, whereas Wendell (1970) and Merriam (1910) believed that the Virgin Valley Formation overlies the Canyon Rhyolite. Additionally, Wendell indicated that tuffaceous sediments underlying the Canyon Rhyolite are part of an older Middle Miocene fluvial sequence. The source of the uncertainty probably lies in distinguishing tuffaceous sedimentary sequences which vary widely in rock type because of both vertical and lateral changes. The range of rock types overlaps to such an extent that correlation on the basis of lithology is difficult.

Table 1: Stratigraphy of the Virgin Valley area, Nevada

Merriam (1910)		Fyock (1963) Cupp and others (1977)		Wendell (1970)		This Report
Mesa Formation		Mesa Formation		Mesa Formation		Mesa Formation
Upper zone	Virgin Valley Formation	Thousand Creek Formation		Thousand Creek Formation		Thousand Creek Formation
Middle zone		Upper Member (welded tuff)	Canyon Rhyolite	Virgin Valley Formation		Virgin Valley
		Middle Member (tuff and breccia)				Canyon Rhyolite - ash-flow tuff member
Lower zone		Lower Member (lava flows)				Formation
Canyon Rhyolite		Virgin Valley Formation		Upper Member (welded tuff)	Canyon Rhyolite	Canyon Rhyolite lava-flow member
				Lower Member (lava flows)		
				Middle Miocene fluvial sequence		Pre-Canyon Rhyolite tuffaceous sediment
				Middle Miocene welded tuff		Older ash-flow tuff (Idaho Canyon Tuff)

Our interpretation, based on reconnaissance field work and summarized in table 1, does not agree completely with that of any of the previous workers and has important implications for the geologic setting of uranium mineralization. Our stratigraphic interpretation and geologic history are derived largely from our own investigation but draw heavily upon the descriptions and interpretations of Wendell and Merriam. Although he did not discuss some possible implications, Wendell, in particular, recognized and described most of the important relationships and rock types. For convenience, we have retained most of the nomenclature of Wendell (derived in part from Merriam), although some revision is warranted. Figure 1 is a geologic map of the area based on previous work and this study.

Stratigraphy

Older Ash-Flow Tuff (Idaho Canyon Tuff)

The oldest volcanic rock exposed in the area examined by us was called Middle Miocene welded tuff by Wendell. It is a pumice-rich, phenocryst-poor, densely welded rhyolitic ash-flow tuff 60 m (200 ft) thick according to Wendell. Phenocrysts are of quartz and sanidine. The Idaho Canyon Tuff, described by Noble and others (1970), is probably the same unit, although petrographic descriptions are not identical and Noble and others give a thickness of 120 m (400 ft). Noble and others found vapor-phase arfvedsonite and sodic amphibole and pyroxene in the groundmass, indicating the rock is peralkaline. Wendell did not mention any peralkaline minerals and considered the Middle Miocene welded tuff

similar to later ash-flow tuffs of the Virgin Valley area that do not contain peralkaline minerals. However, a sample collected during this study also contains arfvedsonite. This and the similarity in field relationships indicate they are the same units.

The older ash-flow tuff (Idaho Canyon Tuff) underlies Pre-Canyon Rhyolite tuffaceous sediment (Wendell's Middle Miocene fluvial sequence) along the upthrown side of the normal fault that bounds the east side of the McGee Mountain - Big Mountain ridge. It does not crop out anywhere in Virgin Valley, but Noble and others (1970) stated that it continues both south and north of the area and thought that it must underlie tuffaceous sediments within Virgin Valley. From stratigraphic relationships, Noble and others (1970) thought the Idaho Canyon Tuff is 15 million years old.

Pre-Canyon Rhyolite Tuffaceous Sediment

The oldest sedimentary sequence observed by us occurs in the division between McGee Mountain and Big Mountain, where a thick section of poorly exposed tuffaceous sediment overlies the older ash-flow tuff. Wendell (1970) called this sequence the Middle Miocene fluvial sequence and considered it distinctly separate from, and older than, the Virgin Valley Formation. The sediments clearly underlie lava flows of Canyon Rhyolite and overlie the older ash-flow tuff. A dike of Canyon Rhyolite cuts these tuffaceous sediments below Big Mountain.

Correlation of the Pre-Canyon Rhyolite tuffaceous sediments within the Virgin Valley Formation is uncertain. The stratigraphically lowest sediments of the Virgin Valley Formation exposed within Virgin Valley are

at least as old as some Canyon Rhyolite lava flows. It is probable that the older sediments are simply an early part of a continuing sequence of tuffaceous sedimentation that includes the Virgin Valley Formation. Alternatively, they could be an older sequence distinct from the Virgin Valley Formation. Detailed work on facies, provenance, and field relationships is necessary to determine which interpretation is correct.

Contact Relationships Between the Lava-Flow Member of the Canyon Rhyolite and the Virgin Valley Formation

The major uncertainty in stratigraphy is the relationship between the Virgin Valley Formation and the Canyon Rhyolite. Within Virgin Valley proper, field relationships show that some of the Virgin Valley beds are derived from the Canyon Rhyolite. North of Thousand Creek Gorge at location VV-15 (figs. 1 and 2), the nose of a rhyolite lava flow contains blocks of flow-banded devitrified rhyolite, obsidian, and pumice in an apparent flow breccia. Sediments extending out from there contain clasts from the breccia. Directly adjacent to the nose, the deposits appear to be purely locally reworked lava flow material, with coarse pumice clasts to 20 cm particularly abundant. Away from the flow, the size of pumice clasts decreases, and within 100 m the sediments consist of fine pumice and ash. Other sediments nearby contain clasts of distinctive flow-banded rhyolite. Immediately to the south of Thousand Creek Gorge, Virgin Valley sediments abut against and are probably derived from the same lava flow as described above. The contact is poorly exposed, but sediments near the contact contain pumice blocks up to 50 cm in diameter.

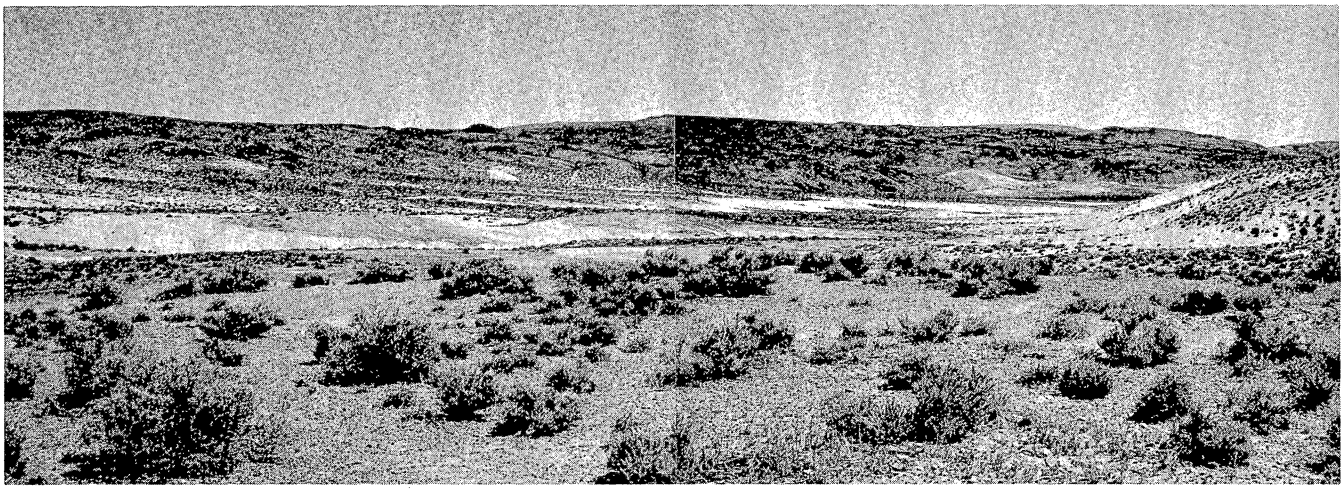

Figure 2. View to southeast across outcrop of Virgin Valley Formation to irregular surface of lava flows of Canyon Rhyolite. Ridge in distance is capped by ash-flow tuff member of Canyon Rhyolite. Sediments of Virgin Valley Formation in left center are derived from lava flows. At right a younger lava flow overlies sediments.

Immediately south of Thousand Creek Gorge, sediments of the Virgin Valley Formation appear to dip under a lava flow (fig. 2). Wendell mapped these sediments as Middle Miocene fluvial sequence. However, the lava flow appears to overlie the flow discussed above; although the sediments cannot be traced perfectly around to the sediments at location VV-15, they are apparently at the same stratigraphic level and are probably correlative. They are part of a continuous sedimentary sequence that was derived from and younger than one flow but overlain by and older than a later flow.

Sediments at location VV-15 were believed to be part of a lower member of the Virgin Valley Formation by both Fyock (1963) and Wendell (1970). Overlying parts of the Virgin Valley Formation thus should be distinctly younger than at least some of the Canyon Rhyolite lava flows. However, the lower member of the Canyon Rhyolite and the Virgin Valley Formation must overlap in age at least partly.

Canyon Rhyolite

Lava-Flow Member

Canyon Rhyolite lava flows form an irregular rim around the present Virgin Valley; the only outlet from the valley is through Thousand Creek Gorge, a deep canyon cut through the flows (fig. 3). The flows evidently were erupted from a high rim around the basin and flowed down into Virgin Valley. The best exposures are along the McGee Mountain - Big Mountain ridge (fig. 4), where the probably viscous lavas formed a series of pressure ridges generally perpendicular to the direction of flow. An aerial

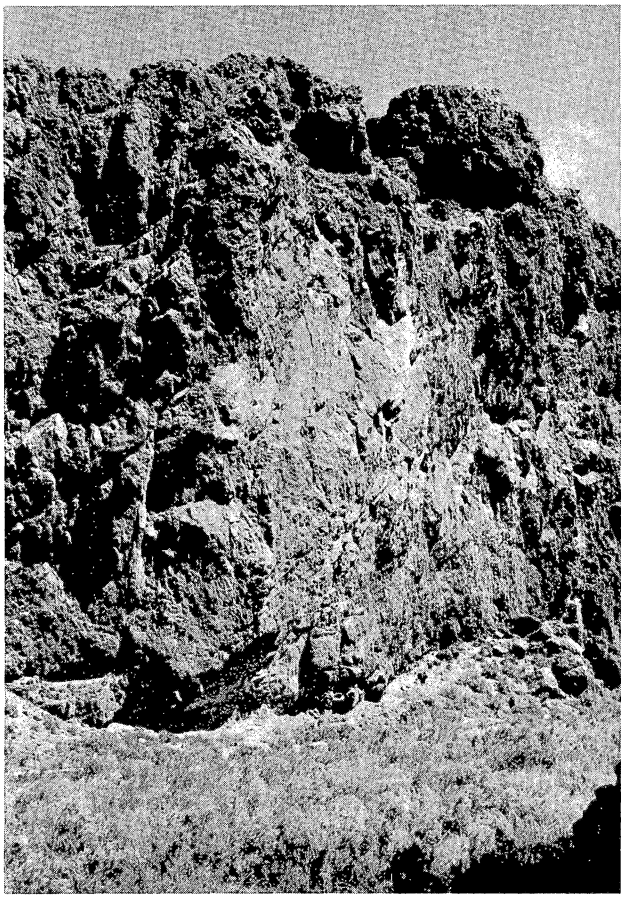

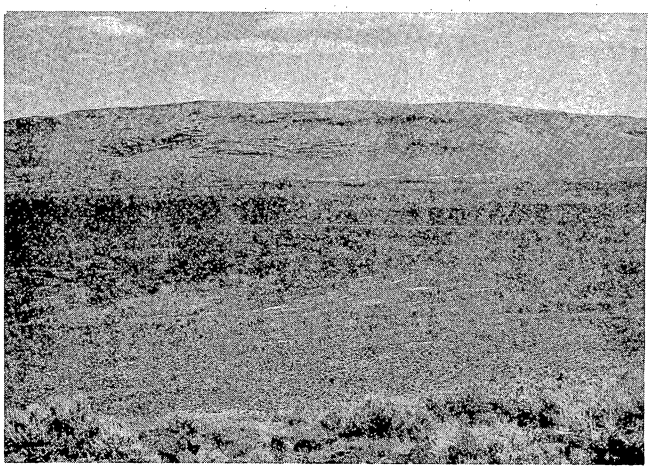

Figure 4. View to east of McGee Mountain capped by ash-flow tuff of Canyon Rhyolite dipping toward observer. Ash-flow tuff overlies lava flows of Canyon Rhyolite.

Figure 3. Outcrop of lava flow of Canyon Rhyolite in entrance to Thousand Creek Gorge. Outcrop is approximately 30 m thick.

photograph shown in Wilden (1964) and Wendell (1970) shows an exhumed lava flow that originated near the north end of McGee Mountain and flowed northwest into Virgin Valley. The flow forms two distinct lobate tongues with curved pressure ridges convex in the direction of flow. It is this flow that overlies tuffaceous sediments just south of the entrance to Thousand Creek Gorge. From the aerial photograph the flow also appears to overlie the flow that was the source of some Virgin Valley sediments at location VV-15. Other good exposures are in the southwest part of

the area in the headwaters of Virgin Creek and in the northwest where roadcuts along highway 8A provide good sections through the flow. Flows to the north, west, and south are largely covered by younger Mesa Basalt.

Lithology varies considerably within individual flows. Commonly the rock is reddish to pink; glassy, perlitic, or devitrified with spherulites; silicified; and flow banded or massive. A few percent quartz and sanidine in subequal amounts make up the phenocrysts. Contorted flow banding and breccias of the rhyolite in a fine-grained groundmass of rhyolite attest to the origin of the rock as a lava flow. Clasts in some of the breccias are rounded and partially grade into the groundmass suggesting high-temperature reassimilation. Different parts of single flows range from totally glassy to totally crystalline. Partly devitrified samples contain abundant spherulites of alkali feldspar and cristobalite aligned along flow bands. In places the rock is highly vesicular and even pumiceous. Thin sections of pumiceous parts show large, irregular shards unlike shards from ash-flow tuffs. Vesicles are irregularly shaped, lined with vapor-phase alkali feldspar and tridymite, and in places contain geopetal fillings of secondary silica (chalcedony and opal). The geopetal structures are all presently horizontal, indicating that no deformation has occurred since their formation.

McKee and Marvin (1974) reported K-Ar ages of 13.7, 16.3, and 22.3 million years of glass, sanidine, and alkali feldspar separates from a single sample of Canyon Rhyolite lava flow. From stratigraphic relations with the Idaho Canyon Tuff, they considered the 22-million-year age unlikely.

Ash-Flow Tuff Member

The ash-flow tuff member of the Canyon Rhyolite occurs only along the McGee Mountain - Big Mountain ridge in four large, separate outcrops capping the ridge (fig. 4). It extends to the south out of the area; otherwise, its distribution outside the area is unknown. The ash-flow tuff member distinctly overlies the lava-flow member of the Canyon Rhyolite, and north of McGee Mountain it overlies tuffaceous sediments mapped by Wendell as Middle Miocene fluvial sequence. Aerial photographs show that sediments there overlie Canyon Rhyolite lavas and are part of the Virgin Valley Formation. Wendell believed rhyolite clasts in the Thousand Creek Formation were derived from the ash-flow tuffs of the Canyon Rhyolite; we agree. Our interpretation of the volcanic history requires that the ash flow be contemporaneous with, and the source of, some of the ash of the Virgin Valley Formation. It may originally have blanketed the basin, but Noble and others (1970), who called it the Tuff of Big Mountain, indicate that its extent outside the immediate area was small.

A section of the ash-flow tuff member of the Canyon Rhyolite exposed south of McGee Mountain consists of a lower part composed of nonwelded ash-flow tuff and water-laid tuff and an upper part composed of a multiple-flow, simple cooling-unit, ash-flow tuff. The lower part includes several nonwelded ash-flow tuffs with clasts of pumice, obsidian, and rhyolite lava flow in a loose, ashy matrix. Clasts of pumice range up to 20 cm in diameter; rock fragments are somewhat smaller. There are a few small (less than 1 mm) sanidine phenocrysts. Laminated, tuffaceous

sediments, probably indicating local reworking, are interbedded with the tuffs.

The upper part consists of an ash-flow tuff that grades from nonwelded but indurated pumice tuff to welded tuff and then back into nonwelded pumice tuff. This sequence is a multiple-flow, simple cooling-unit, ash-flow tuff. The total number of individual flows is uncertain, but irregular breaks within the unit suggest several flows about 3 m thick (fig. 5). The presence of interbedded sediments within the lower ash flows shows that they are not part of the upper cooling unit. The lowest part of the welded tuff is gray, contains devitrified but unflattened pumice up to 2 cm diameter, lithophysal cavities, fewer than 1 percent sanidine phenocrysts to 1 mm, and sparse rocks fragments in a nonwelded groundmass. Welded parts grade from light red to purple with increase in welding and contain rhyolite lava-flow fragments to 5 mm, lithophysal cavities, many of which may replace the pumice, and a few percent chatoyant sanidine phenocrysts to 3 mm. Pumice within the welded parts is flattened and devitrified and increases in size upward. At the bottom of the welded zone pumice fragments are less than 2 cm long; at the top they are up to 5 cm long.

The nonwelded upper part is light gray, and contains fewer than 1 percent sanidine phenocrysts, fragments of rhyolite lava flows and perlite, and unflattened, undevitrified pumice fragments up to 30 cm in diameter.

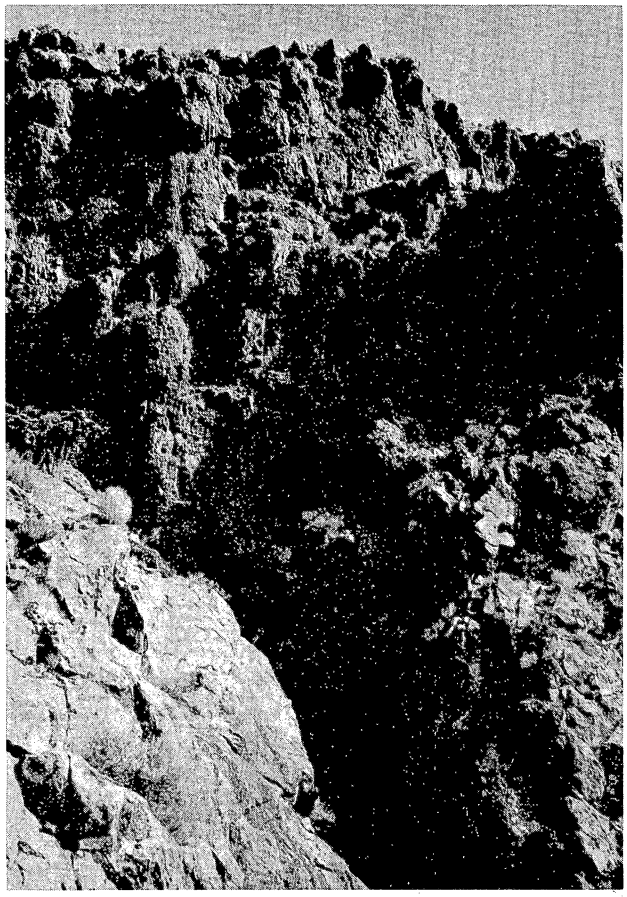

Figure 5. Ash-flow tuff of Canyon Rhyolite showing horizontal partings suggestive of several thin ash flows. Outcrop is approximately 20 m thick and comprises a single densely welded, devitrified cooling unit.

Virgin Valley Formation

Wendell (1970) divided the Virgin Valley Formation into a fluvial-eolian facies and a lacustrine facies and gave a total thickness of at least 375 m (1230 ft). The following discussion is based almost entirely on his work.

The lower part of the Virgin Valley Formation is dominantly fluvial-eolian, whereas the upper part is mostly lacustrine. The fluvial-eolian facies includes volcanic conglomerate, sandstone, and siltstone composed

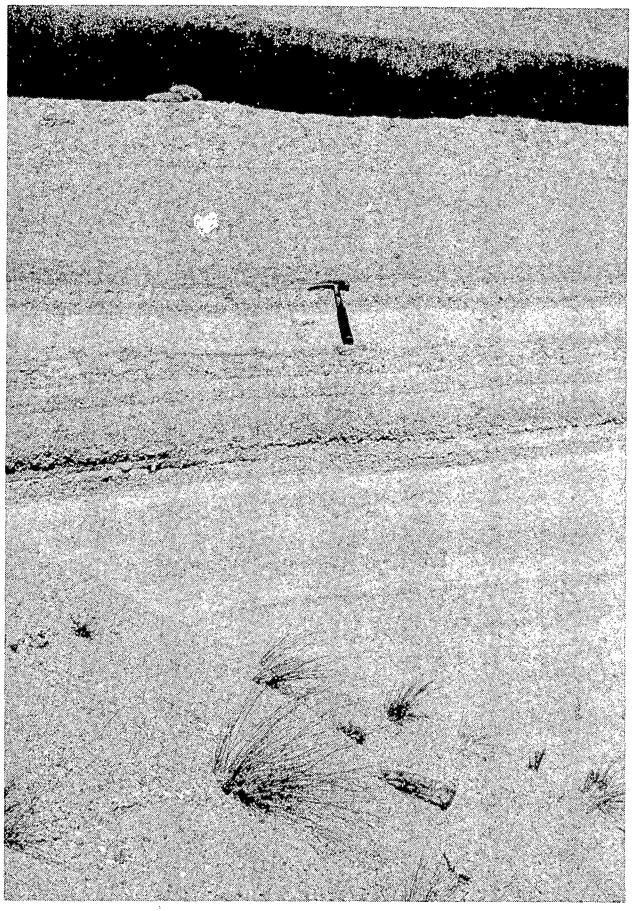

Figure 6. Sediments and possible air-fall tuff of Virgin Valley Formation composed of perlitic pumice fragments.

of pumice fragments and glass shards and minor mineral and rock fragments. Numerous air-fall tuffs are interbedded with the sediments (fig. 6). In the lower part of the formation the fluvial-eolian facies occurs around the edge of the basin and interfingers inward with the lacustrine facies. The lacustrine facies also contains volcanic sandstone and siltstone but includes mudstone, carbonaceous shale, lignite, and diatomite. Much of the vitric material is altered to montmorillonite, but the distribution of altered material was not indicated by Wendell.

The size of the lake in which the lacustrine facies was deposited fluctuated widely during early Virgin Valley sedimentation. During later sedimentation the lake was much larger, and lacustrine facies compose almost all of the upper part of the Virgin Valley Formation. According to Wendell, the diatom assemblage and rush and willow remains in lignite indicate that the lake contained fresh water.

Thousand Creek Formation

The Thousand Creek Formation is in depositional contact with Virgin Valley sediments and Canyon Rhyolite lava flows. Wendell's mapping and our work indicate that the Thousand Creek Formation is probably also younger than the ash-flow tuff member of the Canyon Rhyolite. The Thousand Creek Formation crops out within Virgin Valley almost exclusively below the Mesa Basalt which has protected it from erosion. East of Virgin Valley, it crops out extensively in Thousand Creek flats, the type locality as defined by Merriam (1910). The present distribution suggests that it once blanketed the area capping a surface with mostly little relief. An exception may be below the saddle between McGee Mountain and Big Mountain where Wendell mapped a tongue of Thousand Creek Formation resting on Middle Miocene fluvial sequence (Pre-Canyon Rhyolite tuffaceous sediment of this study). If identification of this unit is correct, it may represent filling of a channel cut deeply into the older rocks. Some outcrops of Canyon Rhyolite lava-flow and ash-flow tuff are above the general level of the Thousand Creek Formation, above even the Mesa Basalt surface, and probably stood up as isolated hills during deposition of the Thousand Creek Formation.

In the Thousand Creek flats area the formation has been downdropped along a major fault along the east side of McGee Mountain - Big Mountain. Neither the base nor any older units is exposed east of this fault.

The Thousand Creek Formation consists of a basal conglomerate overlain by volcanic sandstone and siltstone with interbedded air-fall tuff. The conglomerate contains clasts of rhyolite lava flows and ash-flow tuff identical to the Canyon Rhyolite in a matrix of volcanic sandstone composed of pumice and glass shards (Wendell, 1970). The conglomerate is interbedded with and grades vertically and laterally into fluvial sandstone. Interbedded volcanic siltstone and sandstone overlie the conglomeratic beds and compose the main body of the Thousand Creek Formation.

Mesa Basalt

The Mesa Basalt is the youngest volcanic rock of the area. It caps Big Spring, Gooch, and Rock Spring Tables, north, west, and south of Virgin Valley with flat upper surfaces that dip gently to the north and northeast. The Mesa Basalt may consist of a single, extensive lava flow deposited mostly on the flat upper surface of the Thousand Creek Formation. The Railroad Ridge basalt, which apparently fills an old stream channel east of the Virgin Valley, was regarded by Merriam (1910) as equivalent to the Mesa Basalt. The Mesa Basalt is vesicular and nonporphyritic. The groundmass consists of ophitic clinopyroxene and plagioclase with 10 percent iddingsitized olivine and about 1 percent opaque minerals.

Summary (Geologic History)

The sequence of events as shown by the rock types and locations we examined is as follows. Eruption of the older ash-flow tuff (Idaho Canyon Tuff) was followed by deposition of Pre-Canyon Rhyolite tuffaceous sediments (Wendell's Middle Miocene fluvial sequence). Eruption of lava flows of the Canyon Rhyolite followed, but sedimentation may have been continuous through the entire history of volcanic activity. Confusion over stratigraphy is largely due to a lack of recognition of this fact. Lava flows of the Canyon Rhyolite erupted from vents that formed a rough circle around the present Virgin Valley. Eruptions continued over a sufficient length of time that tuffaceous sediments of the Virgin Valley Formation were deposited between successive lava flows. At least some of the sediments were derived from the lava flows and associated pyroclastic material. The lava flows either created or enhanced a closed basin within which further sedimentation occurred; the lava flows did not fill the basin. Deposition of tuffaceous sediment and air-fall tuffs (Virgin Valley Formation) continued to fill the basin with a general progression of facies from coarser material at the edges to finer material, including lake beds, diatomites, and lignites in the middle. Eruption of the ash-flow tuff member of the Canyon Rhyolite must have occurred during this time, as clasts of welded tuff occur in overlying volcanic sediments. The ash-flow tuff and related pyroclastic eruptions were probably the source for much of the tuffaceous material in Virgin Valley. Continued ash-producing events nearby, depositing ash within the basin, are necessary to provide source material for the Virgin Valley Formation. The ash-

flow tuff is not exposed within Virgin Valley probably because of erosion of Virgin Valley and much of the tuffaceous sediments from within the basin prior to deposition of the Thousand Creek Formation. Eventually the closed basin was filled by sediment and/or breached by a headwardly eroding stream from outside the basin. The stream may have been located near Thousand Creek Gorge, the present outlet of Virgin Valley. As the rim of the basin was breached, erosion began to remove tuffaceous sediments from the basin. Later, for an unknown reason, erosion stopped, and the area was covered by the youngest volcanic sedimentary sequence (Thousand Creek Formation) with a basal conglomerate grading vertically and laterally into volcanic sandstones. Deposition of this unit was probably a more regional phenomenon unrelated to the local volcanic events that produced the older tuffaceous sediments, volcanic rocks, and enclosed basin of Virgin Valley. Deposition produced a nearly level plain upon which the Mesa Basalt lava flows were deposited. The area was cut by regional Basin and Range normal faults following eruption of the Mesa Basalt.

Volcano-Tectonic Setting

Understanding the volcanic setting of Virgin Valley may provide evidence bearing on the reasons for the occurrence of uranium deposits there, on the potential for finding additional deposits there, and on the potential for discovering deposits in other volcanic settings. Critical features which need to be explained are the great volume and thickness of volcanic rocks and volcaniclastic sediments, the circular arrangement of

the Canyon Rholite lava flows, and the origin of the closed basin within Virgin Valley.

A circular volcanic feature suggests a caldera, and a caldera model explains many of the features of Virgin Valley. Smith and Bailey (1968) described seven stages in a caldera's history: (1) regional tumescence from rising of magma, (2) ash-flow tuff eruption, (3) caldera collapse, (4) caldera filling with sediments and volcanic rocks, (5) resurgent doming with ring fracture volcanism, (6) ring fracture volcanism and continued filling of the caldera, and (7) fumarole and hot spring activity. Stages 4 through 7 commonly overlap, and in a complex caldera cycle events can be repeated. Some of these events could have occurred in Virgin Valley; clearly some have not, and for others the evidence is not well exposed.

The observed events in Virgin Valley could fall within stages 4 through 6 of caldera filling and ring fracture volcanism. By this model the Pre-Canyon Rhyolite tuffaceous sediments (Middle Miocene fluvial sequence of Wendell) could be early caldera filling of stage 4. Canyon Rhyolite lava flows represent ring fracture volcanism of stage 5 or 6, and the Virgin Valley Formation sediments and Canyon Rhyolite ash-flow tuff represent late filling and volcanic activity of the caldera.

Let us examine the evidence more carefully. Stage 1 regional tumescence is not evident. However, regional tumescence would be difficult to detect now as the area has been extensively deformed by later volcanic and tectonic activity, including Basin and Range faulting. More important, an older large ash-flow tuff (stage2) whose eruptions could have led to caldera collapse (stage 3) is highly speculative. A caldera-producing

ash-flow tuff would have to exist below the oldest tuffaceous sediments presumed to be caldera fill. The older ash-flow tuff (Idaho Canyon Tuff) is a possible candidate. Noble and others (1970) thought that it was erupted from the Virgin Valley area because the tuff thickens from the southeast and northwest toward Virgin Valley, and the valley is in the approximate center of its distribution. One problem with this interpretation is that the older ash-flow tuff is peralkaline, whereas later volcanic rocks are not. No peralkaline minerals occur in volcanic rocks of Virgin Valley, which should be genetically related to the older ash-flow tuff. Peralkaline and subalkaline silicic volcanic rocks are closely associated in both northern and southern Nevada, however (Noble, 1968; Noble and others, 1970). Also Gibson (1972) demonstrated that volatile alkali loss during ash-flow tuff eruption significantly reduced peralkalinity of post-caldera magmas compared to pre-caldera magmas. Available isotopic age control on the older ash-flow tuff and the Canyon Rhyolite lava flows allows them to be approximately the same age, as is required if they are both parts of caldera volcanism. Thus the early events of the postulated Virgin Valley caldera are not well documented, but the available evidence permits a caldera model and definitely does not disprove it.

Following eruption of the older ash-flow tuff, caldera collapse must have occurred along a series of ring fractures roughly beneath the Big - Mountain - McGee Mountain ridge and circling the valley as shown on figure 1. Canyon Rhyolite lava flows were discharged along this fracture system, are part of the evidence for the fractures, and aid in locating them.

Outcrops of the older ash-flow tuff mapped by Wendell are probably outside the caldera as the thickness remains relatively constant to the south. An ash flow should thicken considerably within a source caldera, so the older ash-flow tuff beneath Virgin Valley may be considerably thicker than where it is exposed.

Initial caldera filling may have been by the Pre-Canyon Rhyolite tuffaceous sediments. The source, transport directions, and depositional environment of this unit are relatively unknown.

Renewal of volcanic activity occurred when Canyon Rhyolite lava flows rose along ring fractures near the edge of the caldera and subsequently flowed out and down into the partly filled caldera. Aerial photographs in Willden (1964) and Wendell (1970) strikingly illustrate the lava flow aspect and show that the flows traveled from higher elevations along the proposed rim into Virgin Valley. Caldera boundary faults should be buried beneath these flows.

Virgin Valley became a closed basin following the eruption and deposition of Canyon Rhyolite lava flows. If the caldera model is correct, the basin was in existence even before this. Study of depositional facies in the Pre-Canyon Rhyolite tuffaceous sediments could resolve this uncertainty, but these rocks are exposed only along the edges of Virgin Valley. Within the basin they occur only in the subsurface.

Virgin Valley sediments were clearly deposited in a closed basin. Sedimentary facies change from relatively coarse fluvial deposits near the edge to finer sediments including lacustrine deposits and lignite within the center of the basin. Inward dips of 2^{o} to 6^{o} of Virgin Valley

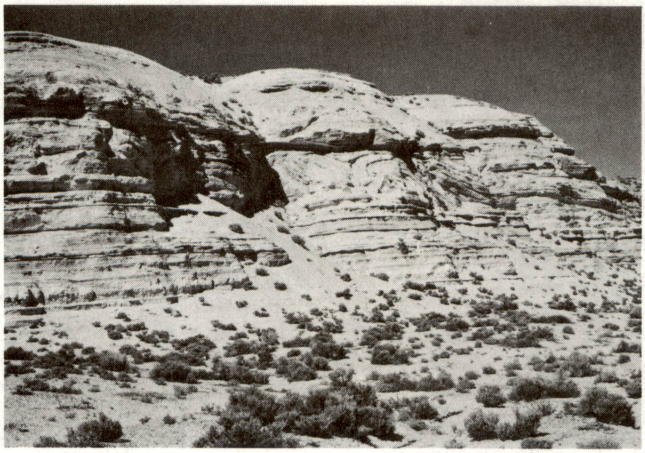

Figure 7. Sediments of Virgin Valley Formation showing soft-sediment deformation caused by slumping of poorly consolidated sediments. Thickness of deformed interval is approximately 4 m.

sediments were interpreted by Wendell (1970) as early folding. More likely they are primary sedimentary dips. Slump structures produced by soft-sediment deformation show that the dips existed immediately following deposition (fig. 7).

Deposition and pyroclastic activity continued concurrently, as indicated by air-fall tuffs and tuffaceous sediments interbedded within the Virgin Valley Formation. Ash-flow tuffs of the Canyon Rhyolite were probably erupted contemporaneously with sedimentation within Virgin Valley

and were probably the source of much of the sedimentary material. Without continued volcanic activity supplying easily erodible debris within the basin, it is unlikely that the basin could have been filled rapidly because the drainage area was very small. Total original extent and volume of the ash-flow tuff of Canyon Rhyolite is not known. The only large outcrop area is along the top of the McGee Mountain - Big Mountain ridge. Noble and others (1970) suggest an original coverage of less than 250 km^2 (100 mi^2). Wendell reports a maximum thickness of 60 m (197 ft) near the summit of McGee Mountain and states that it thins rapidly to the north and south. Preexisting topography may have been an important control on the thickness and distribution. Wendell believed that the ash-flow tuff was erupted from the summit of McGee Mountain because at that location it is thickest and most densely welded. Eruption from this area is consistent with the postulated location of caldera ring fractures. Canyon Rhyolite ash-flow could not have been volumetrically a major ash flow if it were erupted from the Virgin Valley area as there is no evidence for further caldera collapse following its eruption.

Two events of Smith and Bailey's caldera cycle, stage 5, resurgent doming, and state 7, fumarolic activity, are not clearly represented. Evidence for Miocene fumarolic or hot spring activity could be difficult to detect, but some alteration characteristics of rocks of the Virgin Valley area may indicate hot spring activity (discussed below). Resurgent doming clearly has not occurred at Virgin Valley. Smith and Bailey indicate that caldera diameter as it affects the ratio of thickness to diameter in the down-dropped block is a limiting factor on resurgence.

Only calderas greater than 16 km have resurgent domes. The postulated Virgin Valley caldera is approximately 20 km in diameter and may have been too small for resurgence.

Purely caldera-related events ended when caldera-related volcanism and most caldera filling terminated, and breaching of the caldera rim and initiation of erosion of the Virgin Valley Formation began. Subsequently the area was covered by late volcanic sediments of the Thousand Creek Formation. The source, origin, and relationship to volcanism of the Thousand Creek Formation is unknown, but it is probably a distinctly separate event unrelated to the Virgin Valley caldera. Deposition of the Mesa Basalt and Basin and Range faulting followed still later. It may be significant that the normal fault bordering the east side of McGee Mountain and Big Mountain curves from a northwest trend to a northeast trend and closely follows the postulated caldera ring fractures. Although the sense of displacement is opposite to the supposed caldera faults, the location of the fault may be controlled by the preexisting zones of weakness.

The caldera model for Virgin Valley is clearly incomplete. Previous mapping by Wendell was not aimed at discovering a caldera, and our brief reconnaissance left many uncertainties. Nevertheless, it is difficult to explain the circular rim of Canyon Rhyolite, the closed basin, and the great volume of tuffaceous material within the basin by any other mechanism.

URANIUM GEOLOGY

Uraniferous Opal Beds

Uranium deposits have been described in several reports, the most thorough being by Staatz and Bauer (1951). Later reports by Garside (1973) and Cupp and others (1977), add some additional information but are based largely on the earlier report. The brief discussion presented here is derived from all three and from our investigation. Uranium occurs in opal beds both east and west of Virgin Creek in the upper part of the Virgin Valley Formation. Grade is variable ranging from background concentrations up to 0.12 percent. The opal beds consist of thin discontinuous lenses interbedded with air-fall tuff, tuffaceous sediment, and diatomite probably deposited in a lacustrine environment (fig. 8). Individual opal beds are up to a meter thick and as much as 300 m long. The opal resulted from replacement of tuff, tuffaceous sediment, and diatomite. The opalized material grades from mildly silicified to totally opalized; in places opal grades perceptibly into unopalized "ash." The opal is variable in coloration and internal structure.

Uranium is present both as individual uranium minerals and as disseminations in opal. Carnotite and possibly schroeckingerite occur coating fractures, but in some opal no uranium minerals can be identified. In these opals the uranium is finely disseminated uranium minerals. Most if not all of the uranium may have originally been disseminated in opal with the crystalline forms resulting entirely from later remobilization.

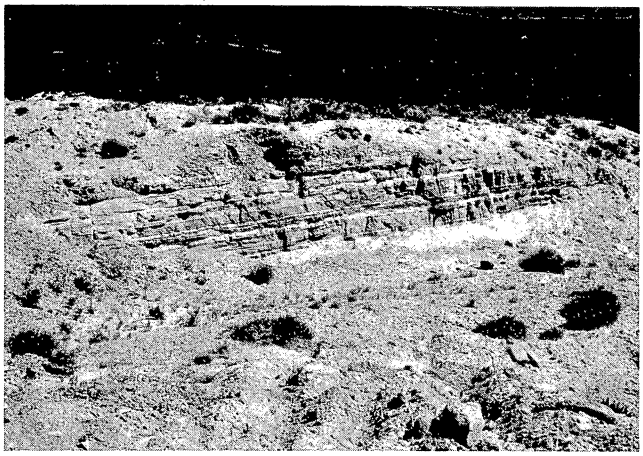

Figure 8. Opal beds interbedded with perlitic pumice and white diatomite.

Sources, Migration, and Concentration of Uranium

Primary Uranium Concentration

Canyon Rhyolite--Ash-Flow Tuff Member

Samples of the ash-flow tuff member of the Canyon Rhyolite (VV-19 series) are arranged in reverse stratigraphic order in table 2. Thus VV-19a is from the base of the tuff; VV-19g and VV-19h are from the top. There is no stratigraphic significance to the order of other samples.

Table 2. Uranium concentrations and alteration of rocks from Virgin Valley, Nevada.

Sample No.	Formation	Rock Type	Mineral Assemblage or Alteration	Uranium Concentration (ppm)
VV-1a	Virgin Valley Formation	Tuff	Opal and clinoptilolite	440
VV-1d	Virgin Valley Formation	Opal	Opal	510
VV-2a	Virgin Valley Formation	Pumice tuff	Hydrated glass	6.3
VV-5a	Canyon Rhyolite	Lava flow	Hydrated glass	8.7
VV-5b	Canyon Rhyolite	Lava flow	Devitrified, minor opal	7.0
VV-5c	Canyon Rhyolite	Lava flow	Devitrified, minor opal	8.3
VV-9	Canyon Rhyolite	Rhyolite dike	Devitrified	6.0
VV-11a	Canyon Rhyolite	Lava flow	Devitrified, vapor phase and opal	11
VV-11b	Canyon Rhyolite	Lava flow	Devitrified, vapor phase and opal	19
VV-11c	Canyon Rhyolite	Lava flow	Devitrified, vapor phase	8.2
VV-14a	Canyon Rhyolite	Lava flow	Devitrified	7.2
VV-15b	Canyon Rhyolite	Lava flow	Glass with opal	18
VV-18a	Idaho Canyon Tuff	Ash-flow tuff	Devitrified, vapor phase	7.5
VV-19a	Canyon Rhyolite	Ash-flow tuff	Glass	7.9
VV-19b	Canyon Rhyolite	Ash-flow tuff	Glass	7.1
VV-19c	Canyon Rhyolite	Ash-flow tuff	Devitrified, vapor phase	7.8
VV-19d	Canyon Rhyolite	Ash-flow tuff	Devitrified, vapor phase and opal	14
VV-19e	Canyon Rhyolite	Ash-flow tuff	Devitrified, vapor phase	6.7
VV-19f	Canyon Rhyolite	Ash-flow tuff	Devitrified, vapor phase and opal	16
VV-19g	Canyon Rhyolite	Ash-flow tuff	Glass	7.6
VV-19h	Canyon Rhyolite	Ash-flow tuff - pumice	Glass	8.6
VV-20a	Canyon Rhyolite	Lava flow	Devitrified, vapor phase	8.2

Four of eight samples from the Canyon Rhyolite ash-flow tuff (VV-19) are still glassy. Uranium concentrations of these samples fall in a narrow range from 7.1 to 8.6 ppm (table 2). The small variation could result entirely from minor analytical imprecision, but differences in amount of dilution with non-uranium-bearing rock and crystal fragments could also be important. A primary uranium concentration around 8 ppm seems well established.

A significant point about these concentrations is that there is little vertical variation in uranium concentration through this complex ash-flow sheet composed of several ash flows and at least two separate cooling units. In addition, any variation is due to the higher uranium concentration of a single pumice fragment (VV-19h). Samples VV-19a and VV-19b are from two nonwelded ash flows, separate cooling units below the thick welded cooling unit. Their uranium concentrations overlap with the uranium concentration of VV-19g, a sample from the upper nonwelded part of the main cooling unit. There was apparently little variation in uranium concentration among several eruptions.

Only one sample of the peralkaline Idaho Canyon Tuff was collected and analyzed. The devitrified sample was 7.5 ppm uranium. Because it is a single devitrified sample, with extensive vapor-phase crystallization, little can be said about its primary concentration or depletion or enrichment. However, the sample is probably genetically related to the other volcanic rocks of Virgin Valley, and its uranium concentration is similar to that of glassy Canyon Rhyolite samples. Its primary concentration may be 7.5 ppm.

Canyon Rhyolite--Lava-Flow Member

The primary uranium concentration of Canyon Rhyolite lava flows can be determined both from the single hydrated, undevitrified sample and also from the consistency of uranium concentrations of some devitrified samples. The perlite sample (VV-5a) contains 8.7 ppm uranium. Several devitrified samples (VV-5b, VV-5c, VV-11c, VV-14a, and VV-20a) that apparently have undergone no significant enrichment or depletion contain 7.0 to 8.3 ppm uranium. These samples are from four different flows within the Canyon Rhyolite. The uranium concentrations are remarkably consistent and are identical to primary uranium concentrations in the Canyon Rhyolite ash-flow tuff.

Sample VV-15b is also glassy but also contains considerable secondary opal coating glass shards in an apparent flow breccia. For reasons discussed more fully below, its uranium concentration of 18 ppm definitely represents enrichment from its primary concentration.

Cupp and others (1977) analyzed three rhyolite samples that contain 6, 11, and 27 ppm uranium. They did not state whether the rhyolites were lava flows or ash-flow tuffs. Based on the results of this study, the sample containing 27 ppm has probably been enriched in uranium; the sample containing 11 ppm may also have been enriched.

Virgin Valley Formation

Perlitized pumice (VV-2a) from the Virgin Valley Formation at one of the opal mines contains 6.3 ppm uranium. All rocks from the Virgin Valley Formation should be genetically related to the Canyon Rhyolite lava and ash flows. Direct comparison of the uranium concentration of VV-2a with

those of the flow rocks, however, is inappropriate for determining minor enrichment or depletion. Nevertheless, the genetic relationship and the similarity in uranium concentration shows that rocks of the Virgin Valley Formation contain high primary uranium concentrations similar to those of the Canyon Rhyolite. Unmineralized Virgin Valley Formation samples collected by Cupp and others (1977) contained 2, 5, and 9 ppm uranium. The sample containing 2 ppm is a claystone and, as will be shown, is probably depleted. The other two samples may be more representative of primary concentrations.

Alteration and Uranium Concentration

Canyon Rhyolite--Ash-Flow Tuff Member

The Canyon Rhyolite ash-flow tuff shows a complete range from densely welded to nonwelded and from glassy to devitrified including vapor-phase crystallization. The glassy samples that were used to determine the primary uranium concentration include (1) VV-19a and VV-19g (fig. 9), which show minor solution and devitrification of glass at the edges of some shards; (2) VV-19b, which shows more extensive (but still minor) devitrification with development of some plumose quartz and alkali feldspar aggregates; and (3) VV-19h, which shows no evidence of devitrification. Among the totally devitrified samples VV-19c is poorly welded, and VV-19d, VV-19e, and VV-19f are densely welded. All are totally devitrified and have undergone moderate vapor-phase crystallization of the groundmass. However, axiolitic and spherulitic devitrification textures are preserved and mafic minerals are not totally oxidized. Pumice fragments in all four samples have undergone extensive vapor-phase crystallization with the

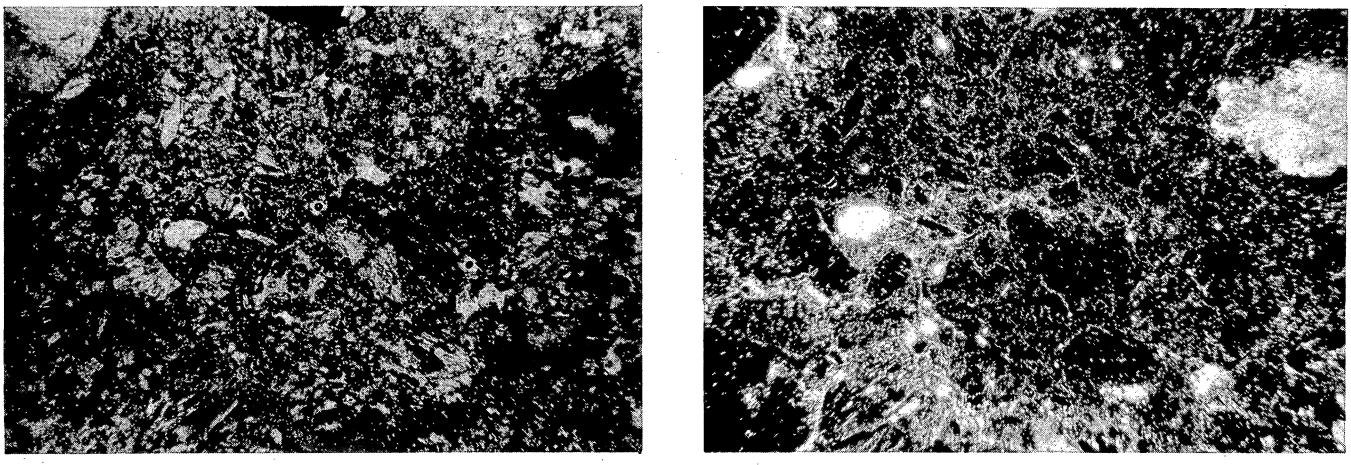

Figure 9. Sample VV-19g. Ash-flow tuff of Canyon Rhyolite. Nonwelded undevitrified ash-flow tuff composed of glass shards, pumice fragments, rock fragments, and phenocrysts. Note thin coating of birefringent montmorillonite? over isotropic glass. Long dimension is approximately 3 mm.

formation of coarse aggregates of quartz and alkali feldspar. Cavities have discontinuous linings of tridymite and alkali feldspar formed at high temperature.

Samples VV-19d and VV-19f also have cavity linings of opal and minor chalcedony (fig. 10). Sample VV-19d has two distinct layers of opal with a final filling of chalcedony in some cavities; VV-19f has several layers of opal separated by a discontinuous layer of chalcedony along with a final filling of chalcedony.

Chalcedony and opal are petrographically distinct. Opal occurs as lightly to darkly colored, colloform coatings of uniform thickness;

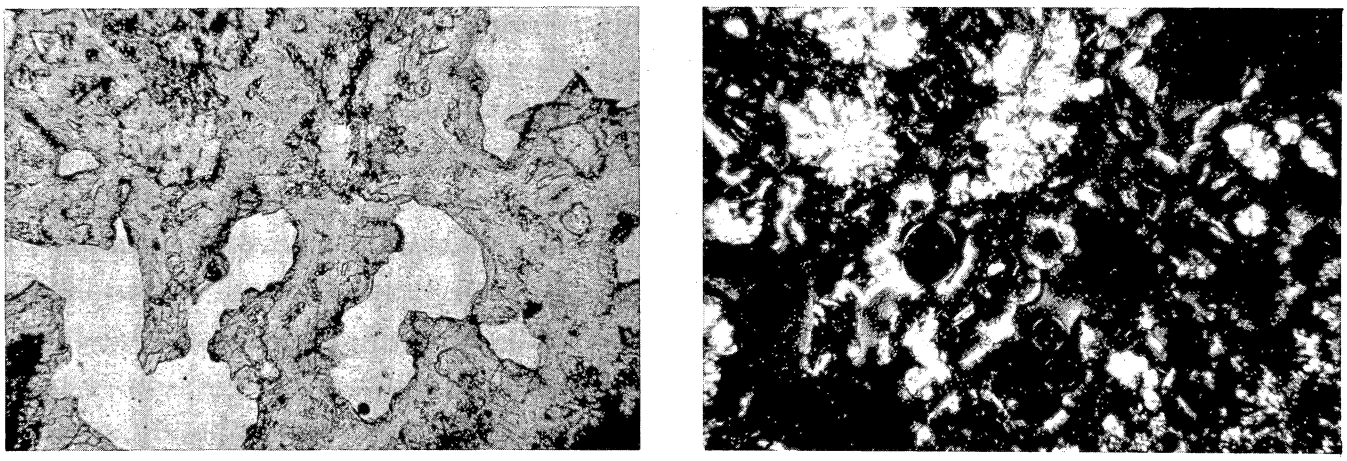

Figure 10. Sample VV-19d. Ash-flow tuff of Canyon Rhyolite. Massive opal coating cavity with devitrification products. Note birefringence of some opal under crossed nicols. Long dimension is approximately 3 mm.

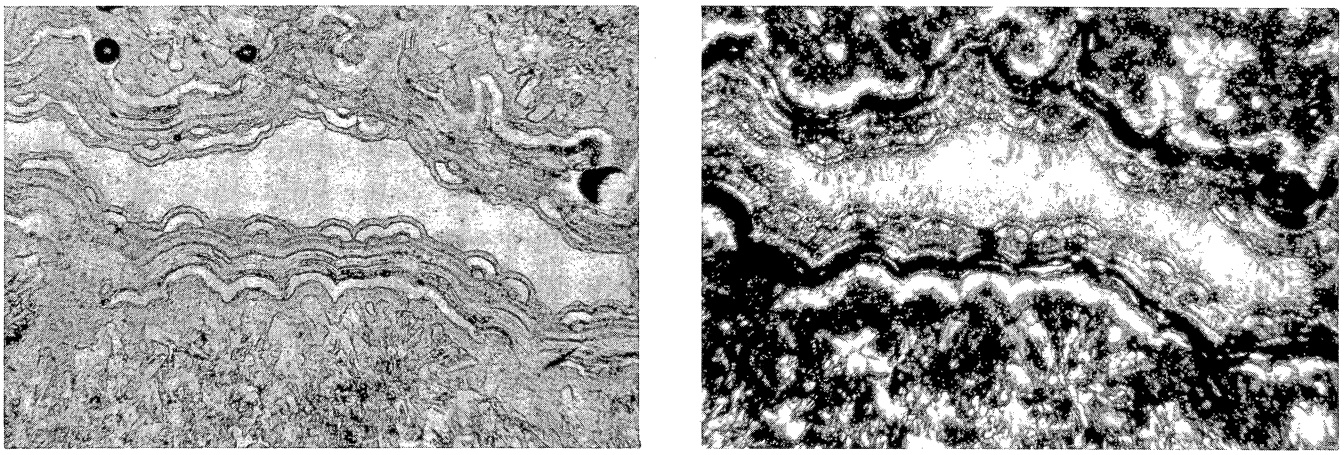

Figure 11. Sample VV-19f. Ash-flow tuff of Canyon Rhyolite. Opal, chalcedony, and quartz filling cavity with tridymite and alkali feldspar devitrification products. Opal precipitated first but is also interlayered with several discontinuous layers of chalcedony. Final filling is by fibrous chalcedony and small area of granular quartz in center. Note difference in relief between opal (high) and chalcedony (low) and birefringence of some opal. Long dimension is approximately 2.5 mm.

wherever opal occurs it completely coats a cavity. Some opal coatings have no observable internal structure, whereas others are fibrous. Chalcedony is colorless and much lower in relief than opal and does not form complete coatings. It occurs as discontinuous, almost spherulitic growths between opal layers and as large irregular fibrous masses completely filling in a cavity. In one cavity in VV-19f small (<.1 mm) quartz grains are the final filling following chalcedony (fig. 11).

Most opal is isotropic, and all chalcedony is distinctly birefringent. However, some material that has all other characteristics of opal is weakly birefringent although the birefringence is much lower than that of chalcedony. This material may represent partial conversion, or a step in the conversion, of opal to another silica mineral, either chalcedony or cristobalite. Samples VV-19c and VV-19e are identical to VV-19d and VV-19f with the exception that the former have no secondary siliceous cavity fillings (fig. 12).

Uranium concentration of the devitrified rocks shows a distinct pattern. Samples VV-19c and VV-19e, which are devitrified with some vapor-phase crystallization but with no secondary silica, contain 7.8 and 6.7 ppm uranium respectively, similar to undevitrified rocks. Samples VV-19d and VV-19f, which also contain opal and chalcedony, have 14 and 16 ppm uranium. Clearly the latter two are enriched in uranium, and the enrichment is somehow related to the presence of opal or chalcedony. By analogy with the uraniferous opal deposits, the uranium is probably within the opal. Uranium has apparently not been depleted from VV-19c or VV-19 to supply the uranium concentrated in VV-19d or VV-19f. Thus high-

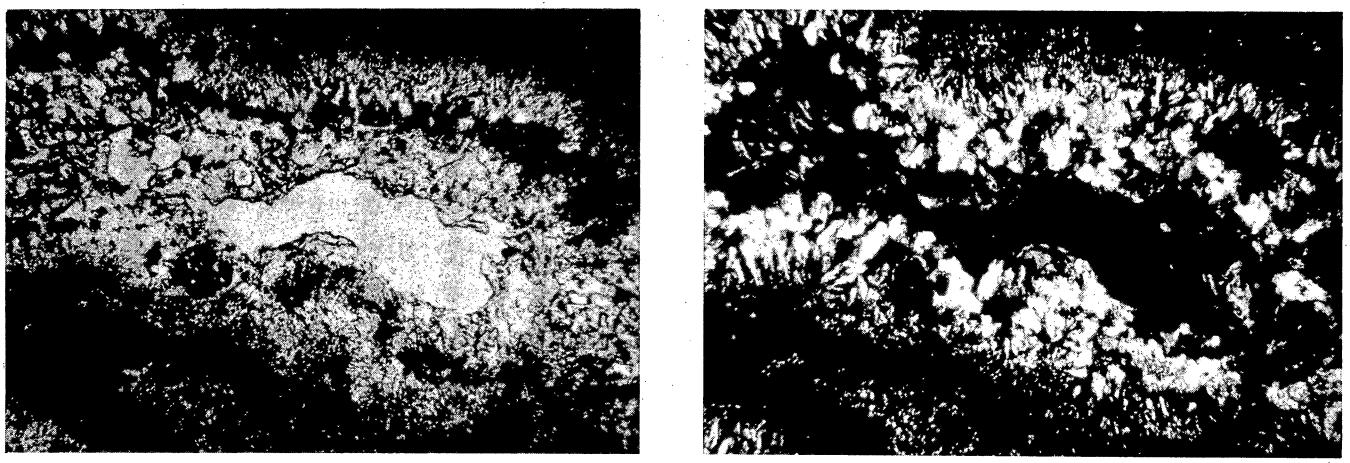

Figure 12. Sample VV-19e. Ash-flow tuff of Canyon Rhyolite. Lithophysal cavity lined with devitrification products but without secondary silica. Long dimension is approximately 2.5 mm.

temperature devitrification and vapor-phase crystallization is an unlikely source for the uranium or secondary silica. Some other process must be supplying these additional constituents. Vapor-phase crystallization is not extensive in the groundmass of these samples. Although vapor-phase crystallization has not affected the uranium concentration here, it is possible that more extensive vapor-phase separation could do so.

Canyon Rhyolite--Lava Flow Member

A very similar pattern of alteration and uranium concentration exists in samples of Canyon Rhyolite lava flow. The one glassy sample (VV-5a) is perlitized with minor devitrification balls (spherulites) and devitrification lenses parallel to flow banding (fig. 13).

Devitrified samples (for example VV-5b and VV-11c) have abundant spherulitic intergrowths and lenses which also follow banding. Different samples show a wide variety of devitrification textures, including spherulites, lenses or trains of spherulites, fine and coarse plumose intergrowths, and irregular intergrowths (fig. 14). The only difference between devitrification in these samples and devitrification in VV-5a is that these samples are totally devitrified. Numerous cavities have formed along and parallel to flow bands in banded rocks or randomly in nonbanded rocks. The cavities are lined with alkali feldspar and tridymite and are probably analogous to the lithophysal cavities of ash-flow tuffs. Volatiles released during devitrification formed pore spaces or were entrapped in existing cavities. Thus devitrification and vapor-phase crystallization were as well developed in these lavas as in the ash-flow tuffs.

Cavity fillings of opal with or without chalcedony are abundant in two devitrified samples VV-11a and VV-11b (fig. 15), and are present to a minor degree in VV-5b and VV-5c. Texturally the opal is similar to opal in the VV-19 samples; it lines cavities and coats vapor-phase minerals. High negative relief but slightly birefringent opal, similar to the birefringent opal of the VV-19 samples, is also present. X-ray patterns show that opal in VV-11b is opal CT (Jones and Segnit, 1971). Chalcedony is a

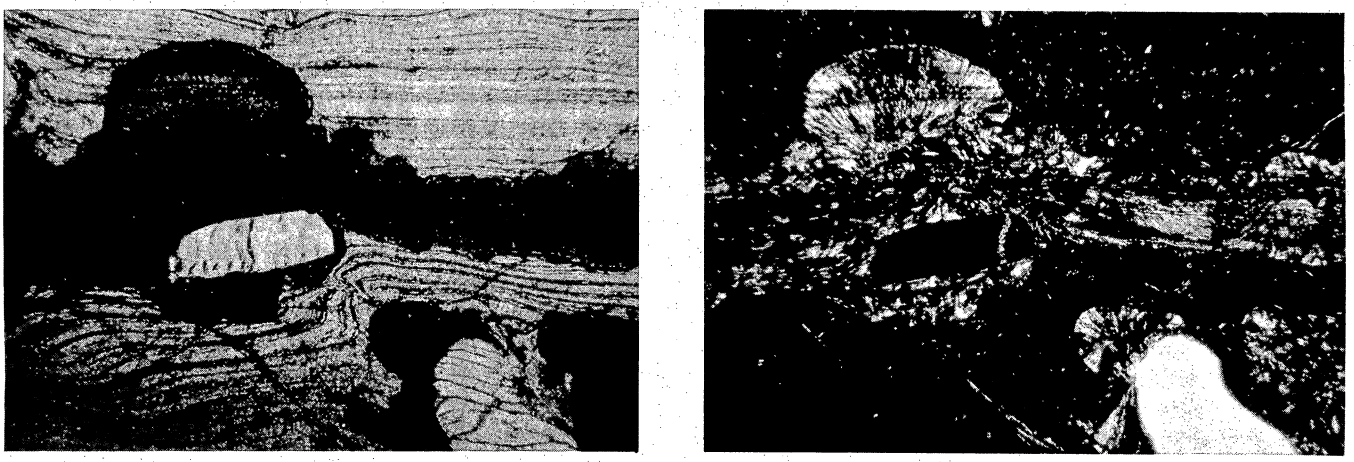

Figure 13. Sample VV-5a. Lava flow of Canyon Rhyolite. Partial spherulitic devitrification of flow-banded rhyolite. Long dimension is approximately 2.5 mm.

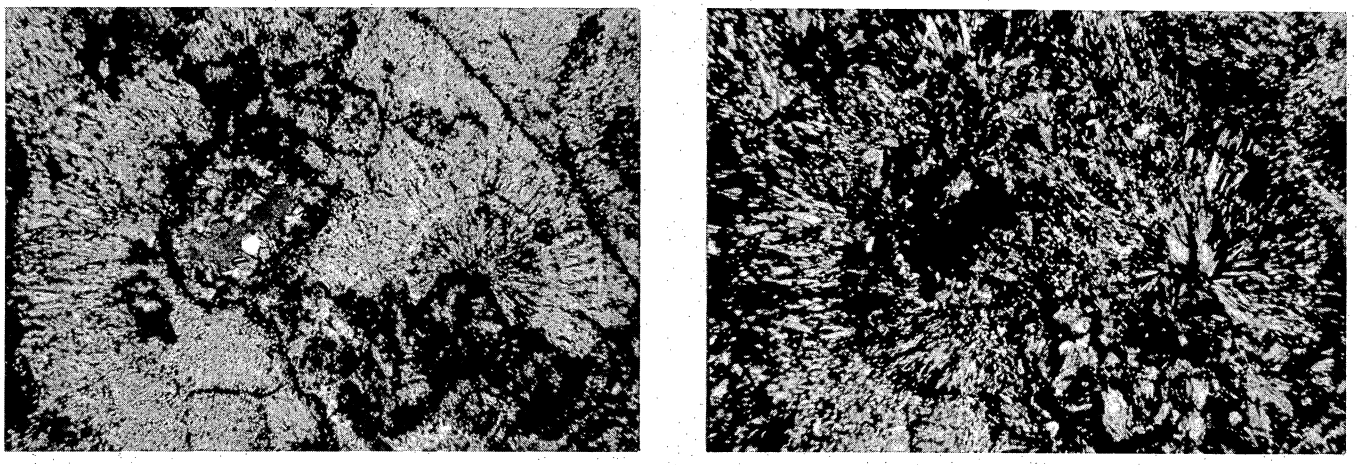

Figure 14. Sample VV-11c. Lava flow of Canyon Rhyolite. Spherulitic devitrification and vapor-phase crystallization of lava flow. Note lack of secondary silica filling of cavity. Long dimension is approximately 3 mm.

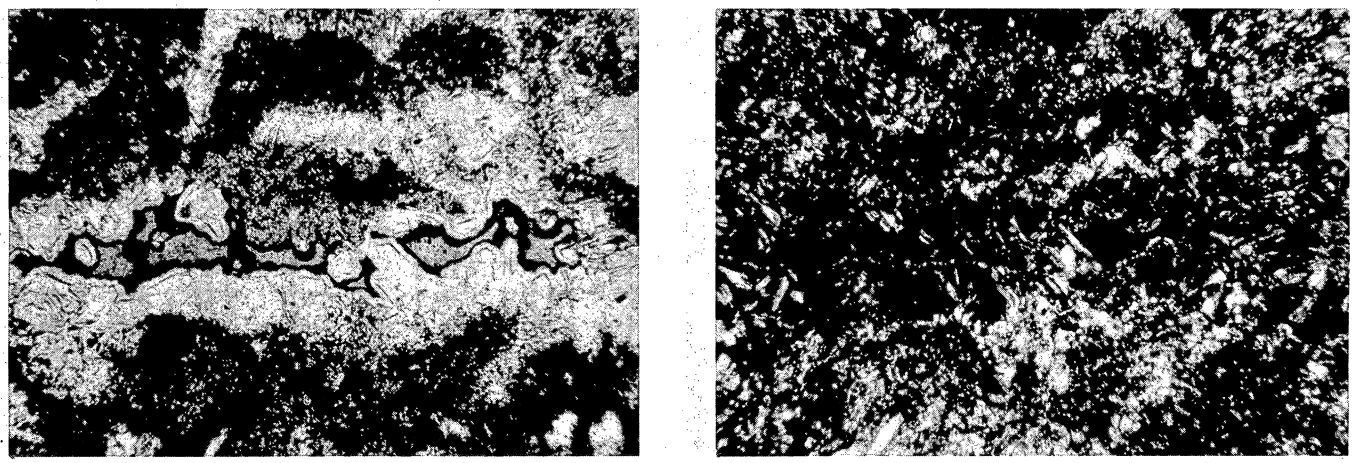

Figure 15. Sample VV-11a. Lava flow of Canyon Rhyolite. Lithophysal cavity in devitrified rhyolite with thin coating of partially birefringent opal over tridymite and alkali feldspar. Long dimension is approximately 2.5 mm.

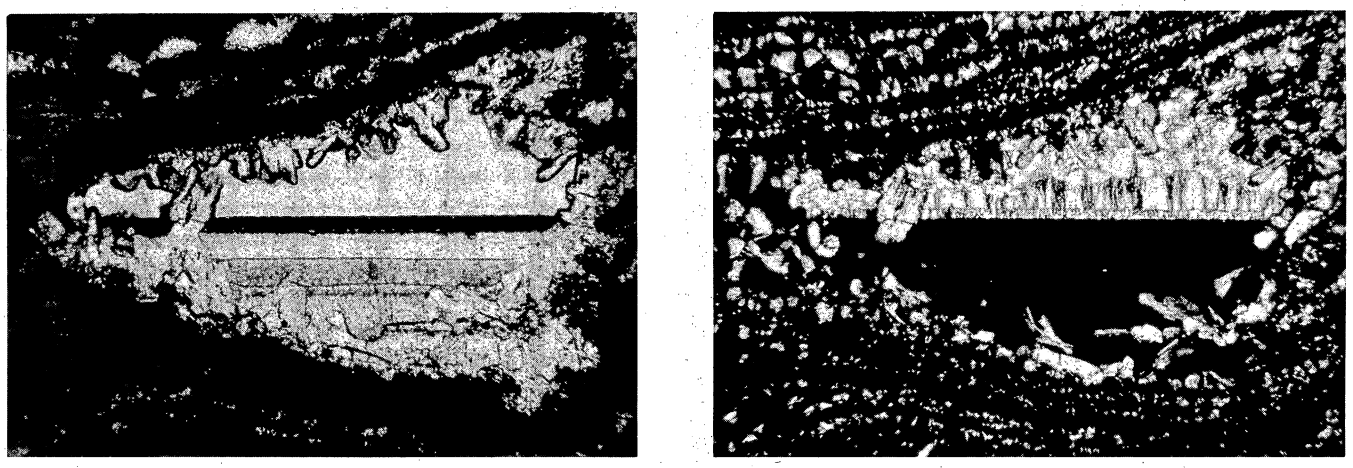

Figure 16. Sample VV-5b. Lava flow of Canyon Rhyolite. Geopetal structure of several layers of opal and final filling of chalcedony in lithophysal cavity in spherulitically devitrified, flow-banded rhyolite. Long dimension is approximately 2.5 mm.

final filling in all of the samples, and in VV-5b and VV-5c it is the dominant silica phase. Opal is present but is not abundant in either of these latter samples, although in VV-5b it forms spectacular geopetal structures (fig. 16). Opal also occurs in the birefringent form and in nearly opaque masses in VV-5b and VV-5c. Sample VV-15b, although almost entirely undevitrified, has opal coatings of glass shards and large (.5 mm) balls of birefringent opal. The lava-flow samples containing opal show several generations of precipitation of opal and chalcedony similar to that in ash-flow tuff samples.

Also similar to the VV-19 samples, uranium concentration is distinctly higher in rocks with abundant opal. Samples VV-11a and VV-11b contain 11 and 19 ppm, and VV-15b contains 18 ppm uranium, all well above the primary concentration of 8 ppm. Samples without opal (fig. 14) all contain about 8 ppm uranium; this concentration indicated that neither enrichment nor depletion has occurred. Samples VV-5b and VV-5c do not entirely follow this pattern. Both contain opal and chalcedony, but neither is enriched in uranium. Neither sample contains as much opal as the other opalized samples, and in both much of the opal is the opaque form; most of the secondary silica in each is chalcedony. It is possible that uranium is not concentrated with chalcedony and that the amount of uraniferous opal is insufficient in these samples to affect the uranium concentration appreciably. Alternatively not all forms of opal are enriched uranium. A complete explanation of this discrepancy is obviously important.

Virgin Valley Formation

Sample VV-1a (440 ppm uranium) is from an opalized tuff bed within the Virgin Valley Formation. The origin of the rock, its contained mineral assemblage, and its uranium concentration are important to understanding the formation of uraniferous opal deposits in both the sedimentary and volcanic rocks of Virgin Valley. The rock contains pumice and ash fragments in a probably crystalline ashy groundmass. The origin of the tuff is uncertain because extensive opalization obscures some of the primary features. It could be air-fall and ash-flow tuff or reworked tuffaceous sediment. Spherulites in both pumice fragments and in groundmass and sparse quartz-alkali feldspar intergrowths suggest emplacement and devitrification at high temperature. However, x-ray data show that quartz and alkali feldspar are at most minor components of the rock.

Abundant low relief and low birefringent, rectangular and wedge-shaped grains in the groundmass and lining cavities were originally thought to be tridymite, which would have made a high-temperature origin of the rock certain. However, x-ray data show that most of the material is clinoptilolite; the presence of a separate tridymite phase cannot be determined because the opal form is opal CT which also gives a tridymite pattern. Tridymite cannot be a major phase, however, because it is only a minor component on the x-ray pattern. Sample VV-1a may also contain Na-montmorillonite because a barely discernible x-ray peak occurred at the appropriate D-spacing. Montmorillonite was not observed in thin section, however. Opal coats clinoptilolite and walls of cavities, filling in and, in places, totally eliminating original pore space (fig. 17).

Figure 17. Sample VV-1a. Opal bed in Virgin Valley Formation. Thin coating of opal over laths of clinoptilolite. Long dimension is approximately 0.8 mm.

Much of the opal shows the slight birefringence observed in the volcanic samples, but, again, in all other respects it has the characteristics of opal. X-ray patterns of VV-1a show no quartz (chalcedony) peak. Primary chalcedony is present but only as a sparse final filling in a few cavities. Note enough occurs to show on x-ray patterns.

Sample VV-1a contains far more uranium than any of the volcanic rocks discussed previously. However, it also contains far more opal; so the uranium concentration actually in opal may be no greater than uranium in opal in the volcanic rocks. Because the opal occurrence in this sample is so similar to the opal occurrences in the volcanic rocks,

it is almost certain that the opal and contained uranium formed by similar processes in each. Samples containing primary chalcedony only are not enriched in uranium; the process that concentrates uranium is apparently tied specifically to the formation of opal. The conversion of opal to chalcedony involves a solution - redeposition mechanism (Keith and others, 1978) that may release uranium. This mechanism could account for the presence of secondary uranium minerals coating opal.

Origin of Uraniferous Opal

The mechanism by which the uraniferous opal forms is critical in determining where similar or larger deposits could form in volcanic rocks and volcaniclastic sediments. The first question is whether or not the uraniferous opal occurrences in Canyon Rhyolite lava flows and ash-flow tuffs and occurrences in the Virgin Valley Formation formed by the same process.

Opal in the volcanic rocks coats high-temperature devitrification products and is followed by or interlayered with chalcedony. Thus its temperature of formation could fall within a wide range from near devitrification temperatures to surface temperatures. However, at devitrification temperatures, quartz, cristobalite, or tridymite are the universal silica phases. Also, opal in the volcanic rocks is not uniformly dispersed through devitrified rock. In fact in a vertical section through the Canyon Rhyolite ash-flow tuff (VV-19) opal occurs in at least two layers separated by nonopalized tuff. If the formation

of opal were intimately connected with devitrification, it would probably occur almost universally in devitrified rocks. The distribution of opal formed from silica and uranium-enriched ground water derived from low- to moderate-temperature alteration of overlying glass would be controlled by the permeability of already devitrified rocks; the opal could be scattered more irregularly through the rock.

Opal in the tuffaceous sediments is more obviously low-temperature in origin. Opal replaces diatomite, which clearly was cold at the time of formation. Opal also coats clinoptilolite and probably was formed as a part of the same process that precipitated the zeolite. Montmorillonite was not definitely found during this study but is reported by Wendell (1970) as occurring in sediments of the Virgin Valley Formation. Clinoptilolite and montmorillonite are associated low-temperature minerals formed by diagenesis, although clinoptilolite may also form during burial metamorphism (Boles, 1977) or by alteration from hot spring waters (Keith and Muffler, 1978).

Another argument against high-temperature deposition of the uranium is the lack of uranium depletion in samples of devitrified ash-flow tuff and lava. Because some rocks are clearly enriched, some others must be depleted. Slight depletion of a large volume of rock could supply sufficient uranium to produce observed deposits in the volcanic rocks and might not be detectable considering analytical limitations and minor uncertainty in the primary uranium concentration. However, if devitrification had released a large portion of the uranium originally in glass, then some of the samples should have measurable depletion. It could be

argued that depleted, devitrified rocks were simply not sampled. It seems fortuitous, however, that of 17 analyzed samples of Canyon Rhyolite none show depletion although 5 show enrichment. Formerly glassy rocks now altered to clay were not sampled in this study, so depletion in these rocks cannot be evaluated. However, Cupp and others (1977) determined a uranium concentration of 2 ppm for a claystone presumably from the Virgin Valley Formation. The low uranium concentration of this sample indicates that it has been depleted. At every known occurrence of uraniferous opal, glassy volcanic rocks or tuffaceous sediments are associated with the opal-bearing rocks. Sample VV-19g, from the upper undevitrified part of the Canyon Rhyolite ash-flow tuff, has thin birefringent coatings on glass shards. The coatings are too small to be identified positively but appear to be montmorillonite and show that some solution of glass has occurred. Nevertheless, more extensive sampling and analysis of altered glass is necessary to confirm that alteration releases uranium.

The probable origin of the uraniferous opal in both flow rocks and tuffaceous sediments is solution of glass by low- to moderate-temperature ground water and deposition of opal from the water. Opal can occur with or without montmorillonite or clinoptilolite in rocks altered by either low (approximately 25^{o}C) or moderate (up to 150^{o}C) water dependent upon the chemical evolution of the water (Walton, 1975; Keith and others, 1978). In the flow rocks, alteration evidently was in an early stage, and opal occurs alone; in the sediments, alteration had progressed to a greater degree, and opal occurs with abundant clinoptilolite and montmorillonite.

Alteration by either hot or cold ground water occurred early in the history of the basin. Hot spring activity would be restricted to the active period of the caldera or to a period of cooling of buried igneous rocks immediately following the active period (stage 7 of the caldera model of Smith and Bailey, 1968). Within a few million years all residual heat would be depleted and hot spring activity would cease.

Deposition of Virgin Valley Formation sediments was also restricted to the active period of the caldera. When igneous activity ceased, abundant tuffaceous material was no longer available for erosion and redeposition. Thus all Virgin Valley sediments were deposited while hot spring activity could be occurring.

Alteration by cold gound water also should have occurred early in the basin's history. Clearly both fluvial and lacustrine sediments were deposited in and by water--so cold ground water was available to dissolve glass. Walter (1975) showed that tuffaceous sediments in Trans-Pecos Texas underwent diagenesis while sedimentation was occurring, and Surdam (1977) showed that diagenesis is an integral part of the history of closed basins. Diagenesis of the sediments of Virgin Valley should also have occurred during sedimentation, although diagenesis could continue today.

Opal beds occur through a considerable vertical range in the Virgin Valley Formation. The stratigraphically highest beds are interbedded with glassy sediment. It is now known if clinoptilolite occurs within these upper opal beds. Clinoptilolite has been found only in one of the lowest opal beds, and it is not known whether more glassy sediments occur

below these lower opal beds. In diagenetically altered sediments in Trans-Pecos, the first appearance of clinoptilolite commonly marks a fairly sharp transition from glassy rock above to totally altered rock below. Formerly glassy rocks in Yellowstone Park are also converted to crystalline assemblages below a distinct transition depth (Keith and others, 1978). Glass persists below that depth only in massive impermeable lava-flow rocks. Closed-basin alteration shows lateral rather than vertical zonation with glass near the margin followed by clinoptilolite and eventually by potassium feldspar in the center of the basin (Surdan, 1977). In all three types of alteration there is a sharp transition from unaltered to altered rock. If a similar transition occurs in Virgin Valley, then sediments below or basinward from the lowest exposed opal beds should have been totally altered and should have released large amounts of uranium. Additional opal beds in the subsurface and other potential host rocks such as carbonaceous shales and lignites within the center of the basin should be highly favorable sites for uranium enrichment.

Although general alteration characteristics would probably be similar whether the water were hot or cold, the difference in flow paths of hot and cold ground water might lead to different distribution of alteration and to different paths for uranium migration. Flow of cold ground water would be entirely from recharge areas in the higher parts of the basin towards the center. Dissolved uranium and other solids would be transported along this path.

Circulation of thermal water would have a significant vertical component. Heated thermal water would arise from below because hot water is less dense than cold water. Only when the hot water reaches the water table near the surface would lateral movement take over. Dissolved material in the water would travel a complex path, first rising from below, then moving basinward. By either method reducing environments in the center of the basin are favorable sites for uranim concentration. However, distribution of uraniferous opal would be controlled by the flow path of the water that precipitated it.

Uranium was probably concentrated in opal by adsorption, as amorphous materials are excellent adsorbents. Colloidal silica is negatively charged and can adsorb positively charged ions. Uranium in high-pH and high-Eh environments characteristic of ground water in volcanic rocks could occur as uranyl-hydroxyl, uranyl-carbonate, uranyl-phosphate complexes (Langmuir, 1978). Only the first is positively charged, but hydroxyl complexes are not important species in water with even low phosphate or carbonate concentrations. A positively charged uranyl-silicate complex can be important at pH 6 but not at high pH. In a high-pH environment (8-10) carbonate complexes are the dominant species except at high temperature ($100^{o}C$) (Langmuir, 1978). The mechanism by which opal incorporates uranium needs to be investigated.

Evaluation of Potential

Virgin Valley Area

The results of this study show that the Virgin Valley area and caldera settings in general are highly favorable for uranium deposits. In

Virgin Valley there are good source rocks; glassy samples of Canyon Rhyolite lavas and ash-flow tuffs and Virgin Valley Formation sediments contain about 8 ppm uranium. There is abundant evidence of redistribution of uranium including (1) uraniferous opal deposits of near-commercial grade, (2) minor uraniferous opal concentrations widespread through the Canyon Rhyolite and Virgin Valley Formation, and (3) depletion of uranium in Virgin Valley Formation sediments altered to clay. The interpretation that opal was formed by alteration of glass and that alteration is far more extensive in the subsurface indicates that uranium migration has probably occurred on a far greater scale than can be recognized at the surface. Finally, favorable host rocks are abundant: not only the known opal hosts but also reducing environments including lignite, carbonaceous shale, and probably reduced sandstones.

Caldera Setting

A caldera setting must be considered highly favorable for uranium mineralization for the following reasons. A caldera creates a closed basin with interior drainage. Uranium in solution in a fluid of any origin is trapped within the basin. For example, uranium separated into volcanic gases and then adsorbed on glass shards may be an important part of the total uranium originally in a magma. The first washing of shards by surface or ground water strips this adsorbed uranium. In a closed basin the uranium cannot leave the system, whereas in an open basin the uranium could enter a throughgoing drainage and be dispersed.

Uranium-bearing fluids could originate from both high-temperature and low-temperature processes within a caldera. Diagenesis by normal

ground water can create uranium-enriched solutions and can occur in any sedimentary basin. Alteration by thermal water can only occur in an area with continued igneous activity such as a caldera. Other high-temperature processes, although not considered important in uranium migration here, could be effective elsewhere and would be best developed in a caldera setting (Pilcher, 1978).

A caldera also creates a special kind of sedimentary basin which in turn determines the kinds of sedimentary deposits that occur within the basin. Lignites and carbonaceous shale along with other reducing sedimentary environments should be common deposits formed by closed-basin sedimentation. Uranium deposits can then form as classical oxidation-reduction deposits without requiring mechanisms unique to volcanic rocks. Volcanic sedimentary aprons exterior to a caldera such as the Tascotal Formation of Trans-Pecos Texas do not commonly have closed basins to concentrate carbonaceous debris or other reductants; seemingly all organic material in the Tascotal Formation has been oxidized. Thus uranium deposits in the Tascotal would necessarily have to have some other concentrating mechanism.

REFERENCES

Boles, J. R., 1977, Zeolites in low-grade metamorphic grades, in Mumpton, F. A., ed., Mineralogy and geology of natural zeolites: Mineralogy Society of America Short Course Notes, v. 4, p. 103-136.

Cupp, G. M., Leedom, S. H., Mitchell, T. P., Kiloh, K. D., and Horton, R. C., 1977, Preliminary study of the favorability for uranium in selected areas in the Basin and Range: U. S. Energy Research and Development Administration GJBX-74(77).

Fyock, T. L., 1963, The stratigraphy and structure of the Virgin Valley--Thousand Creek area, northwestern Nevada: Master's thesis, University of Washington, 50 p.

Garside, L. J., 1973, Radioactive mineral occurrences in Nevada: Nevada Bureau of Mines and Geology Bulletin 81, 121 p.

Gibson, I. L., 1972, The chemistry and petrogenesis of a suite of partellenites from the Ethiopian Rift: Journal of Petrology, v. 13, p. 31-44.

Jones, J. B., and Segnit, E. R., 1971, The nature of opal: 1. Nomenclature and constituent phases: Journal of the Geological Society of Australia, v. 18, p. 57-68.

Keith, T. E. C., and Muffler, L. J. P., 1978, Minerals produced during cooling and hydrothermal alteration of ash flow tuff from Yellowstone drill hole Y-5: Journal of Volcanology and Geothermal Research, v. 3, p. 373-402.

Keith, T. E. C., White, D. E., Beeson, M. H., 1978, Hydrothermal alteration and self-sealing in Y-7 and Y-8 drill holes in northern part of Upper Geyser Basin, Yellowstone National Park, Wyoming: U. S. Geological Survey Professional Paper 1054A, 26 p.

Langmuir, D., 1978, Uranium solution-mineral equilibria at low temperatures with applications to sedimentary ore deposits: Geochimica et Cosmochimica Acta, v. 42, p. 547-569.

McKee, E. H., and Marvin, R. F., 1974, Summary of radiometric ages of Tertiary volcanic rocks in Nevada, Part IV: Northwestern Nevada: Isochron/West no. 10, p. 1-6.

Merriam, J. C., 1910, Tertiary mammal beds of Virgin Valley and Thousand Creek in northwestern Nevada; Part 1 Geologic history: University of California Publication Bulletin, v. 6, p. 21-53.

Noble, D. C., 1968, Kane Springs Wash volcanic oster, Lincoln County, Nevada, in Eckel, E. G., ed., Nevada test site: Geological Society of American Memorandum 110, p. 109-116.

Noble, D. C., McKee, E. H., Smith, J. G., Korringa, M. J., 1970, Stratigraphy and geochronology of Miocene volcanic rocks in northwestern Nevada: U. S. Geological Survey Professional Paper 700-D, p. 23-32.

Pilcher, R. C., 1978, Classification of volcanogenic uranium deposits, in A preliminary classification of uranium deposits: U. S. Department of Energy, GJBX-63(78), p. 41-52.

Smith, R. L., and Bailey, R. A., 1968, Resurgent cauldrons, in Coats, R. R., Hay, R., and Anderson, C., ed., Studies in volcanology: Geological Society of American Memorandum 116, p. 613-662.

Staatz, M. H., and Bauer, H. L., 1951, Virgin Valley opal district, Humboldt County, Nevada: U. S. Geological Survey Circular 142, 7 p.

Surdam, R. C., 1977, Zeolites in closed hydrologic systems, in Mumpton, F. A., ed., Mineralogy and geology of natural zeolites: Mineralogy Society of America Short Course Notes, v. 4, p. 65-92.

Walton, A. W., 1975, Zeolite diagenesis in Oligocene volcanic sediments, Trans-Pecos Texas: Geological Society of America Bulletin 86, p. 615-624.

Wendell, W. G., 1970, The structure and stratigraphy of the Virgin Valley--McGee Mountain area, Humboldt County, Nevada: Master's thesis, Oregon State University, 130 p.

Willden, R., 1964, Geology and mineral deposits of Humboldt County, Nevada: Nevada Bureau of Mines and Geology Bulletin 59, 154 p.

IX. GEOLOGIC SETTING OF THE PEÑA BLANCA URANIUM DEPOSITS, CHIHUAHUA, MEXICO

by Philip C. Goodell, Robert C. Trentham, and Kenneth Carraway[1]

INTRODUCTION

Very little is known concerning the geology of the Peña Blanca region. This study synthesizes knowledge of the area. Data on the chemical alteration in and around mineralized areas are presented.

The Peña Blanca uranium district is situated 50 km north-northeast of Chihuahua, Mexico. The district lies on the eastern side of a Basin and Range horst, and the bulk of the economic mineralization is in Cenozoic volcanic rocks. Ash-flow tuffs overlie Cretaceous limestones in the mine area.

The Peña Blanca range is a part of the Mexican basin and range province, which in this area is characterized by north-trending fault-block mountains. The interior basins rise in elevation from east to west, and the average elevation of the ranges increases likewise (see fig. 1). This general increase in elevation westward culminates within the area under consideration in the Sierra del Nido on the left-hand side of figure 1. This sierra forms the high escarpment on the west side of Federal Highway 45 north of Chihuahua City. This escarpment is the dissected edge of a large volcanic plateau which continues westward to merge with the Sierra Madre Occidental itself. The Peña Blanca

---

[1] Department of Geological Sciences, The University of Texas at El Paso.

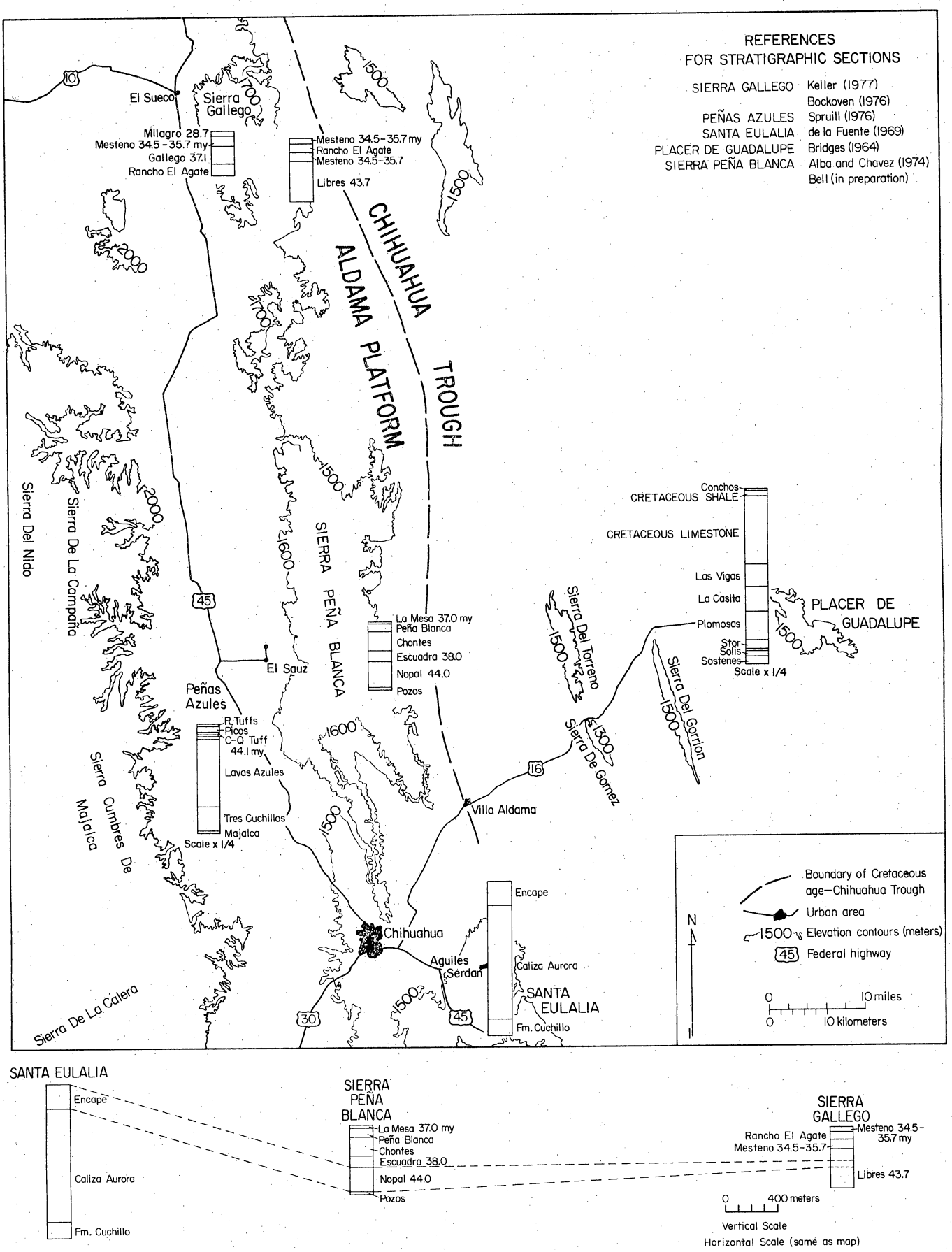

Figure 1. Regional geologic synthesis of the Peña Blanca area.

district, consequently, can be said to lie near the eastern edge of Sierra Madre Occidental Cenozoic volcanic province.

Generally east of the mine area, but also immediately south of it, are Cretaceous limestones upon which the volcanics were deposited. Cretaceous sediments were deposited in a basin known as the Chihuahua Trough. This depositional basin continues eastward to far West Texas; its eastern boundary is at the edge of the Diablo Plateau. The Peña Blanca region is near the western boundary of the carbonate- and evaporite-bearing Chihuahua Trough. The region westward from Peña Blanca is the Aldama Platform (see fig. 1) of Mesozoic time.

The Mesozoic sediments of the Chihuahua Trough have been subjected to extensive folding and thrusting from crustal shortening, and this resulting structural zone is known as the Chihuahua Tectonic Belt. This area was exhumed in the early Tertiary, with the formation of limestone conglomerates on a regional scale. It was in this environment that widespread caldera-related ash-flow tuff deposition took place, at least in the western half of the map area (fig. 1). Localized andesitic stratovolcanoes are present, as indicated by the studies at Sierra Gallego and Peñas Azules. Basalt and rhyolite flows and small intrusions are near the volcanic centers. The eastern edge of the Sierra Madre Cenozoic volcanic province is roughly coincidental with the Aldama Platform - Chihuahua Trough boundary, though the volcanics often overlap into the trough.

Tertiary normal faulting has affected the Mesozoic sediments and the overlying Cenozoic volcanic rocks. It is pertinent to point out that the Chihuahua Trough is succeeded eastward by the West Texas

Cenozoic volcanic province. This volcanic province bears many petrologic and temporal similarities to the eastern Sierra Madre Occidental, and several Peña Blanca type uranium occurrences are known there. The West Texas Province is generally alkaline, in contrast with the calc-alkaline character of the Sierra Madre Occidental.

The geology of the Peña Blanca region is poorly known but has been receiving some recent attention (fig. 1). Approximately 90 km to the north of the district is the Sierra Gallego area. The geology of this region has been the topic of a master's thesis by Bockoven (1976) and a Ph.D. dissertation by Keller (1977) both working at The University of Texas at Austin. Richard Mauger and students at East Carolina University have mapped and radiometrically dated rocks from the Sierra de Majalca area, 45 km southwest of the Peña Blanca district. This group is now working north along the escarpment and is presently northwest of the district. Peter McGaw, a student at U.T. Austin, is currently completing a field study of a large ring structure recognized from Landsat photographs, which lies immediately south of Chihuahua City. The ring structure is caldera related. The Santa Eulalia mining district lies 30 km southeast of Chihuahua City and some 55 km south of the Peña Blanca district. These mines, long operated for lead, zinc, and silver, have been adequately mapped, and de la Fuente (1969) has published the most recent work on that area. Approximately 70 km east of the Peña Blanca area lies the Placer de Guadalupe and Plomosas area. This area has received geologic study because of lead-zinc deposits, and also because of the presence of excellent exposures of Paleozoic and Mesozoic sections. Igneous rocks in this area in the Chihuahua Trough are limited to felsic

dikes, sills, and small intrusives. The geology of each of these surrounding areas will now be discussed in more detail, with particular emphasis on their relationships to Peña Blanca geology.

SIERRA GALLEGO REGION

The Sierra Gallego area (Keller, 1977; Bockoven, 1976) lies 90 km north of Peña Blanca along the boundary between the Sierra Madre volcanic province and the Chihuahua Tectonic Belt. It also straddles the eastern boundary of the Aldama Platform. A 1000-m-thick section of rhyolitic, andesitic, and basaltic volcanics unconformably overlies Cretaceous limestones. Small intrusions and sills are also present. Cenozoic volcanism was initiated 44 million years ago by the deposition of widespread ash-flow tuffs. Limestone conglomerates and epiclastic air-fall and ash-flow tuff deposition continued to approximately 39 million years ago. The volcanics within the Libres Formation are calc-alkaline rhyolites, according to the classification of Irvine and Baragar (1971). A portion of this unit is thought to correlate with the Nopal Formation in the Peña Blanca district. Field relationships suggest a very distant source for this unit. Between 37 and 38 million years ago, 300 m of tholeiitic andesite were extruded in a near-source environment, followed closely by 150 m of near-source calc-alkaline dacite flows. A third sequence of volcanic activity took place 35 million years ago. Widespread sills with localized lava flows, plugs, and flow domes, all calc-alkaline rhyolite, characterize this period. The Mesteño Rhyolite is both an intrusive and extrusive unit as shown in

the stratigraphic section (fig. 1). This period of volcanic activity cannot yet be related to any large-scale, volcano-tectonic event.

Finally, 29 million years ago bimodal calc-alkaline basalt and rhyolites were extruded from local sources. These represent the last event before normal faulting. In general then, the Sierra Gallego region experienced distant caldera eruptions, near-source andesitic and rhyolitic flows, subsequent felsic intrusive and extrusive activity, and later near-source basalt-rhyolite volcanism.

THE SIERRA DE LA CALERA - SIERRA DEL NIDO BLOCK, CHIHUAHUA

The region encompassing this block ranges from 40 km northwest to 60 km southwest of the Peña Blanca district and is from 30 to 100 km north of Chihuahua City. This region has been studied by Mauger and students (Spruill, 1976; Gall, 1977) in studies which are continuing. In the Peñas Azules area (Spruill, 1976), the oldest volcanic unit consists of andesites and tuffs of unknown thickness, some of which have been intensely hydrothermally altered. The next youngest volcanic group consists of 4,000 m of basaltic andesite, tuff, and laharic deposits. The proximity to source or multisource sites of calc-alkaline volcanism is suggested. These units are known as the Peñas Azules volcanic group and are thought to have accumulated in a sinking graben. This volcanic group was tilted and truncated prior to the deposition of the upper volcanic group. The upper group consists of dacite and thick andesite flows with several rhyolitic ash-flow tuffs. The lowermost tuff of this group, the Quintas tuff, has been dated by K-Ar at 44 million years (Mauger, 1976). The age and lithologic description

of this Quintas tuff is similar to that of the Nopal Formation in the Peña Blanca district, which is likewise similar to a portion of the Libres Formation in the Sierra Gallego area. The Ranchería Formation west of Federal Highway 45 is correlatable with the Mesa Formation at Peña Blanca. The unit is thicker to the west.

The 220-m-thick Picos Gemelos andesite flow indicates a moderately near source setting. The relatively uniform ash-flow tuffs indicate a long-term though sporadic caldera activity at some distance. These Oligocene ignimbrites are classified chemically as high-silica rhyolites and subaluminous peralkaline rhyolites (Spruill, 1976). They are compositionally transitional, between the calc-alkaline igneous rocks of the Sierra Madre Occidental and the alkalic volcanic rocks of the West Texas province. A younger volcanic group has also been recognized, and numerous small intrusives and a granite stock have been discovered farther north. Normal faulting postdates the last volcanic activity. Note that the vertical scale on figure 1 in the Peñas Azules area has been reduced 25 percent.

THE SANTA EULALIA AREA, CHIHUAHUA

This region lies 30 km east of Chihuahua City and consists mainly of Cretaceous limestone. About 1,100 m of Aurora Limestone exists with numerous manto and vein deposits of galena and sphalerite. Unconformably on top of the limestones are two ash-flow tuff units indicated by "Encape" in figure 1. A portion is lithologically similar to the Nopal Formation in the Peña Blanca area. The unit has a total thickness of over 250 m although it is variable. Basal limestone conglomerates give

way to thick welded tuffs with the top 50 m or so consisting of alternating conglomerates and flows. Uranium occurrences have been reported in the welded tuffs from underground workings in the district. More study of the volcanic rocks in this area is necessary.

SIERRA DE GUADALUPE AND PLOMOSAS REGION

Note that the stratigraphic column of this area given in figure 1 has been reduced by 25 percent. This area has been included to convey the nature of the Chihuahua Trough. Numerous Paleozoic units are present, dominated by Permian. Late Jurassic and Cretaceous units are well represented. Lower Cretaceous limestones make up over a third of the 7,000 m thickness of the section. No Cenozoic volcanics crop out in the region although several small Tertiary felsic stocks and numerous dikes are present. Of additional interest in this area, however, is the presence of quartz, pyrite, gold, and uraninite veins of Eocene age (Krieger, 1932).

Finally, discussion of the Peña Blanca region is concluded by considering the geology of the southern Peña Blanca range from south to north. Immediately west of Aldama, east of Chihuahua City, are small exposures of Tertiary intrusives of unknown character, along with some extrusives similar to the volcanic section at Peña Blanca. North of this (Tovar and Valencia, 1974) are 1,000 m of Permian flysch-type sediments. These rocks are strongly folded and partly metamorphosed. Commanchean limestones in the form of a broad anticline overlie the Paleozoic rocks forming a part of the Aldama Platform. Younger Cretaceous units appear farther northward within the Sierra de Peña Blanca, until

finally at the Peña Blanca mining district itself, these limestones become covered by the Cenozoic volcanic pile. Massive limestones containing rudistid mounds are common near the mineralized zone and to the south.

GEOLOGY OF THE PEÑA BLANCA DISTRICT

An outcrop map of the district is given in figure 2. Some 200 m of limestone conglomerate, and welded, unwelded, and epiclastic tuffs, form the major volcanic sequence at Peña Blanca. These units range in age from 37 to 44 million years (Alba and Chaves, 1974). Basal limestone conglomerates are common, with two such units having been given formation names, the Pozos and the Chontes (Bell, 1976).

A maximum thickness of 45 m was measured for the Pozos, but both units vary widely in thickness and rock composition. Three volcanic units have prominent welded-tuff members, the Nopal, Escuadra, and Mesa, whereas the Peña Blanca Formation is made up by air fall, epiclastic, and conglomeritic units. The volcanic sequence was laid down on a surface of considerable relief. The Cretaceous rudistid reef complex was apparently being exhumed with the formation of thick local limestone conglomerates prior to the deposition of the Nopal Formation. Missing stratovolcanic units and the inclusion of pebbles of certain units in younger conglomerates, plus the thickening and thinning of clastic and volcanic formations, document the influence of local topographic relief. In the El Cuervo area at the northern margin of the Peña Blanca district, older Tertiary (?) ignimbrites and conglomerates have been included in the folded limestones of the Chihuahua Tectonic Belt. This area has received little study, and these volcanics have not been dated.

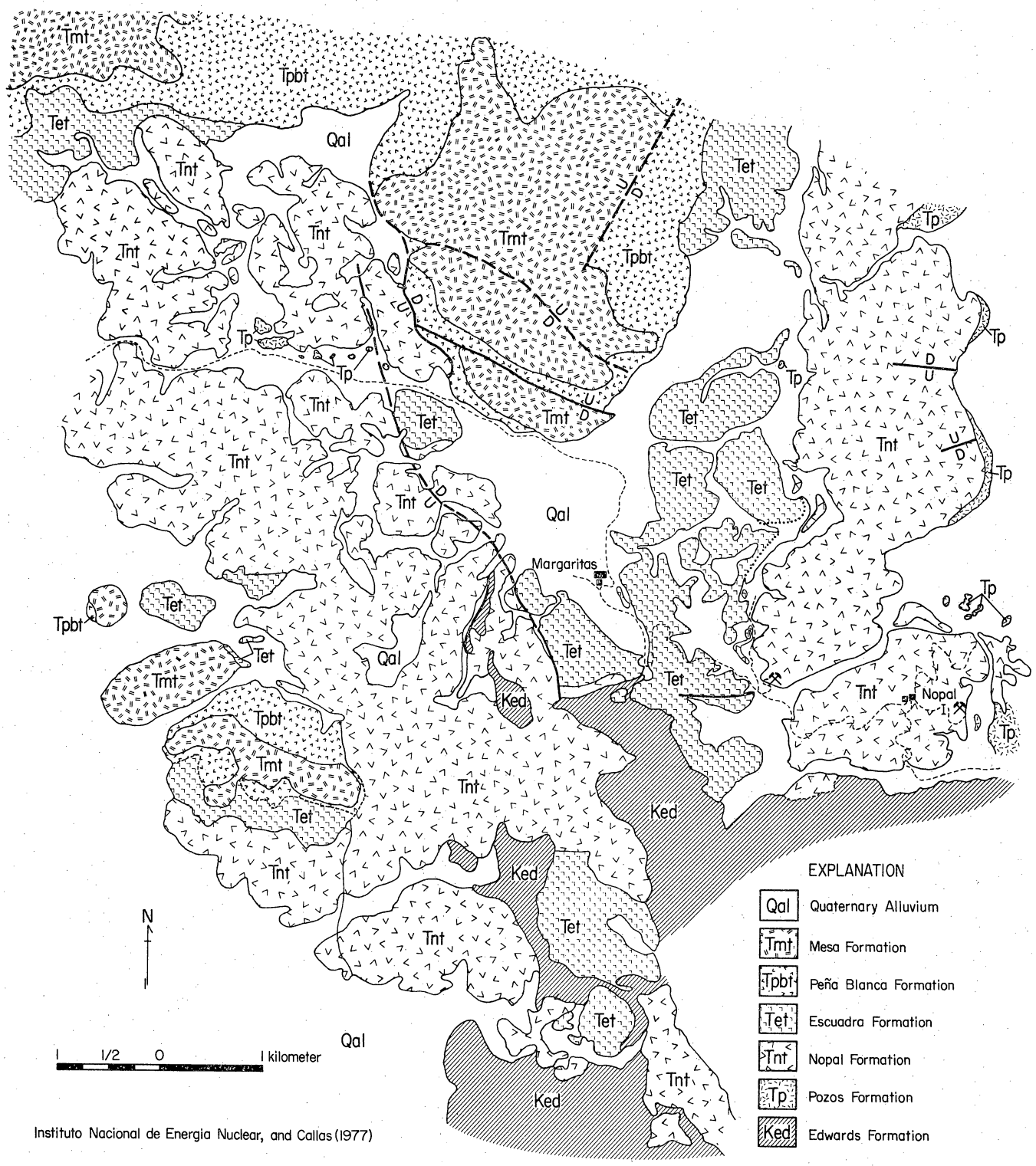

Figure 2. Outcrop map of the Peña Blanca uranium district, Chihuahua, Mexico.

The eastern escarpment of the northern Peña Blanca range consists of a continuous section of volcanic units. Volcanostratigraphic sections (fig. 3; Bell, 1976) measured within the district indicate local variations. The Nopal Formation varies from 70 to 220 m in thickness. The top of the Mesa Formation is never seen, but it has a thickness of up to 200 m. From the regional synthesis given previously, these units appear to have been of widespread distribution. The Escuadra Formation thins to the northeast from a maximum thickness of 100 m near Margaritas. The Peña Blanca epiclastics are locally very thick, and the thinning of the Chontes limestone conglomerate away from the rudistic reef area is documented (fig. 3). From the east-central to southern part of the district, the units overlying the Nopal Formation have been eroded. This region has Nopal exposed at the surface in the form of a succession of westward dipping cuestas. They contain numerous small step faults within the welded members, which is important for the localization of mineralization. The western half of the mine area (fig. 2) has a number of structural complications which are poorly understood. Elevations are much higher in this area and the volcanics are underlain by a carbonate reef. Faulting has raised and tilted this western block, and the volcanic sequence is progressively younger from the south to north.

The characteristic feature of the Peña Blanca volcanic rocks is that they all represent outflow facies distal to caldera-related volcanism. Some speculation can be made as to the sources of these volcanics although very little conclusive data are present. A vertical section is on the right-hand side of figure 3. The Nopal Formation thickens southward to

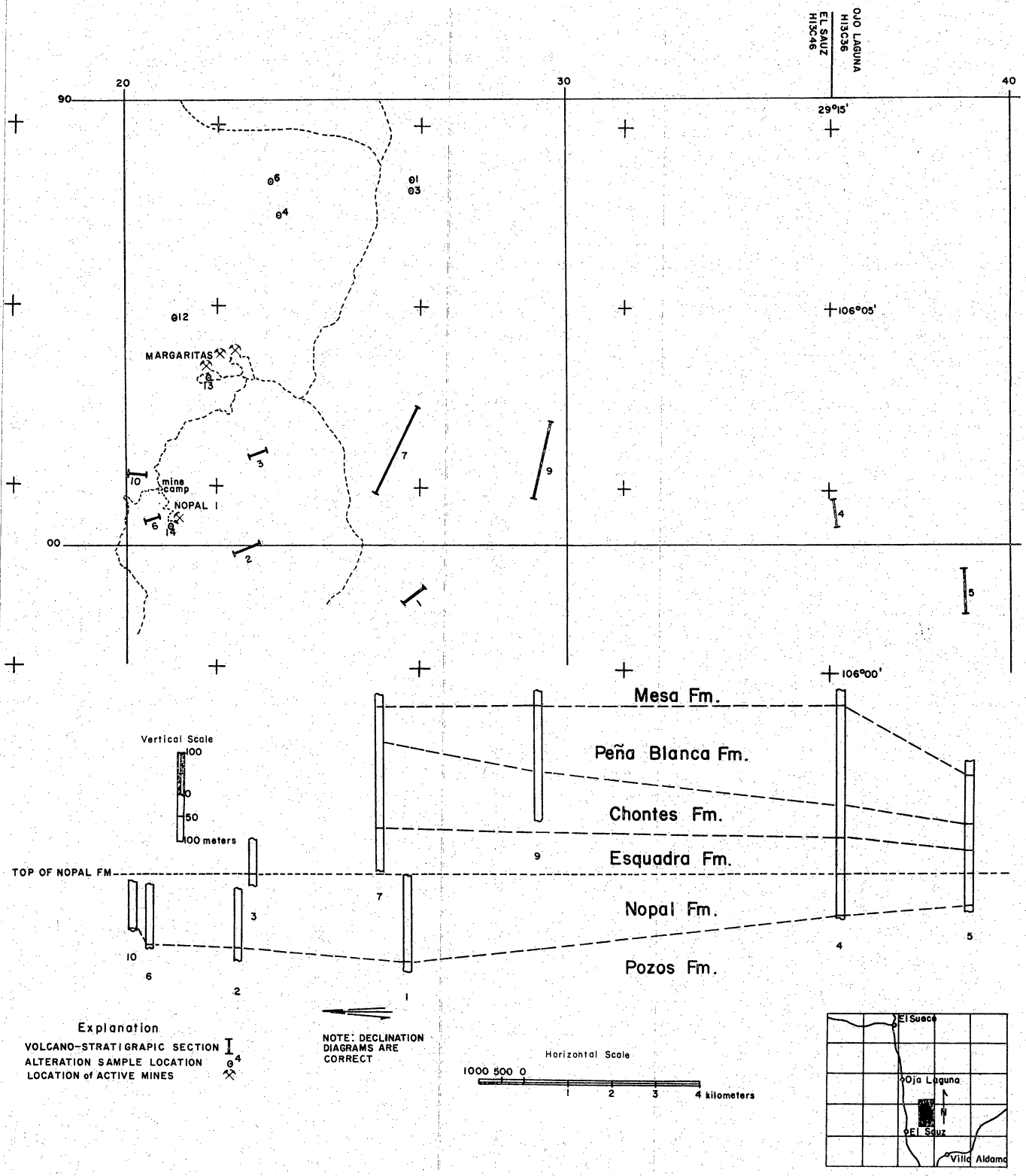

Figure 3. Locations of volcano-stratigraphic sections (Bell, 1976) and alteration samples, Peña Blanca district, Chihuahua, Mexico.

225 m at Sierra Gloria, east of Chihuahua and south of Aldama, and is approximately 200 m thick at Santa Eulalia. This same ash-flow unit appears to thin to approximately 30 m in the Sierra Gallego area. The source of this unit may consequently be the large caldera-like structure found south of Chihuahua City. The Escuadra Formation has not been found in the Sierra Gloria section, and its source is not known.

The Peña Blanca Formation has thicknesses up to 200 m in the mine district. The unit is quite variable in thickness, distribution, and limestone conglomerate content. The upper portion comprises air fall and epiclastic tuffs. The epiclastic component may constitute the reworked, unwelded top of the Escuadra ash-flow tuff. The short timespan between the underlying Escuadra (39 million years old) and the overlying Mesa Formation (37 million years old), suggests a fairly near-source (with respect to the Escuadra) environment.

The Mesa Formation is found over a very large region, including Sierra Gomez to the east, Sierra Gloria to the south, and Sierra de Calera - Sierra Nido area to the west. Eutaxitic structure, thickness variations, and minor structures at the lower contact, all suggest a source area to the west. The Mesa is a prominent ridge-former in the region.

The regional geologic synthesis establishes the outflow-facies nature of the Peña Blanca volcanic sequence. No intrusive rocks crop out within or near the mining district.

DESCRIPTION OF SEVERAL DEPOSITS

Uranium occurs in several different types of environments in the Peña Blanca district. These have been separated, and are illustrated in generalized form in figure 4. More than one environment is frequently mineralized at each mine.

(1) Mineralized step faults in welded members of volcanic units. Jointing or faulting in the brittle, massive ignimbrite provides pathways for solution movement and sites for alteration and precipitation. This environment is exemplified by small high-grade deposits (300 to 500 tons U_3O_8, 0.35 percent upwards) at Nopal 1, 3, and 5. Numerous additional anomalies exist along such step faults in the Nopal Formation. The westward-dipping cuestas of Nopal ignimbrite on the eastern side of the district illustrate this environment.

(2) Mineralization within more porous and permeable units in the volcanostratigraphic column. Such a unit is the lapilli tuff found at the surface at the Margaritas deposit. Porosity was provided by abundant pumice and lithic fragments. Mineralization is stratabound.

(3) Mineralization of the altered vitrophyre at the base of a welded unit, the Nopal Formation. Glassy rock is more chemically reactive than the devitrified welded tuff immediately above it. Vitrophyres are consequently susceptible to alteration, and this altered stratabound layer is more porous and permeable than the surrounding rock. Altered vitrophyres are frequently mineralized and appear to be the host of at least a portion of the large, lower grade deposit at Margaritas. This environment contains the largest amount of reserves in Peña Blanca, and

Figure 4. Diagrammatic sketch of several different uranium depositional environments in volcanogenic areas. The mobilized uranium precipitates for a variety of reasons.

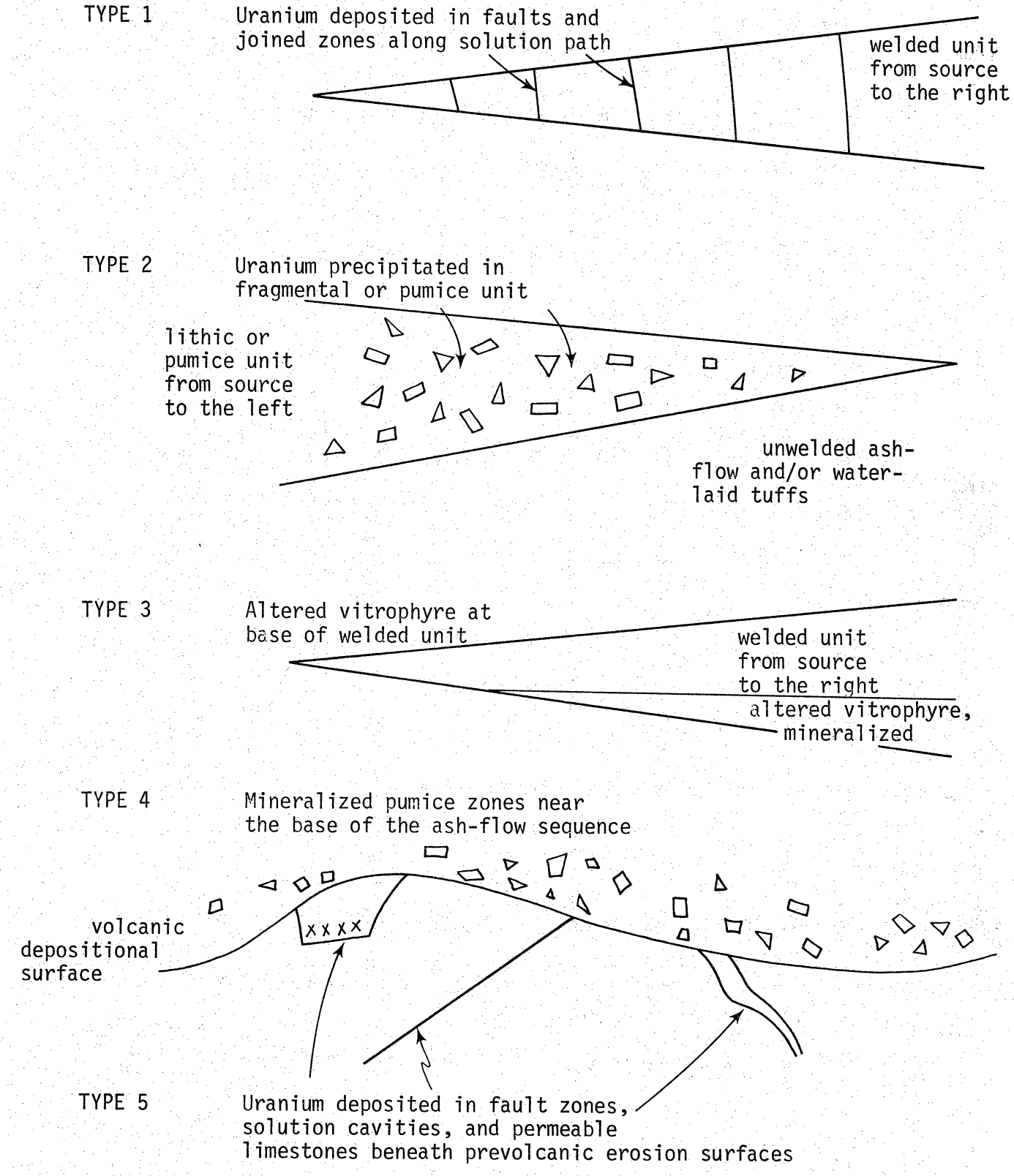

the drilling out of the lower contact of the Nopal ignimbrite is presently the most successful exploration tool. Nopal I appears to undergo a transition from type 1 to this type at depth. El Cuervo area also typifies this environment.

(4) Mineralization of porous pumice zone at base of sequence. A widespread pumice fall preceded the lowest Nopal ignimbrite. This zone is altered and mineralized, mainly at Margaritas.

(5) Mineralization in the underlying Cretaceous limestones. Uranium has been deposited in faults, solution cavities, paleokarsts, and other permeable zones beneath the prevolcanic erosion surface. The Domatilla Mine near Margaritas illustrates this environment. Elsewhere, the El Calvario and Sierra Gomez areas fall within this category.

Several deposits will now be discussed in greater detail.

NOPAL I

The Nopal I is a small high-grade deposit located in a breccia zone at the intersection of two step faults in welded units of the Nopal Formation. These step faults are found within the cuestas on the eastern side of the district and the Nopal I deposit falls at the south end of the southernmost cuesta. In plan the deposit is a 50 by 20 m oval, and extends vertically for over 50 m. The upper part is structurally controlled within the faults in the brittle ignimbrite. Beneath this, in the softer, less consolidated tuff, the mineralization is more widely disseminated and of lower grade. Its shape in these tuffs is that of a cone with apex down. These tuffs

are not noticeably faulted or brecciated, having responded to stress in a manner different from that of the ignimbrite.

The brecciated and oval shape of the ore zone has led to the categorization of the area as a breccia pipe. The pipe designation, plus the presence of some quadravalent uranium as uraninite, has led a number of observers to conclude that the deposit originated from hydrothermal magmatic processes. This origin, however, does not stand the test of careful observation. The deposit averages 0.3 to 0.4 percent U_3O_8, 0.07 percent molybdenum, and has reported reserves of 360 tons of U_3O_8. The mineralogy is uraninite, uranophane, and beta-uranophane. This deposit is presently being mined by open-pit methods and the ore is being stockpiled. Mine geologists are successfully using exploration and development techniques of stepping out along step faults, and particularly, drilling intersections of these faults.

THE MARGARITAS DEPOSIT

Margaritas consists of three different mineralized zones. A lapilli tuff (type 2 category, fig. 4) comprising the lower Escuadra Formation is found at the surface over a limited area. A widespread, stratabound uranium molybdenum deposit has been drilled out just below the base of the lowermost welded unit of the Nopal Formation. The mineralized zone is believed to represent the altered vitrophyre (type 3 category, fig. 4) and/or an altered pumiceous zone (type 4, fig. 4) at the base of the formation. The third mineralized zone consists of fracture and solution cavity fillings in the underlying limestones (type 5, fig. 4). Type 3 mineralization contains most of the reserves of the area.

The widespread stratabound deposit has reported reserves of 4,000 tons U_3O_8 with an average grade of 0.2 percent. It is generally at least 100 to 200 m wide, and extends northwest-southeast for nearly 2 km. The thickness is up to several meters. A portion of this zone is downdropped in a graben-like structure, and this fault zone is equally well mineralized.

All uranium known to date from the Margaritas area is hexavalent, found mainly as uranophane, but also as carnotite and autunite. Sample 13, table 2, is from the type 3 environment. Alteration consists of the formation of montmorillonite (Calas, 1977), and widespread hematitization adjoins the deposit. Molybdenum values are high, averaging 0.3 percent in the ore.

The Margaritas deposit lies adjacent to a prominent rudistid mound-reef complex of the underlying carbonates. The deposit rests above the reef slope. This juxtaposition suggests a possible paleohydrologic influence of the reef complex upon the mineralizing fluids.

SIERRA GOMEZ

Sierra Gomez district lies approximately 15 km east of Peña Blanca, and is in the southern portion of the next range to the east. The range consists mainly of faulted and folded Cretaceous limestones, though the Peña Blanca volcanic sequence is found at both the northern and southern ends of the range.

Hexavalent uranium mineralization is found in faults and solution cavities in limestones, associated with silicification, calcite, siderite, fluorite, and limonite. Mexico's yellow-cake production in the 1960's

came from this area, though the mines are now idle. Small erosional remnants of volcanics indicate that they previously covered the mine area.

Domatilla and El Calvario are other limestone occurrences of this type (type 5, fig. 4).

ALTERATION STUDIES

Rock alteration is intimately associated with the uranium deposits at Peña Blanca, and definite alteration halos exist. The characterization of alteration in the deposits has been undertaken. Comparisons of the altered rocks with fresh ones give indications of the alteration processes, and can provide clues useful in exploration for uranium deposits in volcanic rocks elsewhere. Results of the whole-rock chemistry will be discussed. The altered samples studied, except for sample 13, all come from type 1, figure 4 occurrences.

Sample locations for the alteration studies are given in figure 3 and sample descriptions are found in table 2. For all of these samples, the fresh and altered zones were present within a hand sample, often as little as 4 cm apart. For samples 3, 4, 6, and 12, uranium anomalies at each of these localities had been drilled and/or explored underground, but were not found to be of economic interest. The alteration appears as a bleaching from the normal red color to white.

Partial whole rock analyses of all the samples mentioned are given in table 1. X-ray fluorescence whole-rock analysis was carried out on a wavelength-dispersive x-ray fluorescence unit with a Phillips XRG-3000

Table 1. Partial whole-rock chemical analyses of fresh and altered rocks, Peña Blanca District, Chihuahua. Sample locations are indicated in figure 3.

Values in Weight %

Sample #	SiO_2	Al_2O_3	K_2O	Na_2O	CaO	MgO	MnO	TiO_2	Fe_2O_3
1F	78.20	10.78	6.88	3.47	0.15	0.00	0.045	0.213	1.720
1A	83.60	9.07	5.62	2.52	0.10	0.00	0.021	0.161	0.857
3F	71.05	9.53	6.27	3.45	1.28	0.15	0.020	0.450	1.814
3A	77.16	8.71	5.85	2.99	0.21	0.15	0.007	0.323	0.814
4F	72.69	10.05	7.16	3.34	0.19	0.10	0.23	0.252	1.250
4A	79.10	9.93	6.94	2.94	1.03	0.20	0.610	0.248	0.455
6A-F	66.38	10.72	7.72	3.15	0.35	0.00	0.340	1.390	1.390
6A-A	75.22	11.02	7.51	3.65	0.23	0.00	0.009	0.457	1.280
6B-F	62.22	8.71	7.55	3.17	14.57	0.00	0.390	0.265	1.210
6B-A	73.46	12.29	7.04	2.94	0.23	0.00	0.120	0.385	0.599
12-F	66.71	11.15	8.07	4.24	0.99	0.15	0.63	0.497	2.398
12-A	72.69	10.48	7.41	2.41	0.82	0.15	0.001	0.536	1.690
13	77.00	11.14	7.94	4.46	0.12	0.00	0.010	0.202	1.100
N1-F	73.20	15.70	7.70	0.04	0.05	0.05	0.010	0.340	0.780
N1-A1	82.40	10.40	0.20	0.04	0.43	0.15	0.010	0.180	1.400
N1-A2	88.90	5.50	0.06	0.04	0.49	0.25	0.010	0.290	0.700

Table 2. Sample descriptions.

Sample* designation	Sample** location on map	Description
1	14	Nopal #1 Mine; Nopal Formation; alteration associated with mineralization.
3	3	Nopal Formation; highly fractured zone, alteration zones are numerous, particularly at N10°E, 75°SE. Surface oxidation present in places. No visible uranium minerals; exploration done on an anomaly by three different adits.
4	4	Nopal Formation; highly fractured zone with alteration, general trend north-south. Autunite and tyuyumanite (?) in fractures. Anomaly explored with three adits.
6A	6	Nopal Formation; anomaly explored with six trenches and numerous drill holes. Color of fresh rock is gray; 6A-A is red; 6B-A is white.
6B	6	
12	12	Nopal or Esquadra Formation; anomaly tested by trench. This location is above Domatilla, just to the west of north-south fault.
13	13	Margaritas mine; underground 120 ft. Esquadra Formation?; intensely altered, mineralized.
N1-F	14	Nopal Formation; Nopal #1 mine, fresh rock outside breccia zone.
N1-A1	14	Same as N1-F, but in altered zone.
N1-A2	14	Same as N1-F, but more highly altered.

* Designations ending in F indicate fresh rock; ending in A indicate altered rock.

** These numbers refer to figure 3 where sample locations are indicated by 0 and numbers next to bars, [————————] , indicate stratigraphic section numbers.

Table 3. Factor score coefficients, for factor analysis of chemical data given in table 1.

	Factor 1	Factor 2	Factor 3
SiO_2	0.11325	0.23203	0.28087
Al_2O_3	0.10465	0.30840	0.16954
K_2O	0.37379	0.01206	0.03158
Na_2O	0.27074	0.06296	0.01718
CaO	0.09322	0.04123	0.50477
MgO	0.31837	0.27846	0.22254
MnO	0.15143	0.34377	0.37539
TiO_2	0.24965	0.01768	0.02346
Fe_2O_3	0.02844	0.45389	0.01225

x-ray generator and Phillips tungsten and chrome target tubes. The U.S. Geological Survey standard rock G2 along with several previously analyzed ash-flow tuffs were used as the standards for analysis.

Only clean samples with surface alteration removed were used. Sieving to achieve a uniform size (between 120 and 200 mesh sieve size) was performed. Disk samples were then prepared with boric acid as a backing and pressed at 20,000 psi for one minute. Only disks with no signs of flaking were analyzed.

It should be noted that some of these analyses add up to more than 100 percent. Those with the greater average are richest in silica, and these were 7 percent greater in SiO_2 content than that of the closest standard. The linear extrapolation used to determine these higher silica contents evidently increased the actual silica values.

Differences between fresh and altered rocks are indicated on table 1 by the suffixes F and A. Depletions and enrichments can be seen by inspection. Alteration changes invariably show alkali depletion and silica enrichment. Figure 5 documents these changes using the data from table 1. Arrows are drawn from the fresh to the altered associate of each sample. Two separate samples of no. 6 were analyzed. The arrows consistently show potassium depletion and silica enrichment.

A point of clarification may be necessary for the proper interpretation of these figures. There is frequently a great deal of vertical chemical variability within a volcanostratigraphic unit. This means that the starting points for the alteration arrows in figure 4 may vary by a significant amount. However, tuffs of initially different compositions, when subjected to similar leaching conditions, produce an array of similar trends, as indicated in figure 5.

One group, including samples 3, 4, 6, and 12, have slopes of approximately -1.0 wt. percent/K_2O/10.0 wt. percent SiO_2. The other group, suggested by samples 1 and N1, has similar slopes, which are approximately an order of magnitude smaller, -1.0 wt. percent K_2O/1.25 wt. percent SiO_2. The populations of these two groups are too small for these present observations to be conclusive. However, the 1, N1-A1, and N1-A2 samples are all taken from within the Nopal I mineralized breccia zone. The change in slope in figure 5 between the two groups is undoubtedly reflected by differing mineralogical facies.

Several additional trend diagrams made from the alteration data in table 1 are given in figures 6 through 9. Silicification is indicated in the Si/K, Si/Na, Si/Fe_2O_3, and Si/Al diagrams. The greater degree of silicification in the mineralized zones is shown by samples 1a and N1-A2. These samples, on the Si/Al graph, have similar slopes, which may be fingerprints characteristic of mineralization. Alkali leaching is indicated in the Si/K and Si/Na diagrams, but even more so in the Al/K and Al/Na diagrams. The frequent decrease of alumina during alteration is seen in the Si/Al, Al/Na, and Al/K diagrams.

Trend diagrams do not tell the whole story, and the data in table 1 have been subjected to factor analysis. The data can be reduced to three factors, and the relative weighting of the chemical constituents in the factors is given in table 3. Sodium, potassium, and magnesium are most heavily weighted in factor 1. Iron, aluminum, manganese, and magnesium are most heavily weighted in factor 2, with iron and aluminum being most significant. Factor 3 is most heavily weighted with calcium and manganese. The changes of these three factors during alteration

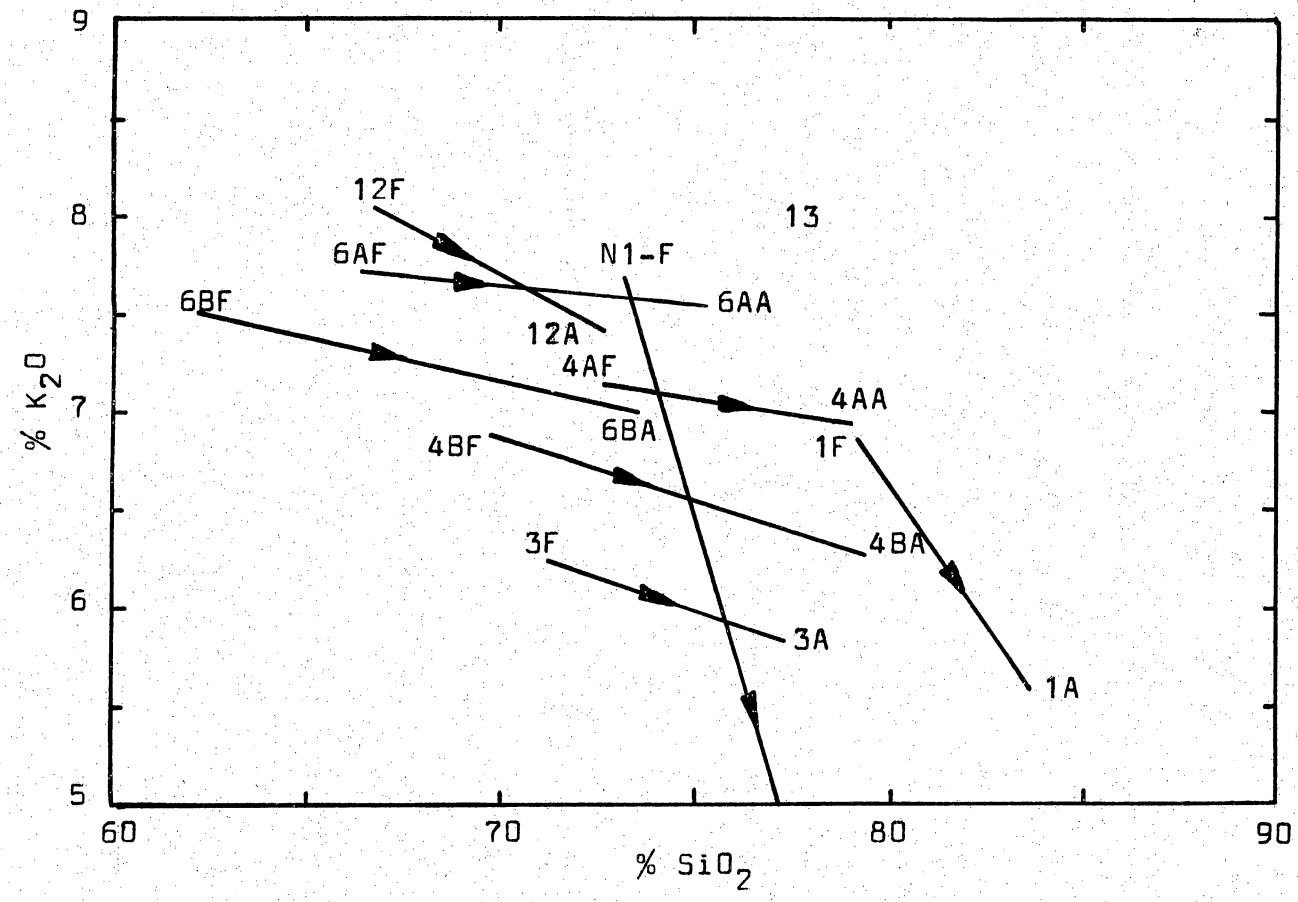

Figure 5. Chemical variation diagram of SiO_2 vs. K_2O

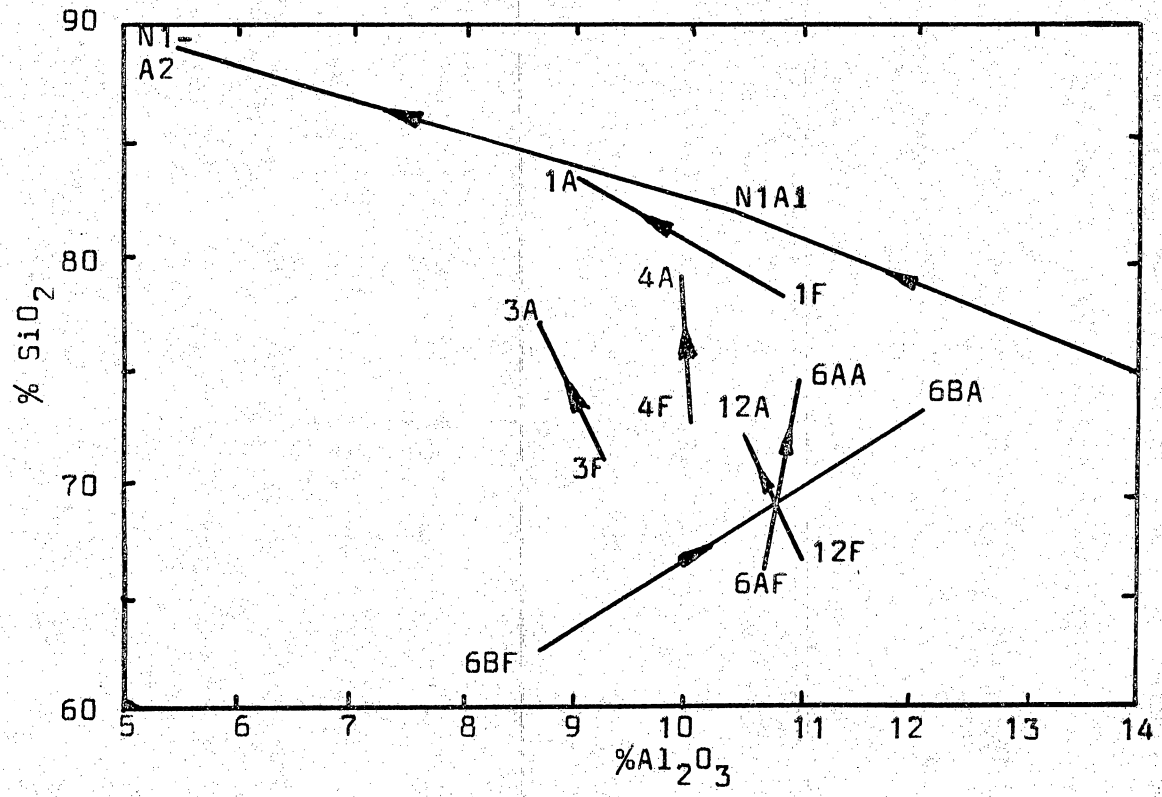

Figure 6. Chemical variation diagram of SiO_2 vs. Al_2O_3.

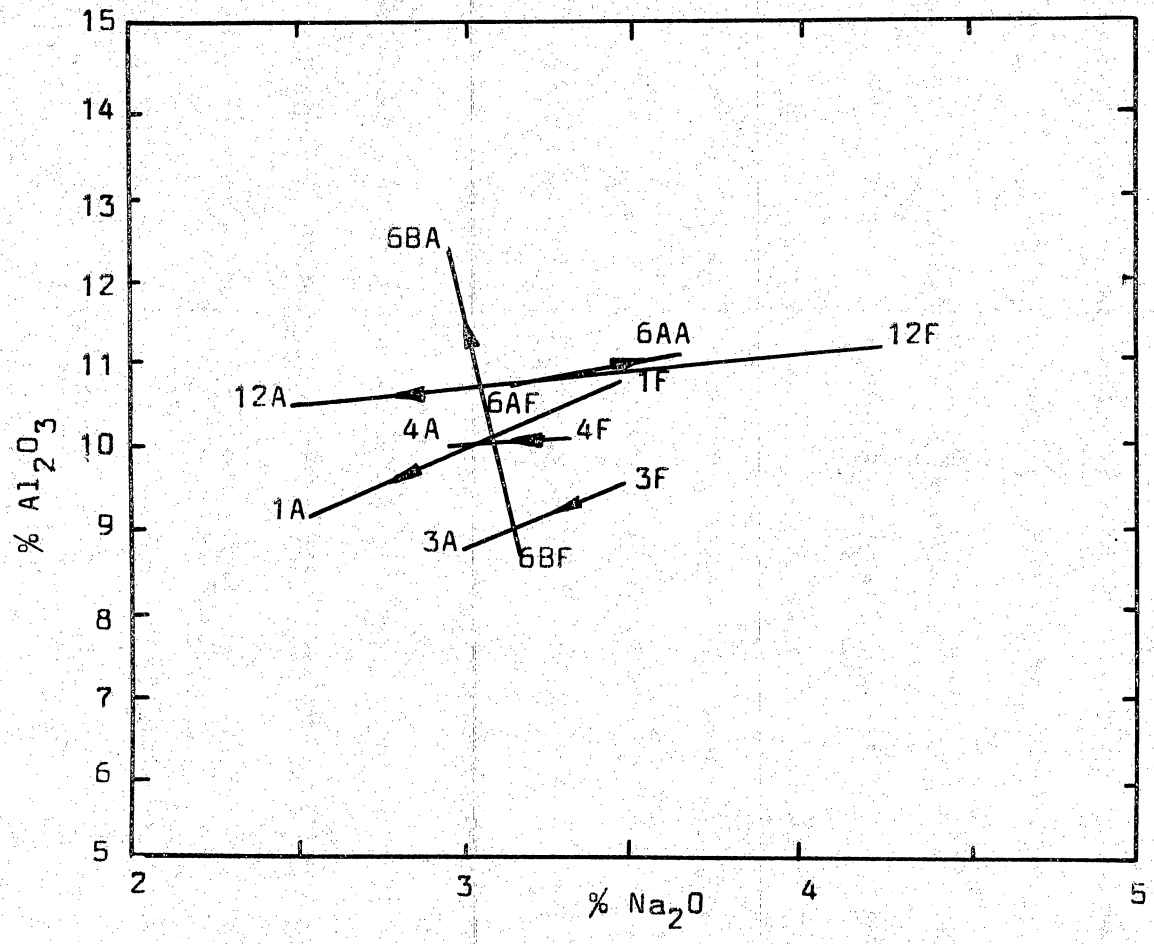

Figure 7. Chemical variation diagram of Al_2O_3 vs. Na_2O.

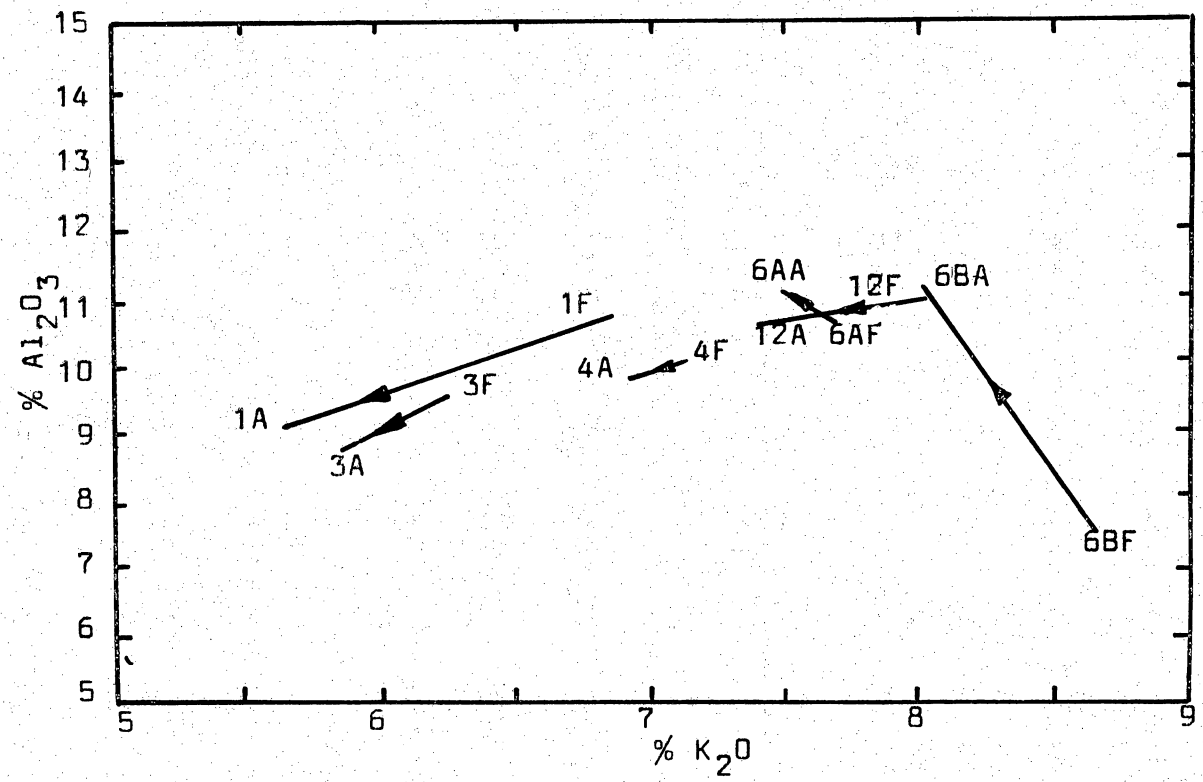

Figure 8. Chemical variation diagram of Al_2O_3 vs. K_2O.

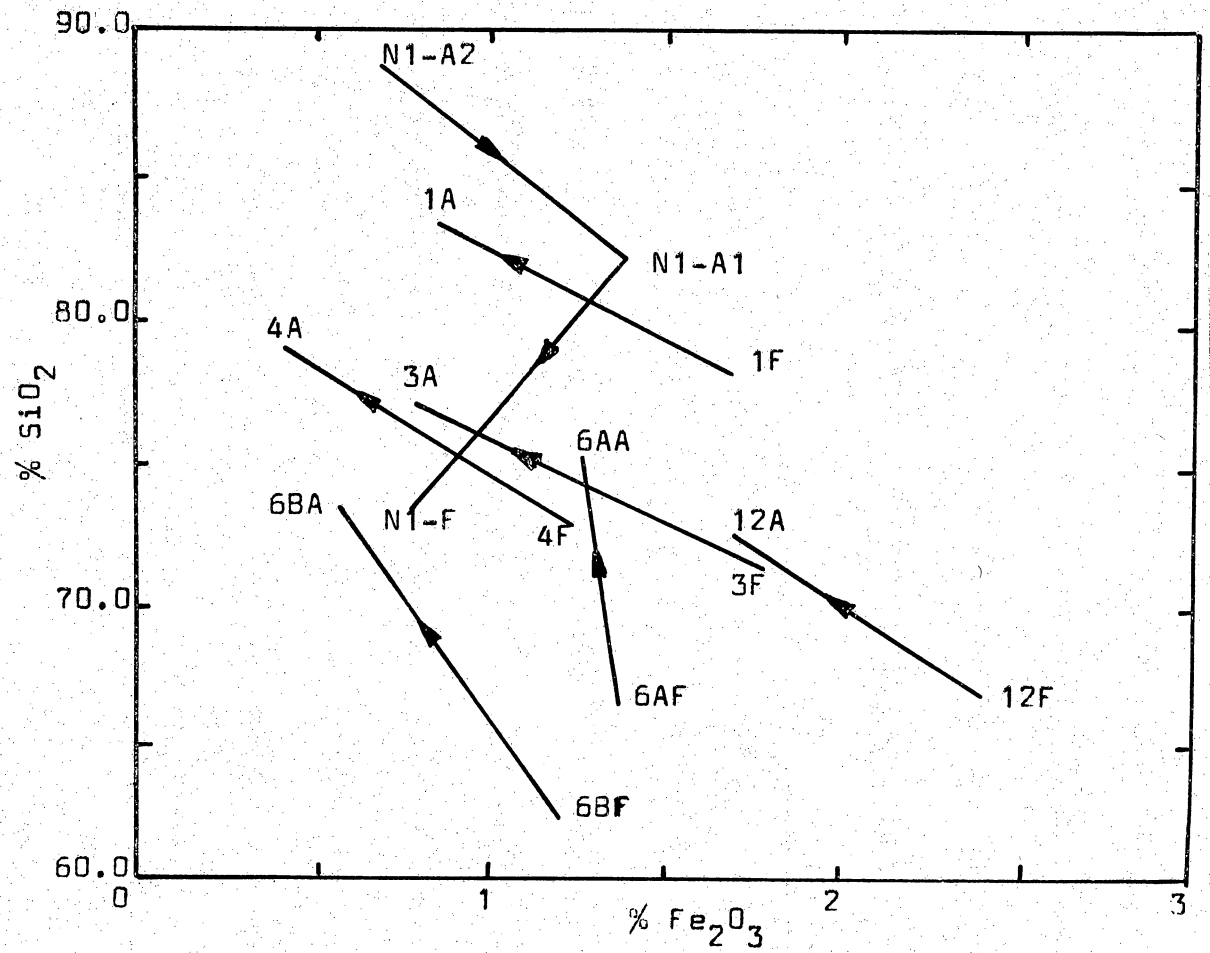

Figure 9. Chemical variation diagram of Fe_2O_3 vs. SiO_2.

processes at Peña Blanca are graphed in figures 10, 11, and 12. It is to be noted that in spite of the silica-variation trends in figures 5 and 6, silica is not heavily weighted in any of the three factors, though it plays a lesser part in factor 3. Figures 5 and 6 should not give the impression that silica variation is the most important aspect of the chemical alteration.

In figure 10, large decreases in factor 2 are generally correlatable with decreases in factor 1, the alkali factor. Figure 11 shows large decreases in factor 3 with the alkali leaching during alteration. At the very low alkali values in Nopal I, this relation reversed itself. Figure 12 is less definite, but may be interpreted as either factor 2 or factor 3 undergoing a significant decrease during alteration.

Rock alteration may be successfully used in seeking uranium deposits in felsic volcanics. Alteration chemistry appears to follow a consistent pattern and becomes more intense closer to major deposits.

GENESIS OF THE PEÑA BLANCA DEPOSITS

The genesis of these deposits is not known; however a number of ideas have been advanced explaining their origin. An attempt will be made to sketch several of these, with an elaboration on a preferred model of genesis. Very little data are present to substantiate any of the suggestions.

The magmatic-hydrothermal model has been proposed largely from the idea that the Nopal I deposit was in a breccia pipe, presumably of intrusive origin, and that the deposit had uraninite which was presumably

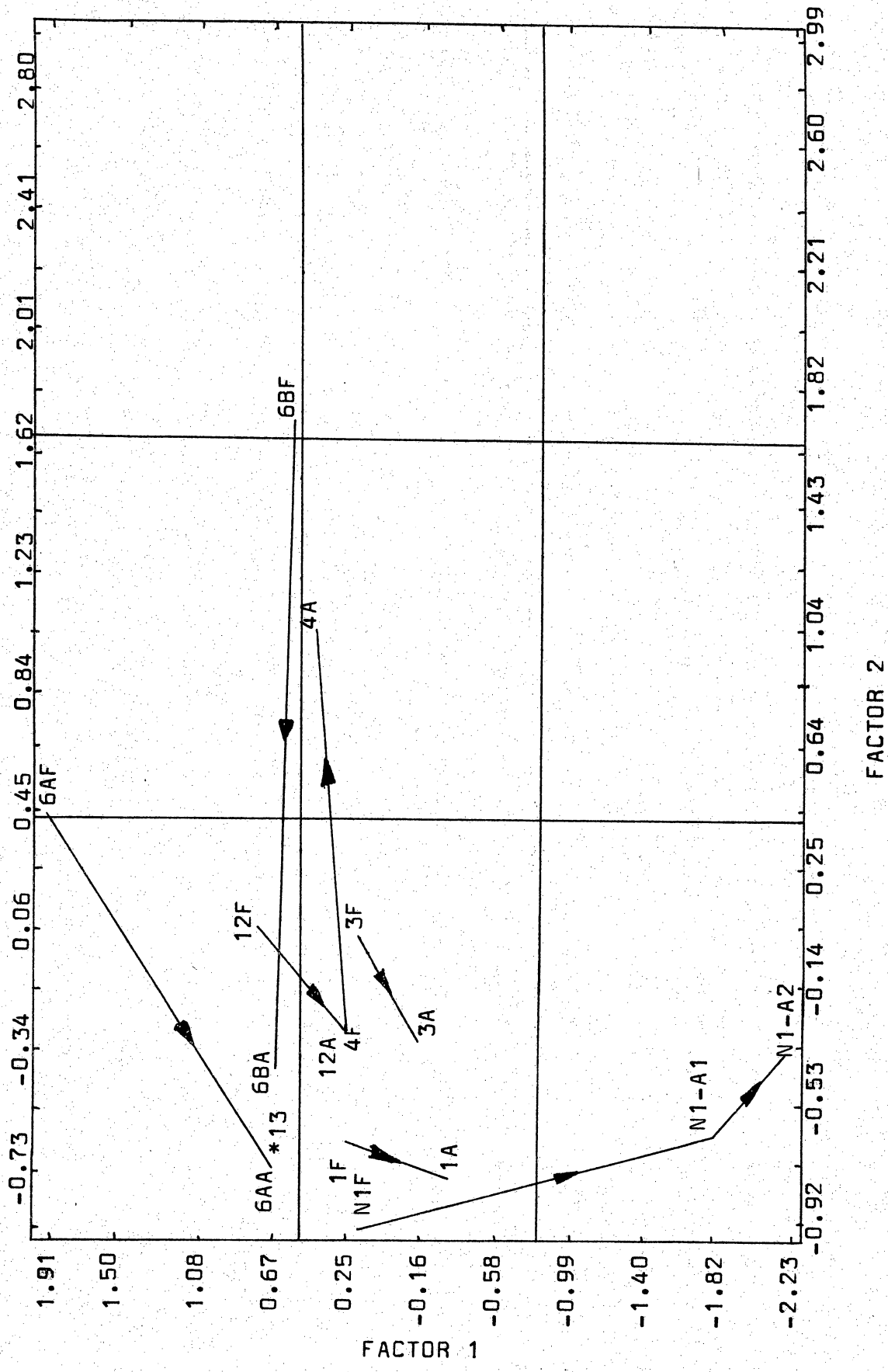

Figure 10. Factor score plots.

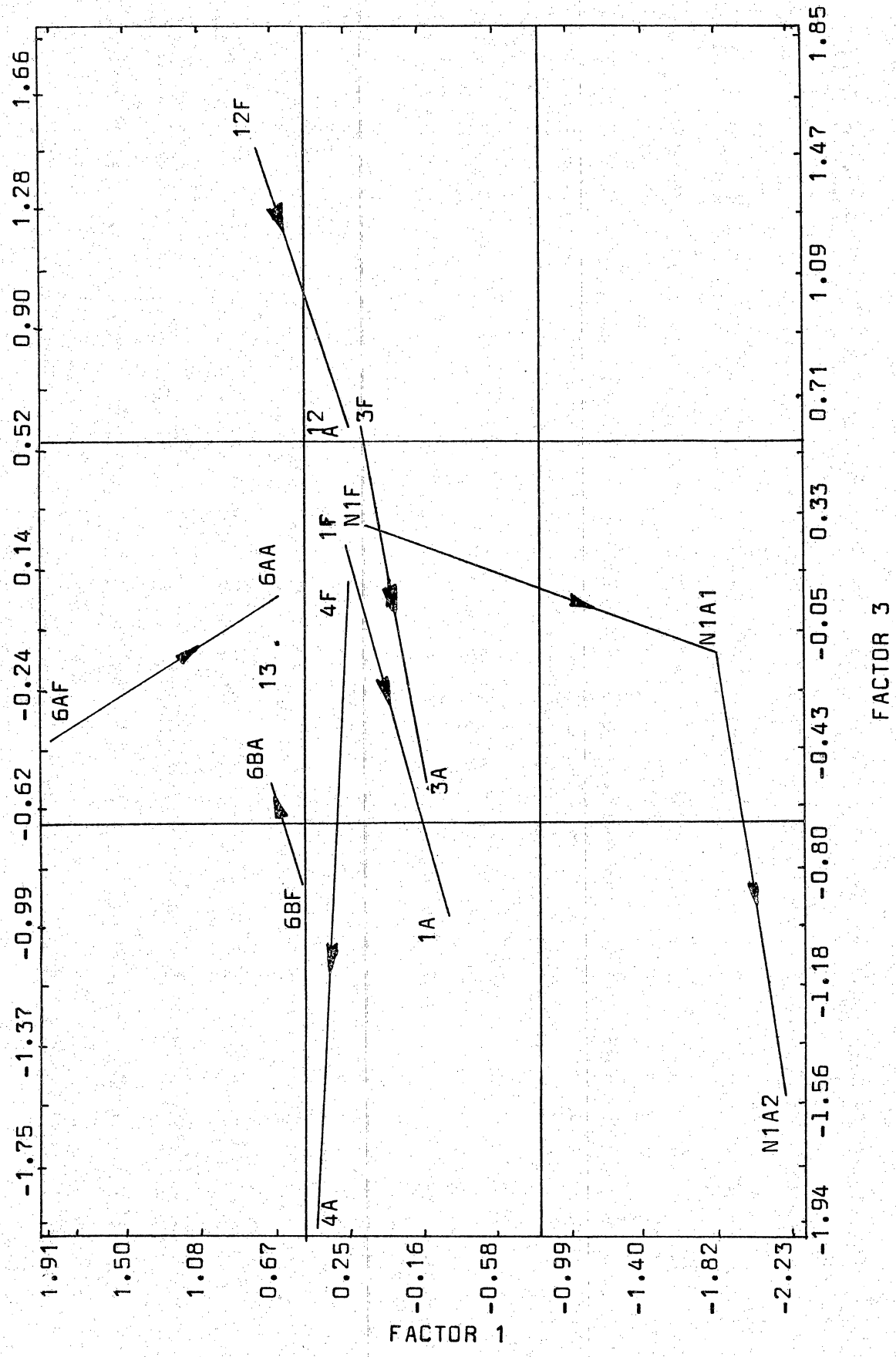

Figure 11. Factor score plots.

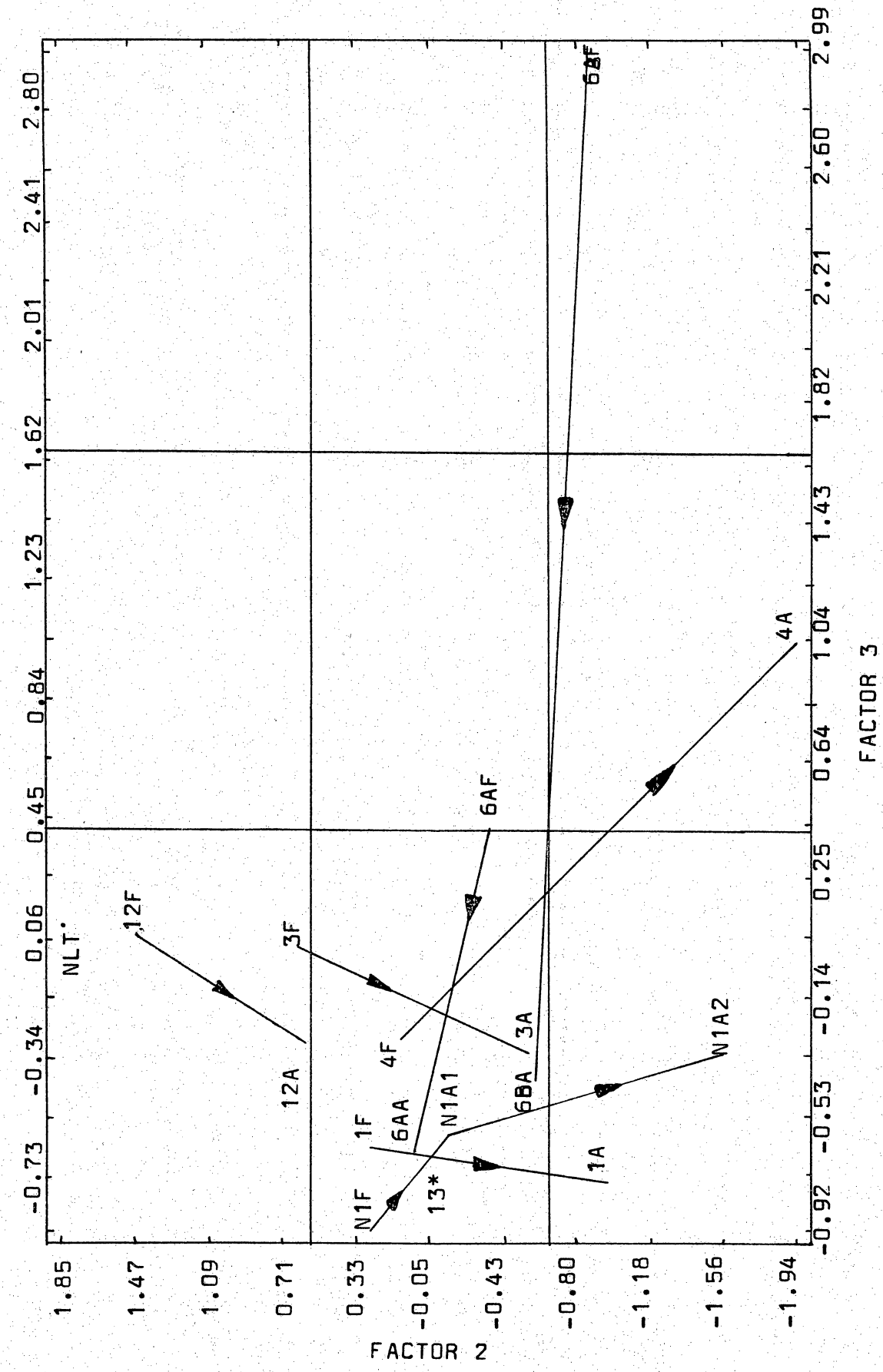

Figure 12. Factor score plots.

"hydrothermal." The pipe can also be interpreted as a breccia zone at the junction of two intersecting step faults in the ignimbrite. Uraninite and marcasite do occur at several localities in the district. Marcasite is not stable above 365° C, and the presence of uraninite is not a good temperature indicator. The presence of these species is only an indicator of reducing conditions. The magmatic-hydrothermal model suffers further from the absence of nearby intrusives.

Given the regional geologic setting of the Peña Blanca deposits, several other modes of origin appear more attractive. The outflow-facies character of the Peña Blanca volcanics precludes near-caldera magmatic activity. The setting of the facies may be envisioned in figure 13, with overlapping ignimbrites, air fall, and epiclastic tuffs. Limestones have not been recognized in the epiclastic zones.

Figure 13 is identical to figure 3 of Goodell (1978). The Peña Blanca setting is only one in a sequence of the movement of uranium through caldera evolution and later events in the volcanic pile.

The transport of uranium at low to moderate temperatures in this geologic environment can take place by several possible mechanisms, and several sources of uranium exist. Possible sources for the Peña Blanca environment are (1) high-grade veins farther "uphill," (2) glass in the volcanic pile, and (3) deeply buried connate waters. Source 2 is the most likely. Possible transport mechanisms that are likely in this environment are (1) ground and surface water applicable to sources 1 and 2 above; (2) diagenetic water applicable to source 2 (and maybe source 1); (3) hydrothermal-connate water heated by caldera-related activity or other intrusive activity, applicable to sources 2 and 3 (and maybe source

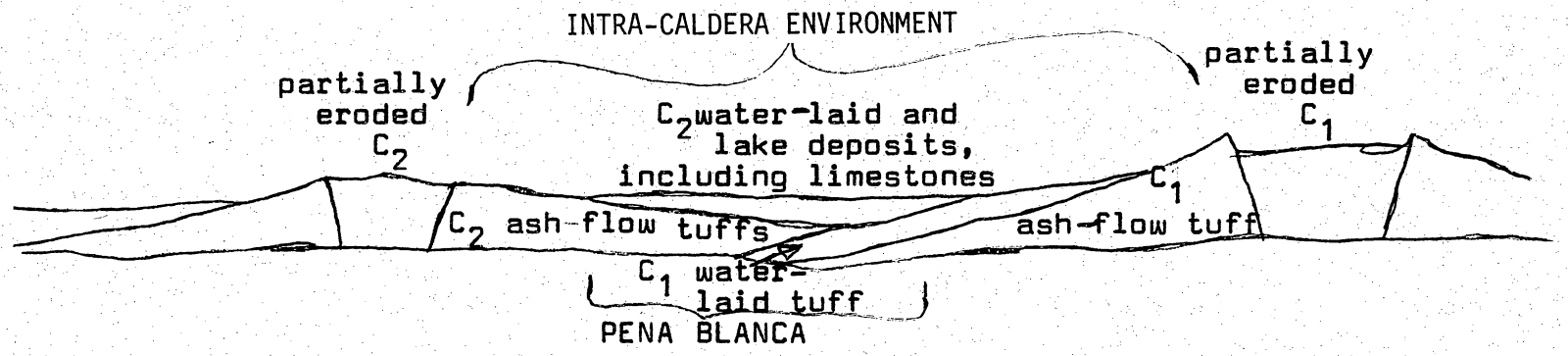

FIGURE 13

Vertical cross section through overlapping caldera environments, showing more detail of the interlayering of ash-flow and water-laid tuffs. Each unit often exhibits facies changes.

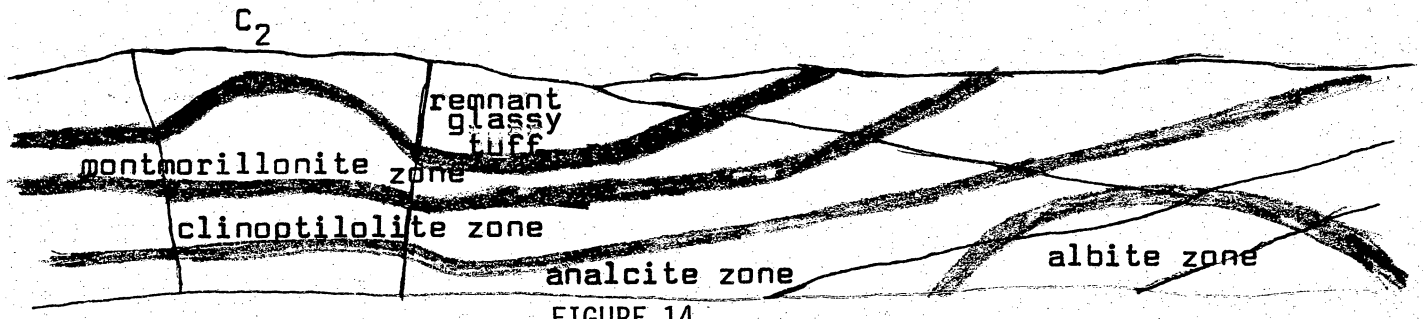

FIGURE 14

Vertical cross section through overlapping caldera environments; progressive diagenetic zeolitization changes are being superimposed over the volcanic pile, as shown by heavy lines. Devitrification, the first of these changes, releases uranium to the ground-water system.

1; source 2 may be most frequent); (4) connate water, with solution movement instigated by later regional extension. Sources 1, 2, and 3 are possible, but sources 2 and 3 would probably be more common. Additional possible sources and transport mediums can undoubtedly be envisioned, but several above appear especially reasonable for the Peña Blanca deposits. Source 2 with transport mechanisms 2 and/or 3 are the ideas which the authors currently favor.

Of great practical significance is the further question of depositional controls. Porosity and permeability have been demonstrated to be very important, as seen by the pumice and lithophyse zones, altered vitrophyre and joints in figure 4. Paleohydrology is important and complex.

The chemical and thermal controls of mineralization are poorly known, largely because of lack of study. With respect to the diagenetic changes commonly experienced in volcanic piles (fig. 14), montmorillonite is common in the Margaritas stratabound deposit, but zeolites have not been carefully sought. The alteration studies included in the present report document alkali leaching in Nopal I (figs. 5 through 12) and widespread silicification throughout. A correlation can be made between the degree of silicification and uranium mineralization. The silicification takes the form of chalcedony and vein quartz, typical of that produced during diagenesis of volcanic piles. Uraniferous chalcedony is common in the area, and preliminary study suggests a uranium-bearing chalcedony halo associated with the deposit. The fact that uranophane, a uranyl silicate, comprises a major ore mineral at

Peña Blanca emphasizes the high-silica activity. However, that uranophane was deposited by initial mineralizing processes and not by recent ground-water activity has not been unequivocally established. It is thought, however, that the initial processes may have deposited hexavalent uranium. Deposition of uranophane along with widespread chalcedony formation can take place simply by neutralizing solutions of pH 8.5 to 10. Waters in equilibrium with volcanic piles undergoing diagenetic changes or alteration can be expected to have such basic pH's. The presence of marcasite and uraninite in the deposits indicates that oxidation potential also may have been variable during deposition. At least some uranium was precipitated because of more reducing environments. Langmuir and Applin (1977) have shown, however, that the Eh value necessary for uraninite precipitation is significantly higher than was previously thought. The organic debris available in sandstone-type uranium deposits is not present in the Peña Blanca volcanics. However, reducing conditions sufficient for uraninite deposition may occur in an only slightly stagnant environment.

In general, then, neutralization from a basic condition, a reducing environment, and intense silicification all seem to be favorable for the formation of Peña Blanca-like uranium deposits. These conditions may be present at the interface of ground water in volcanic terrain and of ground water limestone. Such a ground-water interface was certainly present within or close to the known ore bodies. This interface may be associated with a reaction zone within which deposition of the uranium and alteration of the rock were taking place.

EXPLORATION FOR PEÑA BLANCA-TYPE ENVIRONMENTS

If the uranium is of diagenetic origin, specific geological and chemical techniques besides traditional radiometric methods exist for exploration for these deposits. Peralkaline source rocks appear to be most favorable but may not be necessary in all cases. The diagenetic events of the volcanic pile must mobilize and then precipitate the uranium. Hydrologic channels must be present for the solution movement. Fractures, faults, joints, pumice zones, altered vitrophyres, and lithophysal zones may provide permeability. These features can be mapped and checked for alteration. Alteration in the welded units is readily recognizable in the field and chemically. Mapping of alteration zones can lead to an understanding of the paleohydrology. Uranium content and Th/U in chalcedony may give indications of proximity of an ore zone, and mercury and molybdenum are among the trace-element indicators.

Again, the Peña Blanca environment is only one in a sequence of the geochemical evolution of uranium in caldera environments. It seems to play an intermediate role between deposits at the caldera boundary and the traditional sandstone-coarse clastic environment. Peña Blanca is significant in establishing the fact that important amounts of uranium can indeed get localized at this point in the geochemical cycle. Multitudinous occurrences of uranium exist in environments such as those in figure 4 in the Basin and Range. The utilization of these occurrences in discovering additional uranium resources awaits a refinement of our understanding of uranium in this overall environment.

REFERENCES

Alba, L. A., and Chavez, R., 1974, K-Ar ages of volcanic rocks from the central Sierra Peña Blanca, Chihuahua, Mexico: Isochron West, no. 10, p. 21-23.

Bell, R., 1976, in progress, Master's thesis, The University of Texas at El Paso.

Bridges, L. W., 1964, Stratigraphy of Mina Plomosas - Placer de Guadalupe Area, West Texas Geological Society Field Trip Guidebook No. 64-50, p. 20-29.

Bockoven, N. T., 1976, Petrology and volcanic stratigraphy of the El Sueco Area, Chihuahua, Mexico: Master's thesis, The University of Texas at Austin, 112 p.

Calas, G., 1977, Les phenomenes d'alteration hydrothermale et leur relation avec les mineralisation uraniteres en milieu volcanique: le cas des ignimbrites Tertiaires de la Sierra de Peña Blanca, Chihuahua (Mexique): Sci. Geol., Bulletin 30, 1, p. 3-18, Strasbourg.

de la Fuente L., F. E., 1969, Geología de la Mina el Potosi, distrito minero de Santa Eulalia, Chihuahua: Universidad Nacional Autonoma de Mexico, 138 p.

Gall, D. G., 1977, Geology of a section of ignimbrites near Sacramento, Chihuahua, Mexico: Geological Society of America Abstracts with Programs, v. 9, no. 1, p. 20.

Goodell, P. C., 1978, Uranium and the diagenesis of volcanic piles: NURE Geology of Uranium Symposium, 1977, Bendix Field Engineering Corp, Grand Junction, GJBX-12(78), p. 151-162.

Irvine, T. N., and Baragar, W. R. A., 1971, A guide to the chemical classification of the common volcanic rocks: Canadian Journal of Earth Sciences, v. 8, p. 523-548.

Keller, P. C., 1977, Geology of the Sierra del Gallego area, Chihuahua, Mexico: Ph.D. dissertation, The University of Texas at Austin, 151 p.

Krieger, P., 1932, An association of gold and uraninite from Chihuahua, Mexico: Economic Geology, v. 27, p. 651-660.

Langmuir, D., and Applin, K., 1977, Refinement of the thermodynamic properties of uranium minerals and dissolved species, with application to the chemistry of ground waters in sandstone-type uranium deposits: in Campbell, John A., ed., Short Papers of the U. S. Geological Survey Uranium-Thorium Symposium, 1977, U. S. Geological Survey Circular 753, p. 57-60.

Mauger, R., 1977, A progress report on the geology of the Sierra de la Calera-Sierra del Nido block, Chihuahua, Mexico: Geological Society of America Abstracts with Programs, v. 9, No. 1, p. 62.

Spruill, R. K., 1976, The volcanic geology of the Rancho Peñas Azules area, Chihuahua, Mexico: Master's thesis, East Carolina University, 99 p.

Tovar, J. C., and Valencia, J., 1974, First day road log, Ojinaga to Chihuahua City: Geologic Field Trip Guidebook through the States of Chihuahua and Sinaloa, Mexico, West Texas Geological Society, Publication No. 74-63, p. 7-44.

X. ORIGIN OF URANIFEROUS OPAL

By Christopher D. Henry[1]

INTRODUCTION

Cavity linings of opal and chalcedony are common in volcanic rocks and volcaniclastic sediments of Virgin Valley, Nevada, and the Thomas Range, Utah, and also occur in intrusive rhyolites of the Allen Complex in Trans-Pecos Texas. At all these locations much of the secondary silica is enriched in uranium; at both Virgin Valley and the Thomas Range uraniferous opal occurs in near mineable grade deposits. The origin of the uraniferous silica is critical in understanding how the uranium concentrations formed, how uranium was released from source rocks, and in determining where similar or larger deposits could form.

The key to understanding the opal's origin lies only partly in the opal. More important are the mineral association, distribution, and overall setting of the various occurrences of uraniferous opal. The opal and associated minerals clearly precipitated from ground water that has been in contact with, and dissolved, volcanic glass. At least two questions remain. (1) What was the temperature of the ground water--hot because it was part of a convective geothermal system or cold? (2) Is there something unique to either style of alteration that controls uranium mobility? To answer these questions it is necessary to determine the characteristics of the various occurrences and compare them with characteristics of documented alteration.

---

[1]Bureau of Economic Geology, The University of Texas at Austin.

Characteristics of Diagenesis and Geothermal Alteration

Diagenesis by either open or closed hydrologic systems produces the same mineral association although the zonation of mineralization differs. Alteration in the Vieja Group of Trans-Pecos Texas (Walton, 1975) is characteristic of open-system diagenesis; descriptions of other open systems by Hay and Sheppard (1977) are very similar to that of the Texas occurrence. Diagenetic mineral zones in the Vieja Group from top (least altered) to bottom (most altered) are

1. montmorillonite-opal-glass
2. montmorillonite-opal-clinoptilolite
3. montmorillonite-quartz-clinoptilolite
4. montmorillonite-quartz-analcime
5. quartz and analcime

Potassium feldspar occurs in place of analcime in some other diagenetic sequences but does not occur in Trans-Pecos Texas. Zone boundaries are slightly inclined, and individual zones are several hundred meters thick. Alteration occurred by solution of glass by ground water. The early-formed minerals, opal and montmorillonite, coat glass shards. Clinoptilolite occurs in two ways--as a fibrous cement between shards and as coarse, rectangular crystals filling dissolved shards.

Total thickness of altered tuff is approximately 800 m. Walton (1975) indicates that alteration took place at low temperatures at depths no greater than a few hundred meters. With even a high thermal gradient of 40°C/km maximum temperatures should not exceed 50°C.

Diagenesis in closed hydrologic systems such as saline lakes can produce mineral assemblages similar to those that occur in open hydrologic

systems. However, Hay (1977) also recognized several minerals such as sodium silicate and several zeolites in addition to clinoptilolite. The major difference from open-system diagenesis is in distribution of mineral zones. Zone boundaries are nearly vertical with the least altered at the margin of a basin. The concentric zonation and the inward increase in grade of alteration reflects increasing salinity of water.

Alteration by hot ground water produces many of the same minerals found in diagenesis. This type of alteration is commonly called hydrothermal alteration but needs to be distinguished from the classic hydrothermal alteration of precious- or base-metal ore deposits. It is called here geothermal alteration. Studies of drill core at Yellowstone National Park, Wyoming (Honda and Muffler, 1970; Keith and Muffler, 1978; Keith and others, 1978) show that formerly permeable glassy volcanic debris is altered to montmorillonite, opal, chalcedony, quartz, zeolites including clinoptilolite, mordenite, erionite and analcime, and pottassium feldspar. Honda and Muffler (1970) in particular noted the striking similarity in mineralogic association to diagenetically altered sediments. Montmorillonite was the first mineral to form from glass and opal, clinoptilolite and mordenite seem to be restricted to the coolest, shallowest parts of the alteration (Hay, 1977). Nearly all glass is destroyed below about 10 m and persists below that depth only in massive impermeable lavas. Analcime and potassium feldspar are restricted to the deepest, hottest parts of drill holes, and potassium feldspar does not occur at all in some relatively shallow, cool test holes.

Minerals formed at high temperatures either as phenocrysts or devitrification products such as quartz and alkali feldspar are apparently unaffected by geothermal alteration.

X-ray analysis of montmorillonite shows that almost all of it is sodium montmorillonite, which implies that the waters that deposited the montmorillonite had extremely high sodium/calcium ratios. Calcite solubility decreases with increase in temperature so that high-temperature thermal waters commonly have very low calcium concentrations. Calcite is rare in most drill cores and occurs only where rapid boiling depleted CO_2.

Silica minerals present include quartz, chalcedony, cristobalite, and opal. Opal is restricted to the coolest near-surface parts, and quartz and chalcedony, to deeper, higher temperature environments. Keith and Muffler (1978) believed that much of the chalcedony in higher temperature parts of cores was originally deposited as opal but since converted to chalcedony. Keith and others (1978) recognized a complete gradation from opal to cristobalite to chalcedony and quartz. Conversion of opal to cristobalite resulted from reordering of the solid state with no solution and redeposition, whereas conversion of cristobalite to chalcedony or quartz required solution and redeposition.

Maximum temperatures reached in the holes studied ranged from 140° to 170°C at a depth of about 80 m. In one drill hole a temperature of 70°C was reached at approximately 3 m. The mineral association is very similar to the association produced by diagenesis, but because of the extreme thermal gradient mineral zones are highly compressed. Several mineral zones produced by diagenesis may occur over a vertical range of many hundreds of meters, whereas the same zones produced by geothermal alteration may occur in a single drill hole less than 100 m deep.

In summary, most of the minerals are common to both diagenesis and geothermal alteration, and the general zonation of minerals is similar. That is, the order of appearance of various minerals in increasing degree

of diagenesis or increase in temperature in geothermal alteration is the same. In both, solution of glass leads initially to precipitation of opal, montmorillonite, and clinoptilolite with analcime, quartz, and potassium feldspar restricted to the most intense or highest temperature parts of alteration. A major, possibly diagnostic, difference is in geometry of zonation. Diagenesis in an open hydrologic system produces broad, almost regional zones with nearly flat-lying boundaries and abundant unaltered glass. Intensity of alteration increases downward. Diagenesis in a closed hydrologic system also has broad zones, but the boundaries are more vertical and concentric. Alteration increases inward and glass can be abundant at the margin of alteration. In geothermal alteration boundaries are again largely flat-lying, but the zones are narrow, compressed possibly because of the rapid kinetics of reaction at higher temperatures. Also glass is rare except very near the surface.

Characteristics of Uraniferous Opal Occurrences

Virgin Valley, Nevada

In Virgin Valley, Nevada, opal was apparently deposited in tuffaceous sediments filling a caldera or in lava flows and ash-flow tuffs that were a part of the volcanic activity of the caldera. Opal precipitation probably took place during the active period of the caldera or shortly thereafter.

Opal occurs in tuffaceous sediments as a cavity filling and as a replacement of the sediments and in volcanic rocks as a cavity filling. Analysis of Staatz and Bauer (1951) and this study show that different opal deposits are not uniformly enriched in uranium.

In the volcanic rocks, opal occurs coating high-temperature devitrification products including alkali feldspar, quartz, and tridymite. Chalcedony

in several different textural forms commonly occurs with the opal as a final filling or interlayered with the opal but is not apparently enriched in uranium. Quartz is a rare final filling in one sample. Thus the sequence of silica minerals is the reverse of that found in hydrothermally altered samples (Keith and others, 1978) but is similar to occurrences in volcanic rocks (White and others, 1956). Montmorillonite may occur as a very thin coating of glass shards in some undevitrified samples. Otherwise opal and chalcedony are the only diagenetic or hydrothermal minerals, and glass is abundant in highly permeable nonwelded ash-flow tuff.

In the sediments opal occurs with clinoptilolite and montmorillonite; chalcedony is minor or absent but was looked for in only two samples. Potassium feldspar and other zeolites such as analcime were not found in the few samples collected and examined for them. The altered rocks occur directly below and possibly interbedded with thick sequences of tuffaceous sediment composed of hydrated but otherwise unaltered glass.

In both volcanic and sedimentary rocks, both isotropic and nonisotropic opal occurs. The nonisotropic opal has high negative relief and is texturally similar to the isotropic opal. It may represent partial conversion of opal to chalcedony or other more stable silica minerals. X-ray analysis of opal from both the volcanic and sedimentary rocks shows that at least some of the opal is opal CT (Jones and Segnit, 1971).

Thomas Range, Utah

The Thomas Range, Utah, was a major volcanic center active apparently sporadically from about 40 million years ago to 6 million years ago (Lindsey and others, 1975). The youngest rocks are voluminous alkaline rhyolite lava flows and associated tuff. The uranium-lead age of uraniferous opal at the Autunite No. 8 prospect is 3.5 million years (Zielinski and others,

1977) which allows the opal to have formed from geothermal activity associated with the volcanism or from diagenesis of the volcanic rocks after they had cooled. Related, young (less than 1 million years old), silicic intrusive and volcanic activity of the Mineral Mountains, Utah, is accompanied by abundant geothermal activity (Lipman, and others, 1978).

Opal occurs in ash-flow tuff, lava flow and water-laid and air-fall tuff. Lindsey (1978) stated that some uraniferous opal could be found in almost any tuff of the area that is not densely welded. Three of four opal deposits examined during this study are nearly identical in character. Opal and chalcedony fill fractures in brecciated ash-flow tuff and lava flow. Both isotropic and slightly birefringent forms of opal are present. Opal invariably precipitated first and chalcedony last, but they are commonly interlayered. Opal at the Autunite No. 8 prospect is opal CT. Zielinski (personal communication, 1978) stated that uranium concentration varied in different opal layers at the Autunite No. 8 prospect but was more homogeneous in other opal samples. Opal from an opal-calcite veinlet in air-fall tuff overlying the ash-flow tuff at Autunite No. 8 is opal A. Staatz and Carr (1964) reported grades in uraniferous opal as high as 0.2 percent uranium.

No other secondary minerals besides opal, chalcedony, and calcite are known to occur in the uraniferous opal deposits. However, altered tuff deposits occur extensively throughout the Thomas Range. Lindsey (1975) reported three facies, vitric (predominantly still glassy), zeolitic (altered to clinoptilolite and montmorillonite), and feldspathic (altered to potassium feldspar, quartz, and α-cristobalite). The general pattern of alteration is from vitric facies near the margin of the range to feldspathic facies near the center of the range and is similar to

zonation shown by closed-system diagenesis. Lindsey (1975) attributed alteration to diagenesis and even speculated that uranium lost from the altered tuffs could have been the source for some sedimentary uranium deposits in the area. However, Zielinski and others (1977) and Lindsey (1978) thought that the opal at Autunite No. 8 is hydrothermal in origin. At the Autunite No. 8 locality, overlying tuffs are altered to the zeolite facies.

Allen Complex, Trans-Pecos Texas

The Allen Complex consists of a group of shallow intrusions and possible lava flows lying at the edge of a major caldera center of Trans-Pecos Texas, the Chinati Mountains (Cepeda, 1977; Amsbury, 1958). The Allen Complex is older than the Chinati caldera but may be a part of the igneous activity of an older caldera, largely obliterated by the younger activity.

In the Allen Complex, opal occurs lining cavities in intrusive rhyolites. One analyzed sample is enriched in uranium, but the amount and extent of enrichment is not known.

Most of the opal is slightly birefringent indicating partial conversion to chalcedony. Primary chalcedony is the dominant silica phase and occurs interlayered with opal and as a final filling of most cavities. Chalcedony occurs in several different textural forms. Coarse granular quartz is a final filling after chalcedony in some cavities.

No other alteration minerals occur in the same samples with the opal and chalcedony. However, other samples in the area contain clinoptilolite, montmorillonite, and kaolinite. These minerals probably formed by the same process of ground-water alteration of glass that forms the opal. Uranium in mineralized fractures in the rhyolites may also be derived from

ground-water solution of glass.

Most of the rhyolites of the Allen Complex either devitrified at high temperature or are still glassy. However, most of the glassy rhyolites are massive and impermeable; contact with either hot or cold ground water may have been severely restricted.

Stable Isotope Geochemistry of Opal

Sample Preparation and Analysis

Opal samples were crushed to about pea size and hand picked to remove any noncarbonate oxygen or hydrogen containing impurity. Samples were then ground to less than 62.5 microns and leached with dilute HCl to remove all carbonate. The leached samples were washed with distilled water to remove all HCl. X-ray analysis of the purified samples show that samples VV-1d and Autunite No. 8 are opal CT, whereas the Tuff sample is opal A.

For both oxygen and hydrogen isotopic analysis, purified opal was degassed at 25°C under high vacuum for approximately 16 hours to drive off structurally unbound water. Samples for oxygen analysis were then fused. The oxygen analyzed is thus a combination of both oxygen as SiO_2 and oxygen in structurally bound water. Sample 285 was dehydrated before fusion. Oxygen analyzed is entirely from SiO_2 (Knouth, 1973). The three new samples will be rerun for oxygen after they are heated to higher temperatures to drive off all water. Comparison of δO^{18} (total) and δO^{18} (dehydrated) (Knauth, 1973) indicates that the dehydrated δO^{18} is 1 to 5% greater than the total δO^{18}. The error in temperature calculations introduced by using δO^{18} (total) is discussed below.

Samples for hydrogen analysis were heated to 800°C to drive off all water. Thus the δD values are determined on water released between 25°

and 800°C. Some water may still be retained at 800°C (Knauth, 1973). However, it is such a small fraction of the total water concentration that even if the water were isotopically distinct it would not affect the analyzed δD values. Hydrogen from sample 285 was released in a series of steps of increasing temperature. Hydrogen isotopic compositions reported in table 1 are for the total and >200°C fractions (Knauth, 1973).

Results

Values for δO^{18} and δD and estimated temperature of formation by various methods for the three samples and for an opal sample from Virgin Valley from Knauth (1973) are given in table 1. Because sample 285 was prepared and analyzed using procedures somewhat different from these used here, exact comparisons of results are inappropriate. Knauth (personal communication, 1978) indicated that neither analytical procedures nor fractionation factors for opal are well developed. Temperature estimates for all four samples should be interpreted as $\pm$ 10°C.

Temperatures of formation can be estimated in two ways using empirically derived isotopic fractionation factors for water-silica (Knauth and Epstein, 1976). The first method uses both oxygen and hydrogen isotope ratios and requires no assumptions about the composition of the water from which the opal formed. The second method uses only oxygen isotope ratios and requires knowledge of the composition of the water. Both methods use a fractionation factor for chert (chalcedony) and water derived empirically by Knauth and Epstein (1976). Other fractionation factors for quartz and water (Clayton and others, 1972) and biogenic opal and water (Labeyrie, 1974) were not considered

TABLE 1. Isotopic Compositions and Estimated Temperatures of Formation of Opal from Virgin Valley, Nevada, and Thomas Range, Utah.

Sample	Type of Opal	δD‰	δO^{18}‰	Temperature °C			
				Method 1	Method 2 Using		
					Meteoric Water	5‰ shift from meteoric water	0‰
Utah							
Autunite #8	Opal CT	-103	21	36	6	25	85
Tuff above Autunite #8	Opal A	-145	19	27	13	34	101
Present day meteoric water[A]		-100	-16				
Nevada							
VV-1d	Opal CT	-80	16	60	34	59	128
285[B]		-104(-119)[C]	17.5(20.6)[C]	30-44	15[D]	36[D]	89[D]
Present day meteoric water[A]		-120	-14				

A From Sheppard and others, 1969.

B From Knauth, 1973.

C Values in Parentheses are δD>200°C and δO^{18} dehydrated.

D Calculated using δO^{18} dehydrated.

appropriate for use. Using these other factors would not change the temperature results significantly; the $\pm$ 10°C accuracy stated above includes this uncertainty.

For the first method using both oxygen and hydrogen ratios, the isotopic ratios are plotted in figure 1. Chert precipitated at a given temperature has a unique isotopic composition that falls along one of the diagonal lines. Sample 285 is plotted as a box. The dimensions of the box are determined by the oxygen composition of the total and dehydrated fraction and the hydrogen composition of the total and >200°C fractions. This indicates the uncertainty in the temperature determination. The three new samples use total oxygen compositions only and are thus probably maximum estimates of temperature. Clearly all four samples give low temperatures with the new Virgin Valley sample the highest at about 60°C.

The second method of calculation requires an estimation of the oxygen composition of the precipitation water. The opals were undoubtedly deposited from meteoric water even if the water was from hot spring activity. Many studies have documented that geothermal water is meteoric in origin, although the oxygen isotopic composition is altered, enriched in O^{18}, by exchange with wall rocks (Craig and others, 1956). The composition of present-day meteoric water (Sheppard and others, 1969) for Virgin Valley and the Thomas Range are given in table 1. Studies of Cretaceous and Tertiary ore deposits in the western United States show that the isotopic composition of meteoric water has been very similar throughout the Cenozoic. (Sheppard and others, 1969). Because there have been changes in topographic barriers--for example

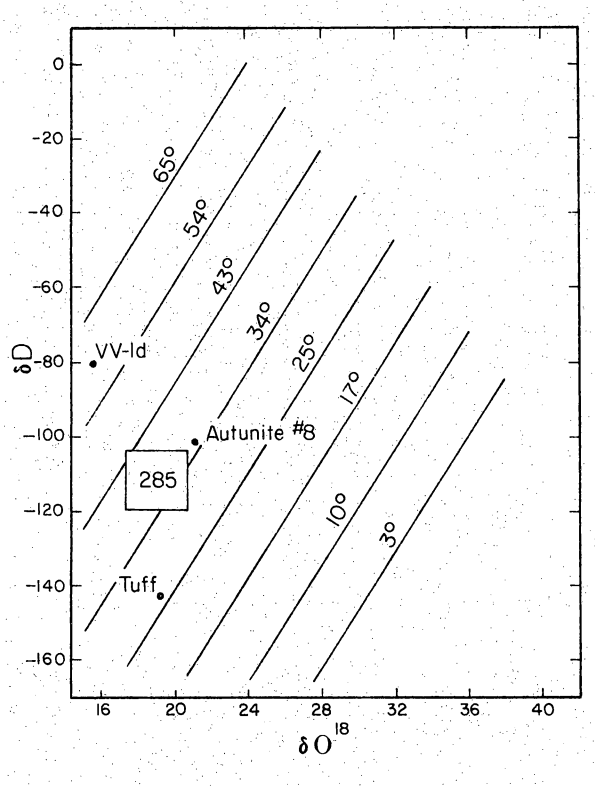

Figure 1. Isotopic composition and estimated temperature of formation of opal using chert-water oxygen isotope fractionation from Knauth and Epstein (1976).

the Sierra Nevada--which control climate, there have probably been changes in the composition of meteoric water. Nevertheless, the present-day ratios are the best available estimates consideraing the youth of the examined opals (6 to 3.5 m.y. for opal in the Thomas Range--Lindsey and others, 1975; Zielinski and others, 1977; less than 14 million years for opal in Virgin Valley--Noble and others, 1970).

Two processes could alter the composition of the water that precipitated opal from the composition of meteoric water. If the waters

were associated with hot spring activity they could be enriched in O^{18}. Observed changes in δO^{18} in active geothermal systems range from 0 to $10^{o}/oo$; most shifts are between 2 and $5^{o}/oo$. Evaporation of water in a closed basin, such as existed in Virgin Valley, can lead to enrichment in both O^{18} and D. Thus both processes can lead to increases in δO^{18}.

Because neither the existence nor the magnitude of an oxygen shift is known for certain, temperatures have been estimated using three compositions. The composition of meteoric water is a reasonable estimate and is one limit on possible compositions. It gives the lowest temperatures. A δO^{18} of $0^{o}/oo$ was used as another limit. It represents a rather extreme and unlikely degree of fractionation but puts a bound on maximum possible temperatures. An intermediate composition was also used with a shift in δO^{18} of $5^{o}/oo$ from meteoric composition. Such a shift is feasible if either evaporative or geothermal waters were involved.

The calculated temperatures range from 6° to 101°C for Thomas Range opals and from 15° to 128°C for Virgin Valley opals. The difference in assumptions clearly has a considerable effect on the temperatures. However, except for those temperatures calculated using $0^{o}/oo$, all temperatures are 60°C or less. Knauth (personal communication, 1978) believed that all the opal samples he analyzed indicated generally low temperatures of origin. The two Thomas Range samples give consistently low temperatures and do not provide evidence for high temperatures of origin. The two Virgin Valley samples show less agreement. However, temperatures calculated for sample 285 use the isotopic composition determined after first driving off structurally bound water, whereas temperatures calculated for VV-1d do not. If the change in oxygen

composition of VV-1d were of the same magnitude as that for sample 285, then calculated temperatures for sample VV-1d would be comparable to temperatures determined for sample 285. Thus the two Virgin Valley samples also indicate fairly low temperatures.

The various uncertainties involved do not allow precise determination of the temperatures. The results indicate low temperatures, but the uncertainty is such that temperatures up to 60°C are feasible. These are temperatures at which opal precipitated. The results do not prove that the water was not geothermal water that cooled before opal precipitated. They simply show that no record of any higher temperature is preserved.

Discussion

A number of factors indicate that the uraniferous opal formed at low temperature by diagenesis. Opal at the three locations--Virgin Valley, Thomas Range, and Allen Complex--is associated with clinoptilolite, montmorillonite, and abundant hydrated but undevitrified glass. In areas of geothermal alteration very little glass is preserved, and clinoptilolite and montmorillonite are restricted to the coolest parts of alteration. Montmorillonite in the Allen Complex is a calcium montmorillonite, whereas almost all montmorillonite in hydrothermally altered material in Yellowstone is sodium montmorillonite. High-temperature geothermal waters generally have low calcium concentrations due to the low solubility of calcite in hot water. Thus the occurrence of calcium montmorillonite in the Allen Complex suggests that the precipitating water was not hot.

Calcite associated with one opal occurrence in the Thomas Range also suggests deposition from cold water. Hot water saturated with calcite will be extremely undersaturated with calcite when the water cools. However, loss of CO_2 during boiling of superheated geothermal waters can lead to precipitation of calcite--so the presence of calcite does not necessarily prove low temperature.

The distribution and zonation of alteration also suggests a low temperature origin by diagenesis. Opal and altered glass is widely distributed in Virgin Valley and in the Allen Complex. Geothermal alteration may be expected to be restricted to specific areas such as ring fracture zones where upwelling thermal waters may occur. Alteration in the Thomas Range shows a distinct zonation from vitric facies at the margins to feldspathic facies in the center of the range. The zonation suggests closed-system diagenesis. In Virgin Valley and in the Allen Complex high-grade diagenetic or high-temperature geothermal minerals such as potassium feldspar and analcime have not been observed. Potassium feldspar does occur in the Thomas Range, but in a seemingly distinct regional zone. Potassium feldspar or analcime can form neither by high-temperature geothermal alteration or by advanced diagenesis, so the absence or presence of potassium feldspar or analcime does not indicate which alteration occurred. However, mineral zonation is apparently highly compressed in areas of geothermal alteration; glass and potassium feldspar can occur in the same section or drill core separated by less than 100 m. In diagenesis of either the open or the closed system, glass and potassium feldspar are separated by either vertical distances of several hundred meters or lateral distances of several kilometers. Thus the lack of potassium feldspar or analcime in

Virgin Valley and in the Allen Complex and the broad zonation in the Thomas Range suggest low-temperature diagenesis.

Finally, stable oxygen and hydrogen isotopic ratios of opal from Virgin Valley and the Thomas Range indicate that the opal precipitated at low temperatures, from either diagenetic fluids or from highly cooled geothermal fluids. Because of the large uncertainty inherent in the analyses, the possibility that the opal precipitated from moderate-temperature (approximately 50°C) geothermal water cannot be excluded.

A few lines of evidence suggest or allow alteration by geothermal water. The geologic setting of all three locations was ideal for the occurrence of hot springs. Similar present-day settings, for example Yellowstone National Park, are the sites of extensive hydrothermal alteration. Conversion of opal to chalcedony is common in Yellowstone drill cores and in opal deposits at all three locations. The similarity in opal conversion and the fact that conversion is aided by contact with high-temperature water through a solution and redeposition mechanism suggest high temperatures. However, time is an equally important factor. Opal can convert to other, more stable silica phases without heating (Kastner and others, 1977). If high-temperature conversion of opal was important, considerable chalcedony should occur-even to the exclusion of opal--particularly in Virgin Valley where opal deposits occur through a wide vertical range.

Thus the uraniferous opal at all three locations appears to have formed from low-temperature diagenesis. It is possible that alteration occurred at different temperatures at different locations. However, alteration by low- or high-temperature water is similar; both types of

alteration are minor variations of the same basic process-solution of glass. Either type of alteration may be equally effective in mobilizing uranium. Thus the particular style of alteration may not be important for uranium mobility. For example, uranium may be transported as a complex that occurs only in one type of water. Organic complexes would be relatively abundant in cold ground water as compared to hot ground water, but possibly not in high-Eh environments which would probably exist in ground water in volcanic rocks. Also, at the high pH characteristics of ground water in volcanic rocks, uranyl carbonate, hydroxyl, and phosphate complexes are major uranium species (Langmuir, 1978). However, at high temperature (100°C) carbonate complexes are relatively unimportant and hydroxyl complexes, more important.

On the other hand, alteration by hot ground water is more complete; little glass is left unaltered. Thus a greater proportion of the total uranium in a volume of rock may be released by solution by high-temperature ground water. Also experiments by Zielinski (1977) show that solution of rhyolitic glass by alkaline, 120°C water released considerable uranium. The only mineral produced by alteration was potassium feldspar. Thus the temperature and alteration products are similar to those of geothermal alteration.

It would be useful to know more about the effectiveness of each process and to know which one produced the observed alteration at the three locations. More thorough studies of the alteration assemblages and zonation at each area would be useful as would a search for more diagnostic criteria for differentiation. Studies of distribution of uranium and other elements in areas where the type of alteration was

better documented would be particularly useful. For example, study of uranium in altered tuffaceous material in Yellowstone National Park provides a unique opportunity to assess the effectiveness of geothermal alteration to mobilize uranium.

REFERENCES

Amsbury, D. L., 1958, Geologic map of Pinto Canyon area, Presidio County, Texas: The University of Texas at Austin, Bureau of Economic Geology Geologic Quadrangle Map 22.

Cepeda, J., 1977, Geology and geochemistry of the igneous rocks of the Chinati Mountains, Presidio County, Texas: Unpublished Ph.D. dissertation, The University of Texas at Austin, 153 p.

Clayton, R. N., O'Neil, J. R., and Mayeda, T. K., 1972, Oxygen isotope exchange between quartz and water: Journal Geophysical Research, v. 77, p. 3057-3067.

Craig, H., Boato, G., and White, D. E., 1956, Isotopic geochemistry of thermal waters, in Nuclear processes in geologic settings: National Research Council, Nuclear Science Series Report 19, o. 19-28.

Hay, R. L., 1977, Geology of zeolites in sedimentary rocks, in Mumpton, F. A., ed., Mineralogy and geology of natural zeolites: Mineralogical Society of America Short Course Notes, v. 4, p. 53-64.

Hay, R. L., and Sheppard, R. A., 1977, Zeolites in open hydrologic systems, Mumpton, F. A., ed., in Mineralogy and geology of natural zeolites: Mineralogical Society of America Short Course Notes, v. 4, p. 93-102.

Honda, S., and Muffler, L. J. P., 1970, Hydrothermal alteration in core from research drill hole Y-1, Upper Geyser Basin, Yellowstone National Park, Wyoming: American Mineralogist, v. 55, p. 1714-1727.

Jones, J. B., and Segnit, E. R., 1971, The nature of opal, 1. Nomenclature and constituent phases: Journal of Geological Society of Australia, v. 18, p. 57-68.

Kastner, M., Keene, J. B., and Gieskes, J. M., 1977, Diagenesis of siliceous oozes--I. Chemical controls on the rate of opal A to opal CT transformation--an experimental study: Geochimica et Cosmochimica Acta, v. 41, p. 1041-1059.

Keith, T. E. C., White, D. E., and Beeson, M. H., 1978, Hydrothermal alteration and self-sealing in Y-7 and Y-8 drill holes in northern part of Upper Geyser Basin, Yellowstone National Park, Wyoming: U.S. Geological Survey Professional Paper 1054-A, 26 p.

Keith, T. E. C. and Muffler, L. J. P., 1978, Minerals produced during cooling and hydrothermal alteration of ash flow tuff from Yellowstone drill hole Y-5: Journal of Volcanology and Geothermal Research, v. 3, p. 373-402.

Knauth, L. P., 1973, Oxygen and hydrogen isotope ratios in cherts and related rocks: Unpublished Ph.D. thesis, California Institute of Technology, 369 p.

Knauth, L. P., and Epstein, S., 1976, Hydrogen and oxygen isotope ratios in nodular and bedded cherts: Geochimica et Cosmochimica Acta, v. 40, p. 1095-1108.

Labeyrie, L., 1974, New approach to surface seawater paleotemperature using O^{18}/O^{16} ratios in silica of diatom frustules: Nature, v. 248, p. 40-42.

Langmuir, D., 1978, Uranium solution-mineral equilibria at low temperatures with applications to sedimentary ore deposits, Geochimica et Cosmochimica Acta, v. 42, p. 547-569.

Lindsey, D. A., Naeser, C. W., and Shawe, D. R., 1975, Age of volcanism, intrusion, and mineralization in the Thomas Range, Keg Mountain, and Desert Mountain, western Utah: U.S. Geological Survey Journal of Research, v. 3, p. 597-604.

Lindsey, D. A., 1975, Mineralization halos and diagenesis in water-laid tuff of the Thomas Range, Utah: U.S. Geological Survey Professional Paper 818-B, 59 p.

_____, 1978, Geology of volcanic rocks and mineral deposits in the Southern Thomas Range, Utah: A brief summary: Brigham Young University Geology Studies, v. 25, pt. 1, p. 25-31.

Lipman, P. W., Rowley, P. D., Mehnert, H. H., Evans, S. H., Nash, W. P., Brown, F. H., Izett, G. A., Naeser, C. W., and Friedman, I., 1978, Pleistocene rhyolite of the Mineral Mountains, Utah--Geothermal and archeological significance: U.S. Geological Survey Journal of Research, v. 6, p. 133-147.

Noble, D. C., McKee, E. H., Smith, J. G., and Korringa, M. J., 1970, Stratigraphy and geochronology of Miocene volcanic rocks in northwestern Nevada: U.S. Geological Survey Professional Paper 700-D, p. 23-32.

Sheppard, S. M. F., Nielsen, R. L., and Taylor, H. P., 1969, Oxygen and hydrogen isotope ratios of clay minerals from porphyry copper deposits: Economic Geology, v. 64, p. 755-777.

Staatz, M. H., and Bauer, H. L., 1951, Virgin Valley opal district, Humboldt County, Nevada: U.S. Geological Survey Circular 142, 7 p.

Staatz, M. H., and Carr, W. J., 1964, Geology and mineral deposits of the Thomas and Dugway Ranges, Juab and Toocle Counties, Utah, U.S. Geological Survey Professional Paper 415, 188 p.

Surdam, R. C., 1977, Zeolites in closed hydrologic systems in Mumpton, F. A., ed., Mineralogy and geology of natural zeolites: Mineralogical Society of America Short Course Notes, v. 4, p. 65-92.

Walton, A. W., 1975, Zeolite diagenesis in Oligocene volcanic sediments, Trans-Pecos Texas: Geological Society of America Bulletin 86, p. 615-624.

White, D. E., Brannoch, W. W., and Murata, K. J., 1956, Silica in hot spring waters: Geochimica et Cosmochimica Acta, v. 10, p. 27-59.

Zielinski, R. A., 1977, Uranium mobility during interaction of rhyolitic glass with alkaline solutions: Dissolution of glass: U.S. Geological Survey Open File Report 77-744, 36 p.

Zielinski, R. A., Ludwig, K. R., and Lindsey, D. A., 1977, Uranium-lead apparent ages of uraniferous secondary silica as a guide for describing uranium mobility in Campbell, J. A., ed., Short papers of the U.S. Geological Survey Uranium-Thorium Symposium: U.S. Geological Survey Circular 753, p. 39-40.